

**Applications and Extensions of Living Ring-Opening Metathesis
Polymerization**

Thesis by

John B. Matson

In partial fulfillment of the requirements

for the degree of

doctor of philosophy

California Institute of Technology

Pasadena, CA

2010

(defended September 4, 2009)

© 2010

John B. Matson

All Rights Reserved

Acknowledgments

I suppose the most chronologically accurate place to begin my thesis acknowledgements is with my Mom and Dad, who long, long ago bought several educational placemats for the kitchen table. I ate breakfast staring at a periodic table at the age of ten, routinely asking my parents what atomic numbers and masses were. The atmosphere in our house growing up taught me to ask questions and created a love of learning that my siblings and I continue to enjoy. Thank you Mom, Dad, Tim, and Abby for teaching me how to learn and how to teach.

While my family may have set the stage, the one who opened the curtain was my high school chemistry teacher, Carolyn Morse. I remember coming home from school and telling Mom and Dad about the polymer demonstrations that she did one day. Remembering my fascination from high school, I decided to take Karen Wooley's polymer chemistry class at WashU during my sophomore year. This led to undergraduate research in her lab, where I was trained by Brooke Van Horn and Maisie Joralemon. I owe Brooke and Maisie a lot for teaching, encouraging, and mostly dealing with all the mistakes I'm sure I made during that time.

My most direct influence and the most important acknowledgement must go to my advisor, Bob Grubbs. After beginning at Caltech, I quickly joined the Grubbs family. Bob provides a research environment that has allowed me to pursue my interests down long, winding, and often quite unexpected paths. While the apparent lack of direction from above was at times difficult, it forced me to learn how to learn and discover on my own, which is truly the goal of a Ph.D. I now leave here prepared to explore my own scientific interests, knowing that I have the base of support from Bob and the extended

Grubbs family and the confidence to investigate important problems in science. Bob has also been a great friend. Whether it was rock climbing, drinking at the Ath, shooting hoops in the gym, or just chatting, Bob was fun to be around. It was during these times that I learned other important things, such as when to use a double-fisherman's knot (almost always), who not to get in a drinking contest with (anyone from Ireland), and what to do when you don't know the answer (mumble). I look forward to more beers and more stories with Bob in the future.

My committee members, Professors Dave Tirrell, Jim Heath, and Mark Davis, were also valuable resources during my time here. Dave was my committee chair and kept everything focused and running smoothly. Jim is great fun to discuss science with because his excitement is contagious and inspiring. Mark was an outstanding resource due to his interest in nanoparticles in cancer therapy. I especially thank him for his comments on my proposals and his friendly, laid-back attitude.

I am also indebted to Scott Virgil, director of the Center for Catalysis and Chemical Synthesis. Scott ran the robot that was a vital component of Chapter 6 of this thesis, but he did so much more than that. Scott took the time to understand the broader goals of my project and contributed valuable ideas that turned into components of the finished product. Additionally, he took care of the meticulous details that I overlooked, as far down as the shape of stirbars and the withdrawal rates of syringes. I am sure that Scott will be an important resource in the department for many students to come.

Every member of the Grubbs group from 2005-2009 deserves acknowledgement, but in the interest of saving trees I will limit this section to those who had a direct and important impact on my work. I joined Bob's group in November of 2004, but I didn't

have space to work until February. At that point I worked in Ron Walker's hood because he was writing his candidacy report. My desk was a flammables cabinet. Ron and Masao Yanagawa helped me hit the ground running, and Ron taught me nearly everything I know about GPC. Erin Guidry and Jason Jordan were also very helpful in those early days. Mike Page came along a little later, working on an offshoot of my project. He was a great guy to discuss chemistry with and a fantastic teacher, and we had a lot of fun traveling to various conferences. The rest of the polymer subgroup was also very helpful along the way. This includes Yan Xia, Rosemary Conrad, Andy Hejl, Irina Gorodetskaya, AJ Boydston, Paul Clark, Grace Chan, Erin Guidry, Jeremiah Johnson, Jasim Uddin, Bahar Bingöl, and several others. Other important folks in the lab were my various baymates: Donde Anderson, Connie Hou, Chris Daeffler (Man Bay), and Masao Yanagawa. Labmates who helped me along the way in various other ways were Jean Li (softball organizer, paper proofreader, back-walker, and group baker), Chris Douglas (organic synthesis czar and Irish car bomb expert), Rosemary Conrad (organic synthesis wisdom and travel buddy), Ian Stewart and Kevin Kuhn (general metathesis knowledge), Cheol Chung (knows everything), AJ Boydston (best guy to read your paper and get you the basketball on the block), Keith Keitz (helping clean up chromium), Matthew Van Wingerden (solvent column apprentice), and Chris Daeffler (country music). A special acknowledgement goes to the 5th Year Braintrust, which includes Kevin Kuhn, Matt Whited, and me. I am both a founding member and the last remaining member of the 5th Year Braintrust, and it was a great honor to be a part of this exclusive organization.

Undergraduate students are highly active in research at Caltech, and I had the pleasure of working with Andrew Freddo for two summers and parts of two school years.

He was a dedicated and enthusiastic student who contributed quite a bit to a chapter in this thesis. He also provided a lot of entertainment in the Man Bay with his music videos and undying love of New Jersey.

My thanks to people outside of the Grubbs group must start with the NanoSystems Biology Cancer Center (NSBCC). I began with the NSBCC when it started in early 2006, and I've learned a lot about biology and cancer from all the people involved in the center. Important people from this group include Jim Heath (NSBCC director), Mike Phelps (director of my project and director of the Crump Institute for Molecular Imaging at UCLA), and Mark Davis (nanoparticle advice). I also would like to pay special thanks to Nagichettiar Satyamurthy (Saty), Phillip Marchis, and Arkadij Elizarov for running radiofluorination reactions on my samples. In addition, thanks go to several others at Caltech who helped along the way, including Raymond Archer and Chris Alabi (DLS training), Peigen Cao (AFM training and tireless help), Udi Vermesh and Ke Xu (SEM), Pat Keon (TEM), Young In Oh, Dave Montgomery and John Phillips (HPLC), Dan Harki (fluorine-18 discussions), and Chris Henry (proposal reading). Michelle Chen at Wyatt Technology was also very helpful with all GPC-related things.

Chemistry department staff members are probably the reason that anything ever gets done here, and I owe them a lot. I especially want to thank Rick Gerhart for fixing my broken glassware and for friendly chats and Dave VanderVelde for NMR assistance with a smile. Linda Syme also deserves thanks for keeping Bob on time and for helping me with travel plans, reimbursements, and lots of paperwork over the years. Dan Nieman, while not a staff member, has also earned acknowledgement for being perhaps the best plumber on the planet. I think I could sail through plumbing school after all he

has taught me while working on the solvent columns. His indefatigable working style, attention to detail, and creative genius would have served him well had he been a Caltech graduate student.

Sports provided a great way to let out the frustrations of lab work. I played softball for several years with the Grubbs group team Imperial Palace, where we won several games and a few championships, both in the Caltech A league and the JPL B league. I also played basketball with a Grubbs group team of rotating players with team names including Brokeback Cowgirls, Black Thunder, and Def Halen Van Journey Snake. We won a few games and usually contended for last place. I was a founding member and am again the last remaining member of the retired WashU swimmers swim team, Pasadena chapter. Once the chapter was reduced to one person, I began swimming with the Caltech Masters Swim Team. Both of these groups provided a nice avenue to swim and socialize.

My friends at Caltech were with me through thick and thin. From celebrating Tar Heel championships to commiserating after painful breakups, Lenny Lucas, Matt Whited and Alon Gorodetsky were with me from the start. The four of us lived together for two awesome years in the Stupid House. Jane Khudyakov and Alex Miller were fellow Tar Heel fans who were great to watch games with from November through (sometimes) April every year. Charlotte (Mason) Whited came along a little later and became a great friend. Paul Clark was a body-boarding buddy and excellent fly fishing instructor. Erin Guidry and Andy Hejl were good drinking and brewing buddies who I've missed having around since they've graduated. Daryl Allen, Jacob Berlin, Tim Funk, and Donde Anderson were also good friends who made my first few years here a lot of fun. Kevin

Metz, Mark Ambrosi, and Nick Graham were friends from WashU that were in the area. We had a lot of great times partying in Hollywood, Hermosa, Westwood, Huntington Beach, and once all around town in a Hummer Limo. I thank all of you for making my time out of lab fun and worthwhile. I'd also like to thank Mariann Ramirez for being on Colorado Boulevard on New Years 2008 and the Ramirez family for treating me like one of their own.

I owe the Athenaeum crew a proverbial round for always being there for a Friday-afternoon, gluten-free outing. The regulars over my years here were Tim Funk, Andy Hejl, Tobias Ritter, Nick Graham, Kate Ashton, Jacob Berlin, Daryl Allen, Matt Whited, Charlotte Whited, Patricio Romero, Ian Stewart, Kevin Kuhn, Rosemary Conrad, Vince Lavallo, Paul Clark, and Keith Keitz. Tim and Andy first invited me, and then I quickly became a regular downstairs or on the lawn in the summertime. Jerry Rodriguez, head of food and beverage, liked to make me the girliest, pinkest drinks he could come up with, and Mike Echevarria, my favorite bartender ever, gave us entirely too many free pitchers. They were also just nice guys to chat with.

Lastly, I'd like to thank everyone in the department for making our community a tight-knit group that looks out for each other. I think nearly everyone in the department has at some point loaned me a chemical, given me advice on a reaction, or trained me on an instrument. More importantly, people came running to help, despite potential harm to themselves, every time I had a chemical emergency...and there were several. This type of culture may not be unique, but I think it is worthy of recognition and acknowledgement.

Abstract

Living ring-opening metathesis polymerization (ROMP) is a polymerization method that has recently become popular in the synthesis of complex polymers due to advances in olefin metathesis catalyst design. The unrivaled degree of functional group tolerance of the method, coupled with a high level of control and synthetic ease, make living ROMP a valuable tool in the assembly of complex nanostructures and functional polymers. Work in this thesis details methods for applying living ROMP in the assembly of complex nanostructures and extending the uses of living ROMP to end-functionalized polymers and to polymers synthesized in a catalyst economical manner.

Chapter 2 describes the synthesis and radiofluorination of fluorine-18 functionalized nanoparticles assembled from polynorbornene block copolymers synthesized via living ROMP. The block copolymers include a hydrophobic photocrosslinkable block made from a novel cinnamate-containing norbornene, as well as a hydrophilic block made from a PEGylated norbornene. Chapter 3 illustrates another application of ROMP-based nanoparticles in which polynorbornene block copolymers are assembled into Janus (hemispherical) nanoparticles.

A method for end-capping ROMP polymers using a symmetrical α -bromoester-containing *cis*-olefin terminating agent is described in Chapter 4. Subsequent atom transfer radical polymerization (ATRP) from the functionalized chain end confirms complete end-functionalization and was used to synthesize mechanistically incompatible block copolymers. Chapter 5 extends this polymer end-functionalization approach to additional functional groups, including alcohols, bromides, thioacetates, fluorescent compounds, biotin, and others.

A thorough study of pulsed-addition ROMP (PA-ROMP) performed using a Symyx robotic system is presented in Chapter 6. Extending the end-capping methodology described in Chapters 4 and 5 to the synthesis of additional polymer chains led to a homo- and block copolymerization strategy that can produce more than one polymer chain per molecule of metal initiator. The PA-ROMP strategy reduces catalyst consumption as much as sevenfold in the synthesis of polynorbornenes.

Appendix 1 describes the synthesis and ROMP of several norbornene monomers, including a copper-64 chelating norbornene, that were not addressed in the previous chapters but that may be useful for future studies on functional ROMP polymers and nanostructures. Appendix 2 contains additional mathematical details on PA-ROMP.

Table of Contents

Acknowledgments	iii
Abstract	ix
List of Figures	xiv
List of Schemes	xvi
List of Tables	xviii
Chapter 1. Introduction	1
<i>Olefin Metathesis</i>	2
General Aspects	2
Recent Developments	5
<i>ROMP</i>	6
General Aspects	6
Living ROMP	7
Biological Applications of ROMP	8
Telechelic ROMP polymers	8
<i>Nanoparticles as in vivo Molecular Imaging Agents</i>	10
<i>Thesis Research</i>	12
<i>References</i>	14
Chapter 2. Synthesis of Fluorine-18 Functionalized Nanoparticles for use as in vivo Molecular Imaging Agents	20
<i>Abstract</i>	21
<i>Introduction</i>	21
<i>Results and Discussion</i>	25
Monomer Syntheses and Evaluations	25
Polymer Syntheses	30
Micelle Formation and Crosslinking	33
Radiofluorination	38
<i>Conclusions</i>	39
<i>Acknowledgement</i>	40
<i>Experimental Section</i>	40
<i>References</i>	51
Chapter 3. A Living Ring-Opening Metathesis Polymerization Route to Janus Nanoparticles	54
<i>Abstract</i>	55
<i>Introduction</i>	55
<i>Results and Discussion</i>	56
Monomer Syntheses	57
Polymer Syntheses	59
Nanoparticle assembly and staining	62
<i>Conclusions</i>	65
<i>Acknowledgement</i>	66
<i>Experimental Section</i>	66
<i>References</i>	74

Chapter 4. ROMP-ATRP Block Copolymers Prepared from Monotelechelic Poly(oxa)norbornenes using a Difunctional Terminating Agent.....	76
<i>Abstract</i>	77
<i>Introduction</i>	77
<i>Results and Discussion</i>	81
<i>Conclusions</i>	89
<i>Acknowledgement</i>	89
<i>Experimental Section</i>	90
<i>References</i>	98
Chapter 5. Monotelechelic Poly(oxa)norbornenes by Ring-Opening Metathesis Polymerization using Direct End-Capping and Cross Metathesis	100
<i>Abstract</i>	101
<i>Introduction</i>	101
<i>Results and Discussion</i>	104
TA Syntheses	106
End-functionalization by direct end-capping.....	108
End-functionalization using CM.....	112
<i>Conclusions</i>	117
<i>Acknowledgment</i>	117
<i>Experimental Section</i>	118
<i>References</i>	131
Chapter 6. Pulsed-Addition Ring-Opening Metathesis Polymerization: Catalyst-Economical Syntheses of Homopolymers and Block Copolymers	134
<i>Abstract</i>	135
<i>Introduction</i>	136
<i>Results and Discussion</i>	139
Pulse Interval Optimization	141
Homopolymers by PA-ROMP	146
Block Copolymers by PA-ROMP.....	160
<i>Acknowledgement</i>	166
<i>Conclusions</i>	167
<i>Experimental Section</i>	168
<i>References</i>	177
Appendix 1. Additional Monomers and Polymers Synthesized	179
<i>Introduction</i>	180
<i>Results and Discussion</i>	180
<i>Acknowledgement</i>	183
<i>Experimental Section</i>	183
<i>References</i>	190

Appendix 2. Theoretical PA-ROMP Molecular Weight Data and Determination of Catalyst Death Rates	191
<i>Introduction</i>	192
<i>Results and Discussion</i>	192
Theoretical PA-ROMP Molecular Weight Data	192
Determination of Catalyst Death Rates	194
<i>References</i>	199

List of Figures

Chapter 1.

Figure 1.1. Olefin metathesis catalysts.	4
Figure 1.2. Comparison of activity and functional group tolerance in olefin metathesis catalysts.	5
Figure 1.3. Monomers typically used in ROMP.	7

Chapter 2.

Figure 2.1. GPC of homopolymer of monomer 3	27
Figure 2.2. Norbornenes designed to test leaving group reactivity.	29
Figure 2.3. GPC traces of block copolymers.	33
Figure 2.4. AFM images of micelles and crosslinked nanoparticles.	35
Figure 2.5. Nanoparticle core crosslinking percentage dependence on irradiation time.	36
Figure 2.6. AFM images of micelles made from block copolymers with values of the PEG chain length.	38
Figure 2.7. RadioTLC of radiofluorinated nanoparticles.	39

Chapter 3.

Figure 3.1. Ruthenium metathesis catalyst (1) and photocrosslinking monomer (2) used in this study.	57
Figure 3.2. AFM image of control nanoparticles on silicon.	64
Figure 3.3. SEM images of Janus nanoparticles and control nanoparticles.	65

Chapter 4.

Figure 4.1. Monomers and metathesis catalyst used in ROMP reactions.	82
Figure 4.2. GPC traces of P(tBENI) homopolymer and P(tBENI- <i>b</i> -S) block copolymer.	84
Figure 4.3. GPC traces of P(tBENI) homopolymer, P(tBENI- <i>b</i> -S) block copolymer and P(tBENI- <i>b</i> -tBA) block copolymer.	88

Chapter 5.

Figure 5.1. Ruthenium olefin metathesis catalysts used in this study.	105
Figure 5.2. Monomers and previously reported TAs used in this study.	106

Chapter 6.

Figure 6.1. Ruthenium olefin metathesis catalysts and monomers used in PA-ROMP reactions.	140
Figure 6.2. GPC traces of products A , B , F , and J from pulse interval optimization experiment.	146
Figure 6.3. GPC traces of P(tBENI) product mixtures K–T from one to ten cycles of PA-ROMP.	149
Figure 6.4. Dependence of M_n and PDI on number of cycles of PA-ROMP for P(tBENI) homopolymers with $M/C = 25$	151

Figure 6.5. GPC trace of PA-ROMP product in single-vial experiment	154
Figure 6.6. GPC traces of P(tBENI) product mixtures U–DD from one to ten cycles of PA-ROMP	155
Figure 6.7. Dependence of M_n and PDI on number of cycles of PA-ROMP for P(tBENI) homopolymers with $M/C = 100$	157
Figure 6.8. GPC traces of P(tBENI) product mixtures EE–NN from one to ten cycles of PA-ROMP	158
Figure 6.9. Dependence of M_n and PDI on number of cycles of PA-ROMP for P(tBENI) homopolymers with $M/C = 25$ at $20\text{ }^\circ\text{C}$ with 60 min pulse interval.....	160
Figure 6.10. GPC traces of block copolymer product mixtures OO–XX from one to ten cycles of PA-ROMP.	163
Figure 6.11. Dependence of M_n and PDI on number of cycles of PA-ROMP for P(tBENI- <i>b</i> -NMONI) block copolymers.	165

Appendix 2.

Figure A2.1. Dependence of M_n (total) on molecular weight on the number of cycles of PA-ROMP from a theoretical data set.....	194
----------------------------------------------------------------------------------------------------------------------------------	-----

List of Schemes

Chapter 1.

Scheme 1.1. Mechanism of olefin metathesis.....	2
Scheme 2.1. Monomer syntheses.....	26

Chapter 2.

Scheme 2.2. Homopolymerization of monomer 3	27
Scheme 2.3. Fluorination of test substrates	29
Scheme 2.4. Synthesis of block copolymers.....	31
Scheme 2.5. Fluorinated Nanoparticle Synthesis.	34

Chapter 3.

Scheme 3.1. Syntheses of complementary hydrogen-bonding monomers.	58
Scheme 3.2. Syntheses of acid-containing monomer and PEGylated monomer.....	59
Scheme 3.3. Synthesis of amphiphilic block copolymer containing ADA H- bonding group	60
Scheme 3.4. Synthesis of amphiphilic block copolymer (12) containing DAD hydrogen-bonding group.....	61
Scheme 3.5. Synthesis of control amphiphilic block copolymer (13).	62
Scheme 3.6. Assembly of Janus nanoparticles.	63
Scheme 3.7. Assembly of control nanoparticles.....	63

Chapter 4.

Scheme 4.1. Synthesis of Vinyl Ether.	81
Scheme 4.2. ROMP and chain termination using vinyl ether followed by ATRP of styrene.....	83
Scheme 4.3. Preparation of terminating agent.....	85
Scheme 4.4. Synthesis of monotelechelic poly(oxa)norbornenes and ROMP- ATRP block copolymers.....	86

Chapter 5.

Scheme 5.1. Synthesis of Several Functionalized Internal <i>cis</i> -Olefins for Poly(oxa)norbornene End-Functionalization.....	107
Scheme 5.2. Synthesis of NHBoc, FITC, and Biotin-Containing TAs.....	108
Scheme 5.3. End-functionalization of P(tBENI) or P(NMONI) using the direct end-capping method.....	109
Scheme 5.4. Removal of Boc and <i>tert</i> -Butyl Ester Groups to Afford Amine- Terminated Polynorbornene.....	111
Scheme 5.5. Synthesis of methylene-capped P(tBENI).....	113
Scheme 5.6. End-functionalization of P(tBENI) or P(NMONI) using cross metathesis.....	114

Chapter 6.

Scheme 6.1. Mechanism of PA-ROMP	138
Scheme 6.2. Experiment designed to determine the optimal pulse interval required for PA-ROMP	143
Scheme 6.3. Synthesis of polynorbornenes by PA-ROMP.....	147
Scheme 6.4. Synthesis of a single batch of low polydispersity homopolymer by PA-ROMP.....	152
Scheme 6.5. Synthesis of P(tBENI- <i>b</i> -NMONI) block copolymers by PA-ROMP.	162

Appendix 1.

Scheme A1.1 Synthesis of DOTA-containing norbornene monomer.	180
Scheme A1.2. ROMP of monomers 3 and 5	181
Scheme A1.3. Synthesis of galactose-containing norbornene monomer.....	182
Scheme A1.4. ROMP of monomer 9	183

List of Tables

Chapter 2.

Table 2.1. Products from fluorination of representative monomers.....	30
Table 2.2. GPC Characterization of Block Copolymers.....	32
Table 2.3. Characterization of Nanoparticles with varied block lengths.....	37
Table 2.4. Characterization of Nanoparticles with varied PEG chain lengths.....	38

Chapter 4.

Table 4.1. Polymer characterization data for monotelechelic poly(oxa)norbornenes and ROMP-ATRP block copolymers.....	87
----------------------------------------------------------------------------------------------------------------------	----

Chapter 5.

Table 5.1. End-capping Efficiency of P(tBENI) or P(NMONI) Polymers using the Direct End-Capping Method.....	110
Table 5.2. End-capping Efficiency of P(tBENI) or P(NMONI) Polymers using Cross Metathesis.....	115

Chapter 6.

Table 6.1. Characterization of the products formed in the pulse interval optimization experiment.....	145
Table 6.2. Characterization of P(tBENI) homopolymer products by GPC from 10 cycles of PA-ROMP at 25 °C with M/C = 25 and a pulse interval of 30 min.....	150
Table 6.3. Addition volumes of monomer solution assuming 8.5% catalyst death rate for each of ten cycles of PA-ROMP.....	153
Table 6.4. Characterization of P(tBENI) homopolymer products by GPC from 10 cycles of PA-ROMP at 25 °C with M/C = 100 and a pulse interval of 30 min.....	156
Table 6.5. Characterization of P(tBENI) homopolymer products by GPC from ten cycles of PA-ROMP at 20 °C with M/C = 25 and a pulse time of 60 min.....	159
Table 6.6. Characterization of P(tBENI- <i>b</i> -NMONI) block copolymer products by GPC from ten cycles of PA-ROMP at 25 °C with M/C = 25 and a pulse interval of 30 min.....	164

Appendix 2.

Table A2.1. Theoretical molecular weight trend over 40 cycles of PA-ROMP.....	193
Table A2.2. Determination of catalyst death rate for P(tBENI) homopolymers with M/C = 25 and a pulse time of 30 min in PA-ROMP.....	195
Table A2.3. Determination of catalyst death rate for P(tBENI) homopolymers with M/C = 25 and a pulse time of 30 min in PA-ROMP.....	196
Table A2.4. Determination of catalyst death rate for P(tBENI) homopolymers with M/C = 25, a temperature of 20 °C and a pulse time of 60 min in PA-ROMP.....	197
Table A2.5. Determination of catalyst death rate for P(tBENI) homopolymers with M/C = 25 and a pulse time of 30 min in PA-ROMP.....	198

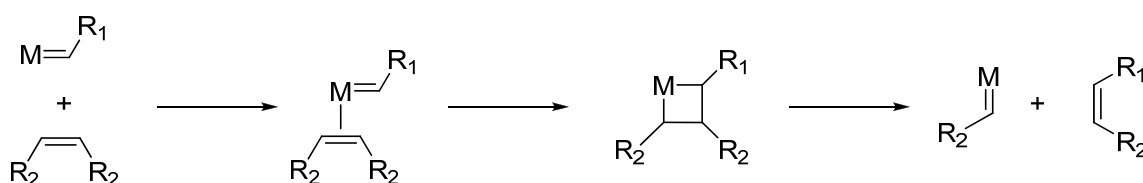
Chapter 1

Introduction

Olefin Metathesis

General Aspects

The olefin metathesis reaction has become a valuable and versatile tool in organic and polymer synthesis over the past few decades.¹ Although several mechanisms for olefin metathesis had been proposed, the now accepted mechanism for the reaction was first described by Chauvin in 1971² and later confirmed by Grubbs in 1975³ and Katz in 1976.⁴ Mediated by a metal carbene species, olefin metathesis in its most basic form is capable of taking two different, symmetrical olefins and forming a new, unsymmetrical olefin (Scheme 1.1). The reaction proceeds via a four-membered metallacyclobutane intermediate and is often reversible and therefore under thermodynamic control.



Scheme 1.1. Mechanism of olefin metathesis.

Olefin metathesis, despite its apparent simplicity, is capable of a wide variety of transformations requiring the making or breaking of carbon-carbon double bonds. Olefin metathesis reactions can be classified into four main categories: ring closing metathesis (RCM),⁵ ring-opening metathesis polymerization (ROMP),⁶ cross metathesis (CM),⁷ and acyclic diene metathesis polymerization (ADMET), which is cross metathesis extended to form polymers.⁸ Several other subcategories also exist, including ring-opening cross metathesis (ROCM),⁹ ethenolysis,¹⁰ ring expansion metathesis polymerization (REMP),¹¹ and others.

In its early years, olefin metathesis was catalyzed by ill-defined, multi-component systems, usually made up of transition metal salts such as WCl_6 and $MoCl_5$ and alkylating agents such as SnR_4 and $AlCl_2R$.¹² These early catalysts were highly active, but they suffered from lack of air, moisture, and functional group tolerance, and their heterogeneous nature made them difficult to study. A single-component, well-defined olefin metathesis catalyst (**1**) was developed by Grubbs in the 1980s¹³ derived from the Tebbe reagent (Figure 1.1).¹⁴ Titanocyclobutane catalyst **1** was the first catalyst capable of mediating the living ROMP of norbornene, affording low polydispersity polymers with control over molecular weight. However, catalyst **1**, unable to tolerate polar monomers, was limited in utility to hydrocarbons. Innovations in molybdenum and tungsten carbenes, such as Schrock's family of catalysts $(NAr)(OR)_2MCHR'$ (**2**),¹⁵ as well as late transition metal salts,¹⁶ improved the state of the art, allowing for greater functional group tolerance. Although many members of the Schrock family of catalysts are still used today due to their high activity and ability to promote stereoselective olefin metathesis reactions, these catalysts exhibit low thermal stability and sensitivity to air, water, and functional groups such as alcohols and aldehydes.¹⁷

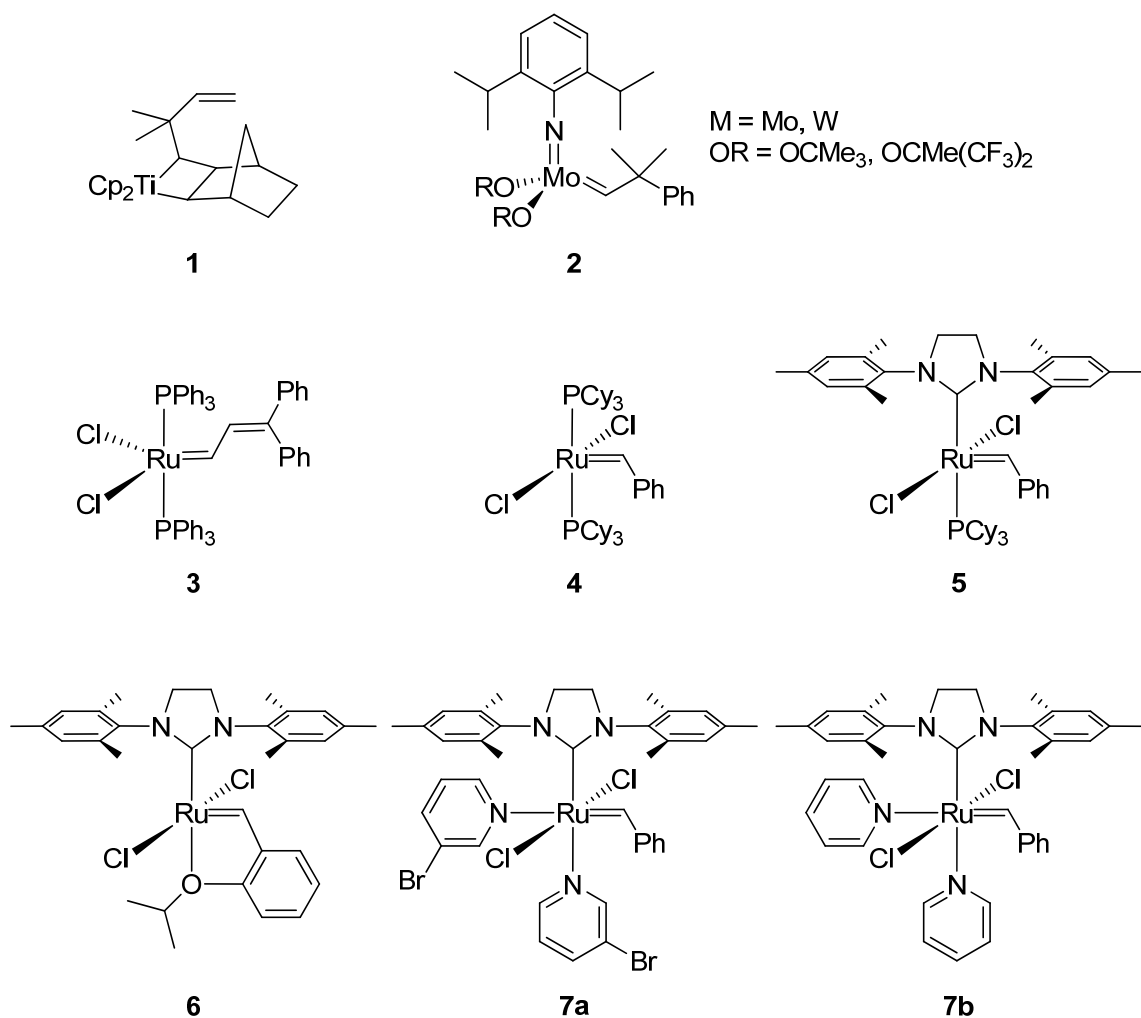


Figure 1.1. Olefin metathesis catalysts.

A 1988 report by Grubbs marked a groundbreaking development in olefin metathesis, detailing the ROMP of norbornene to high conversion in water by ruthenium salts.¹⁸ Ruthenium salts had been previously demonstrated to mediate the ROMP of norbornene in water to low conversion as early as 1965,¹⁹ but these reports were largely overlooked at the time. Grubbs's 1988 study paved the way for a class of well-defined ruthenium metathesis catalysts that is still expanding. The first well-defined ruthenium metathesis catalyst (**3**) was reported in 1992, also by Grubbs.²⁰ This catalyst was found to be tolerant of air, moisture, and most functional groups, including alcohols and acids

(Figure 1.2). However, the catalyst was only active for the ROMP of norbornene. Replacement of the triphenyl phosphine ligands with the bulkier and more electron-donating tricyclohexyl phosphine ligands and changing the vinylidene component to a benzylidene led to the more active and more stable catalyst **4**, first reported by Grubbs in 1996.²¹ Catalyst **4** has the functional group tolerance of catalyst **3** but has an increased substrate scope for CM and RCM and can mediate ROMP of low-strain monomers.²²

	Titanium	Tungsten	Molybdenum	Ruthenium
↑ Increasing Reactivity	Acids	Acids	Acids	Olefins
	Alcohols, Water	Alcohols, Water	Alcohols, Water	Acids
	Aldehydes	Aldehydes	Aldehydes	Alcohols, Water
	Ketones	Ketones	Olefins	Aldehydes
	Esters, Amides	Olefins	Ketones	Ketones
	Olefins	Esters, Amides	Esters, Amides	Esters, Amides
	← Increasing functional group tolerance →			
	← Increasing catalyst reactivity →			

Figure 1.2. Comparison of activity and functional group tolerance in olefin metathesis catalysts (adapted from reference 22).

Recent Developments

The latest major advance in olefin metathesis catalysts came in 1999 with the discovery of N-heterocyclic carbene (NHC) containing ruthenium metathesis catalysts.²³ NHC-based ruthenium metathesis catalysts (catalyst **5** and variations thereof) retain the functional group tolerance of phosphine-based catalysts **3** and **4**, but the active catalytic species performs metathesis several orders of magnitude faster than catalyst **4**.²⁴ In fact, catalyst **4** can effect the ROMP of hundreds to thousands of equivalents of norbornene at

room temperature in just a few seconds.²⁵ Additionally, electron-poor alkenes can undergo metathesis with catalyst **5**, allowing for inclusion of acrylates, trisubstituted olefins, vinyl phosphonates and many other functional groups into the olefin metathesis substrate table.²⁶ Chelating isopropoxy-styrene containing catalysts, such as **6**, have been found to be more stable than their phosphine-containing counterparts.²⁷ Catalysts such as **6** are very useful in RCM and CM, but their utility in ROMP is limited due to their generally slow initiation kinetics. Water-soluble, NHC-containing, ruthenium metathesis catalysts,²⁸ as well as catalysts capable of performing asymmetric metathesis²⁹ and catalysts that can effect RCM of tetrasubstituted olefins³⁰ have also been developed in recent years.

ROMP

General Aspects

ROMP produces polymers with unsaturated backbones through the strain-promoted ring-opening of cyclic olefin monomers (Figure 1.3). Typical monomers are norbornenes, cyclobutenes, cyclooctenes, cyclooctadienes, and cyclopentenes, but many other cyclic olefins have been shown to undergo ROMP. Norbornenes, cyclobutenes, and *trans*-cyclooctenes are generally considered high-strain monomers and can be efficiently polymerized to completion by a number of catalysts. *cis*-Cyclooctenes, cyclooctadienes, and cyclopentenes usually have lower ring strain, and polymerization reactions of these monomers require highly active catalysts and rarely reach full conversion.

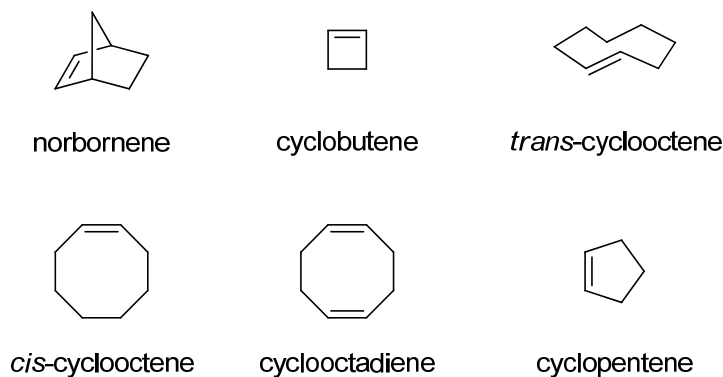


Figure 1.3. Monomers typically used in ROMP.

Living ROMP

Living polymerizations, as first defined by Szwarc,³¹ require that polymerizations proceed in a chain-growth manner without any chain transfer or chain termination reactions.³² Although fast initiation is not a requirement of a living polymerization, an initiation rate greater than or equal to the propagation rate for a given polymerization allows for the production of living polymers with controllable molecular weights and narrow molecular weight distributions. ROMP proceeds in a chain-growth manner, and under the appropriate conditions ROMP can exhibit the requirements of a living polymerization. In the case of living ROMP, polymers with narrow molecular weight distributions (also known as polydispersity indices (PDIs)) are attained when a fast-initiating catalyst is used to mediate the ROMP of a highly-strained olefin monomer. The monomer must also be sterically bulky enough to prevent secondary metathesis reactions between the growing polymer chain end and the polymer backbone. Eliminating secondary metathesis reactions prevents the reaction from reaching thermodynamic equilibrium, yielding a low polydispersity polymer when a fast initiating catalyst is used.

Other techniques, such as adding phosphine or running reactions at reduced temperatures, can be used to prevent secondary metathesis reactions of less bulky monomers.³³ Pyridine-containing catalysts **7a** and **7b** have been shown to initiate ROMP rapidly, resulting in the formation of low polydispersity polymers with low PDIs.³⁴

Biological Applications of ROMP

Highly functional, low polydispersity ROMP polymers have been made for biological applications using various olefin metathesis catalysts.³⁵ ROMP is an ideal polymerization strategy for the synthesis of biologically-relevant polymers because of the functional group and steric tolerance of ruthenium olefin metathesis catalysts. Sugar-containing monomers,³⁶ peptidic monomers,³⁷ and charged monomers³⁸ have all been polymerized with high efficiency using ROMP. There also exist two reports on nanoparticle imaging agents made by ROMP, using magnetic resonance imaging (MRI)³⁹ and near-IR optical imaging.⁴⁰ Chapter 2 of this thesis concerns the synthesis and self-assembly of ROMP block copolymers into nanoparticles for use as *in vivo* molecular imaging agents using positron emission tomography.

Telechelic ROMP polymers

Telechelic polymers, which are polymers that have a desired functionality placed on one (monotelechelic) or both (ditelechelic) chain ends, can be produced by ROMP by taking advantage of secondary metathesis reactions. Synthesis of ditelechelic ROMP polymers is typically done by reacting a small monomer, such as norbornene or cyclooctene, with catalyst in the presence of a symmetrical, disubstituted, linear olefin,

which acts as a chain transfer agent (CTA).⁴¹ Because thermodynamic equilibrium needs to be reached to ensure complete end-functionalization, these reactions are typically run at elevated temperature for 12-24 h. Additionally, the amount of catalyst in such a reaction needs to be as small as possible because the benzylidene fragment of the catalyst competes with CTA in the capping of polymer chains. This process results in polymers with a theoretical PDI of 2.0. High PDIs are acceptable for some purposes, but low PDIs are required for many applications, such as when specific morphologies of block copolymers are desired.

Monotelechelic ROMP polymers have been synthesized with low PDIs (<1.1) via a number of different methods. In all cases secondary metathesis must be prevented. This is typically done by using substituted norbornene monomers to increase steric bulk around backbone olefins. The custom initiator method is one method for synthesizing low PDI, monotelechelic ROMP polymers, by which a ROMP initiator is synthesized and isolated and then used to initiate polymerization.⁴² The custom initiator method is often effective, but it has the downside that a new catalyst must be made for each new desired chain-end-functionality. Custom terminating agents have also been used to produce monotelechelic ROMP polymers. Aldehydes can be used very effectively as terminators in early transition metal-mediated ROMP,⁴³ but the lack of air, moisture, and functional group tolerance of molybdenum metathesis catalysts limits this process to polymers with little functionality. In the case of ruthenium-mediated ROMP, functionalized vinyl ethers have been used to simultaneously end-cap a growing polymer chain and deactivate the metathesis catalyst.⁴⁴ However, end-capping is usually not complete with functionalized vinyl ethers. Other terminating agents include acrylates,⁴⁵ vinyl lactones, and vinyl

carbonates.⁴⁶ More recently the sacrificial monomer method has been developed to produce highly functional, low polydispersity polynorbornenes via ROMP.⁴⁷ This method consists of the ROMP of dioxepine (or another readily degradable monomer) on the end of the desired homopolymer. Subsequent degradation of the poly(dioxipene) block yields an alcohol terminated polymer. This method is limited to a few functional groups, all of which must be further derivatized after polymerization to add any additional functionality. A portion of this thesis addresses the synthetic limitations of end-functionalized ROMP polymers, presenting methodology for the production of mono- and ditelechelic ROMP polymers with high end-capping efficiency.

Nanoparticles as *in vivo* Molecular Imaging Agents

Nanoparticles have recently received a vast amount of interest as imaging and therapeutic agents in cancer.⁴⁸ Much of this interest stems from Maeda's seminal report in 1986 detailing what is now known as the enhanced permeability and retention (EPR) effect.⁴⁹ The EPR effect describes the observation that particles in the range of approximately 10-150 nm are able to selectively penetrate and remain in tumor tissue, while surrounding healthy tissue is left undisturbed.⁵⁰ The EPR effect occurs as a result of hypervascularization, enhanced vasculature permeability, and poor lymphatic system development in tumor tissue.

Many types of nanoparticle systems have been studied for use in tumor imaging and cancer therapy, including liposomes,⁵¹ quantum dots,⁵² dendrimers,⁵³ polymeric micelles,⁵⁴ and other molecular conjugates.⁵⁵ While the type of nanoparticle scaffolds used differ greatly, several characteristics are common to most effective nanoparticle

drug delivery and imaging agents, including a size range of 10-150 nm, near neutral surface charge and a “stealth” surface to minimize opsonization and subsequent removal by the rectoendothelial system.⁵⁶ Adherence to these guidelines appears to be vital for achieving effective nanoparticle drug delivery and imaging agents.

Several methods in tumor imaging using nanoparticles are actively being explored, including magnetic resonance imaging (MRI),⁵⁷ near-IR fluorescence (NIR),⁵⁸ and positron emission tomography (PET).⁵⁹ Of these methods, MRI has received the most attention, but PET may ultimately be a more valuable technique because it is extremely sensitive, and when coupled with computed tomography (CT), it can provide precise information on tumor location. A handful of positron-emitting nuclides exist, providing multiple chemical methods for incorporation into radiotracers. However, due to the very short half-lives of the positron-emitting nuclides of common atoms, greater than 90% of all PET scans are run using fluorine-18 as the radionuclide, mostly in the form of 18-fluorodeoxyglucose. In contrast, nearly every report on tumor imaging using positron-emitting nanoparticles uses copper-64. This disparity is due to the longer half-life and thus easier handling of copper-64 as compared with fluorine-18 (12.7 h vs. 110 min). Synthetic methods to incorporate fluorine-18 into nanoparticles will help to establish PET as a valuable method for the *in vivo* imaging of nanostructured materials. Chapter 2 of this thesis is devoted to incorporating fluorine-18 into nanoparticles to be used as *in vivo* molecular imaging agents.

Thesis Research

Increasing applications for functionally complex polymers and nanostructures in biomedical fields will need to be met by an analogous increase in synthetic methodology to incorporate functionality into macromolecules. ROMP provides a highly functional group tolerant polymerization strategy with which to make functional polymers and nanostructures, yet its uses in biomedical applications remain limited. Work in this thesis details methods for applying living ROMP in the assembly of complex nanostructures and extending the uses of living ROMP to end-functionalized polymers and to polymers synthesized in a catalyst economical manner.

Chapter 2 describes the synthesis and radiofluorination of fluorine-18 functionalized nanoparticles. The nanoparticles are assembled from polynorbornene block copolymers synthesized via living ROMP. The block copolymers include a hydrophobic photo-crosslinkable block made from a novel cinnamate-containing norbornene, as well as a hydrophilic block made from a PEGylated norbornene.

Chapter 3 illustrates another application of ROMP-based nanoparticles in which polynorbornene block copolymers are assembled into Janus (hemispherical) nanoparticles. One hemisphere of the particles was labeled with small gold nanoparticles, and scanning electron microscopy (SEM) was used to image the Janus nanoparticles.

A method for end-capping ROMP polymers using a symmetrical α -bromoester-containing *cis*-olefin terminating agent is described in Chapter 4. Subsequent atom transfer radical polymerization (ATRP) from the functionalized chain end was carried out

to confirm complete end-functionalization and synthesize mechanistically incompatible block copolymers.

Chapter 5 is an extension of Chapter 4, extending the polymer end-functionalization approach described in Chapter 4 to additional functional groups, including alcohols, bromides, thioacetates, fluorescent compounds, biotin, and others.

A thorough study of pulsed-addition ROMP (PA-ROMP) performed using a Symyx robotic system is presented in Chapter 6. Extending the end-capping methodology described in Chapters 4 and 5 to the synthesis of additional polymer chains led to a homo- and block copolymerization strategy that can produce more than one polymer chain per molecule of metal initiator. The PA-ROMP strategy reduces catalyst consumption and ruthenium contamination in the polymer products.

Appendix 1 describes the synthesis and ROMP of several norbornene monomers that were not addressed in the previous chapters, but that may be useful for future studies on functional ROMP polymers and nanostructures. Appendix 2 contains additional mathematical details on PA-ROMP.

References

- (1) Grubbs, R. H. *Handbook of Metathesis*; Wiley-VCH: Weinheim, 2003.
- (2) Herrison, J. L.; Chauvin, Y. *Makromol. Chem.* **1971**, *141*, 161.
- (3) (a) Grubbs, R. H.; Burk, P. L.; Carr, D. D. *J. Am. Chem. Soc.* **1975**, *97*, 3265–3267. (b) Grubbs, R. H.; Carr, D. D.; Hoppin, C.; Burk, P. L. *J. Am. Chem. Soc.* **1976**, *98*, 3478–3483.
- (4) Katz, T. J.; Rothchild, R. *J. Am. Chem. Soc.* **1976**, *98*, 2519–2526.
- (5) For recent reviews see: (a) Grubbs, R. H.; Miller, S. J.; Fu, G. C. *Acc. Chem. Res.* **1995**, *28*, 446. (b) Grubbs, R. H.; Chang, S. *Tetrahedron* **1998**, *54*, 4413. (c) Armstrong, S. K. *J. Chem. Soc. Perkin Trans. 1* **1998**, 371.
- (6) For recent reviews see: (a) Novak, B. M.; Risse, W.; Grubbs, R. H. *Adv. Polym. Sci.* **1992**, *102*, 47. (b) Grubbs, R. H.; Khosravi, E. *Mater. Sci. Tech.*, **1999**, *20*, 65. (c) Buchmeiser, M. R. *Chem. Rev.* **2000**, *100*, 1565. (d) Grubbs, R. H. *Handbook of Metathesis*; Wiley-VCH: Weinheim, 2003, Vol. 3. (e) Bielawski, C. W.; Grubbs, R. H. *Prog. Polym. Sci.* **2007**, *32*, 1–29.
- (7) For recent reviews see: (a) Schuster, M.; Blechert, S. *Angew. Chem.* **1997**, *109*, 2124. (b) Blechert, S. *Pure Appl. Chem.* **1999**, *71*, 1393. (c) Connon, S. J.; Blechert, S. *Angew. Chem., Int. Ed.* **2003**, *42*, 1900.
- (8) (a) Konzelman, J.; Wagener, K. B. *Macromolecules* **1996**, *29*, 7657. (b) Wolfe, P. S.; Gomez, F. J.; Wagener, K. B. *Macromolecules* **1997**, *30*, 714. (c) Lehman, S. E.; Wagener, K. B. *Macromolecules* **2002**, *35*, 48.
- (9) (a) Randall, M. L.; Tallarico, J. A.; Snapper, M. L. *J. Am. Chem. Soc.* **1995**, *117*, 9610–9611. (b) Cuny, G. D.; Cao, J. R.; Hauske, J. R. *Tetrahedron Lett.* **1997**, *38*, 5237–5240.
- (10) Burdett, K. A.; Harris, L. D.; Margl, P.; Maughon, B. R.; Mohkhtar-Zadeh, T.; Saucier, P. C.; Wasserman, E. P. *Organometallics* **2004**, *23*, 2027–2047.
- (11) (a) Bielawski, C. W.; Benitez, D.; Grubbs, R. H. *Science* **2002**, *297*, 2041. (b) Bielawski, C. W.; Benitez, D.; Grubbs, R. H. *J. Am. Chem. Soc.* **2003**, *125*, 8424. (c) Boydston, A. J.; Xia, Y.; Kornfield, J. A.; Gorodetskaya, I. A.; Grubbs, R. H. *J. Am. Chem. Soc.* **2008**, *130*, 12775–12782. (d) Xia, Y.; Boydston, A. J.; Yao, Y.; Kornfield, J. A.; Gorodetskaya, I. A.; Spiess, H. W.; Grubbs, R. H. *J. Am. Chem. Soc.* **2009**, *131*, 2670–2677.
- (12) Truett, W. L.; Johnson, D. R.; Robinson, I. M.; Montague, B. A. *J. Am. Chem. Soc.* **1960**, *82*, 2337–2340.

- (13) (a) Howard, T. R.; Lee, J. B.; Grubbs, R. H. *J. Am. Chem. Soc.* **1980**, *102*, 6876. (b) Lee, J. B.; Ott, K. C.; Grubbs, R. H. *J. Am. Chem. Soc.* **1982**, *104*, 7491. (c) Gilliom, L. R.; Grubbs, R. H. *J. Am. Chem. Soc.* **1986**, *108*, 733.
- (14) Tebbe, F. N.; Parshall, G. W.; Reddy, G. *J. Am. Chem. Soc.* **1978**, *100*, 3611.
- (15) (a) Schrock, R. R.; Murdzek, J. S.; Bazan, G. C.; Robbins, J.; DiMare, M.; O'Regan, M. *J. Am. Chem. Soc.* **1990**, *112*, 3875. (b) Bazan, G. C.; Oskam, J. H.; Cho, H. N.; Park, L. Y.; Schrock, R. R. *J. Am. Chem. Soc.* **1991**, *113*, 6899. (c) Feldman, J.; Schrock, R. R. *Prog. Inorg. Chem.* **1991**, *39*, 1.
- (16) Novak, B. M.; Grubbs, R. H. *J. Am. Chem. Soc.* **1988**, *110*, 960–961.
- (17) Schrock, R. R.; Hoveyda, A. H. *Angew. Chem., Int. Ed.* **2003**, *42*, 4592–4633.
- (18) Novak, B. M.; Grubbs, R. H. *J. Am. Chem. Soc.* **1988**, *110*, 7542–7543.
- (19) Michelotti, F. W.; Keaveny, W. P. *J. Polym. Sci., Part A: Polym. Chem.* **1965**, *3*, 895.
- (20) Nguyen, S. T.; Johnson, L. K.; Grubbs, R. H. *J. Am. Chem. Soc.* **1992**, *114*, 3974–3975.
- (21) Schwab, P.; Grubbs, R. H.; Ziller, J. W. *J. Am. Chem. Soc.* **1996**, *118*, 100.
- (22) Grubbs, R. H. *J. Macromol. Sci. – Pure Applied Chem.* **1994**, *A31*, 1829–1833.
- (23) Scholl, M.; Ding, S.; Lee, C. W.; Grubbs, R. H. *Org. Lett.* **1999**, *1*, 953.
- (24) Sanford, M. S.; Love, J. A.; Grubbs, R. H. *J. Am. Chem. Soc.* **2001**, *123*, 6543–6554.
- (25) Bielawski, C. W.; Benitez, D.; Morita, T.; Grubbs, R. H. *Macromolecules* **2001**, *34*, 8610–8618.
- (26) Chatterjee, A. K.; Choi, T. L.; Sanders, D. P.; Grubbs, R. H. *J. Am. Chem. Soc.* **2003**, *125*, 11360–11370.
- (27) (a) Garber, S. B.; Kingsbury, J. S.; Gray, B. L.; Hoveyda, A. H. *J. Am. Chem. Soc.* **2000**, *122*, 8168–8179. (b) Gessler, S.; Randl, S. *Tetrahedron Lett.* **2000**, *41*, 9973–9976.
- (28) For recent reviews see: (a) Zaman, S.; Curnow, O. J.; Abell, A. D. *Aust. J. Chem.* **2009**, *62*, 91–100. (b) Binder, J. B.; Raines, R. T. *Curr. Opin. Chem. Biol.* **2008**, *12*, 767–773. See also: (c) Gallivan, J. P.; Jordan, J. P.; Grubbs, R. H. *Tetrahedron Lett.* **2005**, *46*, 2577–2580. (d) Hong, S. H.; Grubbs, R. H. *J. Am. Chem. Soc.* **2005**, *127*, 1234–1235.

- Chem. Soc.* **2006**, *128*, 3508–3509. (e) Jordan, J. P.; Grubbs, R. H. *Angew. Chem., Int. Ed.* **2007**, *46*, 5152–5155.
- (29) (a) Fujimura, O.; Grubbs, R. H. *J. Am. Chem. Soc.* **1996**, *118*, 2499–2500. (b) Fujimura, O.; de la Mata, F. J.; Grubbs, R. H. *Organometallics* **1996**, *15*, 1865–1871. (c) Van Veldhuizen, J. J.; Gillingham, D. G.; Garber, S. B.; Kataoka, O.; Hoveyda, A. H. *J. Am. Chem. Soc.* **2003**, *125*, 12502–12508. (d) Van Veldhuizen, J. J.; Garber, S. B.; Kingsbury, J. S.; Hoveyda, A. H. *J. Am. Chem. Soc.* **2002**, *124*, 4954–4955. (e) Seiders, T. J.; Ward, D. W.; Grubbs, R. H. *Org. Lett.* **2001**, *3*, 3225–3228. (f) Funk, T. W.; Berlin, J. M.; Grubbs, R. H. *J. Am. Chem. Soc.* **2006**, *128*, 3508–3509.
- (30) (a) Berlin, J. M.; Campbell, K.; Ritter, T.; Funk, T. W.; Chenlov, A.; Grubbs, R. H. *Org. Lett.* **2007**, *9*, 1339–1342. (b) Stewart, I. C.; Douglas, C. J.; Grubbs, R. H. *Org. Lett.* **2008**, *10*, 441–444. (c) Kuhn, K. M.; Bourg, J. B.; Chung, C. K.; Virgil, S. C.; Grubbs, R. H. *J. Am. Chem. Soc.* **2009**, *131*, 5313–5320.
- (31) Szwarc, M. *Nature* **1956**, *176*, 1168.
- (32) Matyjaszewski, K.; Mueller, A. H. E. ACS, Macromolecular Nomenclature Note No. 12; <http://www.polyacs.org/main/nomenclature.shtml>.
- (33) (a) Myers, S. B.; Register, R. A. *Macromolecules* **2008**, *41*, 6773–6779. (b) Walker, R.; Conrad, R. M.; Grubbs, R. H. *Macromolecules* **2009**, *42*, 599–605.
- (34) Choi, T. L.; Grubbs, R. H. *Angew. Chem., Int. Ed.* **2004**, *42*, 1743–1746.
- (35) For recent reviews see: (a) Ladmiral, V.; Melia, E.; Haddleton, D.M. *Eur. Polym. J.* **2004**, *40*, 431–449. (b) Lee, Y.; Sampson, N. S. *Curr. Opin. Struct. Biol.* **2006**, *16*, 544–550. (c) Smith, D.; Pentzer, E. B.; Nguyen, S. T. *Polym. Rev.* **2007**, *47*, 419–459.
- (36) (a) Mortell, K. H.; Gingras, M.; Kiessling, L. L. *J. Am. Chem. Soc.* **1994**, *116*, 12053–12054. (b) Manning, D. D.; Hu, X.; Beck, P.; Kiessling, L. L. *J. Am. Chem. Soc.* **1997**, *119*, 3161–3162. (c) Gestwicki, J. E.; Strong, L. E.; Kiessling, L. L. *Chem. Biol.* **2000**, *7*, 583–591. (d) Puffer, E. B.; Pontrello, J. K.; Hollenbeck, J. J.; Kink, J. A.; Kiessling, L. L. *ACS Chem. Biol.* **2007**, *2*, 252–262. (e) Fraser, C.; Grubbs, R. H. *Macromolecules* **1995**, *28*, 7248–7255. (f) Nomura, K.; Schrock, R. R. *Macromolecules* **1996**, *29*, 540–545. (g) Camm, K. D.; Castro, N. M.; Liu, Y.; Czechura, P.; Snelgrove, J. L.; Fogg, D. E. *J. Am. Chem. Soc.* **2007**, *129*, 4168–4169. (h) Rawat, M.; Gama, C. I.; Matson, J. B.; Hsieh-Wilson, L. C. *J. Am. Chem. Soc.* **2008**, *130*, 2959–2961.
- (37) (a) Coles, M. P.; Gibson, V. C.; Mazzariol, L.; North, M.; Teasdale, W. G.; Williams, C. M.; Zamuner, D. *J. Chem. Soc., Chem. Commun.* **1994**, 2505–2506. (b) Biagini, S. C. G.; Coles, M. P.; Gibson, V. C.; Giles, M. R.; Marshall, E. L.;

- North, M. *Polymer* **1998**, *39*, 1007–1014. (c) Biagini, S. C. G.; Davies, R. G.; Gibson, V. C.; Giles, M. R.; Marshall, E. L.; North, M.; Robson, D. A. *Chem. Commun.* **1999**, 235–236. (d) Maynard, H. D.; Grubbs, R. H. *Macromolecules* **1999**, *32*, 6917–6924. (e) Maynard, H. D.; Okada, S. Y.; Grubbs, R. H. *Macromolecules*, **2000**, *33*, 6239–6248. (f) Maynard, H. D.; Okada, S. Y.; Grubbs, R. H. *J. Am. Chem. Soc.* **2001**, *23*, 1275–1279. (g) Breitenkamp, R. B.; Ou, Z.; Breitenkamp, K.; Muthukumar, M.; Emrick, T. *Macromolecules* **2007**, *40*, 7617–7624. (h) Biagini, S. C. G.; Parry, A. L. *J. Polym. Sci., Part A: Polym. Chem.* **2007**, *45*, 3178–3190. (i) Sutthasupa, S.; Sandra, F.; Masuda, T. *Macromolecules* **2009**, *42*, 1519–1525.
- (38) (a) Han, H. J.; Chen, F. X.; Yu, J. H.; Dang, J. Y.; Ma, Z.; Zang, Y. Q.; Xie, M. R. *J. Polym. Sci., Part A: Polym. Chem.* **2007**, *45*, 3986–3993. (b) Eren, T.; Som, A.; Rennie, J. R.; Nelson, C. F.; Urgina, Y.; Nusslein, K.; Coughlin, E. B.; Tew, G. N. *Macromol. Chem. Phys.* **2008**, *209*, 516–524.
- (39) Allen, M. J.; Raines, R. T.; Kiessling, L. L. *J. Am. Chem. Soc.* **2006**, *128*, 6534–6535.
- (40) Miki, K.; Kuramochi, Y.; Oride, K.; Inoue, S.; Harada, H.; Hiraoka, M.; Ohe, K. *Biocong. Chem.* **2009**, *20*, 511–517.
- (41) (a) Cramail, H.; Fontanille, M.; Soum, A. *J. Mol. Catal.* **1991**, *65*, 193. (b) Chung, T. C.; Chasmawala, M. *Macromolecules* **1991**, *24*, 3118–3120. (c) France, M. B.; Grubbs, R. H.; McGrath, D. V.; Paciello, R. A. *Macromolecules* **1993**, *26*, 4742. (d) Hillmyer, M. A.; Grubbs, R. H. *Macromolecules* **1993**, *26*, 872–874. (e) Maughon, B. R.; Morita, T.; Bielawski, C. W.; Grubbs, R. H. *Macromolecules* **2000**, *33*, 1929–1935.
- (42) (a) Bielawski, C. W.; Louie, J.; Grubbs, R. H. *J. Am. Chem. Soc.* **2000**, *122*, 12872–12873. (b) Burtscher, D.; Saf, R.; Slugovc, C. *J. Polym. Sci., Part A: Polym. Chem.* **2006**, *44*, 6136–6145.
- (43) (a) Coca, S.; Paik, H. J.; Matyjaszewski, K. *Macromolecules* **1997**, *30*, 6513–6516. (b) Murphy, J. J.; Kawasaki, T.; Fujiki, M.; Nomura, K. *Macromolecules* **2005**, *38*, 1075–1083.
- (44) Owen, R. M.; Gestwicki, J. E.; Young, T.; Kiessling, L. L. *Org. Lett.* **2002**, *4*, 2293–2296.
- (45) Lexer, C.; Saf, R.; Slugovc, C. *J. Polym. Sci., Part A: Polym. Chem.* **2009**, *47*, 299–305.
- (46) Hilf, S.; Grubbs, R. H.; Kilbinger, A. F. M. *J. Am. Chem. Soc.* **2008**, *130*, 11040–11048.

- (47) (a) Hilf, S.; Berger-Nicoletti, E.; Grubbs, R. H.; Kilbinger, A. F. M. *Angew. Chem., Int. Ed.* **2006**, *45*, 8045–8048. (b) Hilf, S.; Kilbinger, A. F. M. *Macromol. Rapid Comm.* **2007**, *28*, 1225–1230. (c) Hilf, S.; Hanik, N.; Kilbinger, A. F. M. *J. Poly. Sci., Part A: Polym. Chem.* **2008**, *46*, 2913–2921. (d) Hilf, S.; Kilbinger, A. F. M. *Macromolecules* **2009**, *42*, 1099–1106.
- (48) For recent reviews see: (a) Brigger, I.; Dubernet, C.; Couvreur, P. *Adv. Drug. Del. Rev.* **2002**, *54*, 631–651. (b) Ferrari, M. *Nat. Rev. Cancer* **2005**, *5*, 161–171. (c) Kim, J.; Piao, Y.; Hyeon, T. *Chem. Soc. Rev.* **2009**, *38*, 372–390.
- (49) Matsumura, Y.; Maeda, H. *Cancer Res.* **1986**, *46*, 6387–6392.
- (50) Maeda, H.; Wu, J.; Sawa, T.; Matsumura, Y.; Hori, K. *J. Cont. Rel.* **2000**, *65*, 271–284.
- (51) (a) Lee, S. M.; Chen, H.; Dettmer, C. M.; O'Halloran, T. V.; Nguyen, S. T. *J. Am. Chem. Soc.* **2007**, *129*, 15096–15097. (b) Torchilin, V. P. *Nat. Rev. Drug Discovery* **2005**, *4*, 145–160.
- (52) (a) Michalet, X.; Pinaud, F. F.; Bentolila, L. A.; Tsay, J. M.; Doose, S.; Li, J. J.; Sundaresan, G.; Wu, A. M.; Gambhir, S. S.; Weiss, S. *Science* **2005**, *307*, 538–544. (b) Smith, A. M.; Ruan, G.; Rhyner, M. N.; Nie, S. M. *Ann. Biomed. Eng.* **2006**, *34*, 3–14. (c) Bagalkot, V.; Zhang, L.; Levy-Nissenbaum, E.; Jon, S.; Kantoff, P. W.; Langer, R.; Farokhzad, O. C. *Nano Lett.* **2007**, *7*, 3065–3070.
- (53) (a) Ihre, H. R.; De Jesus, O. L. P.; Szoka, F. C.; Frechet, J. M. J. *Bioconjugate Chem.* **2002**, *13*, 443–452. (b) Lee, C. C.; MacKay, J. A.; Frechet, J. M. J.; Szoka, F. C. *Nat. Biotechnol.* **2005**, *23*, 1517–1526. (c) Malik, N.; Evagorou, E. G.; Duncan, R. *Anti-Cancer Drug.* **1999**, *10*, 767–776. (d) Jain, N. K.; Asthana, A. *Expert Opin. Drug Deliv.* **2007**, *4*, 495–512.
- (54) (a) Torchilin, V. P. *J. Controlled Release* **2001**, *73*, 137–172. (b) Sun, X. K.; Rossin, R.; Turner, J. L.; Becker, M. L.; Joralemon, M. J.; Welch, M. J.; Wooley, K. L. *Biomacromolecules* **2005**, *6*, 2541–2554. (c) Licciardi, M.; Giammona, G.; Du, J. Z.; Armes, S. P.; Tang, Y. Q.; Lewis, A. L. *Polymer* **2006**, *47*, 2946–2955.
- (55) Heidel, J.; Mishra, S.; Davis, M. E. *Adv. Biochem. Eng. Biot.* **2005**, *99*, 7–39.
- (56) Heath, J. R.; Davis, M. E. *Annual Rev. Med.* **2008**, *59*, 251–265.
- (57) Sun, C.; Lee, J. S. H.; Zhang, M. Q. *Adv. Drug. Del. Rev.* **2008**, *60*, 1252–1265.
- (58) Chen, W. *J. Nanosci. Technol.* **2008**, *8*, 1019–1051.
- (59) (a) Bartlett, D. W.; Su, H.; Hildebrandt, I. J.; Weber, W. A.; Davis, M. E. *Proc. Nat. Acad. Sci. U.S.A.* **2007**, *104*, 15549–15554. (b) Fukukawa, K.; Rossin, R.;

Hagooly, A.; Pressly, E. D.; Hunt, J. N.; Messmore, B. W.; Wooley, K. L.; Welch, M. J.; Hawker, C. J. *Biomacromolecules* **2008**, 1329–1339. (c) Schipper, M. L.; Cheng, Z.; Lee, S. W.; Bentolila, L. A.; Iyer, G.; Rao, J.; Chen, X.; Wu, A. M.; Weiss, S.; Gambhir, S. S. *J. Nucl. Med.* **2007**, 48, 1511–1518.

Chapter 2

Synthesis of Fluorine-18 Functionalized Nanoparticles for use as *in vivo* Molecular Imaging Agents

Portions of the text in this chapter have been reproduced with permission from:

Matson, J. B.; Grubbs, R. H. *J. Am. Chem. Soc.* **2008**, *130*, 6731-6733.

Copyright 2008 American Chemical Society

Abstract

Nanoparticles containing fluorine-18 were prepared from block copolymers made by ring-opening metathesis polymerization (ROMP). Using the fast initiating ruthenium metathesis catalyst $(H_2IMes)(pyr)_2(Cl)_2RuCHPh$, low polydispersity amphiphilic block copolymers were prepared from a cinnamoyl-containing hydrophobic norbornene monomer and a mesyl-terminated, PEG-containing hydrophilic norbornene monomer. Self-assembly into micelles and subsequent crosslinking of the micelle cores by light-activated dimerization of the cinnamoyl groups yielded stable nanoparticles. Incorporation of fluorine-18 was achieved by nucleophilic displacement of the mesylates by the radioactive fluoride ion with 31% incorporation of radioactivity. The resulting positron-emitting nanoparticles are to be used as *in vivo* molecular imaging agents for use in tumor imaging.

Introduction

The diagnosis, imaging, and treatment of cancer have the potential to be revolutionized by the use of nanostructures as vehicles for imaging agents and chemotherapeutics.¹ Research in this area is motivated by the observation that high molecular weight species are known to localize more heavily in tumor tissue than in healthy tissue. This phenomenon, known as the enhanced permeability and retention effect (EPR effect), is due to the leaky vasculature exhibited in the tumor tissue.² Exploitation of the EPR effect is a common strategy for targeting tumor cells, using nanostructures including liposomes,³ quantum dots,⁴ dendrimers,⁵ polymeric micelles,⁶ and other molecular conjugates.⁷

The EPR effect was first observed in the 1980s when Maeda and coworkers reported that large molecules (> 50 kDa) showed a tendency to enter and remain in cancer cells.⁸ They attributed these results to four characteristics of tumor vascularization: a) hypervascularization; b) enhanced vascular permeability; c) little recovery of macromolecules via the blood vessels; and d) little recovery of macromolecules from the lymphatic system. Since then the existence of the EPR effect across many types of tumors has been studied,⁹ and the phenomenon was later found to be consistent across all solid tumors. Interestingly, the maximum size of a molecule that can cross into tumor tissue varies widely, from 100 nm to 2 μ m, depending on the tumor cell line.¹⁰ Currently there are no reports that seek to optimize nanoparticle size to deliver the maximum amount of chemotherapeutic to tumors.

Imaging of tumors using nanostructures designed to exploit the EPR effect has been accomplished using several *in vivo* imaging techniques, including magnetic resonance (MR),¹¹ near-IR fluorescence (NIR),¹² and positron emission tomography (PET).¹³ PET is a specific, highly sensitive and versatile three-dimensional molecular imaging technique, and PET is the most sensitive and accurate method of measuring the temporal pattern in the biodistribution of labeled compounds. The most widespread radionuclide used in PET imaging is fluorine-18, which is the positron-emitting isotope in the commonly used PET tracer 18-fluorodeoxyglucose. Its relatively long half-life ($t_{1/2} = 109$ min) makes fluorine-18-containing radiotracers more synthetically accessible than radiotracers containing other small, positron-emitting nuclides, such as carbon-11 ($t_{1/2} = 20$ min), nitrogen-13 ($t_{1/2} = 10$ min), and oxygen-15 ($t_{1/2} = 2$ min). Its utility in

radiotracer syntheses has led to a dramatic increase in recent years in the production of fluorine-18, which is produced by the proton bombardment of [^{18}O]H₂O in a cyclotron.

While nanoparticles incorporating positron-emitting metals such as copper-64 ($t_{1/2} = 12.7 \text{ h}$)^{13a-c} have been synthesized, rapid and efficient incorporation of fluorine-18 into nanoparticles remains elusive.¹⁴ Incorporation of fluorine-18 into nanoparticles is expected to pave the way for precise and accurate *in vivo* PET imaging using nanostructured materials.

One of the most common imaging agents in PET scanning is 18-fluorodeoxyglucose (FDG).¹⁵ A hydrogen atom in a glucose molecule is replaced by a radioactive fluorine atom, and the positron-emitting compound is injected into the body where it is preferentially consumed by a growing tumor. A problem with FDG, as well as other small molecule imaging agents, is that approximately one out of every thousand FDG molecules has the radioactive label—the rest are unlabeled 19-fluorodeoxyglucose molecules and therefore cannot be visualized using a PET scan. Sites in the body that cannot absorb over one thousand glucose molecules can become saturated with these small molecule imaging agents, and the tumor cells are not imaged.¹⁶ To solve this problem, either more ^{18}F -containing molecules relative to ^{19}F -containing molecules are needed (higher specific activity), or the number of possible fluorination sites per molecule needs to be increased. While significantly increasing the percent of radioactive fluorine is currently both difficult and unsafe, organic nanoparticles can be used to increase the possible fluorination sites per molecule and thus improve tumor imaging.

Organic nanoparticles are typically made by self assembly of amphiphilic block copolymers. By dissolving block copolymers with blocks of approximately equal lengths

at the appropriate concentration in a solvent that is selective for only one of the blocks, the less soluble block will form a tight core, while the soluble block will form a loose shell or corona. Indeed, polymeric micelles have found use in medical diagnostic imaging¹⁷ and drug delivery;¹⁸ however, since there are no covalent bonds holding the micelles together, there is the possibility that they can dissociate into individual polymer chains upon dilution in the bloodstream. Crosslinking either the core or the corona avoids this problem by covalently linking all of the chains, turning the micelles into nanoparticles. Since polymeric micelles are typically comprised of a few dozen to several hundred individual polymer chains, there can be thousands of sites available to incorporate functionality in each nanoparticle. In the case where each nanoparticle possesses thousands of potential radioactive sites, the chances of having a particle without a radioactive label are very low, and the oversaturation problem is avoided.

Due to their predictable self-assembly behavior in forming micelles, their ability to control micelle size by modifying block lengths and ratios,¹⁹ and their potentially high molar specific activity, we selected amphiphilic block copolymers as scaffolds from which to build nanoparticles. Ring opening metathesis polymerization (ROMP) provides a route to very low polydispersity amphiphilic block copolymers without protecting group chemistry.²⁰ This is a distinct advantage over other living polymerization techniques, such as anionic polymerization, cationic polymerization, and controlled free radical polymerization, including atom transfer radical polymerization (ATRP), nitroxide-mediated radical polymerization (NMRP), and reversible addition-fragmentation transfer polymerization (RAFT). Typical syntheses of nanoparticles using these techniques require multiple polymerization steps and one or more deprotection or

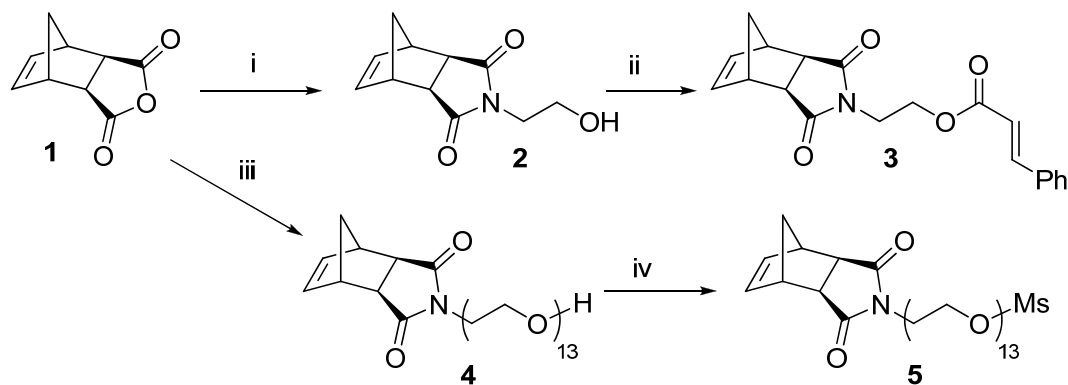
post-polymerization functionalization steps. Additionally, many of the steps performed after polymerization require lengthy purification procedures such as dialysis. ROMP can be used to avoid these steps, which are time-consuming and not atom economical, by allowing for the direct polymerization of a variety of functional monomers.²¹ Living ROMP using substituted norbornenes also produces polymers whose degrees of polymerization can be easily and precisely controlled by adjusting the monomer to catalyst ratio.²² When substituted norbornenes are used as the monomers, ROMP is free of chain-transfer and termination events. Reactions are therefore typically run to complete conversion, allowing for extremely precise control over polymer molecular weight by modifying the monomer to catalyst ratio. Factors affecting nanoparticle size and shape, such as the length and relative ratio of the hydrophilic and hydrophobic blocks, can be easily modified to quickly produce a wide variety of nanoparticle architectures using ROMP. We describe here the synthesis of organic nanoparticles that can be easily synthesized and efficiently functionalized with fluorine-18 using amphiphilic block copolymers made by ROMP.

Results and Discussion

Monomer Syntheses and Evaluations

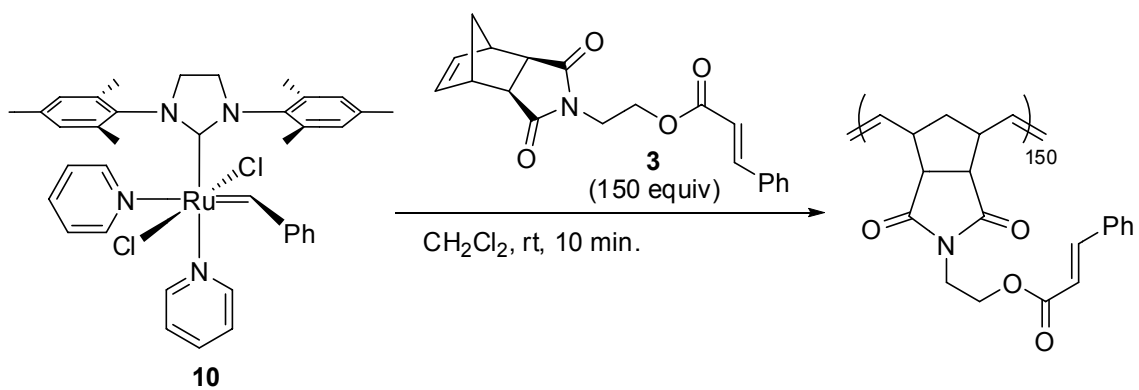
The synthesis of nanoparticles containing functional groups for crosslinking, biocompatibility, and facile radiofluorination required the development of block copolymers that exhibited all of these elements. Substituted *exo*-norbornene imides were selected as the monomers due to their ability to undergo living ROMP, as well as their ability to be easily functionalized. Specifically, norbornene-imide monomers were used

because the condensation of *exo*-anhydride **1** with functionalized amines is a versatile reaction capable of forming a variety of monomers.



Scheme 2.1. Monomer syntheses. Reaction conditions: i) NEt_3 , toluene, reflux, DS-trap. ii) EDC, DMAP, CH_2Cl_2 , rt. iii) C_6H_6 , DS-trap, reflux. iv) MsCl , NEt_3 , $-30\text{ }^\circ\text{C}$.

Hydrophobic monomer **3** was synthesized by reaction of *exo*-norbornene anhydride **1** with aminoethanol to produce norbornene-imide **2**, followed by coupling with *trans*-cinnamic acid using EDC (Scheme 2.1). The cinnamoyl group has recently become popular as a photo-crosslinking group in nanoparticle synthesis since its development by Liu in the mid 1990s.²³ Irradiation with ultraviolet light causes the *trans*-olefin to undergo a [2+2] dimerization, affording a tetrasubstituted cyclobutane ring. The olefin present in the cinnamoyl group of **3** was not expected to participate in metathesis due to its electron deficiency. Homopolymerization of monomer **3** (Scheme 2.2) was carried out in CH_2Cl_2 using catalyst **10** (vide infra) and found to afford a narrowly dispersed polymer product with controllable molecular weight by gel permeation chromatography (GPC) (Figure 2.1).



Scheme 2.2. Homopolymerization of monomer **3**.

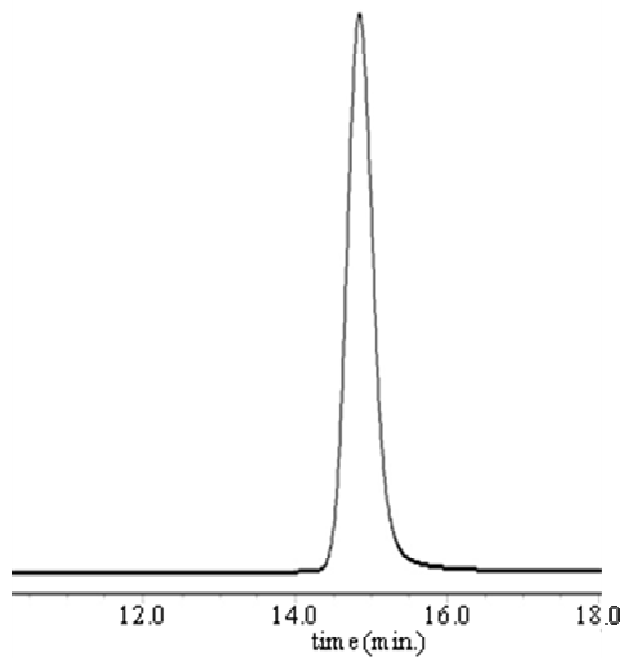


Figure 2.1. GPC of homopolymer of monomer **3**. Polymer characterization data: Theoretical $M_n = 50,300$; Observed M_n (GPC) = 50,000; Observed PDI (GPC) = 1.01.

The PEGylated norbornene imide **4** was synthesized by reaction of a previously reported mono-aminated poly(ethylene glycol) (PEG) chain with *exo*-norbornene anhydride **1**, followed by installment of a mesylate using mesyl chloride to produce hydrophilic monomer **5** (Scheme 2.1). PEG was chosen because it is well-known to be non-immunogenic and non-toxic, and both linear and grafted PEG chains have been shown to provide a stealth coating for nanoparticles in the bloodstream.²⁴ Many lengths of PEG chains were examined, but PEG600 was found to provide the desired solubility while retaining high activity during ROMP.

We chose to incorporate fluorine-18 into the nanoparticles by mimicking well-known small molecule chemistry.²⁵ Many fluorine-18-containing molecular imaging agents rely on nucleophilic displacement of a sulfonate ester by the nucleophilic fluoride-18 anion. These types of reactions are typically run in acetonitrile, using kryptofix-222 to sequester potassium. A variety of simplified norbornene monomers were prepared to test the reactivity of various leaving groups (Figure 2.2). Monomer **7** was designed to be a mimic monomer **5** with a simpler NMR spectrum. Because the oxygen β to the mesylate leaving group in monomer **5** is expected to increase the reaction rate due to anchomeric assistance, monomer **6** was designed with no oxygen β to the mesylate leaving group for comparison. Monomer **8** contains a strongly electron-withdrawing carbonyl group α to the leaving group, which was expected to increase the reaction rate as compared with monomer **7**. Lastly, monomer **9** was prepared with a *p*-nitrophenyl sulfonate ester (nosylate) leaving group, which has been shown to be approximately one order of magnitude more reactive than the mesylate group.²⁶ A monomer containing a triflate

(trifluoromethyl sulfonate ester) leaving group was also synthesized, but it was found to decompose during purification by column chromatography.

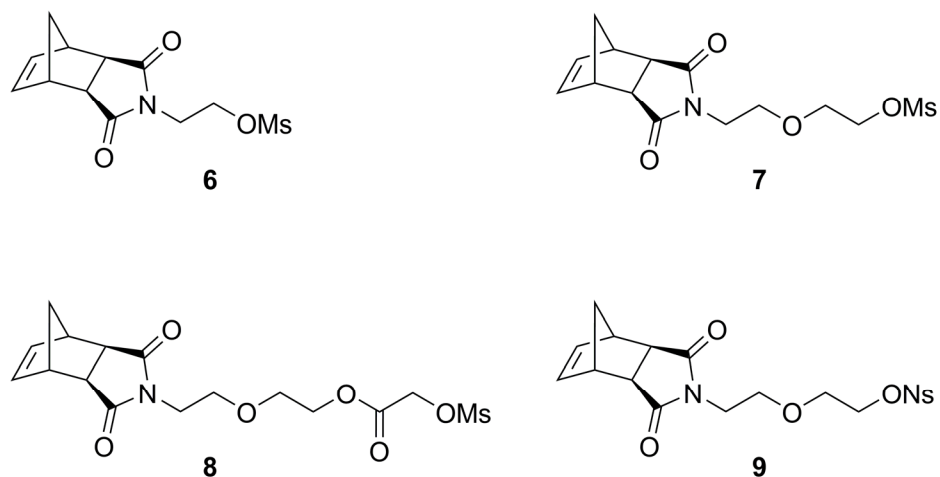
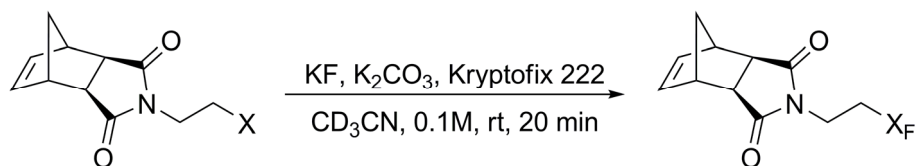


Figure 2.2. Norbornenes designed to test leaving group reactivity.

A standard test reaction was used to approximate the relative reactivities of monomers **6-9** (Scheme 2.3). In this reaction, the desired substrate (0.1 M in CD_3CN) was reacted with KF (3 equiv) in the presence of K_2CO_3 (3.5 equiv) and kryptofix 222 (2 equiv) for 20 min at room temperature.



Scheme 2.3. Fluorination of test substrates.

The products of the reactions were evaluated by ^1H NMR spectroscopy (Table 2.1). Monomer **6** showed a high conversion, but most of the product was the undesired elimination product. Monomer **7** showed 28% conversion to the desired fluoroalkane with no elimination product, most likely due to the presence of the β oxygen. Monomer

8 was expected to be faster than monomer **7**, but only 21% conversion to the desired product was observed. The reason for this slower than expected reactivity is unknown. Monomer **9** was indeed the fastest of the group with complete consumption of starting material, but 19% of the starting material was converted to an unknown side product.

Table 2.1. Products from fluorination of representative monomers.

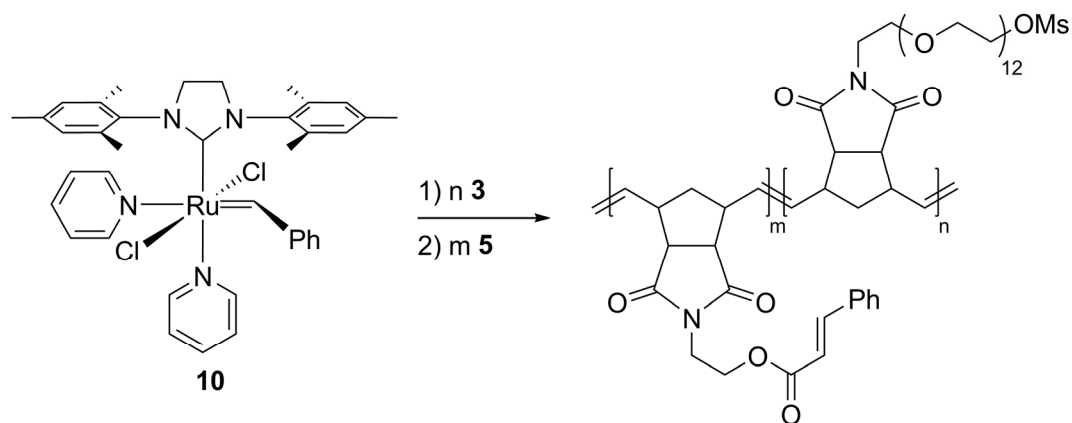
Monomer	% desired product	% elimination product	% other products
6	22	55	0
7	28	0	0
8	21	N/A	0
9	81	0	19

After examining the results of this study, the mesylate group was chosen as the leaving group for displacement by radioactive fluorine-18. Although the nosylate group was faster, the formation of side products was unacceptable. Additionally, the hydrophobic nature of the nosylate group prevented micellization of the block copolymers formed from this monomer.

Polymer Syntheses

To demonstrate the ability of living ROMP in producing a broad range of nearly monodisperse nanoparticles, four block copolymers of varying molecular weights were synthesized (Scheme 2.4). The ruthenium olefin metathesis catalyst

(H₂IMes)(pyr)₂(Cl)₂RuCHPh (**10**) was selected as the initiator due to its ability to produce extremely low polydispersity polymers. Recently, pyridine-containing, fast-initiating ruthenium catalysts such as **10** have shown remarkable reactivity as initiators for living ROMP.^{22,27} The rate of dissociation of the two pyridine ligands from catalyst **6** has been shown to be over five orders of magnitude faster than the rate of phosphine dissociation of the parent complex (H₂IMes)(PCy₃)(Cl)₂RuCHPh,²⁸ leading to polymer syntheses that can be completed in less than a minute.²⁹ Sequential copolymerization of the two monomers was carried out on the benchtop under argon in THF. After polymerization of the first monomer had reached completion (1-2 min), the second monomer was added to the reaction mixture. All reactions reached completion in 30 min. Quenching with ethyl vinyl ether, stirring for 10 min and precipitation into ether/hexanes (1:1) afforded the desired products in excellent yields.



Scheme 2.4. Synthesis of block copolymers.

Table 2.2. GPC Characterization of Block Copolymers.

Entry	m	n	M_n (theo)	M_n (GPC)	PDI
1	50	150	140,400	133,200	1.01
2	100	300	280,500	280,000	1.03
3	200	600	560,100	544,000	1.18
4	400	1200	1,124,000	1,222,000	1.73

Characterization by GPC (Figure 2.3) showed monomodal, low polydispersity peaks for most of the polymers (Table 2, entries 1-3). The PDIs were typical for this catalyst, with the exception of the highest molecular weight polymer (Table 2.2). This broadening is likely due to catalyst death. A block ratio of 3:1 hydrophilic/hydrophobic was chosen after a thorough study of the solubility of nanoparticles with various block lengths. The nanoparticles were found to be soluble in acetonitrile, the solvent used for the radiofluorination reaction, while maintaining a large enough core to allow for crosslinking. Nanoparticles with a smaller hydrophilic/hydrophobic ratio were found to be insoluble in acetonitrile, while polymers with a larger hydrophilic/hydrophobic ratio were difficult to isolate and characterize.

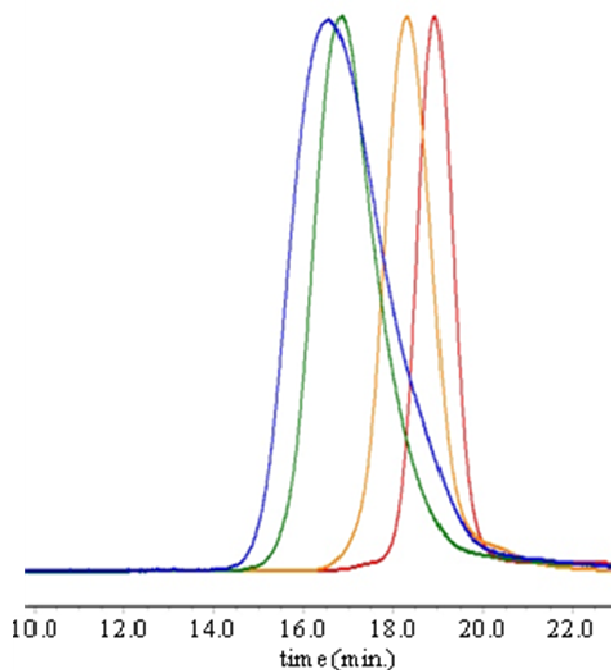
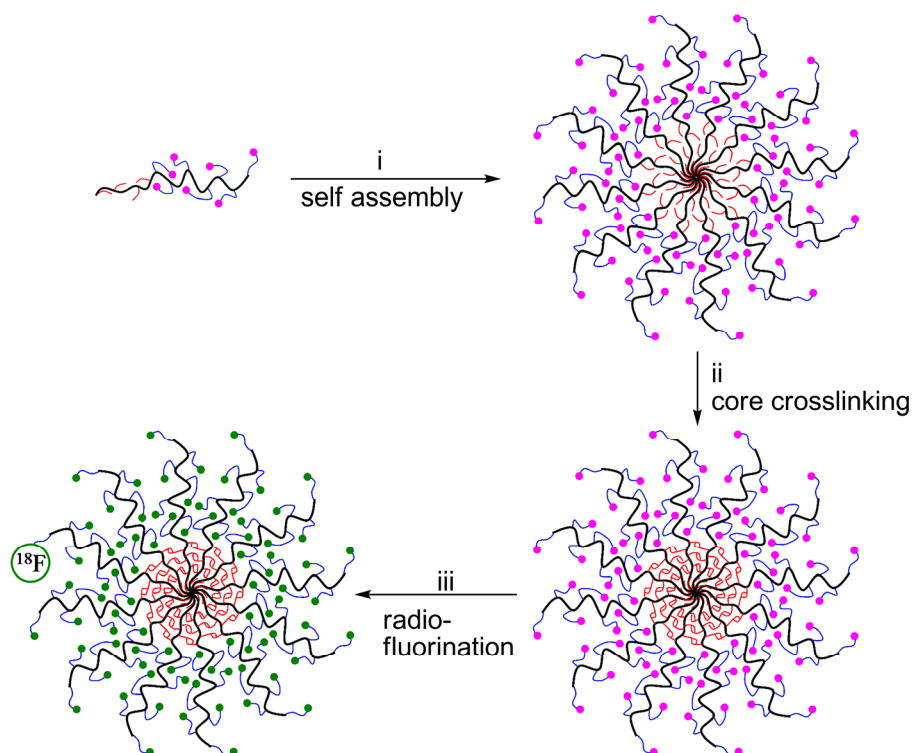


Figure 2.3. GPC traces of block copolymers. Block copolymers of entries 1 (red), 2 (orange), 3 (green) and 4 (blue) from Table 2.2 are shown.

Micelle Formation and Crosslinking

Micelle formation was accomplished by dissolving a given polymer in THF, a good solvent for both blocks, followed by slowly adding water to the solution (Scheme 2.5). The resulting micelle solution was then dialyzed against water to remove the THF. The micelles were analyzed by dynamic light scattering (DLS) and atomic force microscopy (AFM) (Figure 2.4). AFM measurements show that the micelles follow the expected trend of increasing micelle diameters with increasing polymer molecular weight. Additionally, the polydispersity of the micelles can be observed qualitatively by AFM. The largest micelles are clearly more polydisperse, while the smallest micelles are nearly monodisperse, mimicking the PDIs of the constituent block copolymers.



Scheme 2.5. Fluorinated Nanoparticle Synthesis. Black lines represent the polymer backbone; blue lines and red lines represent pendent PEG and cinnamoyl groups, respectively. Purple balls represent mesylate groups and green balls represent fluorine atoms. Conditions: (i) dialysis against H_2O , 24 h. (ii) $h\nu$, 3 min. (iii) (1) K^{18}F , kryptofix 222, K_2CO_3 , BHT, MeCN, 120°C , 60 min; (2) K^{19}F , kryptofix 222, MeCN, 80°C , 30 min.

To ensure that the nanoparticles stay intact upon dilution in the bloodstream, crosslinking of the micelle cores was carried out. Crosslinking was achieved by using UV light from a mercury arc lamp in degassed water at room temperature. The percentage of crosslinking was determined by measurement of the peak absorbance at 278 nm before and after crosslinking. Some amount of intra-chain crosslinking is likely, but this contribution is expected to be small due to the compact nature of the micelle core. Crosslinking was found to increase linearly with time (Figure 2.5). After only 3 min of UV irradiation, samples were typically crosslinked to 10-15%. There is no

evidence that significant crosslinking occurs while the micelle solution is standing in incident light. The extent of the reaction was kept between 15% and 25%, as longer reaction times caused the nanoparticles to become insoluble.

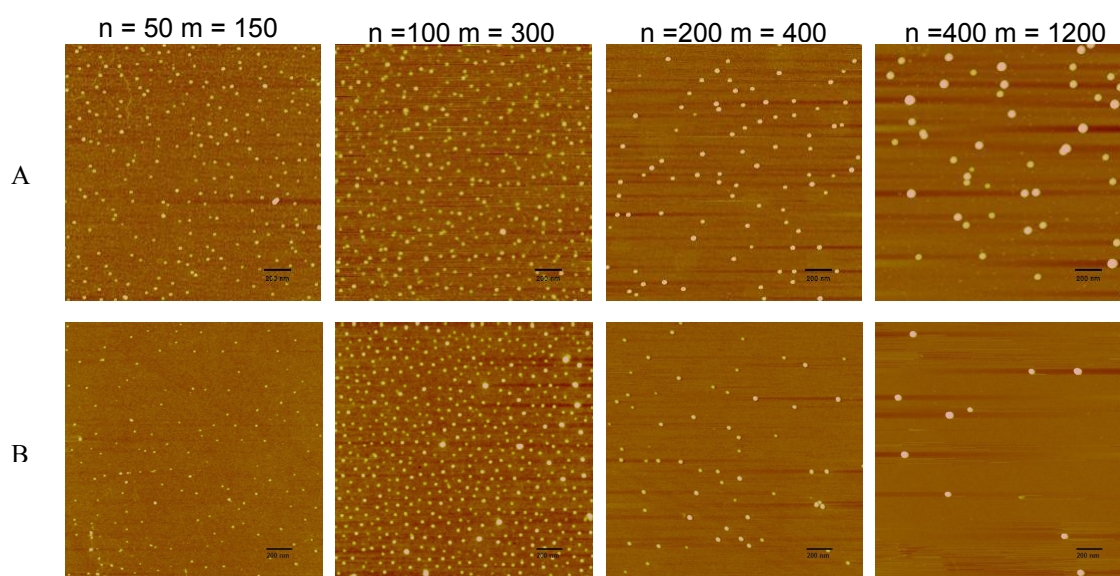


Figure 2.4. A) AFM images of micelles. B) AFM images of crosslinked nanoparticles. The nanoparticle diameters are observed to increase with increasing molecular weight of the constituent block copolymers.

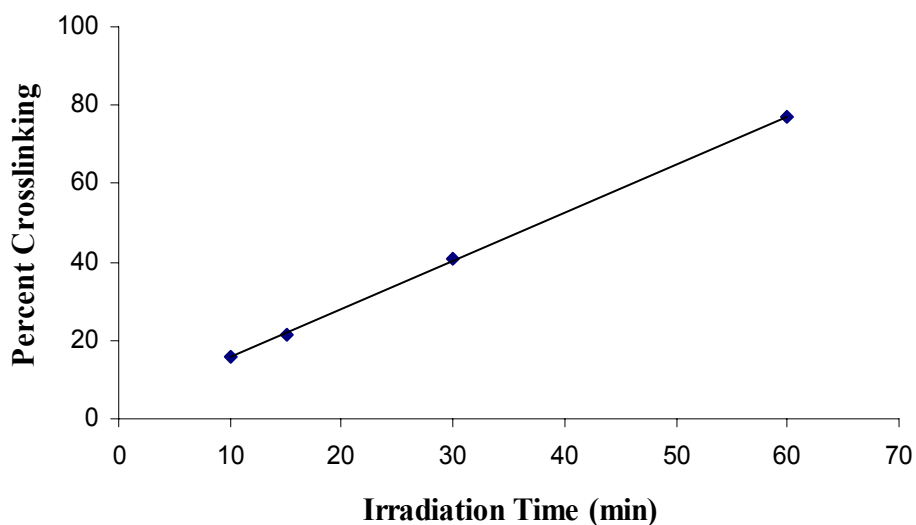


Figure 2.5. Crosslinking percentage dependence on irradiation time.

Characterization of the nanoparticles (Table 2.3) was accomplished in the solid state by AFM, as shown in Figure 2.4, and in solution by DLS. Similar to the micelles, the expected trend of increasing nanoparticle diameter with increasing polymer molecular weight is observed, with nanoparticle diameters ranging from 12.7 nm to 39.7 nm by AFM and 47.4 nm to 142.5 nm by DLS. These data are comparable to the values observed for the micelles. The apparent diameter of the nanoparticles is 2-3 times larger when measured using DLS than when measured using AFM. This effect is likely due to the swelling of the polymer chains in solution as well as the hydration sphere surrounding the particles in aqueous environments. Because AFM measures dehydrated particles on a substrate, hydrodynamic diameter measured by DLS is a better indicator of the particle size *in vivo*. DLS measurements show that the particles fall into the desired range to effectively probe the limits of the EPR effect.^{1d}

Table 2.3. Characterization of Nanoparticles with varied block lengths.

Entry	Polymer M_n	Diameter (AFM)	Diameter (DLS)
1	133,200	12.7 ± 2.6 nm	47.4 ± 7.5 nm
2	280,000	16.4 ± 4.5 nm	58.1 ± 1.8 nm
3	544,000	21.1 ± 3.9 nm	79.7 ± 9.7 nm
4	1,222,000	39.7 ± 4.0 nm	142.5 ± 6.8 nm

We also hypothesized that finer control over nanoparticle size might be attained by varying the length of the PEG chain in monomer **5**. Longer PEG chains are expected to stiffen the polymer backbone compared with shorter PEG chains due to greater steric crowding. Nanoparticles formed from stiffer chains are therefore expected to have a larger diameter. To test this hypothesis, the length of the PEG portion of monomer **5** was varied between 6, 9 and 13 average repeat units, and block copolymers similar to those described above were synthesized and assembled into micelles. The length of the hydrophobic and hydrophilic blocks were kept constant at 50 repeat units for each. AFM images (Figure 2.6) of the micelles with varied PEG chain lengths showed that fine size control was indeed possible by tuning the length of the PEG chain. Table 2.4 shows the size and size distributions of the micelles.

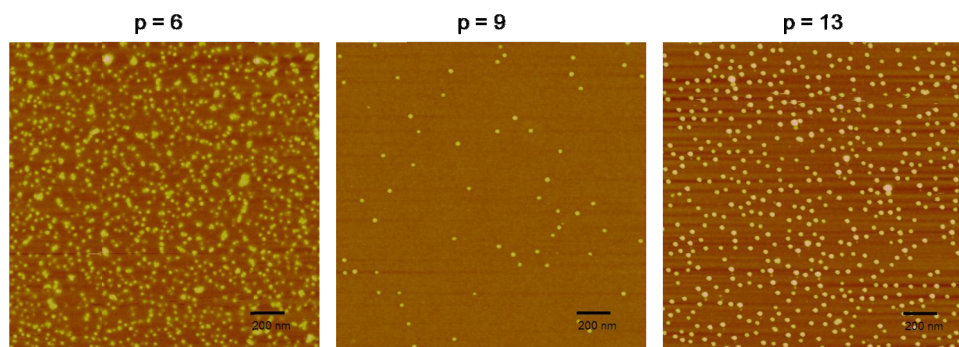


Figure 2.6. AFM images of micelles made from block copolymers with values of the PEG chain length (p) varying from 6 to 13.

Table 2.4. Characterization of Nanoparticles with varied PEG chain lengths.

Entry	p	Diameter (AFM)
1	6	14.0 ± 3.3 nm
2	9	17.3 ± 3.0 nm
3	13	20.3 ± 3.3 nm

Radiofluorination

Lyophilized nanoparticle samples were used for the radiofluorination experiments. Fluorine-18 anion was transported in its hydrated form into the reaction vessel, and solutions of kryptofix 222, K_2CO_3 , and BHT were added. Three consecutive additions and evaporations of acetonitrile were used to remove the water, which is typically detrimental to nucleophilic substitution reactions using fluoride ion.²⁵ The nanoparticles were added to the reaction vessel as a solution in acetonitrile, and the reaction mixture was heated in a sealed vessel for 1 h at 120 °C. The mesylate groups

remaining after radiofluorination were displaced with additional fluorine-19 to avoid undesired reactions *in vivo*. The radiofluorinated particles were isolated by diluting the reaction mixture with water and passing this solution through neutral alumina and strongly-acidic cation exchange resin. These conditions effectively removed all of the kryptofix and most of the unreacted fluoride. The extent of reaction was established by measurement of the radioactivity of the nanoparticles, as well as radioTLC (Figure 2.7), which showed that 31% of the fluorine was incorporated into the nanoparticles. The product was recovered in 61% radiochemical purity.

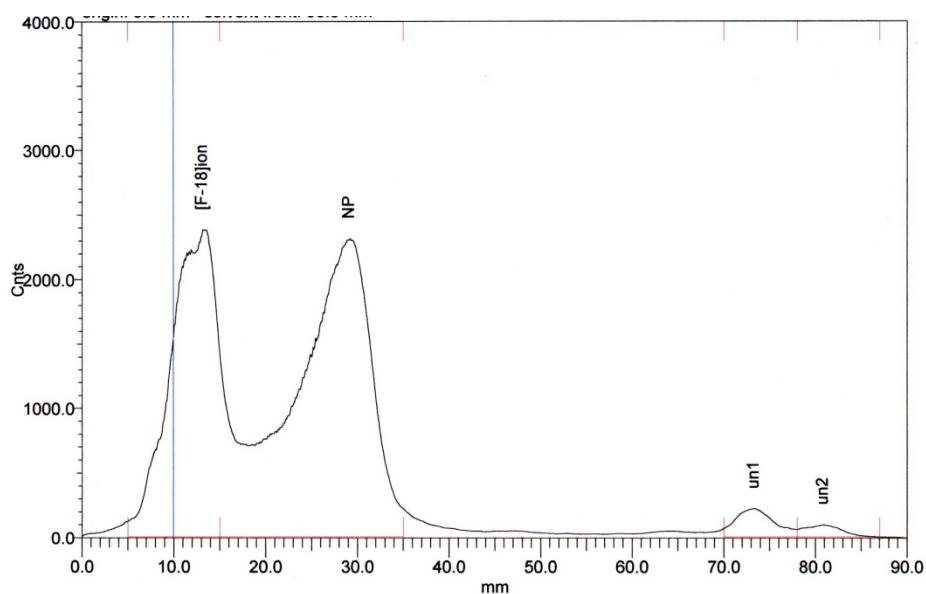


Figure 2.7. RadioTLC of radiofluorinated nanoparticles.

Conclusions

Fluorine-18 functionalized nanoparticles have been synthesized for use as *in vivo* molecular imaging agents. A new, cinnamoyl-functionalized norbornene imide monomer was synthesized to be used as a photocrosslinkable, hydrophobic block, and a PEG-containing, mesylate-terminated norbornene imide monomer was synthesized to be used

as a hydrophilic block. Sequential ROMP of the two monomers followed by dissolution in water yielded aqueous micelles. Crosslinking of the micelles using ultraviolet light yielded discrete nanoparticles that exhibited hydrodynamic diameters from 47 nm to 142 nm. Standard nucleophilic fluorination chemistry was employed to incorporate fluorine-18 into the nanoparticles in 61% radiochemical purity. Ongoing *in vivo* studies in mice will establish the optimal size range of nanoparticles for exploitation of the EPR effect.

Acknowledgement

The author thanks Materia for catalyst as well as Peigen Cao for assistance with AFM and for providing a program for measuring the size and size distribution of the nanoparticles. The group of Mark Davis, especially Raymond Archer and Chris Alabi, assisted in the DLS measurements. Radiofluorination reactions were performed by Arkadij Elizarov and Phillip Marchis. The author also thanks Nagichettiar Satyamurthy for helpful discussions regarding radiofluorination.

Experimental Section

General Information

NMR spectra were measured in CDCl_3 or $\text{DMSO-}d_6$ on Varian Mercury 300 MHz spectrometers unless otherwise noted. ^1H and ^{13}C NMR chemical shifts are reported in ppm relative to CDCl_3 . Flash column chromatography of organic compounds was performed using silica gel 60 (230-400 mesh). High-resolution mass spectra (EI and FAB) were provided by the California Institute of Technology Mass Spectrometry Facility. DLS instrumentation consisted of a Brookhaven Instruments Limited

(Holtsville, NY) system, including a model BI-200SM goniometer, a model BI-9000AT digital correlator, a model HC120-08 photomultiplier, and a laser operated at 659 nm. Measurements were made at 25 °C. Prior to analysis, solutions were centrifuged in a Beckman model TJ-6 centrifuge at 2000 rpm for 5 min to sediment dust particles. Scattered light was collected at a fixed angle of 90°. The digital correlator was operated with 250 ratio spaced channels, an initial delay of 5 μ s, a final delay of 50 ms, and a duration of 10 min. The calculations of the particle size distributions and distribution averages were performed with the ISDA software package (Brookhaven Instruments Company), using CONTIN particle size distribution analysis routines. All measurements were made in triplicate. AFM images were taken using a Nanoscope IV Scanning Probe Microscope Controller (Digital Instruments, Veeco Metrology Group) in tapping mode in air at room temperature using Veeco model TESP tips (spring constant = 20-80 N/m, resonance frequency = 297-335 kHz). The samples were prepared by drop coating onto silicon 111 surfaces that had been prepared by immersion for 5 min at 55 °C in a solution of H₂O/NH₄OH (30% in H₂O)/H₂O₂ (50% in H₂O) (5:1:1) followed by washing with DI water and drying with compressed air. Samples were drop coated onto the substrates, and excess solvent was removed by wicking with filter paper. Photoreactions were done using a 450 W medium pressure mercury arc lamp (Ace Glass). Reactions were done using a water-cooled, quartz jacket surrounding the lamp immersed in the reaction mixture. Gel permeation chromatography (GPC) was carried out in DMF on two I-series MBLMW ViscoGel columns (Viscotek) connected in series with a DAWN EOS multiangle laser light scattering (MALLS) detector and an Optilab DSP differential refractometer (both from Wyatt Technology). No calibration standards were used, and

dn/dc values were obtained for each injection by assuming 100% mass elution from the columns. UV-Vis spectra were taken on a Beckman DU 7400 spectrophotometer.

Materials

CH₂Cl₂ and THF were purified by passage through solvent purification columns.³⁰ (H₂IMes)(pyr)₂(Cl)₂RuCHPh (**10**) was prepared from (H₂IMes)(PCy₃)(Cl)₂RuCHPh, which was obtained from Materia, according to a literature procedure.²⁸ Aminohydroxy(polyethylene glycol) was made according to a literature procedure.³¹ *cis*-5-Norbornene-*endo*-2,3-dicarboxylic anhydride was purchased from Acros Organics. All other commercially available materials were obtained from Aldrich Chemical Company and used as received unless otherwise noted.

***cis*-5-Norbornene-*exo*-2,3-dicarboxylic anhydride (1).** A round-bottom flask was charged with *cis*-5-norbornene-*endo*-2,3-dicarboxylic anhydride (198 g). 200 mL 1,2-dichlorobenzene was added, a condenser was attached, and the reaction apparatus was immersed in an oil bath at 185 °C for 4 h. Once cool, the flask was further cooled to 0 °C, and the precipitate was recovered by filtration and washed with hexanes. This crude product was recrystallized from benzene six times to yield 31 g pure *exo* product (16% yield). ¹H NMR: δ 1.42-1.47 (m, 1H), 1.51 (dt, *J* = 10.2, 1.5 Hz, 1H), 3.01 (d, *J* = 1.5 Hz, 2H), 3.44-3.47 (m, 2H), 6.34 (t, *J* = 1.8 Hz, 2H). ¹³C NMR: δ 171.78, 138.14, 48.95, 47.06, 44.30. HRMS: calculated 164.0474, found 164.0468.

N-(hydroxyethyl)-cis-5-norbornene-exo-2,3-dicarboximide (2). A round-bottom flask was charged with anhydride **1** (2.07g, 1 equiv). To the flask was added 15 mL toluene, followed by 2-aminoethanol (800 μ L, 1.05 equiv) and triethylamine (200 μ L, 0.11 equiv). Stirring caused insoluble clumps to form. A Dean-Stark trap was attached to the flask, and the reaction mixture was heated at reflux for 8 h. Once complete consumption of **1** was observed by TLC, the reaction mixture was concentrated *in vacuo* to yield an off-white solid. This residue was dissolved in 40 mL CH₂Cl₂ and washed with 0.1N HCl (10 mL) and brine (10 mL). The organic layer was dried over MgSO₄ and concentrated *in vacuo* to yield **2** as a white solid in 93% yield. ¹H NMR: δ 1.34 (d, J = 9.9 Hz, 1H), 1.51 (dt, J = 9.9, 1.4 Hz, 1H), 2.3 (s, 1H), 2.71 (d, J = 1.5 Hz, 2H), 3.28 (t, J = 1.5 Hz, 2H), 3.67-3.71 (m, 2H), 3.75-3.79 (m, 2H), 6.29 (t, J = 1.8 Hz, 2H). ¹³C NMR: δ 178.95, 138.00, 60.56, 48.07, 45.45, 42.97, 41.49. HRMS: calculated 208.0974, found 208.0984.

N-(cinnamoyl ethyl)-cis-5-norbornene-exo-2,3-dicarboximide (3). To a 3-necked, round-bottom flask, equipped with a stirbar, a septum, a stopper, and gas inlet, was added alcohol **2** (1.022 g, 1 eq) under argon flow. 10 mL CH₂Cl₂ was added, followed by N-(3-dimethylaminopropyl)-N'-ethylcarbodiimide hydrochloride (1.411 g, 1.49 eq) and 4-dimethylaminopyridine (60 mg, 0.10 eq). *trans*-Cinnamic acid (886 mg, 1.21 eq) was added as a solution in 10 mL CH₂Cl₂ via syringe. The reaction mixture was allowed to stir under argon at room temperature for 7 h, at which point complete consumption of **2** was observed by TLC. The reaction mixture was washed with water (2 x 20 mL) and dried over MgSO₄. The pale yellow residue was purified by silica gel

chromatography (3:2 hexanes/EtOAc) to yield **3** as a clear oil, which solidified into a white solid over several days, in 91% yield. ^1H NMR: δ 1.32 (d, $J = 9.9$ Hz, 1H), 1.49 (dt, $J = 9.9, 1.5$ Hz, 1H), 2.72 (d, $J = 1.2$, 2H), 3.28 (t, $J = 1.8$ Hz, 2H), 3.83-3.87 (m, 2H), 4.34-4.38 (m, 2H), 6.28 (t, $J = 1.8$ Hz, 2H), 6.36 (d, $J = 16.2$ Hz, 1H), 7.37-7.50 (m, 5H), 7.64 (d, $J = 15.9$ Hz, 1H). ^{13}C NMR: δ 178.00, 166.61, 151.02, 145.69, 137.98, 134.40, 130.63, 129.08, 128.35, 117.49, 61.08, 48.02, 45.44, 42.85, 37.76. HRMS: calculated 338.1392, found 338.1381.

N-(hydroxy poly(ethylene glycol))-cis-5-norbornene-exo-2,3-dicarboximide

(4). A round-bottom flask was charged with aminohydroxyPEG (1.428 g, 1 equiv) and 30 mL toluene, followed by anhydride **1** (*exo* anhydride) (367 mg, 1.07 equiv) and triethylamine (40 μL , 0.1 equiv). A Dean-Stark trap was attached, and the reaction mixture was heated at reflux for 19 h, at which point complete consumption of aminohydroxyPEG was observed by TLC. The reaction mixture was concentrated *in vacuo*, and the residue was taken up in CH_2Cl_2 , washed with 0.1 N HCl and brine, and dried over MgSO_4 . The crude product was purified by silica gel chromatography (5% MeOH in CH_2Cl_2) to yield **4** as a clear oil in 80% yield. ^1H NMR: δ 1.35 (d, $J = 9.9$ Hz, 1H), 1.49 (dt, $J = 9.9$ Hz, 1.5 Hz, 1H), 2.67 (s, 2H), 3.26 (m, 2H), 3.56-3.73 (m, 50H), 6.27 (t, $J = 1.8$ Hz, 2H). ^{13}C NMR: δ 178.21, 138.00, 130.92, 70.72, 70.44, 70.01, 67.05, 61.87, 47.99, 45.44, 42.89, 37.88.

N-(mesyl poly(ethylene glycol))-cis-5-norbornene-exo-2,3-dicarboximide (5).

A round-bottom flask was charged with **4** (468 mg, 1 equiv) under an atmosphere of argon. CH_2Cl_2 (6 mL) was added, followed by NEt_3 (175 μL , 2.0 equiv) and the reaction

mixture was cooled to $-35\text{ }^{\circ}\text{C}$. MsCl (73 μL , 1.5 equiv) as a solution in 2 mL CH_2Cl_2 was added dropwise using a syringe pump at a rate of 0.05 mL/min. After complete addition, the reaction mixture was allowed to slowly warm to room temp. After 6 h complete consumption of **4** was observed by TLC, and the reaction mixture was diluted with CH_2Cl_2 (20 mL) and washed with 0.1 N HCl (10 mL) and brine (10 mL), then dried over MgSO_4 . The crude product was purified by silica gel chromatography (5% MeOH in CH_2Cl_2) to yield **5** as a clear oil in 83% yield. ^1H NMR: δ 1.34 (d, $J = 9.9$ Hz, 1H), 1.49 (dt, $J = 9.9$ Hz, 1.5 Hz, 1H), 2.68 (s, 2H), 3.08 (s, 3H), 3.26 (m, 2H), 3.56-3.72 (m, 50H), 3.73 (m, 2H), 4.38 (m, 2H) 6.28 (t, $J = 1.8$ Hz, 2H). ^{13}C NMR: δ 178.19, 138.01, 70.74, 70.03, 69.49, 69.20, 67.06, 47.99, 45.45, 42.90, 37.92.

N-(ethylmesyl)-cis-5-norbornene-exo-2,3-dicarboximide (6). A round bottom flask under argon was charged with alcohol **2** (100 mg, 1 equiv) and CH_2Cl_2 (1 mL). The solution was cooled to 0°C , then NEt_3 (150 μL , 2.2 equiv) was added via syringe. Lastly, MsCl (60 μL , 1.6 equiv) was added dropwise via syringe. The reaction mixture immediately turned dark yellow. After 2 h the reaction was quenched by addition of H_2O (2 mL) to the reaction mixture. The mixture was transferred to a separatory funnel, and the organic layer was removed. The organic layer was then washed with 0.01 N HCl (10 mL) and brine (10 mL) and dried over MgSO_4 . The yellow solid was purified on a plug of silica, eluting with 5% MeOH in CH_2Cl_2 to yield a white powder (94 mg) in 68% yield. ^1H NMR: δ 1.30 (d, $J = 9.9$, 1H), 1.63 – 1.48 (m, 2H), 2.77 (t, $J = 7.4$, 2H), 3.03 (s, 3H), 3.29 (dd, $J = 7.9$, 6.1, 2H), 3.92 – 3.78 (t, 2H), 4.48 – 4.35 (t, 2H), 6.31 (t, $J = 1.8$, 2H).

N-(ethoxy-ethyl-2-(mesyl))-cis-5-norbornene-exo-2,3-dicarboximide (7). N-(ethoxy-2-ethoxy)-cis-5-norbornene-exo-2,3-dicarboximide was first prepared by reaction of anhydride **1** (96 mg, 1 equiv) with $\text{H}_2\text{N}(\text{CH}_2)_2\text{O}(\text{CH}_2)_2\text{OH}$ (70 μL , 1.2 equiv) and NEt_3 (10 μL , 0.1 equiv) in 1 mL toluene. The reaction mixture was heated at reflux with a Dean-Stark trap for 2 h. The solvent was removed by rotary evaporation, and the residue was taken up in CH_2Cl_2 . This solution was washed with 0.1 N HCl and brine then dried over MgSO_4 . A clear oil was recovered (114 mg) and used without further purification in the next step. To this oil in 1 mL dry CH_2Cl_2 was added NEt_3 (120 μL , 2.0 equiv). After cooling to 0°C , MsCl (50 μL , 1.5 equiv) was added dropwise. After 12 h, the reaction was quenched by adding H_2O (2 mL). The mixture was transferred to a separatory funnel, and the organic layer was removed. The organic layer was then washed with 0.1 N HCl (10 mL) and brine (10 mL) and dried over MgSO_4 . The crude yellow oil was purified by silica gel chromatography (5% MeOH in CH_2Cl_2 , I_2 vis) to yield a clear oil (119 mg) in 83% yield. ^1H NMR: δ 1.30 (d, $J = 9.9$, 1H), 1.63 – 1.48 (m, 2H), 2.71 (d, $J = 1.1$, 2H), 3.04 (s, 3H), 3.30 – 3.22 (m, 2H), 3.79 – 3.62 (m, 6H), 4.36 – 4.24 (m, 2H), 6.30 (t, $J = 1.7$, 2H). ^{13}C NMR: δ 178.29, 138.02, 69.18, 68.45, 67.39, 48.06, 45.50, 42.90, 37.89, 37.76.

N-(ethoxy-ethyl-2-(mesyl)acetate)-cis-5-norbornene-exo-2,3-dicarboximide (8). Mesyl-glycolic acid was first prepared from a modified literature procedure.³² Briefly, silver mesylate (520 mg, 1.1 equiv) was added to a 2-necked round-bottom flask under argon flow followed by dry CH_3CN (2 mL). Iodoacetic acid (437 mg, 1 equiv) was massed out into a septum-cap vial, then the vial was evacuated and backfilled with argon,

and CH₃CN was added. This solution was transferred via cannula into the reaction flask, and the flask was covered with aluminum foil. After 20 h, the yellow AgI precipitate was removed by filtering the reaction mixture through Celite. The filtrate was rotovapped to yield a clear oil. The product was extracted from the oil with Et₂O. Concentration of the Et₂O solution yielded a white powder, which was recrystallized from CHCl₃/actone/pet ether (1:1:5) to yield white crystals (105 mg) in 29% yield. ¹H NMR (CD₃COCD₃): δ 3.22 (s, 3H), 4.85 (s, 2H). The pure mesyl-glycolic acid (95 mg, 1 equiv) was then added to a 2-necked round-bottom flask under argon with CH₂Cl₂ (1 mL). EDC (185 mg, 1.9 equiv) and DPTS (15 mg, 0.1 equiv) were added to the reaction mixture, and the reaction mixture became cloudy yellow over several minutes. N-(ethoxy-2-ethoxy)-*cis*-5-norbornene-*exo*-2,3-dicarboximide, prepared as described previously, was added to the reaction mixture in 1 mL CH₂Cl₂. The reaction mixture became clear within 1 min. After 3.5 h, the reaction was quenched by addition of H₂O (3 mL). The CH₂Cl₂ layer was separated off, washed with H₂O and brine, and dried over MgSO₄ to yield a pale yellow oil. The product was purified by column chromatography to yield a clear oil (24 mg) in 12% yield. ¹H NMR: δ 1.31 (d, *J* = 9.8, 1H), 1.48 (d, *J* = 9.8, 1H), 2.69 (s, 2H), 3.34 – 3.16 (m, 5H), 3.78 – 3.59 (m, 6H), 4.38 – 4.23 (m, 2H), 4.80 (s, 2H), 6.30 (t, *J* = 1.7, 2H). ¹³C NMR: δ 178.19, 166.99, 137.97, 68.00, 67.14, 64.89, 47.99, 45.43, 42.82, 39.29, 37.65.

N-(ethoxy-ethyl-2-(nosyl))-*cis*-5-norbornene-*exo*-2,3-dicarboximide (9). N-(ethoxy-2-ethoxy)-*cis*-5-norbornene-*exo*-2,3-dicarboximide (136 mg, 1 equiv), prepared as described previously, was added to a round-bottom flask containing nosyl chloride

(165 mg, 1.4 equiv). CH_2Cl_2 (1 mL) was added, and the flask was cooled to 0 °C. NEt_3 (110 μL , 1.5 equiv) was then added dropwise. After 15 h, the reaction was quenched by adding H_2O (3 mL). The mixture was transferred to a separatory funnel, and the organic layer was removed. The organic layer was then washed with 0.1 N HCl (10 mL) and brine (10 mL) and dried over MgSO_4 . The crude orange oil was purified by silica gel chromatography (5% MeOH in CH_2Cl_2 , I_2 vis) to yield an orange oil (48 mg) in 20% yield. ^1H NMR: δ 1.29 (d, $J = 9.9$, 1H), 1.55 – 1.41 (m, 1H), 2.68 (d, $J = 1.2$, 2H), 3.31 – 3.19 (m, 2H), 3.73 – 3.54 (m, 6H), 4.27 – 4.15 (m, 2H), 6.28 (t, $J = 1.7$, 2H), 8.19 – 8.06 (m, 2H), 8.50 – 8.37 (m, 2H). ^{13}C NMR: δ 178.23, 138.00, 128.51, 124.71, 70.41, 67.90, 67.30, 48.02, 45.47, 42.88, 37.73.

Cold Fluorination Procedure. In an N_2 -filled glovebox, KF (11 mg, 3.0 equiv), K_2CO_3 (30 mg, 3.5 equiv), and kryptofix 222 (45 mg, 2.0 equiv) were massed into a 2-necked, round-bottom flask. The flask was capped with a septum and a greased stopper. In a separate vial, the substrate to be fluorinated (1 equiv) was dissolved in 0.75 mL CH_3CN . The vial and the flask were brought out of the box, and the CH_3CN solution was transferred via cannula to the reaction flask. After stirring for 20 min at room temp, the reaction was quenched by addition of a small amount of H_2O . The reaction mixture was concentrated, and the product distribution was evaluated by ^1H NMR spectroscopy.

Polymerization Procedure. In a typical polymerization, a vial was charged with hydrophobic norbornene **3** (2.9 mg) and a stirbar under argon flow. THF (0.2 mL) was added to the vial. The desired amount of catalyst **10** as a stock solution in THF (2.5

mg/mL) was then injected into the vial. The reaction was allowed to proceed at room temperature under argon flow for 1-2 min, then hydrophilic norbornene **5** (21.2 mg) was added as a solution in THF (0.2 mL). All reactions were quenched by addition of ethyl vinyl ether (0.2 mL) that had been purified by passage through a short column of silica gel. The reaction mixture was allowed to stir for an additional 15 min before precipitation into 20 mL Et₂O/hexanes (1:1). The products were recovered in 87-99% yield by decanting off the supernatant and scraping the gooey solids off of the sides of the beaker. ¹H NMR δ 1.30-1.70 (br s), 1.95 (s), 1.85-2.55 (br s), 2.90-3.05 (br s), 3.07 (s), 3.63 (br s), 3.75 (m), 4.36 (m), 5.38-5.80 (br m), 6.32-6.44 (br d), 7.30-7.55 (br d), 7.58-7.70 (m).

Micelle Formation Procedure. Block copolymer (10 mg) was dissolved in filtered (0.02 μm) THF (5 mL). Once homogeneous, filtered (0.02 μm) DI water (5 mL) was added dropwise over 10 min. The micelle solution was then transferred to dialysis tubing (8000 MWCO) and dialyzed against water for 24-48 h while protected from light.

Micelle Crosslinking Procedure. A photochemical reactor was charged with cloudy, aqueous micelle solution (8 mL). The solution was degassed by bubbling with argon for 20 min. A UV lamp (450 W medium pressure) was inserted into the photochemical reactor, and the solution was irradiated for 3 min. Samples were lyophilized while protected from light before use in radiofluorination reactions.

Radiofluorination Procedure. A 5 mL reaction vessel in a fume hood with a leaded glass sash was charged with hydrated $K^{18}F$ (361 mCi). K_2CO_3 (1 mg) and kryptofix 222 (10 mg) in 1 mL CH_3CN/H_2O (94:4) were added to the vessel. The solvent was boiled off by submersing the vessel in an oil bath at 120 °C while bubbling N_2 through the reaction mixture. BHT in dry CH_3CN (1 mL) was then added to the vessel, followed by solvent removal in the same way. Two more additions and evaporations of dry CH_3CN were performed to ensure complete removal of H_2O . A lyophilized nanoparticle sample (5.7 mg) was dissolved in 3 mL dry CH_3CN and added to the vessel. The vessel was sealed and heated at 120 °C for 60 min. In order to displace the excess mesylates, $K^{19}F$ (1.5 mg) and kryptofix 222 (6.5 mg) in 0.5 mL CH_3CN were added to the vessel. The vessel was sealed and heated for an additional 30 min at 80 °C. At this point the reaction mixture was diluted with water and passed through a column containing Dowex strongly acidic macroreticular ion exchange resin, followed by a short plug of alumina. RadioTLC was used to analyze the radiochemical purity of the product.

References

- (1) (a) Brigger, I.; Dubernet, C.; Couvreur, P. *Adv. Drug Delivery. Rev.* **2002**, *54*, 631–651. (b) Sinha, R.; Kim, G. J.; Nie, S. M.; Shin, D. M. *Mol. Cancer Ther.* **2006**, *5*, 1909–1917. (c) Moghimi, S. M.; Hunter, A. C.; Murray, J. C. *FASEB J.* **2005**, *19*, 311–330. (d) Ferrari, M. *Nat. Rev. Cancer* **2005**, *5*, 161–171. (e) Heath, J. R.; Davis, M. E. *Annu. Rev. Med.* **2008**, *59*, 251–265.
- (2) Maeda, H.; Wu, J.; Sawa, T.; Matsumura, Y.; Hori, K. *J. Controlled Release* **2000**, *65*, 271–284.
- (3) (a) Lee, S. M.; Chen, H.; Dettmer, C. M.; O'Halloran, T. V.; Nguyen, S. T. *J. Am. Chem. Soc.* **2007**, *129*, 15096–15097. (b) Torchilin, V. P. *Nat. Rev. Drug Discovery* **2005**, *4*, 145–160.
- (4) (a) Michalet, X.; Pinaud, F. F.; Bentolila, L. A.; Tsay, J. M.; Doose, S.; Li, J. J.; Sundaresan, G.; Wu, A. M.; Gambhir, S. S.; Weiss, S. *Science* **2005**, *307*, 538–544. (b) Smith, A. M.; Ruan, G.; Rhyner, M. N.; Nie, S. M. *Ann. Biomed. Eng.* **2006**, *34*, 3–14. (c) Bagalkot, V.; Zhang, L.; Levy-Nissenbaum, E.; Jon, S.; Kantoff, P. W.; Langer, R.; Farokhzad, O. C. *Nano Lett.* **2007**, *7*, 3065–3070.
- (5) (a) Ihre, H. R.; De Jesus, O. L. P.; Szoka, F. C.; Frechet, J. M. J. *Bioconjugate Chem.* **2002**, *13*, 443–452. (b) Lee, C. C.; MacKay, J. A.; Frechet, J. M. J.; Szoka, F. C. *Nat. Biotechnol.* **2005**, *23*, 1517–1526. (c) Malik, N.; Evagorou, E. G.; Duncan, R. *Anti-Cancer Drug.* **1999**, *10*, 767–776. (d) Jain, N. K.; Asthana, A. *Expert Opin. Drug Deliv.* **2007**, *4*, 495–512.
- (6) (a) Torchilin, V. P. *J. Controlled Release* **2001**, *73*, 137–172. (b) Sun, X. K.; Rossin, R.; Turner, J. L.; Becker, M. L.; Joralemon, M. J.; Welch, M. J.; Wooley, K. L. *Biomacromolecules* **2005**, *6*, 2541–2554. (c) Licciardi, M.; Giammona, G.; Du, J. Z.; Armes, S. P.; Tang, Y. Q.; Lewis, A. L. *Polymer* **2006**, *47*, 2946–2955.
- (7) Heidel, J.; Mishra, S.; Davis, M. E. *Adv. Biochem. Eng. Biot.* **2005**, *99*, 7–39.
- (8) Matsumura, Y.; Maeda, H. *Cancer Res.* **1986**, *46*, 6387–6392.
- (9) (a) Maeda, H.; Seymour, L. W.; Miyamoto, Y. *Bioconjugate Chem.* **1992**, *3*, 351–362. (b) Baban, D. F.; Seymour, L. W. *Adv. Drug Delivery Rev.* **1998**, *34*, 109–119. (c) Reddy, L. H. *J. Pharm. Pharmacol.* **2005**, *57*, 1231–1242.
- (10) Hobbs, S. K.; Monsky, W. L.; Yuan, F.; Roberts, W. G.; Griffith, L.; Torchilin, V. P.; Jain, R. K. *Proc. Natl. Acad. Sci. U.S.A.* **1998**, *95*, 4607–4612.
- (11) (a) Morawski, A. M.; Lanza, G. A.; Wickline, S. A. *Curr. Opin. Biotechnol.* **2005**, *16*, 89–92. (b) Seo, W. S.; Lee, J. H.; Sun, X. M.; Suzuki, Y.; Mann, D.; Liu, Z.; Terashima, M.; Yang, P. C.; McConnell, M. V.; Nishimura, D. G.; Dai, H. J. *Nat.*

- Mater.* **2006**, *5*, 971–976. (c) Mulder, W. J. M.; Koole, R.; Brandwijk, R. J.; Storm, G.; Chin, P. T. K.; Strijkers, G. J.; Donega, C. D.; Nicolay, K.; Griffioen, A. W. *Nano Lett.* **2006**, *6*, 1–6. (d) Kobayashi, H.; Brechbiel, M. W. *Adv. Drug Delivery Rev.* **2005**, *57*, 2271–2286.
- (12) Yang, Z.; Zheng, S. Y.; Harrison, W. J.; Harder, J.; Wen, X. X.; Gelovani, J. G.; Qiao, A.; Li, C. *Biomacromolecules* **2007**, *8*, 3422–3428.
- (13) (a) Pressly, E. D.; Rossin, R.; Hagooley, A.; Fukukawa, K. I.; Messmore, B. W.; Welch, M. J.; Wooley, K. L.; Lamm, M. S.; Hule, R. A.; Pochan, D. J.; Hawker, C. J. *Biomacromolecules* **2007**, *8*, 3126–3134. (b) Bartlett, D. W.; Su, H.; Hildebrandt, I. J.; Weber, W. A.; Davis, M. E. *Proc. Nat. Acad. Sci. U.S.A.* **2007**, *104*, 15549–15554. (c) Fukukawa, K.; Rossin, R.; Hagooley, A.; Pressly, E. D.; Hunt, J. N.; Messmore, B. W.; Wooley, K. L.; Welch, M. J.; Hawker, C. J. *Biomacromolecules* **2008**, *9*, 1329–1339. (d) Schipper, M. L.; Cheng, Z.; Lee, S. W.; Bentolila, L. A.; Iyer, G.; Rao, J.; Chen, X.; Wu, A. M.; Weiss, S.; Gambhir, S. S. *J. Nucl. Med.* **2007**, *48*, 1511–1518.
- (14) Since the publication of this work, two reports concerning the synthesis of fluorine-18-containing nanoparticles have been published: (a) Devaraj, N. K.; Keliher, E. J.; Thurber, G. M.; Nahrendorf, M.; Weissleder, R. *Bioconjugate Chem.* **2009**, *20*, 397–401. (b) Herth, M. M.; Barz, M.; Moderegger, D.; Allmeroth, M.; Jahn, M.; Thews, O.; Zentel, R.; Rösch, F. *Biomacromolecules* **2009**, *10*, 1697–1703.
- (15) (a) Nabi, H. A.; Zubeldia, J. M. *J. Nucl. Med. Technol.* **2002**, *30*, 3–9. (b) Rohren, E. M.; Turkington, T. G.; Coleman, R. E. *Radiology* **2004**, *231*, 305–332.
- (16) Jagoda, E. M.; Vaquero, J. J.; Seidel, J.; Green, M. V.; Eckelman, W. C. *Nucl. Med. Biol.* **2004**, *31*, 771–779.
- (17) (a) Torchilin, V. P. *J. Controlled Release* **2001**, *73*, 137–172. (b) Torchilin, V. P. *Colloids Surf., B* **1999**, *16*, 305–319.
- (18) Adams, M. L.; Lavasanifar, A.; Kwon, G. S. *J. Pharm. Sci.* **2003**, *92*, 1343–1355.
- (19) Stubenrauch, K.; Moitzi, C.; Fritz, G.; Glatter, O.; Trimmel, G.; Stelzer, F. *Macromolecules* **2006**, *39*, 5865–5874.
- (20) Bielawski, C. W.; Grubbs, R. H. *Prog. Polym. Sci.* **2007**, *32*, 1–29.
- (21) (a) Maynard, H. D.; Okada, S. Y.; Grubbs, R. H. *Macromolecules* **2000**, *33*, 6239–6248. (b) Rawat, M.; Gama, C. I.; Matson, J. B.; Hsieh-Wilson, L. C. *J. Am. Chem. Soc.* **2008**, *130*, 2959–2961. (c) Ilker, M. F.; Nüsslein, K.; Tew, G. N.; Coughlin, E. B. *J. Am. Chem. Soc.*, **2004**, *126*, 15870–15875.

- (22) Choi, T. L.; Grubbs, R. H. *Angew. Chem. Int. Ed.* **2003**, *42*, 1743–1746.
- (23) (a) Liu, G. J.; Hu, N. X.; Xu, X. Q.; Yao, H. *Macromolecules* **1994**, *27*, 3892–3895. (b) Guo, A.; Liu, G. J.; Tao, J. *Macromolecules* **1996**, *29*, 2487–2493. (c) Henselwood, F.; Liu, G. J. *Macromolecules* **1997**, *30*, 488–493.
- (24) Gref, R.; Minamitake, Y.; Peracchia, M. T.; Trubetskoy, V.; Torchilin, V. P.; Langer, R. *Science* **1994**, *263*, 1600–1603.
- (25) Cai, L.; Lu, S.; Pike, V. W. *Eur. J. Org. Chem.* **2008**, *17*, 2853–2873.
- (26) Noyce, D. S.; Virgilio, J. A. *J. Org. Chem.* **1972**, *37*, 2643–2647.
- (27) (a) Camm, K. D.; Castro, N. M.; Liu, Y. W.; Czechura, P.; Snelgrove, J. L.; Fogg, D. E. *J. Am. Chem. Soc.* **2007**, *129*, 4168–4169. (b) Slugovc, C.; Demel, S.; Stelzer, F. *Chem. Commun.* **2002**, *21*, 2572–2573.
- (28) Love, J. A.; Morgan, J. P.; Trnka, T. M.; Grubbs, R. H. *Angew. Chem., Int. Ed. Engl.* **2002**, *41*, 4035–4037.
- (29) Bielawski, C. W.; Benitez, D.; Morita, T.; Grubbs, R. H. *Macromolecules* **2001**, *34*, 8610–8618.
- (30) Pangborn, A. B.; Giardello, M. A.; Grubbs, R. H.; Rosen, R. K.; Timmers, F. J. *Organometallics* **1996**, *15*, 1518–1520.
- (31) Menger, F. M.; Zhang, H. *J. Am. Chem. Soc.* **2006**, *128*, 1414–1415.
- (32) Chen, W. S.; Bohlken, D. P.; Plapp, B. V. *J. Med. Chem.* **1982**, *24*, 190–193.

Chapter 3

A Living Ring-Opening Metathesis Polymerization Route to Janus Nanoparticles

Abstract

Asymmetric (Janus) nanoparticles with two distinct hemispheres were prepared by comicellization of AB and BC amphiphilic block copolymers followed by photocrosslinking. The block copolymers were synthesized by living ring-opening metathesis polymerization (ROMP) using the fast-initiating ruthenium metathesis catalyst $(\text{H}_2\text{IMes})(\text{pyr})_2(\text{Cl})_2\text{RuCHPh}$. Incorporated into the common, hydrophobic, photocrosslinkable, poly(cinnamoyl ethyl norbornene imide) block were complementary hydrogen-bonding monomers to favor Janus micelle formation over mixed micelle formation. One hydrophilic block was comprised of poly(carboxymethyl norbornene imide) (P(CMNI)), while the other was comprised of poly(triethylene glycol norbornene imide). To confirm the asymmetrical character of the Janus nanoparticles, 1.5 nm gold nanoparticles were covalently attached to the P(CMNI) hemisphere of the Janus nanoparticles. The gold-stained Janus nanoparticles were then compared to gold-stained, symmetrical nanoparticles using scanning electron microscopy (SEM).

Introduction

Janus nanoparticles have attracted a significant amount of attention in the past decade due to their unique features and synthetic challenge.^{1,2} Named for the two-faced Roman god Janus, ruler of doorways and gates, Janus particles have two chemically distinct hemispheres. The multiple faces of a nanoparticle make Janus nanoparticles intriguing structures due to their potential as drug carriers,³ emulsion stabilizers,⁴ and in electronic⁵ and propulsion applications.⁶ Additionally, the synthesis of Janus particles

represents a significant chemical challenge, as most methods used to make nanoparticles rely on self-assembly techniques that yield almost exclusively symmetrical particles.

Several protocols for the synthesis of Janus nanoparticles have been developed, including directed self-assembly,^{2a-c,2f} controlled phase separation,^{2g,7} microfluidics,^{2d,3,8} and selective surface modification using various protection strategies.⁹ The directed self-assembly method of Janus nanoparticle formation was particularly intriguing to us due to our recent interest in the synthesis of nanoparticles from block copolymers.¹⁰ Theoretical studies on the self-assembly of mixtures of block copolymers into nanoparticles have been done by Potemkin.^{2c} In this work, Potemkin notes that a mixture of AB and BC block copolymers will not yield Janus micelles unless some additional interactions between the blocks are provided. Liu recently reported that sufficient additional interactions between the B blocks were achieved when AB and BC block copolymers were forced to comicellize by adding complementary hydrogen bonding groups to the common B blocks of each block copolymer.^{2c} Photocrosslinking of the B blocks was used to lock the structure into a Janus nanoparticle. Inspired by Liu's report, we hoped to extend this method to block copolymers prepared by living ROMP.

Results and Discussion

ROMP provides an ideal method for accessing complex macromolecular structures due to the air, moisture, and functional group tolerance of ruthenium metathesis catalysts.¹¹ Over the past several years, ROMP polymers containing peptides,¹² sugars,¹³ charged groups,¹⁴ and grafted polymer chains¹⁵ have been synthesized. Hydrogen-bonding groups have also been incorporated into ROMP

polymers, indicating that some unprotected Lewis basic functional groups are also compatible with ruthenium metathesis catalysts.¹⁶ Ruthenium metathesis catalyst $(\text{H}_2\text{IMes})(\text{Cl})_2(\text{pyr})_2\text{RuCHPh}$ (**1**) has recently become popular for the synthesis of living ROMP polymers due to its fast initiation, long benchtop stability, and functional group tolerance (Figure 3.1).^{10,17} In this study, we used catalyst **1** with several novel monomers to construct Janus nanoparticles.

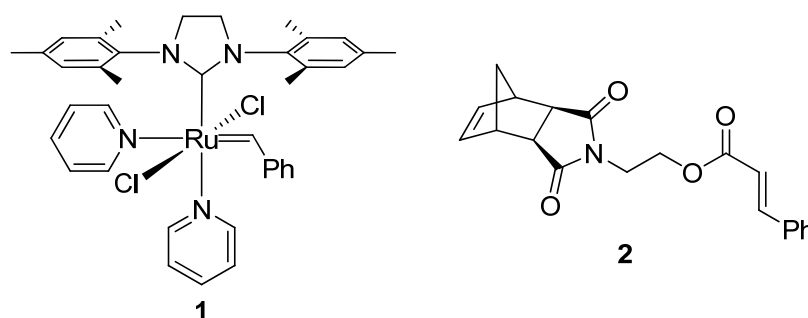
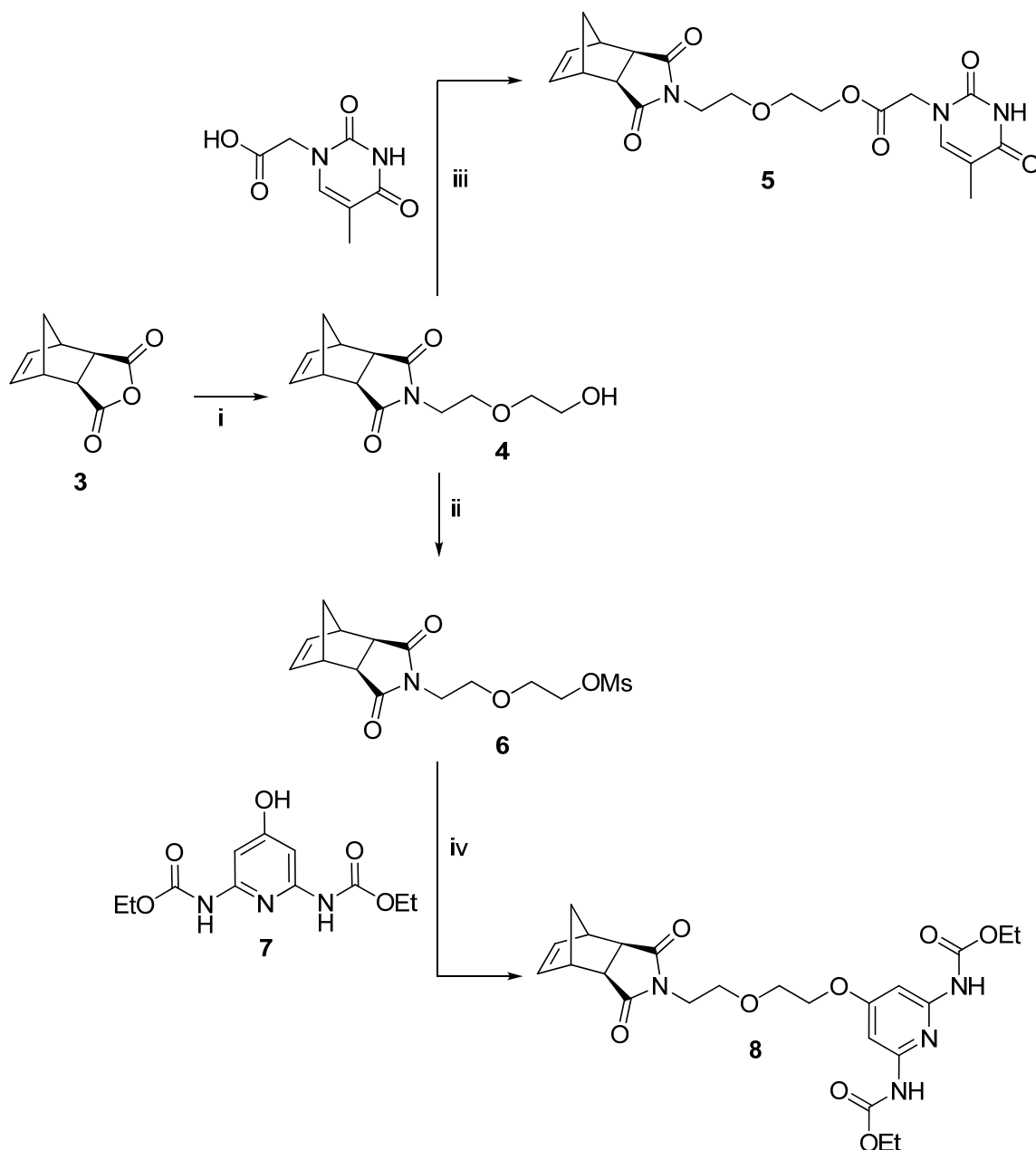


Figure 3.1. Ruthenium metathesis catalyst (**1**) and photocrosslinking monomer (**2**) used in this study.

Monomer Syntheses

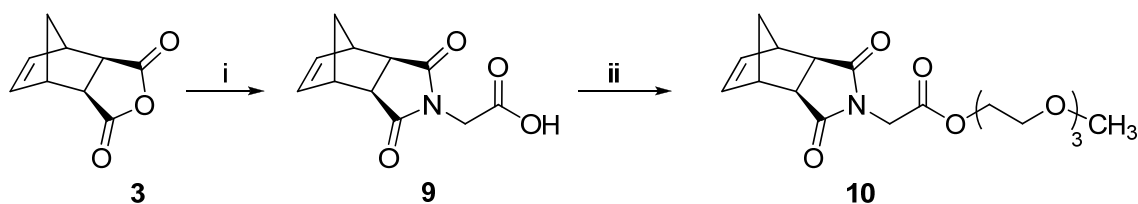
We set out to synthesize a pair of complementary hydrogen-bonding monomers that could be incorporated into block copolymers. Borrowing techniques from Rotello,¹⁸ we chose an acceptor-donor-acceptor (ADA) hydrogen-bonding pattern coupled with a donor-acceptor-donor (DAD) pattern. First, 2-(2-aminoethoxy)ethanol was added to norbornene anhydride **3**, removing water with a Dean-Stark trap, to afford norbornene alcohol **4** (Scheme 3.1). The ADA hydrogen-bonding pattern was added to the monomer by coupling thymine-1-acetic acid to alcohol **4** using *N*-(3-dimethylaminopropyl)-*N*'-

ethylcarbodiimide (EDC) to afford ADA monomer **5**. DAD monomer **8** was made by reacting DAD diaminopyridine complex **7**, which was prepared according to a literature procedure,¹⁸ with mesylated norbornene **6**. Monomers **5** and **8** were both found to undergo homopolymerization smoothly.



Scheme 3.1. Syntheses of complementary hydrogen-bonding monomers. Reaction conditions: i) 2-(2-aminoethoxy)ethanol, NEt_3 , toluene, DS-trap. ii) MsCl , NEt_3 , CH_2Cl_2 . iii) EDC, DPTS, CH_2Cl_2 . iv) K_2CO_3 , DMF.

Three additional norbornene monomers were prepared for the synthesis of the A, B and C blocks of the block copolymers. Carboxymethylene norbornene imide (CMNI) (**9**) was made by reacting norbornene anhydride **3** with glycine (Scheme 3.2). Triethylene glycol monomethyl ether was coupled to monomer **9** using EDC to yield triethyleneglycol norbornene imide (TEGNI) (**10**). Cinnamoyl ethyl norbornene imide (CENI) (**2**) was used as the hydrophobic, crosslinking monomer and was prepared as described previously.¹⁹

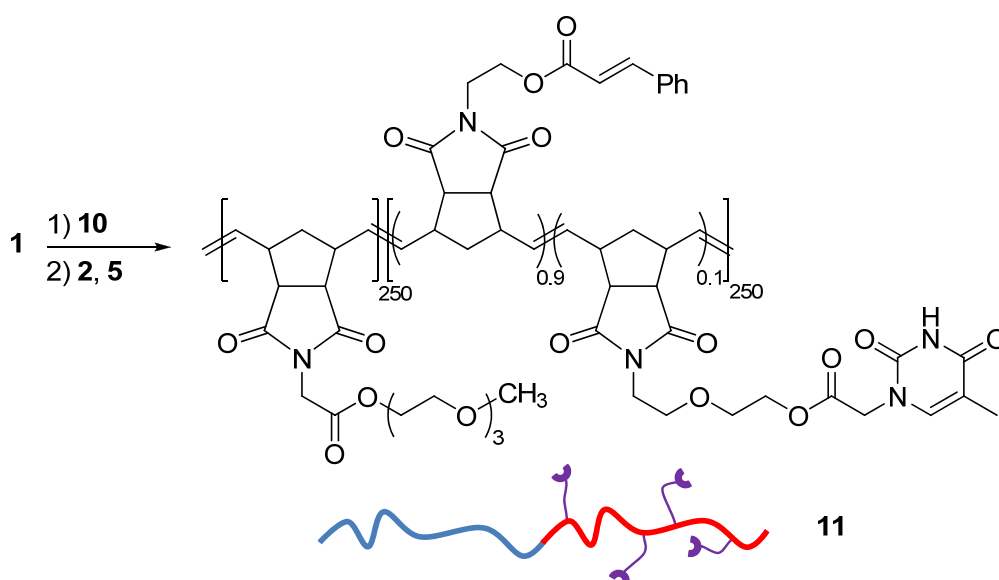


Scheme 3.2. Syntheses of acid-containing monomer (**9**) and PEGylated monomer (**10**). Reaction conditions: i) glycine, NEt₃, toluene, DS-trap. ii) triethylene glycol monomethyl ether, EDC, DPTS.

Polymer Syntheses

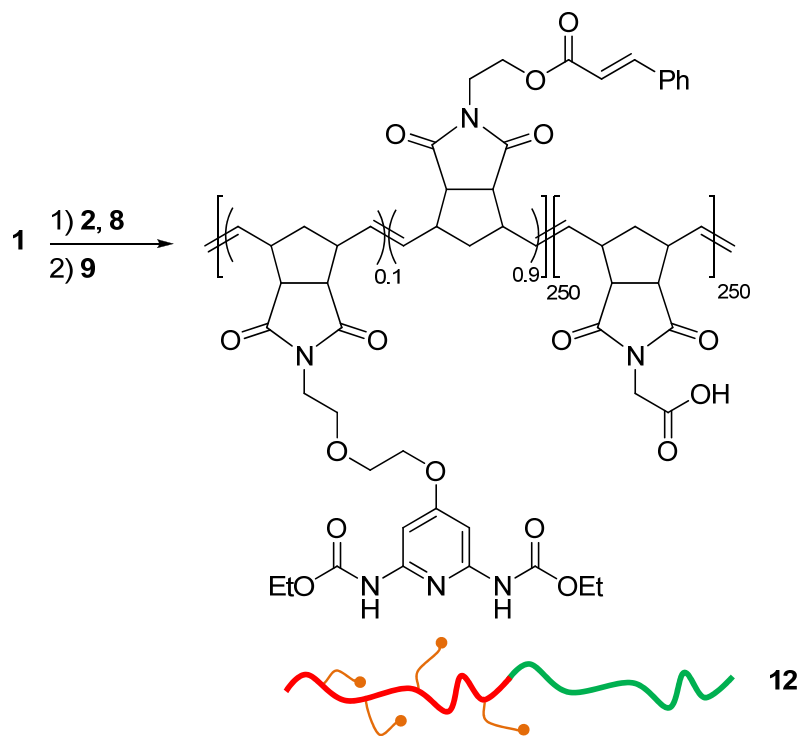
We hoped to exploit the tendency of most polymer mixtures to show phase separation to form Janus micelles by forcing AB and BC block copolymers to comicellize. It was expected that a mixture of AB and BC block copolymers with block A derived from monomer **9** and block B derived from monomer **10** would phase separate, with separation potentially depending on the pH of the solution. To establish that Janus nanoparticles were synthesized, we hoped to selectively react the poly(carboxylate) hemisphere with mono-amino gold nanoparticles for visualization by electron

microscopy. To this end, two different amphiphilic block copolymers with complementary hydrogen-bonding units were synthesized for assembly into Janus nanoparticles. The first polymer, P(TEGNI-*b*-(CENI-*ran*-ADA)) (**11**) was made according to Scheme 3.3. A block of P(TEGNI) was first grown by injecting a solution of catalyst **1** into a solution of monomer **10**. After complete consumption of monomer **10**, a solution of monomers **2** and **5** were added in a molar ratio of approximately 9:1. The polymer product was recovered by precipitation into Et₂O/hexanes (1:1).



Scheme 3.3 Synthesis of amphiphilic block copolymer (**11**) containing ADA H-bonding group. In the cartoon the blue line represents the hydrophilic P(TEGNI) segment, the red line represents the hydrophobic P(CENI) block, and the purple lines with the semicircles represent the ADA monomer.

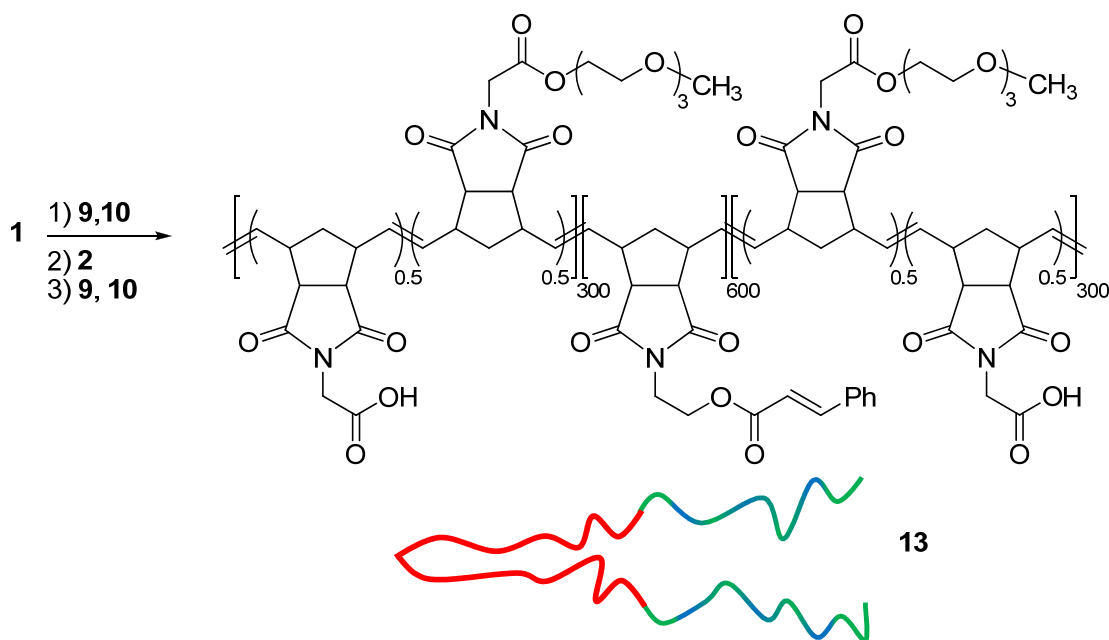
The second polymer, P((CENI-*ran*-DAD)-*b*-CMNI) (**12**), was made in a similar fashion (Scheme 3.4). First, catalyst **1** was injected into a solution of monomers **2** and **8**, also in a 9:1 molar ratio. After complete monomer consumption, a solution of monomer **9** was added. The polymer product was recovered by precipitation into Et₂O/hexanes (1:1).



Scheme 3.4. Synthesis of amphiphilic block copolymer (**12**) containing DAD hydrogen-bonding group. In the cartoon the green line represents the hydrophilic P(CMNI) segment, the red line represents the hydrophobic P(CENI) block, and the orange lines with the spheres represent the DAD monomer.

We also synthesized a polymer for assembly into traditional, symmetrical nanoparticles for comparison by electron microscopy to Janus nanoparticles. This polymer, P((CMNI-*ran*-TEGNI)-*b*-CENI-*b*-(CMNI-*ran*-TEGNI)) (**13**), was designed to have no hydrogen-bonding pairs and to have the hydrophilic units randomly distributed throughout the nanoparticle corona. This would allow for attachment of gold nanoparticles onto the entire surface of the organic nanoparticle, providing a completely contrasted organic nanoparticle for imaging using electron microscopy. Polymer **13** was synthesized by first injecting a solution of catalyst **1** into a solution of monomers **9** and **10** in a 1:1 molar ratio (Scheme 3.5). After complete monomer consumption, a solution of monomer **2** was added. Once monomer **2** had been completely consumed, another

solution of monomers **9** and **10** in the same ratio was added. The product was recovered by precipitation into Et₂O/hexanes (1:1). A simpler P(CENI-*b*-(CMNI-*ran*-TEGNI)) would be expected to be equally effective for assembling the control nanoparticles, but polymer **13** was used instead because it had already been prepared for a different study.

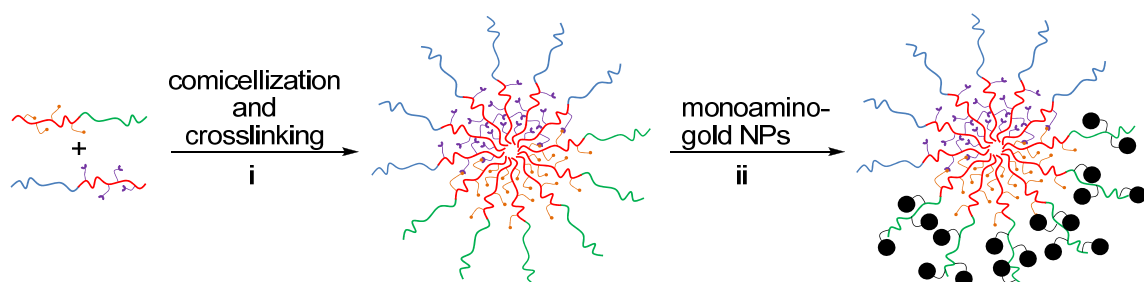


Scheme 3.5. Synthesis of control amphiphilic block copolymer (**13**). The red line represents the hydrophobic P(CMNI) block and the mixed blue and green line represents the random P(CMNI-*ran*-TEGNI) hydrophilic block.

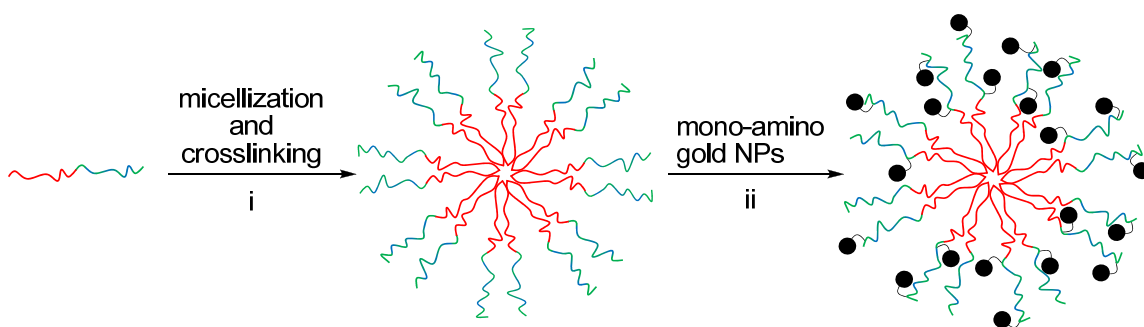
Nanoparticle assembly and staining

With the polymers in hand, we set out to assemble Janus nanoparticles along with control nanoparticles for comparison. The Janus nanoparticles were assembled first by comicellizing polymers **11** and **12** (Scheme 3.6) in a solution of THF and pentane. The complementary hydrogen-bonding units in the hydrophobic portion were expected to drive comicellization, favoring Janus particle formation over mixed micelle formation.

The THF/pentane micelle solution was photocrosslinked in a procedure described previously¹⁹ to afford stable nanoparticles. Removal of the pentane and dialysis of the micelle solution in THF against water afforded aqueous nanoparticles. Symmetrical, control nanoparticles were made in a similar fashion (Scheme 3.7). An atomic force microscopy (AFM) image of the control nanoparticles (Figure 3.2) shows particles of about 40 nm with relatively low polydispersity and limited tendency to aggregate. AFM images of the Janus particles were difficult to obtain due to aggregation.



Scheme 3.6. Assembly of Janus nanoparticles. Black spheres with lines represent 1.5 nm mono-amino gold nanoparticles. Reaction conditions: i) 1) dissolution in THF followed by slow addition of pentane; 2) $h\nu$ followed by dialysis against H_2O . ii) mono-amino gold nanoparticles, EDC, sulfated N-hydroxysuccinimide, aqueous phosphate buffer.



Scheme 3.7. Assembly of control nanoparticles. Black spheres with lines represent 1.5 nm mono-amino gold nanoparticles. Reaction conditions: i) 1) dissolution in THF followed by slow addition of H_2O and dialysis against H_2O ; 2) $h\nu$, H_2O . ii) gold nanoparticles, EDC, sulfated N-hydroxysuccinimide, H_2O .

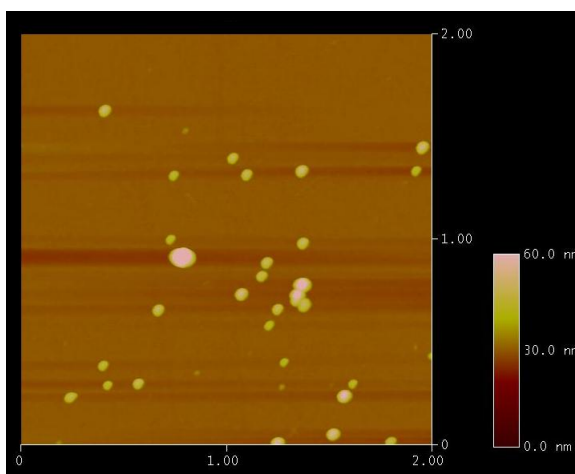


Figure 3.2 AFM image of control nanoparticles on silicon.

To confirm the Janus character of the nanoparticles, we devised a method to preferentially stain one hemisphere of the organic nanoparticles. Mono-amino gold nanoparticles (1.5 nm in diameter) were purchased and attached to the P(CMNI) portion of the organic nanoparticles using standard alcohol-amine coupling chemistry (Scheme 3.6). Excess reagents were removed by dialysis against water to afford a light brown solution. The gold nanoparticles were expected to stain only the P(CNMI) hemisphere of the Janus nanoparticles while staining the entire surface of the control organic nanoparticles

The stained nanoparticles were imaged by SEM to examine whether Janus nanoparticles had indeed been synthesized (Figure 3.3). Nanoparticle samples were drop-deposited onto silicon 111 surfaces that had been cleaned and treated with basic piranha solution. The nanoparticle samples tended to aggregate despite addition of various salts and testing at a range of pH values. As a result, only the occasional individual particle could be carefully examined. Figure 3.3A shows what appears to be a nanoparticle with one dark side, which we believe to be a Janus nanoparticle. Similar

particles could not be found in the control sample (Figure 3.3B). Further experiments need to be done to conclude whether Janus particles have definitely been synthesized, including transmission electron microscopy. Additionally, particles that do not tend to aggregate would be necessary to view a large population of Janus nanoparticles. This might be accomplished by avoiding PEG as one of the hydrophilic groups.

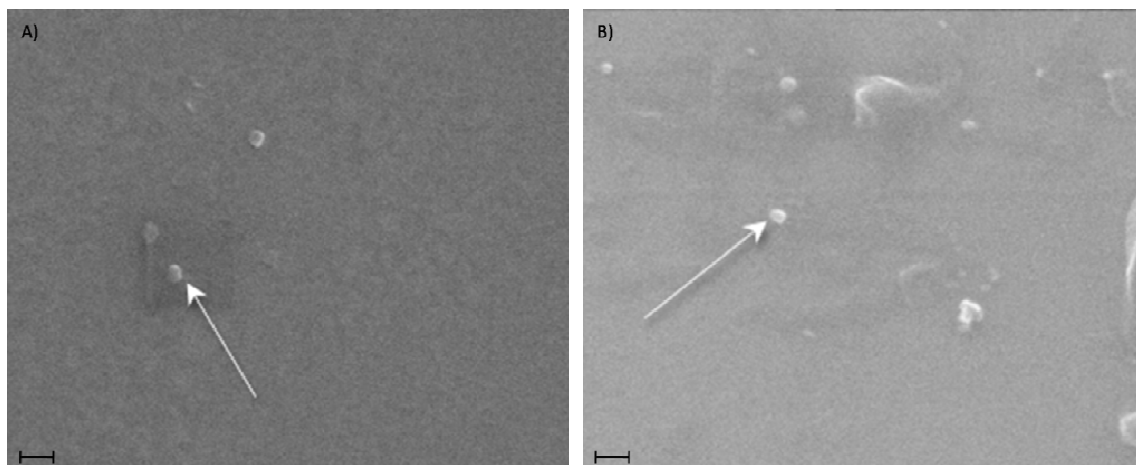


Figure 3.3. A) SEM image of Janus nanoparticle sample. B) SEM image of control nanoparticle sample. Scale bar equal to 100 nm. Arrows point to individual nanoparticles.

Conclusions

We have shown that living ROMP is an effective synthetic route to producing nanoparticles that may have asymmetrical or Janus character. Several new norbornene monomers were synthesized and polymerized using living ROMP to produce AB and BC block copolymers. Incorporation of complementary hydrogen-bonding groups into the B blocks of each polymer was used to favor comicellization of the two different polymers. The micelles were then photocrosslinked to avoid disturbing chain segregation in aqueous solution. Covalent attachment of small mono-amino gold nanoparticles to the

Janus nanoparticles was accomplished using standard EDC coupling chemistry. Though not conclusive, SEM shows what appears to be the desired Janus character of the nanoparticles. Future studies on the micelles using TEM may help to definitively establish the hemispherical symmetry of the nanoparticles.

Acknowledgement

The author thanks Materia for catalyst as well as Andrew Freddo for carrying out many of the experiments detailed in this chapter. Udi Vermesh, Dr. Ke Xu, and Dr. Bradley Olsen are acknowledged for help with electron microscopy. Dr. Ron Walker is acknowledged for a generous donation of complex 7.

Experimental Section

General Information

NMR spectra were measured in CDCl_3 or $\text{DMSO-}d_6$ on Varian Mercury 300 MHz spectrometers unless otherwise noted. ^1H and ^{13}C NMR chemical shifts are reported in ppm relative to CDCl_3 . Flash column chromatography of organic compounds was performed using silica gel 60 (230-400 mesh). High-resolution mass spectra (EI and FAB) were provided by the California Institute of Technology Mass Spectrometry Facility. AFM images were taken using a Nanoscope IV Scanning Probe Microscope Controller (Digital Instruments, Veeco Metrology Group) in tapping mode in air at room temperature using Veeco model TESP tips (spring constant = 20-80 N/m, resonance frequency = 297-335 kHz). The samples were prepared by drop coating onto silicon 111 surfaces that had been prepared by immersion for 5 min at 55 °C in a solution of

H₂O/NH₄OH (30% in H₂O)/H₂O₂ (50% in H₂O) (5:1:1) followed by washing with DI water and drying with compressed air. Samples were drop coated onto the substrates, and excess solvent was removed by wicking with filter paper. Photoreactions were done using a 450 W medium pressure mercury arc lamp (Ace Glass). Reactions were done using a water cooled quartz jacket surrounding the lamp immersed in the reaction mixture. Gel permeation chromatography (GPC) was carried out in THF on two I-series MBLMW ViscoGel columns (Viscotek) connected in series with a DAWN EOS multiangle laser light scattering (MALLS) detector and an Optilab DSP differential refractometer (both from Wyatt Technology). No calibration standards were used, and dn/dc values were obtained for each injection by assuming 100% mass elution from the columns.

Materials

CH₂Cl₂ was purified by passage through solvent purification columns.²⁰ Anhydrous DMF was purchased from Acros Chemical Company and used as received. (H₂IMes)(pyr)₂(Cl)₂RuCHPh (**1**) was prepared according to a literature procedure from (H₂IMes)(PCy₃)(Cl)₂RuCHPh (obtained from Materia).²¹ Monomer **2** was prepared as described previously.¹⁹ Diaminopyridine complex **7** was prepared according to a literature procedure.¹⁸ Dimethylaminopyridinium *p*-toluene sulfonate (DPTS) was prepared according to a literature procedure.²² Mono-amino gold nanoparticles were purchased from Nanoprobe. All other materials were purchased from Aldrich Chemical Company and used as received.

N-(hydroxy diethylene glycol)-cis-5-norbornene-exo-2,3-dicarboximide (4).

A round-bottom flask was charged with anhydride **3** (393 mg, 1 equiv), 2-(2-aminoethoxy)ethanol (273 mg, 1.08 equiv), NEt₃ (35 μ L, 0.1 equiv) and toluene (6 mL). A Dean-Stark trap was attached to the flask, and the reaction mixture was heated at 135 °C for 2 h. The reaction mixture was concentrated *in vacuo* and the residue was taken up in CH₂Cl₂, washed with 0.1 N HCl and brine, and dried over MgSO₄. Concentration *in vacuo* yielded **4** as a clear oil in 84% yield (505 mg) that was of sufficient purity for further steps. ¹H NMR: δ 1.32 (dt, $J = 9.9$ Hz, 1.5 Hz, 1H), 1.49 (dt, $J = 9.9$ Hz, 1.5 Hz, 1H), 2.49 (s, 1H), 2.68 (d, $J = 1.5$ Hz, 2H), 3.25 (t, $J = 1.8$ Hz, 2H), 3.52-3.71(m, 8H), 6.27 (t, $J = 1.8$ Hz, 2H). ¹³C NMR: δ 178.54, 137.98, 72.31, 67.59, 61.87, 48.00, 45.46, 42.80, 38.27. HRMS: calculated: 252.1236; found: 252.1245.

N-(thymine ester diethylene glycol)-cis-5-norbornene-exo-2,3-dicarboximide

(5). A round-bottom flask under argon was charged with thymine-1-acetic acid (90 mg, 1.2 equiv). CH₂Cl₂ (2 mL) was added, followed by EDC (124 mg, 1.6 equiv) and DPTS (12 mg, 0.1 equiv). Alcohol **4** was then added as a solution in CH₂Cl₂ (2 mL). The cloudy reaction mixture became clear over several hours of stirring at room temperature. After 20 h the reaction mixture was washed with H₂O and brine and dried over Na₂SO₄. The white, powdery residue was taken up in CH₂Cl₂ and precipitated into Et₂O. The solids were removed, and the filtrate was concentrated to afford **5** as a white powder in 51% yield (83 mg). ¹H NMR: δ 1.23 (d, $J = 9.9$ Hz, 1H), 1.41 (d, $J = 9.9$ Hz, 1H), 1.85 (s, 3H), 2.61 (d, $J = 1.2$ Hz, 2H), 3.17 (t, $J = 1.8$ Hz, 2H), 3.54-3.61 (m, 6H), 4.20 (m, 2H), 4.42 (s, 2H), 6.19 (t, $J = 1.8$ Hz, 2H), 7.07 (d, $J = 1.2$ Hz, 1H), 9.31 (s, 1H). ¹³C NMR: δ

178.32, 167.83, 164.45, 151.16, 140.72, 137.95, 111.20, 68.14, 67.02, 64.66, 48.57, 48.00, 45.41, 42.88, 37.88, 12.48. HRMS: calculated: 418.1614; found: 418.1613.

N-(mesyl diethylene glycol)-cis-5-norbornene-exo-2,3-dicarboximide (6).

Alcohol **4** (110 mg, 1 equiv) and NEt_3 (120 μL , 2.0 equiv) were dissolved in CH_2Cl_2 (1 mL) in a round-bottom flask, and the solution was cooled to 0 °C. Methane sulfonyl chloride (50 μL , 1.5 equiv) was added dropwise, and the reaction mixture was allowed to warm to room temperature. After 12 h the reaction was quenched with H_2O (2 mL). The organic layer was removed, washed with brine, and dried over MgSO_4 . The product was purified by silica gel chromatography (5% MeOH in CH_2Cl_2) to yield **6** as a clear oil in 83% yield (119 mg). ^1H NMR: δ 1.32 (dt, $J = 9.9$ Hz, 1.5 Hz, 1 H), 1.53 (dt, $J = 9.9$ Hz, 1.5 Hz, 1H), 2.69 (d, $J = 1.2$ Hz, 2H), 3.04 (s, 3H), 3.27 (t, $J = 1.8$ Hz, 2H), 3.69 (m, 6H), 4.28 (m, 2H), 6.28 (t, $J = 1.8$ Hz, 2H). ^{13}C NMR: δ 178.27, 137.98, 69.16, 68.42, 67.35, 48.02, 45.46, 42.87, 37.87, 37.72. HRMS: calculated: 330.1011; found: 330.1007.

N-(diethyl 4-ethoxy(2-ethoxy)pyridine-2,6-diyl)dicarbamate)-cis-5-norbornene-exo-2,3-dicarboximide (8). An oven-dried, 2-necked, round-bottom flask under argon was charged with diaminopyridine complex **7** (34 mg, 1.1 equiv) and K_2CO_3 (22 mg, 1.4 eq). DMF (1 mL) was added, followed by mesylate **6** (43 mg, 1 equiv). After 18 h the solvent was removed and the residue was filtered and concentrated. The product was purified on a plug of neutral alumina, eluting with 10% MeOH in CH_2Cl_2 to yield **8** as a tan, waxy solid in 62% yield (40 mg). ^1H NMR: δ 1.14 (t, $J = 7.5$ Hz, 6H), 1.25 (dt, $J = 9.9$ Hz, 1.5 Hz, 1H), 1.40 (dt, $J = 9.9$ Hz, 1.5 Hz), 2.30 (q, $J = 7.5$ Hz, 4H),

2.60 (d, $J = 1.2$ Hz, 2H), 3.15 (t, $J = 1.8$ Hz, 2H), 3.62 (s, 4H), 3.70 (m, 2H), 4.02 (m, 2H), 6.19 (t, $J = 1.8$ Hz, 2H), 7.33 (s, 2H). ^{13}C NMR: δ 178.49, 173.24, 168.34, 150.92, 137.79, 96.02, 68.61, 67.67, 67.08, 47.86, 45.26, 42.63, 37.79, 30.52, 9.31.

N-(carboxy methyl)-cis-5-norbornene-exo-2,3-dicarboximide (9). A round-bottom flask was charged with anhydride **3** (4.47 g, 1 equiv) and glycine (2.13 g, 1.04 equiv). To the flask was added 25 mL toluene, followed by NEt_3 (450 μL , 0.10 equiv). A Dean-Stark trap was attached to the flask, and the reaction mixture was heated at 135 $^\circ\text{C}$ for 10 h. The reaction mixture was concentrated *in vacuo* and the residue was taken up in EtOAc (50 mL) and washed with a solution of 0.2N HCl (2 x 20 mL). The organic layer was then concentrated *in vacuo* to yield a white solid. This residue was taken up in 35 mL sat. aq. NaHCO_3 and washed with CH_2Cl_2 (2 x 10 mL). The aqueous layer was acidified to pH=2, forming a thick slurry. The aqueous mixture was extracted with CHCl_3 (4 x 40 mL), and the combined organic layers were dried over MgSO_4 and concentrated *in vacuo* to yield **9** as a white solid in 88% yield (5.30 g). ^1H NMR: δ 1.48 (dt, $J = 9.9, 1.5$ Hz, 1H), 1.51 (d, $J = 9.9$, 1H), 2.77 (d, $J = 1.2$ Hz, 2H), 3.31 (t, $J = 1.5$ Hz, 2H), 4.28 (s, 2H), 6.30 (t, $J = 1.8$ Hz, 2H), 10.76 (s, 1H). ^{13}C NMR: δ 177.54, 172.24, 138.22, 48.26, 45.64, 43.07, 39.38. HRMS: calculated: 222.0766; found: 222.0769.

N-(methoxy triethylene glycol)-cis-5-norbornene-exo-2,3-dicarboximide (10). Carboxylic acid-containing monomer **9** (497 mg, 1.1 equiv) was dissolved in anhydrous CH_2Cl_2 (5 mL). EDC (870 mg, 2.1 eq) and DPTS (46 mg, 0.07 equiv) were added.

Triethylene glycol monomethyl ether (349 mg, 1 equiv) was added as a solution in CH₂Cl₂ (3 mL), and the reaction mixture was stirred at room temperature for 2 d. The reaction mixture was washed with water (2 x 50 mL) and brine (1 x 25 mL), and the organic layer was dried over MgSO₄. The crude product was purified by silica gel chromatography (6% MeOH in CH₂Cl₂) to yield **10** as a clear oil in 59% yield (459 mg). ¹H NMR: δ 1.53 (dt, *J* = 9.9 Hz, 1.5 Hz, 1H), 1.72 (dt, *J* = 9.9 Hz, 1.5 Hz, 1H), 2.75 (d, *J* = 1.5 Hz, 2H), 3.38 (s, 3H), 3.53-3.71 (m, 10H), 4.26 (s, 2H), 4.29 (m, 2H), 6.31 (t, *J* = 1.8 Hz, 2H). ¹³C NMR: δ 177.31, 167.15, 138.18, 72.12, 70.83, 70.78, 68.96, 65.09, 59.23, 48.20, 45.62, 43.06, 39.59. HRMS: calculated: 368.1707; found: 368.1707.

P(TEGNI-*b*-(CENI-*ran*-ADA)) (11). To a stirring solution of monomer **10** (24.5 mg, 250 equiv) in CH₂Cl₂ (1.2 mL) was added catalyst **1** (0.20 mg, 1 equiv) in CH₂Cl₂ (0.025 mL). After 10 min, a solution of monomer **2** (22.1 mg, 225 equiv) and monomer **5** (3.3 mg, 25 equiv) in CH₂Cl₂/MeOH (6:1) (0.7 mL) was added to the reaction mixture. After an additional 20 min, ethyl vinyl ether (0.5 mL) was added. The reaction mixture was stirred for another 10 min then precipitated into Et₂O/hexanes (1:1) (40 mL). The product was recovered by filtration (32 mg). GPC: *M*_n: 202000, *M*_w/*M*_n = 1.06.

P((CENI-*ran*-DAD)-*b*-CMNI) (12). To a stirring solution of monomer **2** (30.8 mg, 225 equiv) and monomer **8** (4.7 mg, 25 equiv) in CH₂Cl₂ (1.2 mL) was added catalyst **1** (0.30 mg, 1 equiv) in CH₂Cl₂ (0.15 mL). After 15 min monomer **9** (25.1 mg, 250 equiv) was added to the reaction mixture in MeOH (0.5 mL). After an additional 15 min, ethyl vinyl ether (0.5 mL) was added. The reaction mixture was stirred for another

10 min then precipitated into Et₂O/hexanes (1:1) (40 mL). The product was recovered by filtration (48 mg). GPC: M_n : 663000, $M_w/M_n = 1.06$.

P((CMNI-*ran*-TEGNI)-*b*-CENI-*b*-(CMNI-*ran*-TEGNI)) (13). To a stirring solution of monomer **9** (9.4 mg, 150 equiv) and monomer **10** (16.3 mg, 150 equiv) in CH₂Cl₂ (0.6 mL) was added catalyst **1** (0.20 mg, 1 equiv) in CH₂Cl₂ (0.1 mL). After 10 min monomer **2** (56.7 mg, 600 equiv) was added in CH₂Cl₂ (0.6 mL). After an additional 10 min the same mixture of monomers **9** and **10** was added to the reaction mixture again in CH₂Cl₂ (0.6 mL). After an additional 15 min, ethyl vinyl ether (0.5 mL) was added. The reaction mixture was stirred for another 10 min then precipitated into Et₂O/hexanes (1:1) (60 mL). The product was recovered by filtration (79 mg). Severe aggregation was observed by GPC in THF, preventing molecular weight and polydispersity analysis.

Janus nanoparticle formation procedure. A mixture of polymers **11** and **12** (5 mg each) was dissolved in THF (18 mL). After complete dissolution, pentane (2 mL) was added dropwise, causing the solution to become slightly cloudy. The micelle solution was allowed to stir for 12 h. The THF/pentane solution was then transferred to a photoreactor and degassed by bubbling argon through the solution for 20 min. The sample was then irradiated for 3 min to crosslink the micelles. After crosslinking, the sample was concentrated *in vacuo* to 2 mL, then the sample was diluted to 5 mL with THF. Water (5 mL) was added dropwise to the THF solution, and the cloudy THF/water solution was transferred to dialysis tubing (8000 MWCO) and dialyzed against water while protected from light.

Control nanoparticle formation procedure. Polymer **13** (19 mg) was dissolved in DMF (10 mL). Once complete dissolution occurred, water (10 mL) was added slowly to the stirring DMF solution. The cloudy micelle solution was transferred to dialysis tubing (8000 MWCO) and dialyzed against water while protected from light. The aqueous micelle solution was transferred to a photoreactor and degassed by bubbling argon through the solution for 20 min. The sample was then irradiated for 3 min to crosslink the micelles.

Mono-amino gold nanoparticle attachment procedure. Organic nanoparticle solution (0.2 mL from stock solution of 1 mg/mL) was diluted to 0.4 mL with phosphate buffer (pH = 8.0). The gold nanoparticles were taken up in a 1:1 mixture of water to phosphate buffer (pH = 8.0) and added to the organic nanoparticle solution. Sulfonated N-hydroxysuccinimide (1.1 mg, 60 equiv relative to COOH groups) and EDC (7.6 mg, 500 equiv relative to COOH groups) were then added, and the reaction mixture was allowed to stand at room temperature for 2 d. The reaction mixture was then transferred to dialysis tubing (8000 MWCO) and dialyzed against water. The product was recovered from the dialysis bag as a clear, brown solution.

References

- (1) For recent reviews see: (a) Walther, A.; Müller, A. H. E. *Soft Matter* **2008**, *4*, 663–668. (b) Perro, A.; Reculosa, S.; Ravaine, S.; Bourgeat-Lami, E.; Duguet, E. *J. Mater. Chem.* **2005**, *15*, 3745–3760.
- (2) (a) Erhardt, R.; Boker, A.; Zettl, H.; Kaya, H.; Pyckhout-Hintzen, W.; Krausch, G.; Abetz, V.; Müller, A. H. E. *Macromolecules* **2001**, *34*, 1069–1075. (b) Erhardt, R.; Zhang, M.; Boker, A.; Zettl, H.; Abetz, C.; Frederik, P.; Krausch, G.; Abetz, V.; Müller, A. H. E. *J. Am. Chem. Soc.* **2003**, *125*, 3260–3267. (c) Hu, J.; Liu, G. *Macromolecules*, **2005**, *38*, 8058–8065. (d) Nie, Z.; Li, W.; Seo, M.; Xu, S.; Kumacheva, E. *J. Am. Chem. Soc.* **2006**, *128*, 9408–9412. (e) Palyulin, V. V.; Potemkin, I. I. *Macromolecules* **2008**, *41*, 4459–4463. (f) Cheng, L.; Zhang, G.; Zhu, L.; Chen, D.; Jiang, M. *Angew. Chem., Int. Ed.* **2008**, *47*, 10171–10174. (g) Higuchi, T.; Tajima, A.; Motoyoshi, K.; Yabu, H.; Shimomura, M. *Angew. Chem., Int. Ed.* **2008**, *47*, 8044–8046.
- (3) Roh, K. H.; Yoshida, M.; Lahann, J. *Materialwiss. Werkstofftech.* **2007**, *38*, 1008–1011.
- (4) (a) Takahara, Y. K.; Ikeda, S.; Ishino, S.; Tachi, K.; Ikeue, K.; Sakata, T.; Hasegawa, T.; Mori, H.; Matsumura, M.; Ohtani, B. *J. Am. Chem. Soc.* **2005**, *127*, 6271–6275. (b) Walther, A.; Hoffmann, M.; Müller, A. H. *Angew. Chem., Int. Ed.* **2008**, *47*, 711.
- (5) Nisisako, T.; Torii, T.; Takahashi, T.; Takizawa, Y. *Adv. Mater.*, **2006**, *18*, 1152–1156.
- (6) (a) Howse, J. R.; Jones, R. A. L.; Ryan, A. J.; Gough, T.; Vafabakhsh, R.; Golestanian, R. *Phys. Rev. Lett.*, **2007**, *99*, 048102. (b) Golestanian, R.; Liverpool, T. B.; Ajdari, A. *Phys. Rev. Lett.*, **2005**, *94*, 220801.
- (7) (a) Vilain, C.; Goettmann, F.; Moores, A.; Floch, P. L.; Sanchez, C. *J. Mater. Chem.* **2007**, *17*, 3509. (b) Kim, S. H.; Tan, J. P. K.; Nederberg, F.; Fukushima, K.; Yang, Y. Y.; Waymouth, R. M.; Hedrick, J. L. *Macromolecules* **2009**, *42*, 25–29.
- (8) Nisisako, T.; Torii, T.; Takahashi, T.; Takizawa, Y. *Adv. Mater.* **2006**, *18*, 1152–1156.
- (9) (a) Perro, A.; Reculosa, S.; Pereira, F.; Delville, M. H.; Mingotaud, C.; Duguet, E.; Bourgeat-Lami, E.; Ravaine, S. *Chem. Commun.* **2005**, *44*, 5542–5543. (b) Lattuada, M.; Hatton, T. A. *J. Am. Chem. Soc.* **2007**, *129*, 12878–12899.
- (10) Matson, J. B.; Grubbs, R. H. *J. Am. Chem. Soc.* **2008**, *130*, 6731–6733.

- (11) (a) Grubbs, R. H. *Handbook of Metathesis*; Wiley-VCH: Weinheim, 2003. (b) Trnka, T. M.; Grubbs, R. H. *Acc. Chem. Res.* **2001**, *34*, 18–29.
- (12) (a) Maynard, H. D.; Okada, S. Y.; Grubbs, R. H. *Macromolecules*, **2000**, *33*, 6239–6248. (b) Breitenkamp, R. B.; Ou, Z.; Breitenkamp, K.; Muthukumar, M.; Emrick, T. *Macromolecules* **2007**, *40*, 7617–7624. (c) Biagini, S. C. G.; Parry, A. L. *J. Polym. Sci., Part A: Polym. Chem.* **2007**, *45*, 3178–3190. (d) Sutthasupa, S.; Sandra, F.; Masuda, T. *Macromolecules* **2009**, *42*, 1519–1525.
- (13) (a) Fraser, C.; Grubbs, R. H. *Macromolecules* **1995**, *28*, 7248–7255. (b) Puffer, E. B.; Pontrello, J. K.; Hollenbeck, J. J.; Kink, J. A.; Kiessling, L. L. *ACS Chem. Biol.* **2007**, *2*, 252–262. (c) Rawat, M.; Gama, C. I.; Matson, J. B.; Hsieh-Wilson, L. C. *J. Am. Chem. Soc.* **2008**, *130*, 2959–2961.
- (14) (a) Han, H. J.; Chen, F. X.; Yu, J. H.; Dang, J. Y.; Ma, Z.; Zang, Y. Q.; Xie, M. R. *J. Polym. Sci., Part A: Polym. Chem.* **2007**, *45*, 3986–3993. (b) Eren, T.; Som, A.; Rennie, J. R.; Nelson, C. F.; Urgina, Y.; Nüsslein, K.; Coughlin, E. B.; Tew, G. N. *Macromol. Chem. Phys.* **2008**, *209*, 516–524.
- (15) Xia, Y.; Kornfield, J. A.; Grubbs, R. H. *Macromolecules* **2009**, *42*, 3761–3766.
- (16) (a) Stubbs, L. P.; Weck, M. *Chem. Eur. J.* **2003**, *9*, 992–999. (b) Scherman, O. A.; Lighthart, G. B. W. L.; Ohkawa, H.; Sijbesma, R. P.; Meijer, E. W. *Proc. Nat. Acad. Sci.* **2006**, *103*, 11850–11855. (c) Higley, M. L.; Pollino, J. M.; Hollembeak, E.; Weck, M. *Chem. Eur. J.* **2005**, *11*, 2946–2953.
- (17) (a) Choi, T. L.; Grubbs, R. H. *Angew. Chem., Int. Ed.* **2003**, *42*, 1743–1746. (b) Camm, K. D.; Castro, N. M.; Liu, Y. W.; Czechura, P.; Snelgrove, J. L.; Fogg, D. E. *J. Am. Chem. Soc.* **2007**, *129*, 4168–4169. (c) Colak, S.; Tew, G. N. *Macromolecules* **2008**, *41*, 8436–8440. (d) Kolonko, E. M.; Kiessling, L. L. *J. Am. Chem. Soc.* **2008**, *130*, 5626–5627. (e) Kratz, K.; Breitenkamp, K.; Hule, R.; Pochan, D.; Emrick, T. *Macromolecules* **2009**, *42*, 3227–3229.
- (18) Ilhan, F.; Gray, M.; Rotello, V. M. *Macromolecules* **2001**, *34*, 2597–2601.
- (19) See chapter 2.
- (20) Pangborn, A. B.; Giardello, M. A.; Grubbs, R. H.; Rosen, R. K.; Timmers, F. J. *Organometallics* **1996**, *15*, 1518–1520.
- (21) Love, J. A.; Morgan, J. P.; Trnka, T. M.; Grubbs, R. H. *Angew. Chem., Int. Ed. Engl.* **2002**, *41*, 4035–4037.
- (22) Moore, J. S.; Stupp, S. I. *Macromolecules* **1990**, *23*, 65–70.

Chapter 4

ROMP-ATRP Block Copolymers Prepared from Monotelechelic Poly(oxa)norbornenes using a Difunctional Terminating Agent

Portions of the text in this chapter have been reproduced with permission from:

Matson, J. B.; Grubbs, R. H. *Macromolecules* **2008**, *41*, 5626-5631.

Copyright 2008 American Chemical Society

Abstract

Novel block copolymers were prepared by combining ROMP and ATRP. Using the fast initiating ruthenium metathesis catalyst $(H_2IMes)(Cl)_2(pyr)_2RuCHPh$ and (*Z*)-but-2-ene-1,4-diyl bis(2-bromopropanoate) as a terminating agent, three different monotelechelic poly(oxa)norbornenes were synthesized. Complete end-functionalization was shown by carrying out the ATRP of styrene and *tert*-butylacrylate from the poly(oxa)norbornenes using a CuBr/PMDETA catalyst system. GPC showed no remaining homopolymer, and all block copolymers were found to have matching theoretical and observed molecular weights and low polydispersities.

Introduction

Combination of multiple distinct types of living polymerization methods has been the subject of intense study in recent years.¹ This research is driven by the fact that while the number of cheap, accessible monomers is relatively low, the different types of materials that can be produced from these monomers is much higher due to copolymerization and manipulation of microstructure. Still, many monomer combinations cannot be copolymerized using a single method due to the diverse conditions, requirements, and monomer types of the various living polymerization methods,² such as living anionic polymerization, controlled/living radical polymerization (CRP), and living ring opening metathesis polymerization (ROMP). This problem is typically overcome by the development of multifunctional initiators, monomers, and chain-transfer agents that allow for multiple polymerization techniques to be used in the preparation of a single polymer.

ROMP polymers provide unique materials because unlike radical, anionic, and cationic polymerizations, no unsaturation in the monomer is lost.³ These types of unsaturated-backbone polymers, such as poly(oxa)norbornenes, polycyclooctenes, and polycyclobutenes, are either unattainable or have imperfect microstructure when made using radical and ionic polymerization techniques. While great efforts have been made at merging various types of CRP polymerization methods in a single polymer synthesis,² only a few reports exist that show the combination of living ROMP with any other polymerization method.⁴ Reliable techniques for joining living ROMP with other living polymerization methods will provide synthetic routes to new materials inaccessible by any other means. We chose to investigate combining living ROMP with ATRP because of the ability of both methods to easily produce highly functional polymers under mild conditions.

Most of the reports that describe the combination of ROMP and living radical polymerization techniques use functionalized ROMP monomers capable of initiating ATRP, also known as inimers.^{4c-h,5} Both grafting-from and grafting-through approaches have been used to synthesize polymers with a backbone made by ROMP and side chains made by ATRP. While useful in making brush polymers, inimers have limited utility because they cannot be used to reliably make other polymer structures.

Linear polymers have been made by combining ROMP and ATRP by using a difunctional chain-transfer agent (CTA).⁶ The resulting telechelic ROMP polymers were used to initiate ATRP, producing ABA triblock copolymers. This strategy suffers from the drawback that the middle B block is not made in a living fashion, so a polydisperse product is obtained. Additionally, only monomers that can undergo secondary metathesis

(backbiting) can be used in these reactions, leaving out substituted norbornene monomers from these types of materials.

A synthetic method for the preparation of monotelechelic ROMP polymers could allow for incorporation of an ATRP initiator on the chain end. This would facilitate the synthesis of low polydispersity linear ROMP-ATRP block copolymers, which could be further end-functionalized in a variety of ways, expanding the scope of ROMP-ATRP hybrid materials to more complex graft copolymers, star polymers, multiblock copolymers, and others. Monotelechelic ROMP polymers have been made through either the custom initiator method or the end-capping method. The custom initiator method is typically carried out by exchanging the benzylidene on the metathesis catalyst for an alkylidene with the desired functionality.⁷ This strategy, while effective, suffers from the necessity of synthesizing a new catalyst for each new desired end-functional group. The end-capping method involves the addition of a small molecule that is added onto the end of the polymer chain by reaction with the living chain end. End-capping chains with aldehydes is a reliable technique for end-functionalization of ROMP polymers made using early transition metal catalysts,^{4b,8} but until recently no reliable techniques existed for this type of transformation using the more air, moisture and functional group tolerant ruthenium metathesis catalysts.

Hilf et al. described the sacrificial monomer method of producing hydroxyl-terminated ROMP polymers.⁹ This technique involves the synthesis of a diblock copolymer with one block composed of the desired monomer, followed by a second short block composed of a dioxepine monomer. Subsequent cleavage of the poly(dioxepine) yields the hydroxyl-functionalized monotelechelic polymer. These types of

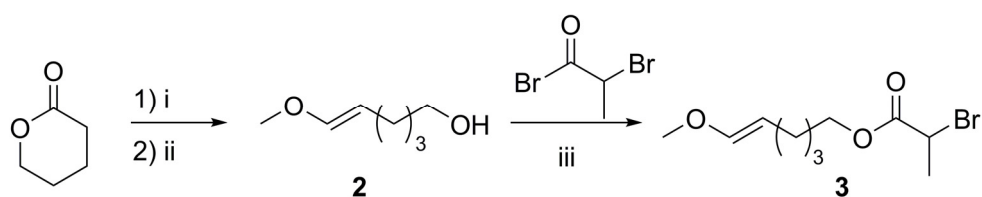
monotelechelic polymers have been used to make all-ROMP graft copolymers,¹⁰ as well as poly(norbornene)-*b*-poly(ethylene glycol) copolymers by further end-functionalization of the ROMP polymer.¹¹ While the sacrificial monomer strategy could be used to create many types of polymer architectures, the alcohol-functionalized polymer must always be further derivatized to enable further reactivity. This process requires long reaction times and often does not reach completion. Hilf et al. also recently described methods for installing aldehydes or carboxylic acids at the polymer chain end.¹² In this example, the single turnover substrates vinylene carbonate and 3*H*-furanone were used to end-cap the growing polymer chain. The methods described above are effective if the desired chain-end-functionality is an alcohol, aldehyde, or carboxylic acid, but a technique that could directly incorporate any desired functional group onto the polymer by reaction with the living chain end would allow for the incorporation of diverse chain end-functionality without the need to perform difficult post polymerization transformations.

We are aware of one report that utilizes this type of transformation. Li et al. used the ruthenium initiator $(\text{PCy}_3)_2(\text{Cl})_2\text{RuCHPh}$ to prepare liquid crystalline block copolymers using a symmetrical olefin to place an α -bromoester on one end of the ROMP polymer.^{4a} They were then able to initiate the ATRP of *n*-butyl acrylate from the functionalized chain end. However, recent reports have shown that the ruthenium metathesis catalyst $(\text{H}_2\text{IMes})(\text{Cl})_2(\text{pyr})_2\text{RuCHPh}$ (**1**) and related structures afford living polymers of extremely low polydispersity much faster than with previous catalysts.¹³ Polymerizations with catalyst **1** are often complete in only a few minutes, and synthesis of block copolymers can be achieved.¹⁴ These qualities, as well as its air and moisture tolerance and its long benchtop stability, make catalyst **1** an ideal initiator for the facile

synthesis of end-functionalized ROMP polymers. We sought to extend the approach of Li et al. to this highly active ruthenium metathesis catalyst and to examine the scope of this type of transformation.

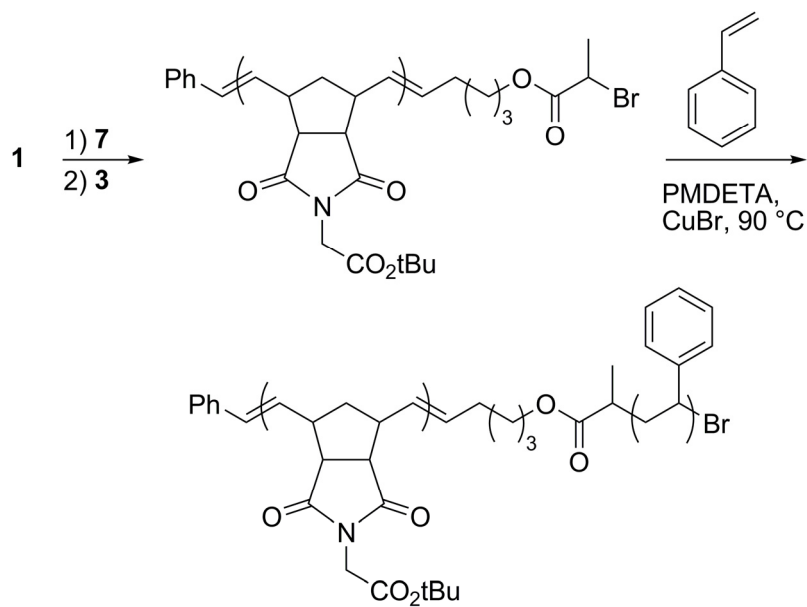
Results and Discussion

Functionalized vinyl ethers were used to end-cap poly(norbornenes) in an example by Owen et al. using $(\text{PCy}_3)_2(\text{Cl})_2\text{RuCHPh}$ as the metathesis catalyst.¹⁵ Although their capping efficiencies were not 100%, we chose to reexamine this route using catalyst **1** in hopes that the more active catalyst would enable complete end-capping. To test this hypothesis, we prepared α -bromoester end-functionalized polymers using vinyl ether **3** to terminate the reaction. Vinyl ether **3** was synthesized by reduction of δ -valerolactone with DIBAL, followed by transformation of the aldehyde to vinyl ether **2** by a Wittig reaction with a phosphonium ylide as previously reported.¹⁶ Addition of 2-bromopropionyl bromide afforded vinyl ether **3** (Scheme 4.1).



Scheme 4.1. Synthesis of Vinyl Ether Reaction conditions: i) DIBAL, THF, $-40\text{ }^\circ\text{C}$. ii) $\text{ClPh}_3\text{PCH}_2\text{OCH}_3$, sec-BuLi , THF, $0\text{ }^\circ\text{C}$. iii) THF, NEt_3 , $0\text{ }^\circ\text{C}$.

ROMP was carried out by reacting ruthenium initiator **1** with *tert*-butyl ester norbornene imide monomer (tBENI) **7** (Figure 4.1) in CH_2Cl_2 until complete (3 min), followed by addition of 10 equiv of vinyl ether **3** (Scheme 4.2). The reaction mixture



Scheme 4.2. ROMP and chain termination using vinyl ether followed by ATRP of styrene.

To determine the extent of end capping, polymer **4** was used as a macroinitiator to initiate the ATRP of styrene using a CuBr/PMDETA catalyst system, yielding block copolymer product **5**. As seen in the low molecular weight shoulder in the GPC trace in Figure 4.2, a significant amount of unreacted homopolymer remains, further corroborating the results found by Owen et al.¹⁵ We attribute the incomplete end-capping to an initial undesirable cross metathesis reaction between the living polymer chain end and **3** that puts the vinyl ether instead of the α -bromoester onto to polymer chain. Further cross metathesis between the vinyl ether functionalized polymer and the α -bromoester-functionalized ruthenium complex is expected to be slow, limiting the ability of this strategy to afford the desired product before catalyst death occurs. With this knowledge in hand, we decided to abandon the functionalized vinyl ether route and pursue a new strategy.

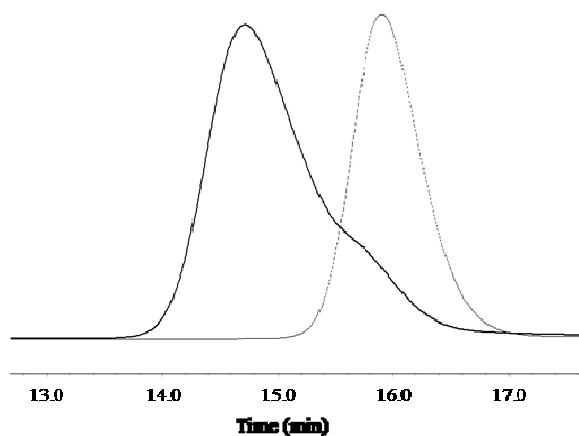
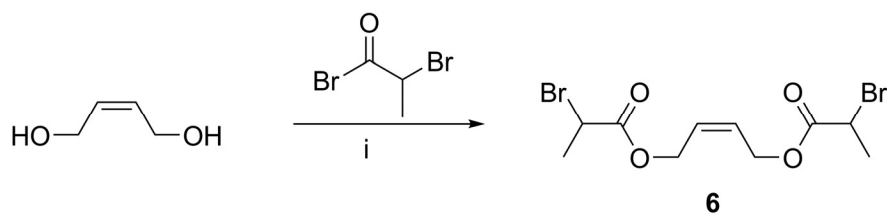


Figure 4.2. GPC traces of P(tBENI) homopolymer **4** (dashed line) and P(tBENI-*b*-S) block copolymer **5** (solid line).

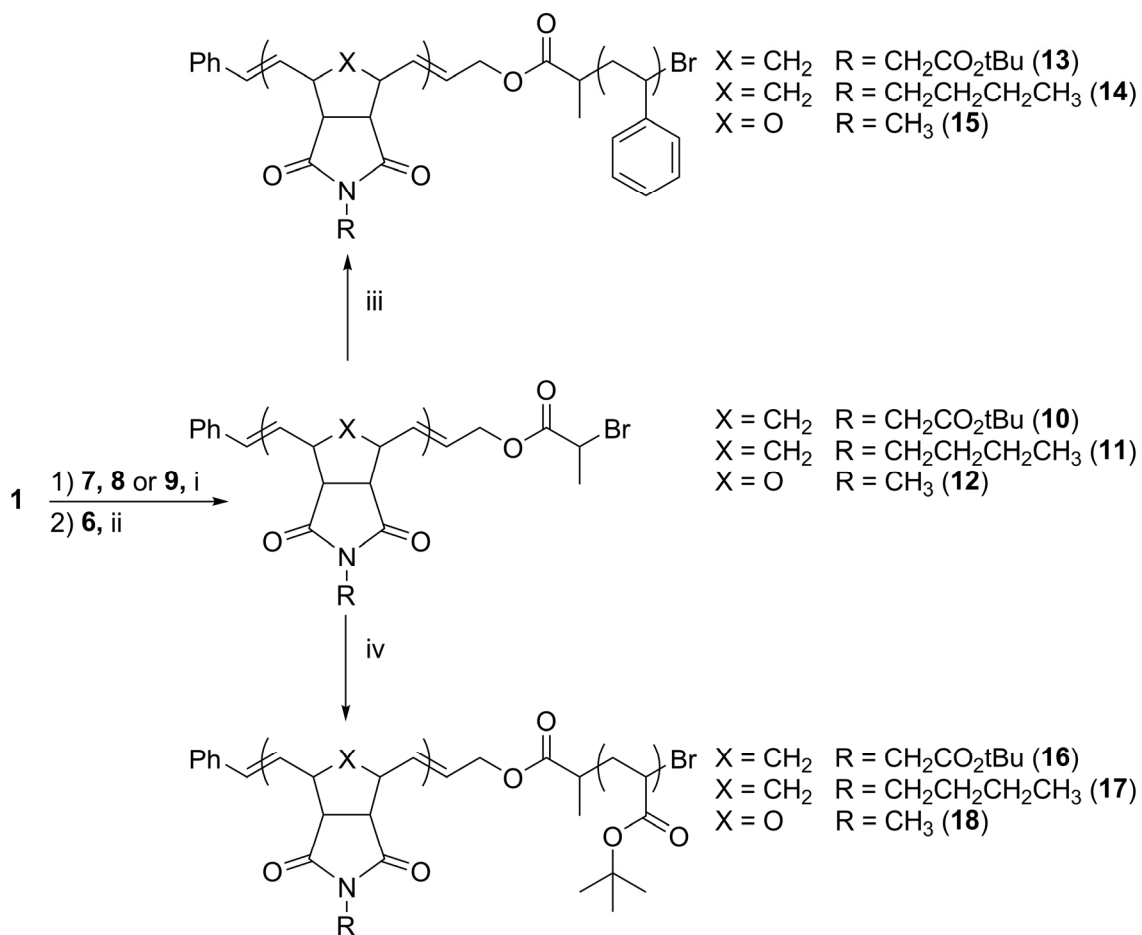
When a cyclic olefin is sterically unencumbered enough to undergo secondary metathesis, internal *cis* olefins are widely used as CTAs to afford telechelic polymers.^{1e, 6a,17} In polymers with repeat units that are too bulky to undergo secondary metathesis, a *cis* olefin can act instead as a terminating agent (TA).^{4a} In this case, reaction with only the living polymer chain end affords the monotelechelic polymer and the free ruthenium alkylidene in a ring-opening cross metathesis reaction. Any further reaction between the functionalized chain end and the ruthenium alkylidene is redundant due to the symmetrical nature of the TA. The other chain end containing the phenyl group derived from the initiator is expected to be too deactivated to participate in further metathesis reactions.

We prepared TA *cis*-2-butene-1,4-diyl bis(2-bromopropanoate) (**6**) in one step by addition of two equivalents of 2-bromopropionyl bromide to commercially available *cis*-2-butene-1,4-diol (Scheme 4.3). Poly(oxa)norbornenes were prepared from tBENI, N-butyl norbornene imide (NBNI) and N-methyl oxanorbornene imide (NMONI) (**7-9**) using the same reaction conditions described above (Scheme 4.4). Eight equiv of TA **6**

were added to the reaction mixture after 3 min, and the reaction was quenched by precipitation after 3 h. These polymers (**10-12**) were found to be narrowly dispersed, and molecular weights were in agreement with theoretical values (Table 4.1).



Scheme 4.3. Preparation of terminating agent. Reaction conditions: i) 2-bromopropionyl bromide, THF, NEt₃, 0 °C.



Scheme 4.4. Synthesis of monotelechelic poly(oxa)norbornenes and ROMP-ATRP block copolymers. Reaction conditions: i) 0.3 M in CH_2Cl_2 , 3 min. ii) 8 equiv in CH_2Cl_2 , 3 h. iii) styrene, CuBr , PMDETA, 90°C . iv) tBA, DMF, CuBr , PMDETA, 70°C .

Table 4.1. Polymer characterization data for monotelechelic poly(oxa)norbornenes and ROMP-ATRP block copolymers.

Polymer	Structure	$M_n(\text{theo})^a$	$M_n(\text{NMR})$	$M_n(\text{GPC})^b$	PDI
10	P(tBENI)	7460	10200	8520	1.03
11	P(NBNI)	6820	5230	7190	1.01
12	P(NMONI)	4790	4490	4840	1.06
13	P(tBENI- <i>b</i> -S)	19800	18800	19100	1.07
14	P(NBNI- <i>b</i> -S)	29100	27000	25800	1.13
15	P(NMONI- <i>b</i> -S)	28400	40300	28600	1.21
16	P(tBENI- <i>b</i> -tBA)	27500	24900	25300	1.10
17	P(NBNI- <i>b</i> -tBA)	27500	24300	26800	1.07
18	P(NMONI- <i>b</i> -tBA)	28800	32100	28000	1.06

^aDetermined by monomer catalyst ratio (**11-13**) or percent monomer conversion as determined by ¹H NMR spectroscopy (**14-19**). ^b Measured in THF eluent using RI and MALLS detectors.

Next, a PS block was added to each of polymers **7-9** using a CuBr/PMDETA catalyst system in neat styrene at 90 °C to produce polymers **13-15**. Figure 4.3 shows the GPC traces of homopolymer **10** and block copolymer **13**. Unlike block copolymer **5**, a monomodal peak was observed, establishing that complete end-functionalization of the polymer was accomplished and that full initiation of the α -bromoester had occurred. Complete disappearance of the homopolymer peak was observed for polymers **14** and **15** as well. Polymer polydispersities remained low, and the molecular weights were close to theoretical values based on monomer conversion. The molecular weight data confirm that only the living chain end reacted with the TA, leaving the phenyl group derived from

initiator **1** untouched. Interestingly, when THF was used as the solvent for the ROMP reaction, P(tBENI-*b*-S) block copolymers showed a low molecular weight shoulder with the same peak retention time as the homopolymer, indicating that P(tBENI) end-functionalization was incomplete. This observation is in agreement with previous reports demonstrating that the rate of secondary metathesis during ROMP using ruthenium catalysts is slower in THF than in CH₂Cl₂.¹⁸

To explore the utility of this reaction with other α -olefins, *tert*-butylacrylate (tBA) was added to each of the poly(oxa)norbornenes homopolymers using the same CuBr/PMDETA catalyst system in DMF at 70 °C to produce polymers **16-18**. GPC analysis of these polymers also showed monomodal peaks, and molecular weights measured by NMR spectroscopy and GPC matched the theoretical values. These polymer syntheses demonstrate the generality of this approach, and it is expected that many other acrylates and styrenes can be used to make multi-block copolymers using this method.

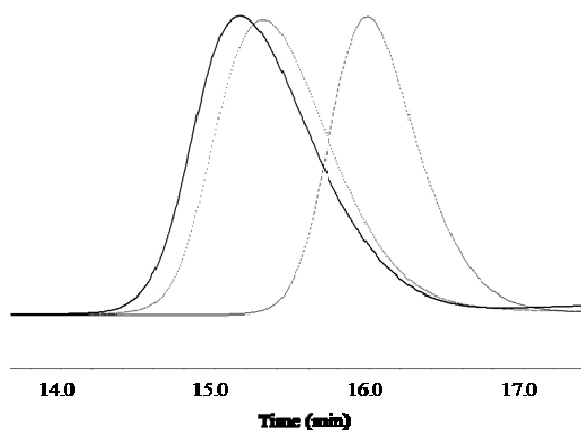


Figure 4.3. GPC traces of P(tBENI) homopolymer **10** (dashed line), P(tBENI-*b*-S) block copolymer **13** (dotted line), and P(tBENI-*b*-tBA) block copolymer **16** (solid line).

Conclusions

In summary, we have demonstrated a method for making monotelechelic poly(oxa)norbornenes containing α -bromoesters as ATRP initiators using a symmetrical *cis*-olefin TA. Both PS and PtBA blocks were grown from the chain ends, and a complete shift in the GPC peak was observed. The data indicate that complete end-functionalization and initiation of ATRP from the poly(oxa)norbornenes occurred. Many more types of multi-block copolymers using this strategy can be envisioned, including diblocks and triblocks of both the ROMP and ATRP portions. Additionally, any strained cyclic olefin that can undergo living ROMP could be used, so the possible types of multi-block copolymers are not limited to poly(oxa)norbornenes. We also expect this method to be general for the preparation of monotelechelic living ROMP polymers, allowing for the incorporation of virtually any functionality to be placed onto the polymer chain end, as long as it is compatible with the ruthenium catalyst and an appropriate TA can be synthesized. Future work includes the synthesis of novel tri- and tetra- block copolymers and end-functionalized polymers to be used in biological applications.

Acknowledgement

The author thanks Materia for catalyst as well as Dr. Ron Walker, Paul Clark, and Yan Xia for helpful discussions.

Experimental Section

General Information

NMR spectra were measured in CDCl_3 or $\text{DMSO-}d_6$ on Varian Mercury 300 MHz spectrometers unless otherwise noted. ^1H and ^{13}C NMR chemical shifts are reported in ppm relative to CDCl_3 . Flash column chromatography of organic compounds was performed using silica gel 60 (230-400 mesh). High-resolution mass spectra (EI and FAB) were provided by the California Institute of Technology Mass Spectrometry Facility. Gel permeation chromatography (GPC) was carried out in THF on two PLgel 10 μm mixed-B LS columns (Polymer Labs) connected in series with a DAWN EOS multiangle laser light scattering (MALLS) detector and an Optilab DSP differential refractometer (both from Wyatt Technology). No calibration standards were used, and dn/dc values were obtained for each injection by assuming 100% mass elution from the columns. Infrared spectra were recorded using a Perkin Elmer Spectrum BXII spectrometer.

Materials

CH_2Cl_2 and THF were purified by passage through solvent purification columns.¹⁹ $(\text{H}_2\text{IMes})(\text{pyr})_2(\text{Cl})_2\text{RuCHPh}$ (**1**) was prepared from $(\text{H}_2\text{IMes})(\text{PCy}_3)(\text{Cl})_2\text{RuCHPh}$ (obtained from Materia) according to a literature procedure.²⁰ *cis*-5-Norbornene-*endo*-2,3-dicarboxylic anhydride was purchased from Acros Organics, and *cis*-5-norbornene-*exo*-2,3-dicarboxylic anhydride was prepared as previously described.²¹ 6-Methoxyhex-5-en-1-ol (**2**) was prepared according to a literature procedure and isolated as 76% *trans* product.¹⁶ Styrene and tBA were passed

through a column of basic alumina immediately before use. *cis*-2-Butene-1,4-diol was distilled from CaH₂. All other materials were obtained from Aldrich Chemical Company and used as received unless otherwise noted.

6-methoxyhex-5-enyl 2-bromopropanoate (3). An oven-dried, 2-necked, round-bottom flask under argon was charged with 6-methoxyhex-5-en-1-ol (**2**) (82 mg, 1 equiv) in 1 mL THF. NEt₃ (0.22 mL, 2.5 equiv) was added, and the flask was cooled to 0 °C. 2-bromopropionyl bromide (0.13 mL, 2.0 eq) was added dropwise to the reaction mixture, and a white precipitate developed. After stirring at room temperature for 6 h, the reaction mixture was diluted with CH₂Cl₂ and water. The organic layer was removed, and the aqueous layer was extracted with CH₂Cl₂. The organic layers were combined and washed with brine and dried over MgSO₄. The crude product was purified by silica gel chromatography (5% EtOAc in hexanes) to give **6** as a clear oil in 88% yield (77% *trans* product). ¹H NMR: δ 1.45 (m, 2H), 1.66 (m, 2H), 1.81-1.90 (m, 5H), 1.93-2.11 (m, 3H), 3.51-3.58 (m, 4H), 4.07-4.40 (m, 3.2H), 4.70 (m, 0.8H), 5.88 (d, *J* = 3.3 Hz, 0.2H), 6.28 (d, *J* = 12.3 Hz, 0.8H). ¹³C NMR: δ 170.51, 170.42, 147.64, 146.75, 102.49, 66.21, 66.12, 65.12, 56.12, 44.15, 40.43, 40.20, 33.17, 29.27, 28.08, 27.89, 27.42, 27.27, 27.04, 26.03, 23.48, 21.88. HRMS: calculated 265.0440, found 265.0439.

(Z)-But-2-ene-1,4-diyl bis(2-bromopropanoate) (6). An oven-dried, 3-necked, round-bottom flask under argon was charged with *cis*-2-butene-1,4-diol (2.0 mL, 1 equiv) in 40 mL THF. NEt₃ (9.0 mL, 2.5 equiv) was added, and the flask was cooled to 0 °C. 2-bromopropionyl bromide (7.7 mL, 3.0 equiv) was added dropwise to the reaction

mixture, and a white precipitate developed. After stirring at room temperature for 6 h, the reaction mixture was diluted with CH₂Cl₂ and water. The organic layer was removed, and the aqueous layer was extracted with CH₂Cl₂. The organic layers were combined, washed with brine, and dried over MgSO₄. The crude product was purified by silica gel chromatography (10% EtOAc in hexanes) to give **6** as a clear oil in 63% yield. Further purification was accomplished by Kugelrohr distillation. ¹H NMR: δ 1.83 (d, *J* = 6.9 Hz, 6H), 4.38 (q, *J* = 6.9, 2H), 4.80 (d, *J* = 4.8, 4H), 5.81 (m, 2H). ¹³C NMR: δ 170.12, 128.11, 61.50, 39.95, 21.78. HRMS: calculated 358.9317, found 358.9309.

***tert*-Butyl ester norbornene imide (tBENI) (7)**. A 100 mL round-bottom flask was charged with glycine-*tert*-butyl ester (3.88 g, 1.1 equiv) in 45 mL C₆H₆. *cis*-5-Norbornene-*exo*-2,3-dicarboxylic anhydride (4.25 g, 1 equiv) and NEt₃ (0.375 mL, 0.1 equiv) were added, and the reaction mixture quickly solidified. The flask was immersed in an oil bath and heated at reflux with a Dean-Stark trap. The solids slowly dissolved, leaving a clear solution. After 2 h the heat was removed and the solvent was removed *in vacuo*. The residue was taken up in CH₂Cl₂ and washed with 0.1 N HCl, H₂O and brine, then dried over MgSO₄. A pale yellow oil was recovered, which solidified after 10 h under high vacuum. The solid was purified by sublimation, yielding a white powder in 50% yield. ¹H NMR: δ 1.43 (s, 9H), 1.51 (dt, *J* = 9.9, 1.5 Hz, 1H), 1.71 (d, *J* = 9.9 Hz, 1H), 2.71 (d, *J* = 1.2 Hz, 2H), 3.29 (t, *J* = 1.5 Hz, 2H), 4.10 (s, 2H), 6.28 (t, *J* = 1.8 Hz, 2H). ¹³C NMR: δ 177.37, 165.91, 138.12, 83.00, 48.14, 45.51, 43.13, 40.37, 28.16. HRMS: 278.1392, found 278.1389.

N-butyl norbornene imide (NBNI) (8). A 100 mL round-bottom flask was charged with *cis*-5-norbornene-*exo*-2,3-dicarboxylic anhydride (1.0 g, 1 equiv) and 25 mL glacial acetic acid. Once homogeneous, *n*-butylamine (0.66 mL, 1.1 equiv) was added slowly to the flask. A condenser and a drying tube were attached, and the flask was immersed in an oil bath at 120 °C. After 2 h, the heat was removed, and once cool, the contents of the flask were added to 50 mL chilled H₂O. The cloudy solution was extracted with toluene three times. The combined organic layers were washed with H₂O and brine and dried over MgSO₄ to yield a pale yellow oil. The oil was purified by elution in CH₂Cl₂ through a column of neutral alumina. ¹H NMR: δ 0.93 (t, *J* = 7.2 Hz, 3H), 1.21-1.36 (m, 3H), 1.48-1.62 (m, 3H), 2.67 (d, *J* = 1.2 Hz, 2H), 3.27 (m, 2H), 3.46 (t, *J* = 7.5 Hz, 2H), 6.28 (t, *J* = 1.8 Hz, 2H). ¹³C NMR: δ 178.33, 138.04, 48.00, 45.37, 42.92, 38.72, 30.04, 20.43, 13.84. HRMS: calculated 220.1338, found 220.1344.

N-methyl oxanorbornene imide (NMONI) (9). A Schlenk tube was charged with *N*-methyl maleimide (4.11 g, 1 equiv), followed by Et₂O (25 mL) and furan (5.2 mL, 1.9 equiv). Three freeze-pump-thaw cycles were performed, and the tube was sealed under argon. The tube was immersed in an oil bath at 90 °C, and the solids slowly dissolved. After 4 h the heat was removed and the tube was allowed to cool. The white precipitate was collected by filtration and purified by recrystallization from EtOAc in 48% yield. ¹H NMR: δ 2.86 (s, 2H), 2.98 (s, 3H), 5.28 (s, 2H), 6.52 (s, 2H). ¹³C NMR: δ 176.42, 136.64, 80.95, 47.63, 25.04. HRMS: calculated 180.0661, found 180.0657.

General Polymerization Procedure for monotelechelic poly(oxa)norbornenes

(4, 10-12). A 2 dram vial with a septum cap was charged with the desired amount of monomer and a stirbar under argon flow. CH_2Cl_2 (0.1 M) was added to the vial. The desired amount of catalyst 1 as a stock solution in CH_2Cl_2 was quickly added to the vigorously stirring monomer solution. After stirring at room temperature for 3 min under argon flow, vinyl ether **3** or TA **6** was added as a solution in CH_2Cl_2 . The reaction mixture was allowed to stir for 3 to 24 h. The reaction mixture was precipitated into a large volume of Et_2O /hexanes (1:1), and the product was recovered by filtration and multiple washings with ether, followed by drying under vacuum.

Poly(tBENI) (10). The product was recovered as a tan powder in 93% yield. GPC: $M_n = 8520$, $M_w/M_n = 1.03$. IR: 2979, 2931, 1779, 1742, 1710, 1415, 1394, 1369, 1324, 1235, 1160, 919, 846, 750. ^1H NMR: δ 1.20-1.80 (m, 9n H), 1.82 (d, 3H) 2.00-2.30 (m, n H), 2.70-3.40 (m, 4n H), 4.05 (s, 2n H), 4.38 (q, 1H), 4.65 (d, 2H), 5.40-5.80 (d, 2n H).

Poly(NBNI) (11). The product was recovered as a tan powder in 93% yield. GPC: $M_n = 7190$, $M_w/M_n = 1.02$. IR: 2956, 2872, 1771, 1698, 1436, 1397, 1368, 1341, 1265, 1190, 1135, 1046, 970, 922, 763. ^1H NMR: δ 0.80-1.00 (m, 3n H), 1.20-1.40 (m, 2n H), 1.40-1.80 (m, 4n H), 1.82 (d, 3H), 1.95-2.40 (m, n H), 2.60-3.60 (m, 5n H), 4.38 (q, 1H), 4.65 (d, 2H), 5.40-5.80 (d, 2n H).

Poly(NMONI) (12). The product was recovered as a tan powder in 76% yield. GPC: $M_n = 4840$, $M_w/M_n = 1.06$. IR: 3604, 3464, 3059, 2952, 2890, 1778, 1713, 1436, 1383, 1328, 1283, 1131, 1031, 971, 920, 807, 734, 700, 632. ^1H NMR: δ 1.82 (d, 3H), 2.85-3.00 (s, 3n H), 3.20-3.45 (s, 2n H), 4.30-4.60 (m, nH + 1H), 4.70-5.00 (m, n H), 5.70-6.10 (m, 2n H).

ATRP of S and tBA from monotelechelic poly(oxa)norbornenes (5, 13-18). A dry vial with a septum cap was charged with the desired macroinitiator (**4**, **10**, **11** or **12**) (0.050 mmol) and a stirbar. Neat monomer (0.25 mL) was added, followed by DMF (0.2 mL) and PMDETA (1.0 μL , 0.050 mmol). Three freeze-pump-thaw cycles were performed on this solution. The vial was backfilled with argon, and CuBr (0.7 mg, 0.050 mmol) was added. Two more freeze-pump-thaw cycles were performed, then the vial was sealed under argon and placed in an oil bath at 90 °C (**5**, **13-15**) or 70 °C (**16-18**). Monomer conversion was measured by ^1H NMR spectroscopy, and reactions were quenched at the desired conversion by removal of heat, exposure to air, and dilution with THF. The copper catalyst was removed by passing the reaction mixture through a column of alumina, eluting with THF. The polymer solution was concentrated and precipitated into a large volume of methanol (**5**, **13-15**) or methanol/H₂O (70:30) (**16-18**). The product was recovered by filtration (**5**, **13-15**) or by decanting off the supernatant (**16-18**). All products were dried under vacuum for several hours.

Poly(tBENI-*b*-S) (13). The product was recovered as a white, fluffy powder in 34% yield. GPC: $M_n = 19100$, $M_w/M_n = 1.07$. IR: 3026, 2924, 2853, 1779, 1743, 1710,

1601, 1493, 1453, 1415, 1394, 1369, 1324, 1236, 1168, 1071, 1029, 970, 846, 750, 698.

^1H NMR: δ 1.20-2.40 (m, 10n + 2m H), 2.70-3.40 (m, 4n H), 4.05 (s, 2n H), 5.40-5.80 (d, 2n H), 6.30-7.25 (m, 5m H)

Poly (NBNI-*b*-S) (14). The product was recovered as a white, fluffy powder in 50% yield. GPC: $M_n = 25800$, $M_w/M_n = 1.13$. IR: 3060, 3026, 2926, 2853, 1944, 1771, 1700, 1602, 1493, 1453, 1397, 1368, 1343, 1266, 1190, 1136, 1029, 968, 908, 758, 698. ^1H NMR: δ 0.80-1.00 (m, 3n H), 1.20-2.40 (m, 7n + 2m H), 2.60-3.60 (m, 5n H), 5.40-5.80 (d, 2n H) 6.30-7.25 (m, 5m H).

Poly (NMONI-*b*-S) (15). The product was recovered as a white, fluffy powder in 20% yield. GPC: $M_n = 28600$, $M_w/M_n = 1.21$. IR: 3618, 3060, 3026, 2925, 2850, 1944, 1870, 1778, 1704, 1602, 1493, 1452, 1382, 1283, 1130, 1029, 968, 909, 758, 698. ^1H NMR: δ 1.20-2.30 (m, 2m H) 2.85-3.00 (s, 3n H), 3.20-3.45 (s, 2n H), 4.30-4.60 (m, nH), 4.70-5.00 (m, n H), 5.70-6.10 (m, 2n H) 6.30-7.25 (m, 5m H).

Poly (tBENI-*b*-tBA) (16). The product was recovered as a hard, white solid in 38% yield. GPC: $M_n = 25300$, $M_w/M_n = 1.10$. IR: 2978, 2931, 1980, 1731, 1456, 1417, 1393, 1368, 1326, 1257, 1153, 846, 737, 701. ^1H NMR: δ 1.20-1.80 (m, 9n + 10.5m H), 1.80-2.00 (m, 0.5m H), 2.00-2.30 (m, n H + m H), 2.70-3.40 (m, 4n H), 4.05 (s, 2n H), 5.40-5.80 (d, 2n H).

Poly (NBNI-*b*-tBA) (17). The product was recovered as a hard, white solid in 60% yield. GPC: $M_n = 26800$, $M_w/M_n = 1.07$. IR: 2978, 2944, 2873, 1771, 1728, 1700, 1480, 1448, 1394, 1367, 1258, 1150, 1038, 846, 751. $^1\text{H NMR}$: δ 0.80-1.00 (m, 3n H), 1.20-2.00 (m, 6n + 11m H), 1.95-2.40 (m, n H + m H), 2.60-3.60 (m, 5n H), 5.40-5.80 (d, 2n H).

Poly (NMONI-*b*-tBA) (18). The product was recovered as a hard, white solid in 43% yield. GPC: $M_n = 28000$, $M_w/M_n = 1.06$. IR: 2978, 2932, 1728, 1447, 1393, 1368, 1257, 1149, 1034, 846, 752. $^1\text{H NMR}$: δ 1.20-2.00 (m, 11m H), 2.10-2.40 (m, m H) 2.85-3.00 (s, 3n H), 3.20-3.45 (s, 2n H), 4.30-4.60 (m, nH), 4.70-5.00 (m, n H), 5.70-6.10 (m, 2n H).

References

- (1) (a) For recent reviews see: (a) Yagci, Y.; Tasdelen, M. A. *Prog. Polym. Sci.* **2006**, *31*, 1133–1170. (b) Lopez, R. G.; D'Agosto, F.; Boisson, C. *Prog. Polym. Sci.* **2007**, *32*, 419–454. See also: (c) You, Y. Z.; Hong, C. Y.; Wang, W. P.; Lu, W. Q.; Pan, C. Y. *Macromolecules* **2004**, *37*, 9761–9767. (d) Stalmach, U.; de Boer, B.; Videlot, C.; van Hutten, P. F.; Hadziioannou, G. *J. Am. Chem. Soc.* **2000**, *122*, 5464–5472. (e) Mahanthappa, M. K.; Bates, F. S.; Hillmyer, M. A. *Macromolecules* **2005**, *38*, 7890–7894.
- (2) Braunecker, W. A.; Matyjaszewski, K. *Prog. Polym. Sci.* **2008**, *33*, 93–165.
- (3) Bielawski, C. W.; Grubbs, R. H. *Prog. Polym. Sci.* **2007**, *32*, 1–29.
- (4) (a) Li, M. H.; Keller, P.; Albouy, P. A. *Macromolecules* **2003**, *36*, 2284–2292. (b) Coca, S.; Paik, H. J.; Matyjaszewski, K. *Macromolecules* **1997**, *30*, 6513–6516. (c) Charvet, R.; Novak, B. M. *Macromolecules* **2004**, *37*, 8808–8811. (d) Cheng, C.; Khoshdel, E.; Wooley, K. L. *Nano Lett.* **2006**, *6*, 1741–1746. (e) Kriegel, R. M.; Rees, W. S.; Weck, M. *Macromolecules* **2004**, *37*, 6644–6649. (f) Morandi, G.; Mantovani, G.; Montebault, V.; Haddleton, D. M.; Fontaine, L. *New J. Chem.* **2007**, *31*, 1826–1829. (g) Morandi, G.; Montebault, W.; Pascual, S.; Legoupy, S.; Fontaine, L. *Macromolecules* **2006**, *39*, 2732–2735. (h) Runge, M. B.; Dutta, S.; Bowden, N. B. *Macromolecules* **2006**, *39*, 498–508.
- (5) Liaw, D. J.; Huang, C. C.; Ju, I. Y. *J. Poly. Sci., Part A: Polym. Chem.* **2006**, *44*, 3382–3392.
- (6) (a) Bielawski, C. W.; Morita, T.; Grubbs, R. H. *Macromolecules* **2000**, *33*, 678–680. (b) Katayama, H.; Fukuse, Y.; Nobuto, Y.; Akamatsu, K.; Ozawa, F. *Macromolecules* **2003**, *36*, 7020–7026.
- (7) (a) Bielawski, C. W.; Louie, J.; Grubbs, R. H. *J. Am. Chem. Soc.* **2000**, *122*, 12872–12873. (b) Burtscher, D.; Saf, R.; Slugovc, C. *J. Poly. Sci., Part A: Polym. Chem.* **2006**, *44*, 6136–6145.
- (8) Murphy, J. J.; Kawasaki, T.; Fujiki, M.; Nomura, K. *Macromolecules* **2005**, *38*, 1075–1083.
- (9) Hilf, S.; Berger-Nicoletti, E.; Grubbs, R. H.; Kilbinger, A. F. M. *Angew. Chem., Int. Ed.* **2006**, *45*, 8045–8048.
- (10) Hilf, S.; Kilbinger, A. F. M. *Macromol. Rapid Comm.* **2007**, *28*, 1225–1230.
- (11) Hilf, S.; Hanik, N.; Kilbinger, A. F. M. *J. Poly. Sci., Part A: Polym. Chem.* **2008**, *46*, 2913–2921.

- (12) Hilf, S.; Grubbs, R. H.; Kilbinger, A. F. M. *J. Am. Chem. Soc.* **2008**, *130*, 11040–11048.
- (13) (a) Choi, T. L.; Grubbs, R. H. *Angew. Chem., Int. Ed.* **2003**, *42*, 1743–1746. (b) Camm, K. D.; Castro, N. M.; Liu, Y. W.; Czechura, P.; Snelgrove, J. L.; Fogg, D. E. *J. Am. Chem. Soc.* **2007**, *129*, 4168–4169.
- (14) Matson, J. B.; Grubbs, R. H. *J. Am. Chem. Soc.* **2008**, *130*, 6731–6733.
- (15) Owen, R. M.; Gestwicki, J. E.; Young, T.; Kiessling, L. L. *Org. Lett* **2002**, *4*, 2293–2296.
- (16) Liu, B.; Duan, S. Q.; Sutterer, A. C.; Moeller, K. D. *J. Am. Chem. Soc.* **2002**, *124*, 10101–10111.
- (17) (a) Xia, Y.; Verduzco, R.; Grubbs, R. H.; Kornfield, J. A. *J. Am. Chem. Soc.* **2008**, *130*, 1735–1740. (b) Bielawski, C. W.; Scherman, O. A.; Grubbs, R. H. *Polymer* **2001**, *42*, 4939–4945.
- (18) (a) Nguyen, S. T.; Grubbs, R. H.; Ziller, J. W. *J. Am. Chem. Soc.* **1993**, *115*, 9858–9859. (b) Wu, Z.; Wheeler, D. R.; Grubbs, R. H. *J. Am. Chem. Soc.* **1992**, *114*, 146–151. (c) Walker, R.; Conrad, R. M.; Grubbs, R. H. *Macromolecules* **2009**, *42*, 599–605.
- (19) Pangborn, A. B.; Giardello, M. A.; Grubbs, R. H.; Rosen, R. K.; Timmers, F. J. *Organometallics* **1996**, *15*, 1518–1520.
- (20) Love, J. A.; Morgan, J. P.; Trnka, T. M.; Grubbs, R. H. *Angew. Chem., Int. Ed.* **2002**, *41*, 4035–4037.
- (21) See Chapter 2.

Chapter 5

Monotelechelic Poly(oxa)norbornenes by Ring-Opening Metathesis

Polymerization using Direct End-Capping and Cross Metathesis

Abstract

Two different methodologies for the end-functionalization of poly(oxa)norbornenes prepared by living ring-opening metathesis polymerization (ROMP) are presented. The first method, termed direct end-capping, is carried out by adding an internal *cis*-olefin terminating agent (TA) to the reaction mixture immediately after the completion of the living ROMP reaction. The second method relies on cross metathesis (CM) between a methylene-terminated poly(oxa)norbornene and a *cis*-olefin TA mediated by the ruthenium olefin metathesis catalyst $(\text{H}_2\text{IMes})(\text{Cl})_2\text{Ru}(\text{CH}-o\text{-OiPrC}_6\text{H}_4)$ ($\text{H}_2\text{IMes} = 1,3\text{-dimesitylimidazolidine-2-ylidene}$). TAs containing various functional groups, including alcohols, acetates, bromides, α -bromoesters, thioacetates, *N*-hydroxysuccinimidyl esters, and Boc-amines, as well as fluorescein and biotin groups, were synthesized and tested. The direct end-capping method typically resulted in >90% end-functionalization efficiency, while the CM method was nearly as effective for TAs without polar functional groups or significant steric bulk. End-functionalization efficiency values were determined by ^1H NMR spectroscopy.

Introduction

Ring-opening metathesis polymerization (ROMP) has become a widely used method for the synthesis of both industrially relevant and academically interesting polymers.¹ Among the many types of interesting polymer architectures accessible by ROMP are block,² hyperbranched,³ dendronized,⁴ brush,⁵ and cyclic polymers.^{6,4c} Many of these architectures can be produced with a high degree of molecular weight control and with narrow polydispersities. Control of both polymer architecture and molecular

weight is a result of developments in olefin metathesis catalyst design, using mainly ruthenium and molybdenum catalysts.⁷ With the wide variety of polymers that olefin metathesis catalysts have enabled, it is remarkable that narrow polydispersity, telechelic ROMP polymers remain difficult to prepare.

Telechelic polymers are linear polymers in which a desired functionality is placed at one (monotelechelic) or both (ditelechelic) of the chain ends. Functionalized chain ends can then be used for a number of applications, including growing another polymer block using a different polymerization mechanism,⁸ attaching biomolecules,⁹ or cyclizing to form cyclic polymers.¹⁰ A number of strategies for making low polydispersity, telechelic ROMP polymers have been employed to produce hybrid block copolymers,¹¹ fluorescent polymers,¹² and graft polymers.¹³ However, the synthetic methods currently available for producing narrow polydispersity, telechelic ROMP polymers all result in either less than quantitative end-capping or are limited in the types of functional groups that can be appended to the chain end.

Telechelic ROMP polymers are traditionally synthesized by reacting a small, strained olefin such as norbornene or cyclooctene with an internal olefin chain transfer agent (CTA) in the presence of an olefin metathesis catalyst.¹⁴ At thermodynamic equilibrium, every CTA molecule is incorporated into the polymer chain, and the molecular weight is controlled by controlling the monomer to CTA molar ratio. The resulting polymers have high degrees of chain-end-functionality, but because the polymerization mechanism is dominated by chain transfer, the products have polydispersity indexes (PDIs) of around 2.0. High PDIs are acceptable for some

purposes, but low PDIs are required for many applications, such as when specific morphologies of block copolymers are desired.

Methods for synthesizing low PDI, telechelic ROMP polymers have been developed by several groups over the past decade. The custom initiator method is one such process, by which a ROMP initiator is synthesized, isolated, and then used to initiate polymerization.^{12,15} The custom initiator method can be effective, but it has the drawback that a new catalyst must be made for each new chain-end-functionality. Synthesis of new olefin metathesis catalysts can be difficult and low yielding, especially when complex functionality is desired. In a different strategy, custom TAs have also been used to produce monotelechelic ROMP polymers.¹⁶ In the case of ruthenium-mediated ROMP, functionalized vinyl ethers are most commonly used to simultaneously end-cap a growing polymer chain and deactivate the metathesis catalyst. Typically end-capping is not complete with functionalized vinyl ethers, as we have shown previously.^{11f} Other TAs include acrylates,¹⁷ as well as vinyl lactones and vinyl carbonates.¹⁸ Aldehydes can be used very effectively as terminators in molybdenum-mediated ROMP,^{11d,19} but the lack of air, moisture, and functional group tolerance of molybdenum metathesis catalysts limits this process to polymers with minimal functionality. Another more recent end-functionalization strategy is the sacrificial monomer method.²⁰ The sacrificial monomer method requires the synthesis of a block copolymer with one block comprised of the desired monomer and the other block comprised of a readily degradable monomer. Subsequent degradation of the sacrificial block yields an end-functionalized polymer. The sacrificial monomer method is quite effective, but it is limited to only a

few functional groups, all of which must be further derivatized after polymerization to add any additional functionality.

We recently described a direct method of ROMP polymer end-capping utilizing an internal *cis*-olefin as a TA.^{11f} Because the backbone olefins of substituted poly(oxa)norbornenes are too sterically hindered to undergo metathesis, the TA adds only to the ω end of the polymer. Any further metathesis reactions are degenerate. Using a TA containing α -bromoester groups, we observed complete end-capping to form a low polydispersity, monotelechelic polymer with an α -bromoester group. Subsequent atom-transfer radical polymerization (ATRP), using the end-capped polynorbornene as a macroinitiator, showed a complete shift in the GPC peaks from homopolymer to block copolymer, indicating that end-capping was quantitative and occurred only on the ω end of the polymer. We also recently reported an extension of this method to ditelechelic polymers by reacting the catalyst with the desired symmetrical *cis*-olefin before addition of monomer.²¹ Now we report on the development of this direct end-capping method to include other functional groups. In addition, we describe a post-polymerization method of end-functionalization of the ω -end of ROMP polymers using cross metathesis.

Results and Discussion

Recently, pyridine-containing ruthenium olefin metathesis catalysts **1** and **2** (Figure 1) have found use as mediators of ROMP due to their fast-initiation rates and high functional group tolerance.^{2d,16c,22} Catalysts **1** and **2** have been shown to effect the living ROMP of a wide variety of strained cyclic olefin monomers, including many with high levels of functionality, such as saccharides,^{22b,23} peptides,²⁴ and charged groups.^{22d,25}

All new TAs were designed with these criteria in mind. In addition, TAs **6** and **7** (Figure 2), which are known to be active cross metathesis substrates, were included in this study.

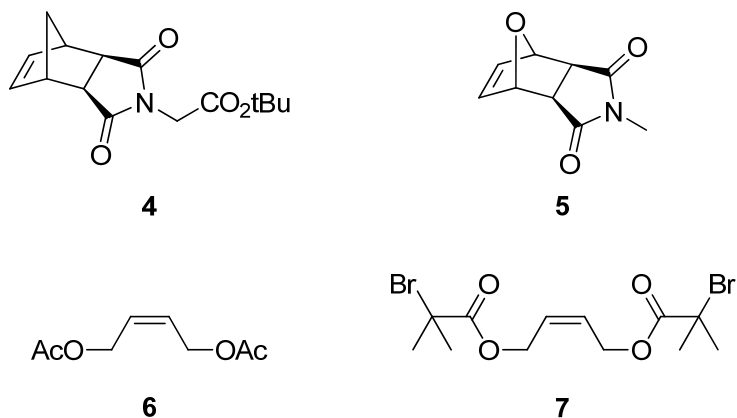
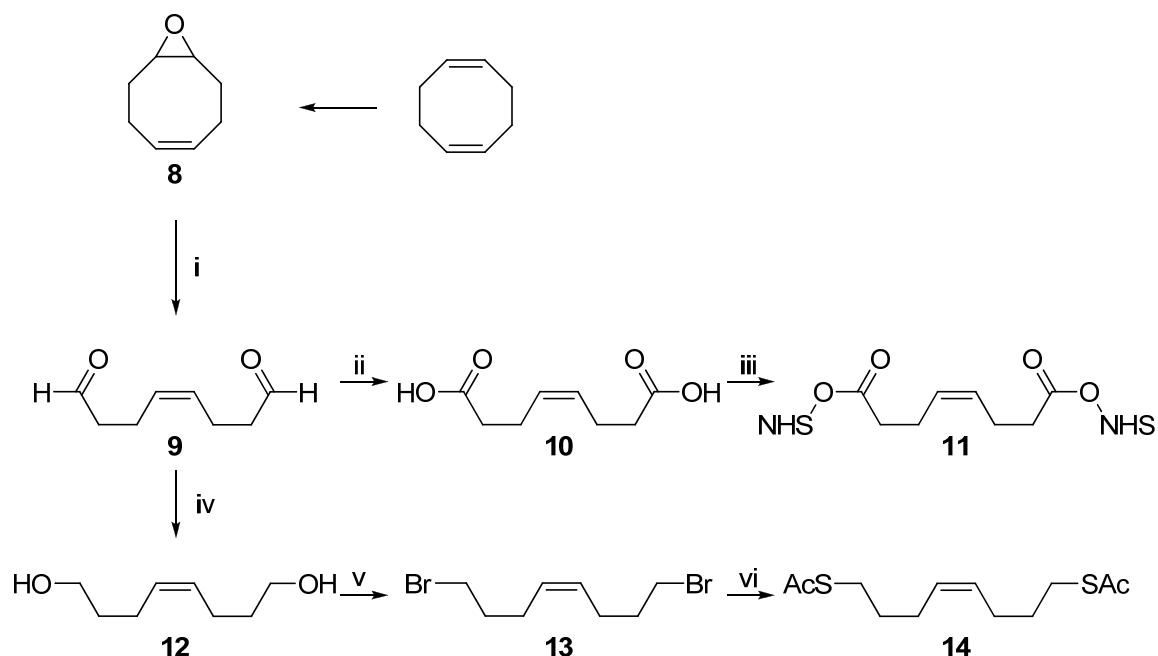


Figure 5.2. Monomers (**4** and **5**) and previously reported TAs (**6** and **7**) used in this study.

TA Syntheses

To quickly synthesize a variety of TAs with varying functionality, we began with previously reported epoxide **8**.²⁷ Oxidation of **8** using periodic acid afforded dial **9**, which was further oxidized using Jones reagent to diacid **10**. Diacid **10** was derivatized to NHS ester-containing TA **11** by an EDC coupling reaction to enable amine conjugation to a polynorbornene terminus. Reduction of dial **9** to diol **12** was accomplished using NaBH₄. Diol **12** was then converted to dibromide **13**, with potential use in copper-catalyzed azide-alkyne cycloaddition when converted to the azide after end-capping, a process that has been demonstrated using a similar TA.²⁸ A diazide TA was also synthesized from dibromide **13**, but it was found to quickly deactivate the metathesis catalyst. Finally, dibromide **13** was converted to dithioacetate **14** using potassium thioacetate. Removal of the acetate groups using LiAlH₄ to afford a dithiol

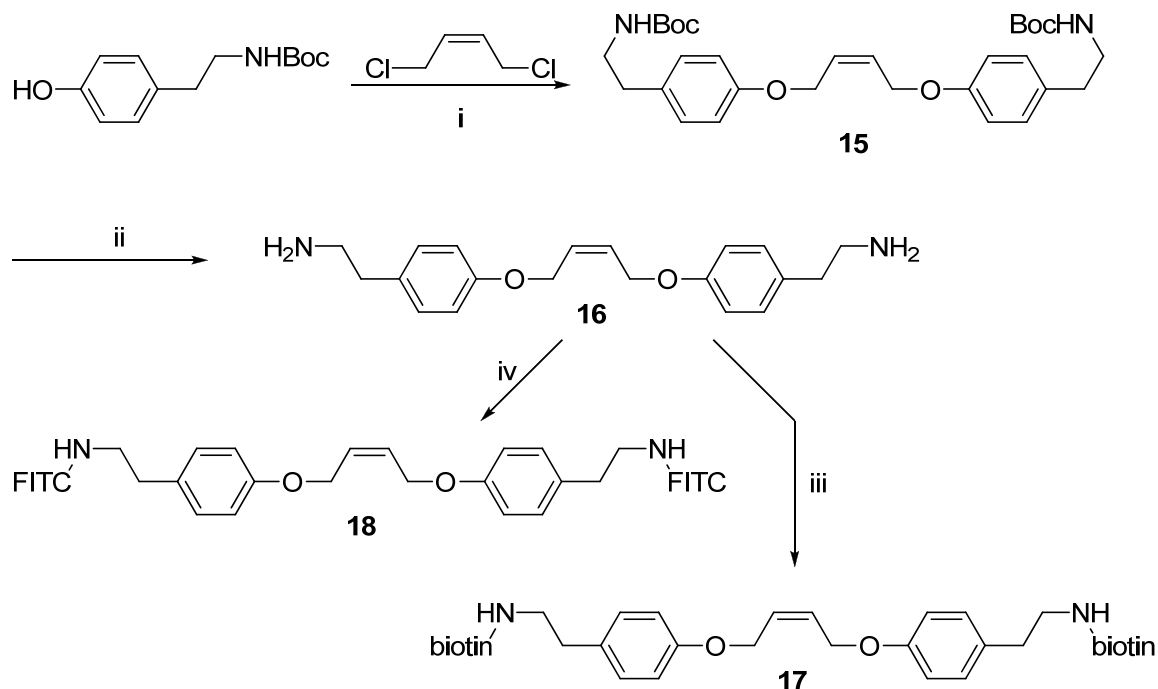
was successful, but the resulting TA appeared to be incompatible with the metathesis catalyst.



Scheme 5.1. Synthesis of Several Functionalized Internal *cis*-Olefins for Poly(oxa)norbornene End-Functionalization. Reagents and conditions: (i) I(O)(OH)₅, *p*-dioxane/H₂O, 0 °C to rt; (ii) Jones reagent, acetone, 0 °C to rt; (iii) N-hydroxysuccinimide, EDC, DPTS, CH₂Cl₂, rt; (iv) NaBH₄, Et₂O/EtOH, 0 °C to rt; (v) CBr₄, PPh₃, CH₂Cl₂, 0 °C to rt; (vi) KSAc, DMF, 65 °C.

In order to incorporate olefins with allylic substitution into this study, we also synthesized a Boc-amine-containing TA (**15**) by the reaction of 1,4-dichloro-*cis*-2-butene with Boc-tyramine (Scheme 2). Removal of the Boc-groups using trifluoroacetic acid afforded diamine **16**. Coupling of diamine **16** with biotin using EDC afforded the biotin-containing TA, **17**. Biotin end-capped polynorbornenes have been reported once before using 30 equiv of a functionalized vinyl ether;²⁹ a method that requires less of the expensive and difficult to remove biotin TA could be useful for biological applications of ROMP polymers. A fluorescein-containing TA (**18**) was also synthesized from diamine

16 by addition of fluorescein isothiocyanate (FITC). With a set of symmetrical *cis*-olefins with varied functionality in hand, we set out to examine their reactivity in end-functionalization reactions.

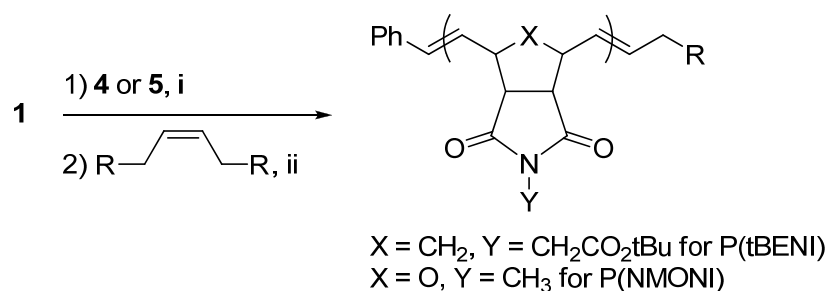


Scheme 5.2. Synthesis of NHBoc, FITC, and Biotin-Containing TAs. Reagents and conditions: (i) K_2CO_3 , DMF, 90 °C; (ii) TFA, CH_2Cl_2 , rt; (iii) biotin, EDC, DPTS, DMF, rt; (iv) FITC, DMF, rt.

End-functionalization by direct end-capping

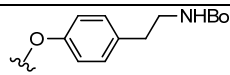
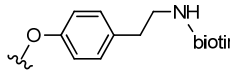
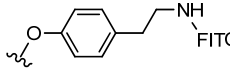
Using our previously described method,^{11f} end-capping of P(tBENI) or P(NMONI) chains with TAs **6**, **7**, **9**, **11-15**, **17**, and **18** was carried out (Scheme 3). Briefly, a solution of catalyst **1** was injected into a rapidly stirring vial of monomer **4** (25 equiv) in CH_2Cl_2 under argon on the benchtop. After 3 min, the desired TA (5 equiv) was added as a solution in CH_2Cl_2 or MeOH (for TAs **17** and **18**). Biotin-containing TA

17 was not soluble in MeOH at the concentrations used, so it was added as a slurry. The reaction mixture was stirred at room temperature under argon for an additional 6 h, at which point ethyl vinyl ether was added to quench the reaction. The polymer products were isolated in high purity in most cases by precipitation of the reaction mixture into a large volume of diethyl ether/hexanes (or isopropanol/hexanes) (1:1), followed by filtration and washing with diethyl ether. In cases where the TA was not soluble in the precipitation solvent mixture, the precipitated polymer products were further purified by dialyzing the reaction mixture against DMSO or DMF and then water, followed by lyophilization. NMR spectroscopy was used to confirm complete removal of the excess TA. Carboxylic acid-containing TA **10** and primary amine-containing TA **16** were found to deactivate the catalyst, presumably due to coordination to the metal center. All polymers were characterized by gel permeation chromatography (GPC) and showed the expected narrow polydispersity and molecular weight of approximately 7000 Daltons.



Scheme 5.3. End-functionalization of P(tBENI) or P(NMONI) using the direct end-capping method. Reagents and conditions: (i) CH_2Cl_2 , rt, 3 min; (ii) CH_2Cl_2 or MeOH, rt, 6 h.

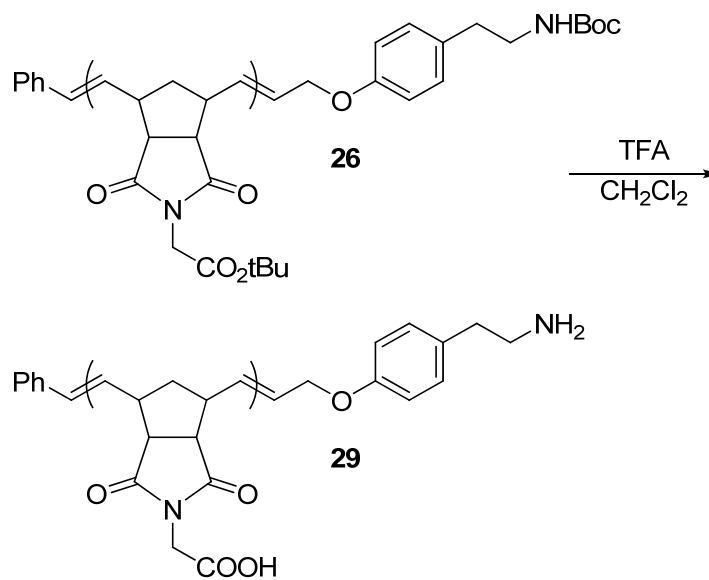
Table 5.1. End-capping Efficiency of P(tBENI) or P(NMONI) Polymers using the Direct End-Capping Method.

Entry	TA	R =	% efficiency ^a
19	6	OAc	97
20	7	OC(O)C(CH ₃) ₂ Br	>98
21	9	CH ₂ C(O)H	59
22	11	CH ₂ C(O)NHS	80
23	12	CH ₂ CH ₂ OH	97
24	13	CH ₂ CH ₂ Br	>98
25	14	CH ₂ CH ₂ SAc	91
26	15		>98
27	17		93
28	18		>98

^aEfficiency determined from the ¹H NMR integral ratio of the phenyl end group protons derived from catalyst **1** to the newly-installed end group protons.

¹H NMR spectroscopy was used to evaluate the percentage of end-capping by comparing the integral values of the phenyl end groups derived from catalyst **1** with the integral values of the appended functional group. A relaxation delay of 10 s was used to ensure precise integral values, and NMR spectra were taken on a 500 MHz spectrometer for a high level of resolution. The results, summarized in Table 1, show that most TAs are capable of near-quantitative end-capping. Notably, FITC-containing TA **18** showed a high degree of end-capping, providing a simple, direct method to fluorescent,

monotelechelic polynorbornenes. Biotin-containing TA **17**, which is only sparingly soluble in CH₂Cl₂/MeOH mixtures, reached 93% end-capping efficiency, indicating that the direct end-capping methodology is sufficiently robust to compensate for poorly soluble TAs.



Scheme 5.4. Removal of Boc and *tert*-Butyl Ester Groups to Afford Amine-Terminated Polynorbornene.

To synthesize an amine-terminated polynorbornene, polymer **26** was treated with trifluoroacetic acid in CH₂Cl₂ to remove the Boc protecting group as well as the *tert*-butyl ester groups on the repeating units (Scheme 4). ¹H NMR spectroscopy showed complete removal of both the Boc and the *tert*-butyl ester groups, affording amine-terminated poly(carboxymethylene norbornene imide) (P(CMNI)) **29**. This simple route to amine-terminated ROMP polymers may prove useful for appending biomolecules or other large groups to polymer termini using standard amine-carboxylic acid coupling chemistry.

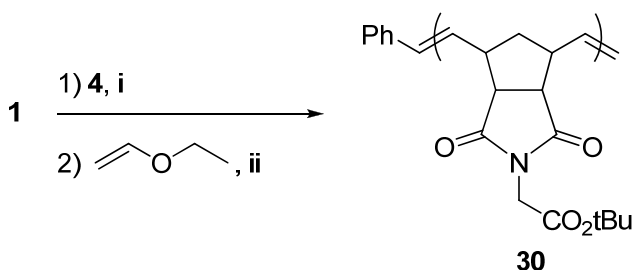
End-functionalization using CM

As an alternative to direct end-capping, we sought to develop a post-polymerization method for poly(oxa)norborene end-functionalization. Post-polymerization end-functionalization would provide an alternative route to monotelechelic polynorbornenes that might be useful in cases where direct end-capping is not feasible due to solubility or other concerns. Noting that most ROMP reactions are quenched with ethyl vinyl ether, we thought CM would be an effective end-capping reaction. Uses of CM in polymer synthesis remain almost exclusively limited to acyclic-diene metathesis polymerization (ADMET).^{1a} Considering the capability of CM to make highly-functional olefins in small molecules, we sought to extend the use of CM in polymer synthesis to polymer end-functionalization.

Previous studies in our group have shown that CM between a terminal olefin and a disubstituted olefin is a highly effective method for olefin homologation and functionalization.³⁰ In fact, CM between a terminal olefin and an internal, disubstituted olefin is considerably more effective than CM between two terminal olefins. This result is attributed to the greater stability of a propagating ruthenium alkylidene versus a propagating ruthenium methylidene.³¹ In a CM reaction between a terminal olefin and a disubstituted olefin, the propagating ruthenium alkylidene is greatly favored over the methylidene. The TAs described earlier in this study represent a group of internal olefins that would be expected to perform well in CM and showed high reactivity in direct end-capping. We used these same TAs in the CM portion of this study for the sake of convenience and to compare the efficiencies of the two methods, but it should be noted that *trans*-olefins or mixtures of *cis*- and *trans*-olefins would be expected to perform

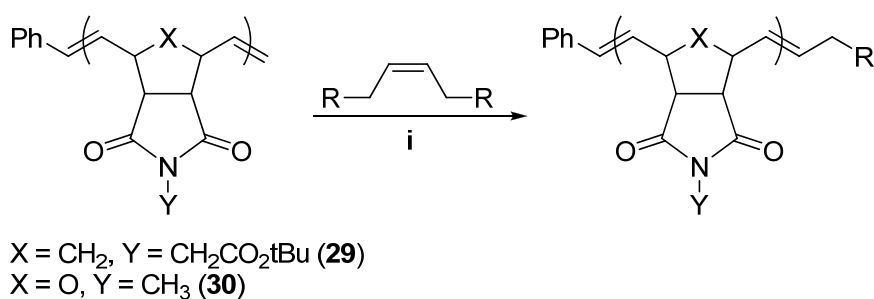
similarly because in CM *cis*-olefins are often quickly isomerized to their *trans* forms, indicating that the initial stereochemistry of the olefin is irrelevant.

To prepare an olefin-terminated polymer to act as the terminal olefin cross partner, the ROMP of monomer **4** was again carried out using catalyst **1** (Scheme 5). P(tBENI) polymer **30** was prepared by injecting catalyst **1** from a stock solution into a vigorously stirring solution of monomer **4** (25 equiv). After 3 min polymerization was terminated using ethyl vinyl ether to end-cap the polymer with a methylene end group. Polymer **30** showed the low PDI and controllable molecular weight expected from catalyst **1**. As noted earlier, previous work from our group has indicated that end-capping using vinyl ethers does not result in 100% end-capping with a terminal olefin.^{11f} The remaining end groups are believed to be vinyl ethers derived from ethyl vinyl ether termination. We assumed that the vinyl ether-capped portion of polymer **30**, which is not visible by ¹H NMR spectroscopy due to overlapping signals with backbone protons, would also be active in CM when run at the temperatures and with catalyst loadings described here.



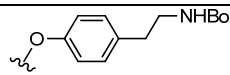
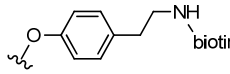
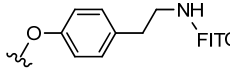
Scheme 5.5. Synthesis of methylene-capped P(tBENI). Reagents and conditions: (i) CH₂Cl₂, 3 min, rt; (ii) rt, 15 min.

We chose to use the chelating-ether ruthenium olefin metathesis catalyst $(\text{H}_2\text{IMes})(\text{Cl})_2\text{Ru}(\text{CH-}o\text{-OiPrC}_6\text{H}_4)$ (H_2IMes = 1,3-dimesitylimidazolidine-2-ylidene) (**3**) in this study due to its longer lifetime and higher efficiency in CM than catalysts **1** and **2**. A solvent screen showed that toluene was the best solvent for this reaction, with common metathesis solvents THF and CH_2Cl_2 performing considerably worse. The optimal temperature was found to be $40\text{ }^\circ\text{C}$, at which the reaction was complete in 12 h and there was no significant loss of the phenyl end group on the α end of the polymer. Higher temperatures led to some cross metathesis of the phenyl-norbornenyl internal olefin. Under no circumstances, including higher temperatures, higher catalyst loadings, and longer reaction times, was there any indication that the backbone norbornenyl-norbornenyl olefins underwent metathesis, as indicated by GPC before and after CM. Additionally, our group previously reported that CM between two methylene-capped polymer chains can be used to dimerize the polymer;³² we observed no polymer-polymer CM when TA was present.



Scheme 5.6. End-functionalization of P(tBENI) or P(NMONI) using cross metathesis. Reagents and conditions: (i) catalyst **3** (50 mol% relative to polymer), toluene or toluene/MeOH, $40\text{ }^\circ\text{C}$, 12 h.

Table 5.2. End-capping Efficiency of P(tBENI) or P(NMONI) Polymers using Cross Metathesis.

Entry	TA	R =	% efficiency ^a
31	6	OAc	89
32	7	OC(O)C(CH ₃) ₂ Br	>90
33	9	CH ₂ C(O)H	36
34	11	CH ₂ C(O)NHS	44
35	12	CH ₂ CH ₂ OH	60
36	13	CH ₂ CH ₂ Br	>90
37	14	CH ₂ CH ₂ SAc	70
38	15		>90
39	17		69
40	18		40

^aEfficiency determined from the ¹H NMR integral ratio of the phenyl end group protons derived from catalyst **1** to the newly-installed end group protons.

Using the optimized conditions of catalyst **3** (50 mol% relative to polymer) in toluene at 40 °C for 12 h with 5 equiv of TA, we examined the CM of polymers **19** and **20** on TAs **6**, **7**, **9**, **11-15**, **17**, and **18** (Scheme 6). All reactions were run under argon on the benchtop, and end-capping reactions using **17** and **18** were run in 4:1 toluene/methanol to aid in solubility. The polymer products were isolated using the same procedures as described in the direct end-capping section. The results from the CM reactions are summarized in Table 2. TAs **6**, **7**, **13**, and **15** showed high degrees of end-

capping efficiency (>85%), as was seen using the direct end-capping method, indicating that polymer end-functionalization using the CM method is highly efficient when sterically unencumbered TAs and TAs without polar functionalities are used. TAs containing polar functional groups were generally less effective, with dial TA **9** and diol TA **12** showing only 36 and 60% end-functionalization efficiency, respectively. The polar functional groups on TAs **9**, **11**, and **12** may limit the efficiency of CM only for these particular TAs due to coordination of the Lewis basic functionality to the metal center after the initial metathesis event, but further studies on TAs with longer spacer groups between the olefin and the functional group are warranted.

We attribute the higher efficiency of the direct end-capping method compared with the CM method to the necessity for only a single metathesis turnover in the case of direct end-capping. In the case of CM, several metathesis steps need to occur to effect end-functionalization, including reaction of the TA with the catalyst, reaction of the functionalized catalyst with the polymer chain end, and productive metathesis to release the catalyst and functionalized polymer. The CM method, while generally not as effective as the direct end-capping method, may prove useful in cases where a TA is not soluble in CH_2Cl_2 or in cases where the study of a single batch of polymer with varying end groups is needed. Moreover, this method facilitates the synthesis and use of poly(oxa)norbornenes as pivotal macromolecular building blocks which can be prepared on large scale, stored indefinitely, then functionalized as desired. Additionally, it should be noted that this methodology is not limited to polynorbornenes; theoretically CM would be capable of end-functionalizing many olefin-terminated polymers.

Conclusions

We have presented two methods for the end-functionalization of poly(oxa)norbornenes to afford monotelechelic ROMP polymers. The direct end-capping method involves a single metathesis turnover between the ruthenium metal center on a living polymer chain and an internal olefin TA. This method was found to be highly effective for a wide variety of TAs, including fluorescein and biotin-containing TAs, demonstrating the versatility of this approach. We expect that the direct end-capping methodology will find use in a variety of areas, including bioconjugation, surface attachment, and in the synthesis of mechanistically incompatible block copolymers. The CM method is a two-step procedure requiring termination of ROMP with ethyl vinyl ether, followed by CM of the methylene-capped polymer with an internal olefin TA. Though generally less effective than direct end-capping, end-functionalization by CM may also find use in cases where direct end-capping is not feasible or with olefin-terminated polymers made by methods other than ROMP.

Acknowledgment

The author thanks Materia for catalyst. Paul G. Clark and Yan Xia are also acknowledged for generous donations of DPTS and TA **7**, respectively. The author also thanks Paul G. Clark for NMR assistance. Dr. Andrew J. Boydston, Yan Xia, and Dr. Ron Walker are acknowledged for helpful discussions.

Experimental Section

General Information

NMR spectra of small molecules were measured in CDCl_3 on Varian Mercury 300 MHz spectrometers unless otherwise noted. NMR spectra of polymers were measured on Varian Inova 500 or 600 MHz spectrometers with a relaxation delay of 10 s in CD_2Cl_2 unless otherwise noted. ^1H and ^{13}C NMR chemical shifts are reported in ppm relative to proteosolvent resonances. Flash column chromatography of organic compounds was performed using silica gel 60 (230-400 mesh). High-resolution mass spectra (EI and FAB) were provided by the California Institute of Technology Mass Spectrometry Facility. Gel permeation chromatography (GPC) was carried out in THF on two PLgel 10 μm mixed-B LS columns (Polymer Labs) connected in series with a DAWN EOS multiangle laser light scattering (MALLS) detector and an Optilab DSP differential refractometer (both from Wyatt Technology). No calibration standards were used, and the dn/dc values used were 0.109 for tBENI polymers and 0.135 for NMONI polymers, as calculated by averaging several runs assuming 100% mass elution from the columns.

Materials

CH_2Cl_2 , Et_2O and toluene were purified by passage through solvent purification columns and degassed.³³ MeOH was dried over Mg and distilled. Anhydrous DMF was obtained from Acros Chemical Company and used as received. $(\text{H}_2\text{IMes})(\text{PCy}_3)(\text{Cl})_2\text{RuCHPh}$ and $(\text{H}_2\text{IMes})(\text{Cl})_2\text{RuCH}(o\text{-OiPrC}_6\text{H}_4)$ (**3**) were provided by Materia. $(\text{H}_2\text{IMes})(\text{pyr})_2(\text{Cl})_2\text{RuCHPh}$ (**1**) was prepared from

(H₂IMes)(PCy₃)(Cl)₂RuCHPh according to a literature procedure.³⁴ *tert*-Butyl ester norbornene imide (**4**) was prepared as described previously.^{11f} *cis*-2-Butene-1,4-diyl bis(2-bromo-2-methylpropanoate) (**6**) was prepared similarly to a procedure described previously.^{11f} *cis*-1,4-Dichloro-2-butene was obtained from Aldrich Chemical Company and distilled prior to use. *cis*-1,2-Epoxy-5-cyclooctene (**8**) and *cis*-4-octene-1,8-diol (**12**) were prepared according to a literature procedure.²⁷ Deuterated solvents were obtained from Cambridge Isotope Labs. Dimethylaminopyridium *p*-toluene sulfonate (DPTS) was prepared according to a literature procedure.³⁵ All other materials, including *N*-(3-dimethylaminopropyl)-*N'*-ethylcarbodiimide (EDC), were obtained from Aldrich Chemical Company and used as received.

***cis*-4-Octene-1,8-dial (9)**. To a solution of *cis*-1,2-epoxy-5-cyclooctene (**8**) (1.00 g, 1 equiv) in *p*-dioxane (10 mL) at 0 °C was added periodic acid (2.12 g, 1.15 equiv) dropwise in 10 mL H₂O. The reaction mixture was allowed to warm to room temperature. After 2.5 h, the reaction mixture was extracted with Et₂O (3 x 30 mL). The combined organic layers were dried over Na₂SO₄, and the residue was purified by Kugelrohr distillation to afford **9** as a clear oil in 58% yield (650 mg). ¹H NMR: δ 2.38 (m, 4H), 2.56 (m, 4H), 5.28 (t, *J* = 4.5 Hz, 2H), 9.76 (m, 2H). ¹³C NMR: δ 201.99, 120.04, 43.69, 20.11. HRMS: calculated: 140.0837; found: 140.0832.

***cis*-4-Octene-1,8-dioic acid (10)**. To a solution of dial **9** (400 mg, 1 equiv) in acetone (20 mL) at 0 °C was added Jones reagent dropwise until the orange color persisted. The reaction mixture was then allowed to stir at room temperature. After 90

min the acetone was removed *in vacuo* and the green residue was taken up in H₂O (20 mL). The H₂O layer was extracted with EtOAc (3 x 25 mL), and the combined organic layers were washed with brine (10 mL) and dried over Na₂SO₄. Removal of the solvent *in vacuo* yielded a white powder that was recrystallized from EtOAc/hexanes to afford **10** as a white solid in 60% yield (293 mg). ¹H NMR (10% CD₃OD in CDCl₃): δ 2.30-2.39 (m, 8H), 4.96 (br s, 2H), 5.37 (t, *J* = 4.5 Hz, 2H). ¹³C NMR: δ 177.11, 129.12, 34.08. 22.75. HRMS: calculated: 172.0736; found: 172.0738.

***cis*-4-Octene-1,8-bis(N-hydroxysuccinimidyl) ester (11)**. An oven-dried, 2-necked, round-bottom flask under argon was charged with diacid **10** (100 mg, 1 equiv). CH₂Cl₂ (5 mL) was added to the flask, followed by EDC (657 mg, 5.9 equiv) and DPTS (30 mg, 0.2 equiv). N-hydroxysuccinimide (348 mg, 5.2 equiv) was added, and the reaction mixture was allowed to stir at room temperature. After 20 h H₂O (10 mL) was added, and the CH₂Cl₂ layer was separated off, washed with brine and dried over Na₂SO₄. The crude product was purified by passage through a plug of silica (eluting with EtOAc) followed by recrystallization from toluene or toluene/hexanes to afford **11** as a white powder in 39% yield (84 mg). ¹H NMR (acetone-*d*₆): δ 2.52 (m, 4H), 2.72 (t, *J* = 6.9 Hz, 4H), 2.80-2.95 (m, 8H), 5.54 (t, *J* = 4.8 Hz, 2H). ¹³C NMR (acetone-*d*₆): δ 170.59, 169.33, 129.63, 31.30, 26.34, 23.11. HRMS: calculated: 367.1141; found: 367.1139.

***cis*-4-Octene-1,8-dibromide (13)**. A round-bottom flask was charged with diol **7** (763 mg, 1 equiv) in CH₂Cl₂ (20 mL). CBr₄ (3.70 g, 2.1 equiv) was added, and the

reaction mixture was cooled to 0 °C. Once cool, PPh₃ (3.09 g, 2.2 equiv) was added, and the reaction mixture was allowed to warm to room temperature. After 16 h the solvent was removed *in vacuo*, affording a pale yellow oil. Hexanes (30 mL) was added, causing white solids to crash out. The suspension was stirred and sonicated, and the solids were filtered off. The filtrate was concentrated *in vacuo*, affording a pale yellow oil. The product was purified by silica gel chromatography (5% EtOAc in hexanes) to yield **13** as a clear oil in 78% yield (1.12 g). ¹H NMR: δ 1.86 (quintet, *J* = 7.2 Hz, 4H), 2.16 (m 4H), 3.35 (t, *J* = 6.6 Hz, 4H), 5.33 (m, 2H). ¹³C NMR: δ 129.43, 33.48, 32.68, 25.87. HRMS: calculated: 269.9442; found: 269.9473.

S,S'-cis-4-octene-1,8-diyl diethanethioate (14). A round-bottom flask was charged with dibromide **13** (584 mg, 1 equiv) and DMF (10 mL). Potassium thioacetate (720 mg, 2.9 equiv) was added, and the reaction mixture was heated at 65 °C. After 30 min the solvent was removed *in vacuo*. The residue was taken up in CH₂Cl₂ and filtered, and the solvent was removed *in vacuo*. The crude product was purified by silica gel chromatography (5% EtOAc in hexanes) to yield **14** as a pale orange oil in 79% yield (442 mg). ¹H NMR: δ 1.63 (quintet, *J* = 7.2 Hz, 4H), 2.12 (dd, *J* = 7.2 Hz, 5.7 Hz, 4H), 2.33 (s, 6H), 2.87 (t, *J* = 7.2 Hz, 4H), 5.37 (t, *J* = 4.5 Hz, 2H). ¹³C NMR: δ 196.06, 129.61, 30.85, 29.57, 28.82, 26.52. HRMS(M+H): calculated: 261.0983; found: 261.0994.

Boc-amine-containing TA 15. A round-bottom flask was charged with Boc-tyramine (2.30 g, 2.2 equiv), K₂CO₃ (2.02 g, 3.3 equiv), and DMF (30 mL). 1,4-

Dichloro-*cis*-2-butene (500 μ L, 1 equiv) was added, and the reaction mixture was heated at 90 $^{\circ}$ C. After 3 h the solvent was removed *in vacuo*, and the residue was taken up in CH_2Cl_2 , washed with water and brine, and dried over Na_2SO_4 . The product was purified by silica gel chromatography (2% MeOH in CH_2Cl_2) to yield **15** as a white powder in 45% yield (1.07 g). ^1H NMR: δ 1.43 (s, 18H), 2.73 (t, $J = 7.2$ Hz, 4H), 3.33 (q, $J = 6.6$ Hz, 4H), 4.52 (s, 2H), 4.65 (d, $J = 4.5$ Hz, 4H), 5.93 (t, $J = 4.5$ Hz, 2H), 6.85 (m, 4H), 7.25 (m, 4H). ^{13}C NMR: δ 157.17, 156.03, 131.59, 129.92, 128.75, 114.90, 79.28, 64.34, 42.10, 35.44, 28.56. HRMS: calculated: 527.3121; found: 527.3115.

Amine-containing TA 16. A round-bottom flask was charged with bis(Boc-amine) **15** (1.07 g, 1 equiv) in CH_2Cl_2 (20 mL). TFA (1.5 mL, 10 equiv) was added, and the flask was capped with a septum with a needle through it. After 24 h the reaction was quenched with 5% aqueous NH_4OH and then diluted with water (20 mL). The CH_2Cl_2 layer was removed, and the aqueous layer was washed with CH_2Cl_2 (3 x 15 mL). The organic layers were combined and dried over Na_2SO_4 . The solvent was removed *in vacuo* to afford **16** as a pale yellow oil in 98% yield (651 mg) in sufficient purity for future reactions. ^1H NMR: δ 2.66 (t, $J = 6.9$ Hz, 4H), 2.89 (t, $J = 6.9$ Hz, 4H), 4.63 (d, $J = 3.9$ Hz, 4H), 5.90 (t, $J = 3.3$ Hz, 2H), 6.85 (m, 4H), 7.09 (m, 4H). ^{13}C NMR: δ 156.98, 132.19, 129.89, 128.70, 114.79, 64.30, 43.58, 38.99. HRMS: calculated: 327.2073; found: 327.2067.

Biotin-containing TA 17. An oven-dried, 2-necked, round-bottom flask under argon was charged with D-biotin (173 mg, 2.6 equiv). DMF (3 mL) was added, followed

by EDC (160 mg, 3.1 equiv) and DPTS (15 mg, 0.2 equiv). Diamine **16** (88 mg, 1 equiv) was then added as a solution in DMF (3 mL). The colorless reaction mixture was allowed to stir at room temperature under argon. After 40 h the DMF was removed *in vacuo*, and the residue was triturated with H₂O. Recrystallization of the crude product from toluene/MeOH (4:1) afforded a white powder in 45% yield (95 mg). ¹H NMR (DMSO-*d*₆): δ 1.20-1.59 (m, 12H), 2.01 (t, *J* = 7.2 Hz, 4H), 2.53-2.63 (m, 6H), 2.77-2.83 (m, 2H), 3.00-3.08 (m, 4H), 3.15-3.22 (m, 4H), 4.08-4.11 (m, 4H), 4.26-4.30 (m, 2H), 4.65 (d, *J* = 3.6 Hz, 4H), 5.81 (t, *J* = 3.2 Hz, 2H), 6.34 (s, 2H), 6.40 (s, 2H), 6.84 (d, *J* = 8.4 Hz, 4H), 7.07 (d, *J* = 8.4 Hz, 4H), 7.80 (t, *J* = 5.4 Hz, 2H). ¹³C NMR (DMSO-*d*₆): δ 171.88, 162.70, 156.48, 131.69, 129.57, 128.46, 114.49, 63.77, 61.03, 59.18, 55.42, 40.29, 35.19, 34.34, 28.18, 28.04, 25.30. HRMS (M+H): calculated: 779.3625; found: 779.3629.

FITC-containing TA 18. An oven-dried, 2-necked, round-bottom flask under argon was charged with FITC (180 mg, 2.1 equiv). Diamine **10** (70 mg, 1 equiv) was then added in DMF (2 mL). The reaction vessel was covered with foil and allowed to stir at room temperature. After 16 h the solvent was removed *in vacuo*. The crude product was taken up in MeOH (1 mL) and precipitated into Et₂O (60 mL). The product was recovered by filtration to yield **12** as a bright orange powder in 80% yield (202 mg). ¹H NMR (CD₃OD): δ 2.83 (s, 4H), 2.95 (s, 2H), 3.76 (s, 4H), 4.54 (d, *J* = 3.3 Hz, 4H), 5.72 (t, *J* = 3.3 Hz, 2H), 6.48-7.09 (m, 22H), 7.56 (dd, *J* = 8.4 Hz, 1.8 Hz, 1.7 H, major isomer), 7.83 (d, *J* = 8.4 Hz, 0.3 H, minor isomer), 8.02 (s, 1.7 H, major isomer), 8.22 (s, 0.3 H, minor isomer). ¹³C NMR: δ 182.34, 171.05, 166.59, 164.82, 161.43, 158.48,

154.15, 149.63, 142.28, 141.92, 132.54, 131.96, 130.92, 130.36, 129.60, 129.07, 125.84, 119.35, 120.18, 116.24, 115.92, 113.74, 111.43, 103.57, 47.09. HRMS: calculated 1105.2788, found 1105.2795.

Typical end-functionalization procedure using the direct end-capping method. To a stirring solution of monomer (0.069 mmol, 25 equiv) in CH₂Cl₂ (0.6 mL) under argon was added catalyst **1** (0.00275 mmol, 1 equiv) as a solution in CH₂Cl₂ (0.1 mL) quickly via syringe. After 3 min TA (0.0137 mmol, 5 equiv) was added to the reaction mixture as a solution in CH₂Cl₂ (or MeOH for TAs **17** and **18**) (0.2 mL). The vial was sealed under argon and stirred for 6 h, at which point ethyl vinyl ether (0.3 mL) was added. The reaction mixture was then precipitated into Et₂O/hexanes (1:1) (20 mL), and the products were recovered by filtration and dried under vacuum. Yields were typically > 90%. In the case of TAs **17** and **18**, the reaction mixture was diluted with DMSO or DMF to 4 mL, and this solution was dialyzed against DMSO or DMF (8000 MWCO) for 3 d, followed by water for 1 d. The aqueous polymer mixture was then lyophilized to afford the clean polymer product. Yields were typically 60-80% in this case.

P(tBENI)=CHCH₂OAc by direct end-capping (19). ¹H NMR: δ 1.20-1.80 (m, 10n H), 2.00-2.30 (m, n H), 2.70-3.40 (m, 4n H), 4.00-4.20 (br s, 2n H), 4.51-4.58 (m, 2H), 5.40-5.80 (d, 2n H), 7.20-7.45 (m, 5H). GPC: $M_n = 7450$, $M_w/M_n = 1.06$.

P(tBENI)=CHCH₂OC(O)C(CH₃)₂Br by direct end-capping (20). ¹H NMR: δ 1.20-1.80 (m, 10n H), 1.91 (s, 6H), 2.00-2.30 (m, n H), 2.70-3.40 (m, 4n H), 4.00-4.20 (br s, 2n H), 4.65-4.75 (m, 2H), 5.40-5.80 (d, 2n H) 7.20-7.45 (m, 5H). GPC: $M_n = 8660$, $M_w/M_n = 1.02$.

P(tBENI)=CHCH₂CH₂C(O)H by direct end-capping (21). ¹H NMR: δ 1.20-1.80 (m, 10n H), 2.00-2.30 (m, n H), 2.70-3.40 (m, 4n H), 4.00-4.20 (br s, 2n H), 5.40-5.80 (d, 2n H), 7.20-7.45 (m, 5H), 9.78 (s, 1H). GPC: $M_n = 5300$, $M_w/M_n = 1.06$.

P(NMONI)=CHCH₂CH₂C(O)NHS by direct end-capping (22). ¹H NMR: δ 2.76-2.85 (m, 4H), 2.90-3.00 (s, 3n H), 3.20-3.45 (s, 2n H), 4.30-4.60 (m, n H), 4.70-5.00 (m, n H), 5.70-6.10 (m, 2n H) 7.30-7.50 (m, 5H). GPC: $M_n = 5590$, $M_w/M_n = 1.02$.

P(tBENI)=CHCH₂CH₂CH₂OH by direct end-capping (23). ¹H NMR: δ 1.20-1.80 (m, 10n H), 2.00-2.30 (m, n H), 2.70-3.40 (m, 4n H), 3.58-3.65 (m, 2H), 4.00-4.20 (br s, 2n H), 5.40-5.80 (d, 2n H), 7.20-7.45 (m, 5H). GPC: $M_n = 6600$, $M_w/M_n = 1.06$.

P(tBENI)=CHCH₂CH₂CH₂Br by direct end-capping (24). ¹H NMR: δ 1.20-1.80 (m, 10n H), 2.00-2.30 (m, n H), 2.70-3.40 (m, 4n H), 3.42-3.52 (m, 2H), 4.00-4.20 (br s, 2n H), 5.40-5.80 (d, 2n H), 7.20-7.45 (m, 5H). GPC: $M_n = 7450$, $M_w/M_n = 1.04$.

P(NMONI)=CHCH₂CH₂CH₂Sac by direct end-capping (25). ¹H NMR: δ 1.68-1.75 (m, 2H), 2.33 (s, 3H), 2.90-3.00 (s, 3n H), 3.20-3.45 (s, 2n H), 4.30-4.60 (m, n

H), 4.70-5.00 (m, n H), 5.70-6.10 (m, 2n H) 7.30-7.50 (m, 5H). GPC: $M_n = 5170$, $M_w/M_n = 1.03$.

P(tBENI)=CHCH₂O-*p*-CH₂CH₂NHBoc-C₆H₄ by direct end-capping (26). ¹H NMR: δ 1.20-1.80 (m, 10n H), 2.00-2.30 (m, n H), 2.70-3.40 (m, 4n H), 4.00-4.20 (br s, 2n H), 5.40-5.80 (d, 2n H), 6.91-6.96 (m, 2H), 7.20-7.45 (m, 5H), 7.12-7.17 (m, 2H). GPC: $M_n = 5420$, $M_w/M_n = 1.06$.

P(tBENI)=CHCH₂O-*p*-CH₂CH₂NHbiotin-C₆H₄ by direct end-capping (27). ¹H NMR (DMSO-*d*₆): δ 1.20-1.80 (m, 10n H), 2.00-2.30 (m, n H), 2.70-3.40 (m, 4n H), 4.00-4.20 (br s, 2n H), 4.27 (t, $J = 3.6$ Hz, 1H), 4.45 (s, 2H), 5.40-5.80 (d, 2n H), 6.31 (s, 1H), 6.38 (s, 1H), 6.82 (m, 2H), 7.07 (m, 2H), 7.20-7.45 (m, 5H), 7.78 (s, 1H). GPC: $M_n = 8560$, $M_w/M_n = 1.01$.

P(tBENI)=CHCH₂O-*p*-CH₂CH₂NHFITC-C₆H₄ by direct end-capping (28). ¹H NMR (DMSO-*d*₆): δ 1.20-1.80 (m, 10n H), 2.00-2.30 (m, n H), 2.70-3.40 (m, 4n H), 4.00-4.20 (br s, 2n H), 5.40-5.80 (d, 2n H), 6.48-6.80 (m, 10H), 6.85-7.00 (m, 2H), 7.10-8.30 (m, 8H). GPC: $M_n = 10000$, $M_w/M_n = 1.06$.

P(CMNI)=CHCH₂O-*p*-CH₂CH₂NH₂-C₆H₄ (29). Polymer **26** (37.5 mg, 1 equiv) was dissolved in CH₂Cl₂ (1 mL), and trifluoroacetic acid (105 μ L, 10 equiv relative to OtBu and NHBoc groups) was added. The vial was capped with a septum with a needle through it, and the reaction mixture was allowed to stir at room temperature

for 2 d. The reaction mixture was then precipitated into a large volume of Et₂O/hexanes (1:1), and the polymer product was recovered by filtration (29.2 mg). ¹H NMR(DMSO-*d*₆): δ 1.40-1.60 (s, n H), 1.90-2.05 (s, n H), 2.60-2.70 (s, n H), 2.76 (m, 2H), 2.90-3.10 (m, 3n H), 3.90-4.05 (s, 2n H), 5.35-5.70 (m, 2n H), 6.88 (m, 2H), 7.13 (m, 2H), 7.18-7.42 (m, 5H), 12.80-13.20 (s, n H).

P(tBENI)=CH₂ (30). To a stirring solution of monomer **4** (507 mg, 25 equiv) in CH₂Cl₂ (5 mL) under argon was added catalyst **1** (53.2 mg, 1 equiv) as a solution in CH₂Cl₂ (0.3 mL) quickly via syringe. The reaction mixture was allowed to stir under argon for 3 min, at which point ethyl vinyl ether (1 mL) was added. After an additional 10 min, the reaction mixture was precipitated into Et₂O/hexanes (1:1) (200 mL). Polymer **19** was recovered by filtration as a light brown powder in 93% yield (480 mg). ¹H NMR: δ 1.20-1.80 (m, 10n H), 2.00-2.30 (m, n H), 2.70-3.40 (m, 4n H), 4.00-4.20 (br s, 2n H), 5.05-5.25 (m, 2H), 5.40-5.80 (d, 2n H) 7.20-7.45 (m, 5H). GPC: $M_n = 7500$, $M_w/M_n = 1.02$.

Typical end-functionalization procedure using CM. Methylene-terminated polymer **19** or **20** was dissolved in toluene (0.3 mL) in a septum-capped vial under argon. TA was added as a solution in toluene or MeOH (for TAs **17** and **18**) (0.1 mL), and catalyst **3** was added as a solution in toluene (0.1 mL). The vial was sealed under argon and allowed to stir for 12 h at 40 °C (or 60 °C for TAs **15**, **17**, and **18**). Products were recovered using the same methods described for the direct end-capping procedure.

P(tBENI)=CHCH₂OAc by CM (31). ¹H NMR: δ 1.20-1.80 (m, 10n H), 2.00-2.30 (m, n H), 2.70-3.40 (m, 4n H), 4.00-4.20 (br s, 2n H), 4.51-4.58 (m, 2H), 5.40-5.80 (d, 2n H), 7.20-7.45 (m, 5H). GPC: $M_n = 7510$, $M_w/M_n = 1.03$.

P(tBENI)=CHCH₂OC(O)C(CH₃)₂Br (32). ¹H NMR: δ 1.20-1.80 (m, 10n H), 1.91 (s, 6H), 2.00-2.30 (m, n H), 2.70-3.40 (m, 4n H), 4.00-4.20 (br s, 2n H), 4.65-4.75 (m, 2H), 5.40-5.80 (d, 2n H) 7.20-7.45 (m, 5H). GPC: $M_n = 7340$, $M_w/M_n = 1.04$.

P(tBENI)=CHCH₂CH₂C(O)H by CM (33). ¹H NMR: δ 1.20-1.80 (m, 10n H), 2.00-2.30 (m, n H), 2.70-3.40 (m, 4n H), 4.00-4.20 (br s, 2n H), 5.40-5.80 (d, 2n H), 7.20-7.45 (m, 5H), 9.78 (s, 1H). GPC: $M_n = 7240$, $M_w/M_n = 1.04$.

P(tBENI)=CHCH₂CH₂C(O)NHS by CM (34). To minimize overlapping peaks in the NMR spectrum, the *tert*-butyl ester group was removed by treatment with trifluoroacetic acid as in polymer **29**. The product was characterized as P(CMNI)=CHCH₂CH₂C(O)NHS. ¹H NMR(DMSO-*d*₆): δ 1.40-1.60 (s, n H), 1.90-2.05 (s, n H), 2.60-2.70 (s, n H), 2.80 (s, 2H), 2.90-3.10 (m, 3n H), 3.90-4.05 (s, 2n H), 5.35-5.70 (m, 2n H), 6.88 (m, 2H), 7.13 (m, 2H), 7.18-7.42 (m, 5H), 12.80-13.20 (s, n H). GPC was not performed due to low solubility in THF.

P(tBENI)=CHCH₂CH₂CH₂OH by CM (35). ¹H NMR: δ 1.20-1.80 (m, 10n H), 2.00-2.30 (m, n H), 2.70-3.40 (m, 4n H), 4.00-4.20 (br s, 2n H), 3.58-3.65 (m, 2H), 5.40-5.80 (d, 2n H), 7.20-7.45 (m, 5H). GPC: $M_n = 7060$, $M_w/M_n = 1.08$.

P(tBENI)=CHCH₂CH₂CH₂Br by CM (36). ¹H NMR: δ 1.20-1.80 (m, 10n H), 2.00-2.30 (m, n H), 2.70-3.40 (m, 4n H), 3.42-3.52 (m, 2H), 4.00-4.20 (br s, 2n H), 5.40-5.80 (d, 2n H), 7.20-7.45 (m, 5H). GPC: $M_n = 7650$, $M_w/M_n = 1.03$.

P(tBENI)=CHCH₂CH₂CH₂SAc by CM (37). To minimize overlapping peaks in the NMR spectrum, the *tert*-butyl ester group was removed by treatment with trifluoroacetic acid as in polymer **29**. The product was characterized as P(CMNI)=CHCH₂CH₂CH₂SAc. ¹H NMR(DMSO-*d*₆): δ 1.40-1.60 (s, n H), 1.90-2.05 (s, n H), 2.32 (s, 3H), 2.60-2.70 (s, n H), 2.82 (m, 2H), 2.90-3.10 (m, 3n H), 3.90-4.05 (s, 2n H), 5.35-5.70 (m, 2n H), 6.88 (m, 2H), 7.13 (m, 2H), 7.18-7.42 (m, 5H), 12.80-13.20 (s, n H). GPC was not performed due to low solubility in THF.

P(tBENI)=CHCH₂O-*p*-CH₂CH₂NHBoc-C₆H₄ by CM (38). ¹H NMR: δ 1.20-1.80 (m, 10n H), 2.00-2.30 (m, n H), 2.70-3.40 (m, 4n H), 4.00-4.20 (br s, 2n H), 5.40-5.80 (d, 2n H), 6.91-6.96 (m, 2H), 7.20-7.45 (m, 5H), 7.12-7.17 (m, 2H). GPC: $M_n = 6940$, $M_w/M_n = 1.04$.

P(tBENI)=CHCH₂O-*p*-CH₂CH₂NHbiotin-C₆H₄ by CM (39). ¹H NMR (DMSO-*d*₆): δ 1.20-1.80 (m, 10n H), 2.00-2.30 (m, n H), 2.70-3.40 (m, 4n H), 4.00-4.20 (br s, 2n H), 4.27 (t, $J = 3.6$ Hz, 1H), 4.45 (s, 2H), 5.40-5.80 (d, 2n H), 6.31 (s, 1H), 6.38 (s, 1H), 6.82 (m, 2H), 7.07 (m, 2H), 7.20-7.45 (m, 5H), 7.78 (s, 1H). GPC: $M_n = 8000$, $M_w/M_n = 1.02$.

P(tBENI)=CHCH₂O-*p*-CH₂CH₂NHFITC-C₆H₄ by CM (40). ¹H NMR (DMSO-*d*₆): δ 1.20-1.80 (m, 10n H), 1.90-2.10 (m, n H), 2.60-3.40 (m, 4n H), 4.00-4.20 (br s, 2n H), 5.40-5.80 (d, 2n H), 6.48-6.80 (m, 10H), 6.85-7.00 (m, 2H), 7.10-8.30 (m, 8H). GPC: $M_n = 10000$, $M_w/M_n = 1.06$.

References

- (1) (a) Grubbs, R. H. *Handbook of Metathesis*; Wiley-VCH: Weinheim, 2003, Vol. 3. (b) Bielawski, C. W.; Grubbs, R. H. *Prog. Polym. Sci.* **2007**, *32*, 1–29.
- (2) (a) Bertin, P. A.; Watson, K. J.; Nguyen, S. T. *Macromolecules* **2004**, *37*, 8364–8372. (b) South, C. R.; Burd, C.; Weck, M. *Acct. Chem. Res.* **2007**, *40*, 63–74. (c) Kluger, C.; Binder, W. H. *J. Poly. Sci., Part A: Polym. Chem.* **2007**, *45*, 485–499. (d) Matson, J. B.; Grubbs, R. H. *J. Am. Chem. Soc.* **2008**, *131*, 6731–6733. (e) Kolonko, E. M.; Pontrello, J. K.; Mangold, S. L.; Kiessling, L. L. *J. Am. Chem. Soc.* **2009**, *131*, 7327–7333.
- (3) (a) Gorodetskaya, I. A.; Choi, T. L.; Grubbs, R. H. *J. Am. Chem. Soc.* **2007**, *129*, 12672–12673. (b) Gorodetskaya, I. A.; Gorodetsky, A. A.; Vinogradova, E. V.; Grubbs, R. H. *Macromolecules*, **2009**, *42*, 2895–2898.
- (4) (a) Helms, B.; Mynar, J. L.; Hawker, C. J.; Fréchet, J. M. J. *J. Am. Chem. Soc.* **2004**, *126*, 15020–15021. (b) Boydston, A. J.; Holcombe, T. W.; Unruh, D. A.; Fréchet, J. M. J.; Grubbs, R. H. *J. Am. Chem. Soc.* **2009**, *131*, 5388–5389.
- (5) Xia, Y.; Grubbs, R. H. *Macromolecules* **2009**, *42*, 3761–3766.
- (6) (a) Boydston, A. J.; Xia, Y.; Kornfield, J. A.; Gorodetskaya, I. A.; Grubbs, R. H. *J. Am. Chem. Soc.* **2008**, *130*, 12775–12882. (b) Xia, Y.; Boydston, A. J.; Yao, Y.; Kornfield, J. A.; Gorodetskaya, I. A.; Spiess, H. W.; Grubbs, R. H. *J. Am. Chem. Soc.* **2009**, *131*, 2670–2677.
- (7) Trnka, T. M.; Grubbs, R. H. *Acc. Chem. Res.* **2001**, *34*, 18–29.
- (8) Yagci, Y.; Tasdelen, M. A. *Prog. Polym. Sci.* **2006**, *31*, 1133–1170.
- (9) (a) Chen, B. Z.; Metera, K.; Sleiman, H. F. *Macromolecules* **2005**, *38*, 1084–1090. (b) Boyer, C.; Liu, J.; Bulmus, V.; Davis, T. P.; Barner-Kowollik, C.; Stenzel, M. H. *Macromolecules* **2008**, *41*, 5641–5650.
- (10) (a) Laurent, B. A.; Grayson, S. A. *J. Am. Chem. Soc.* **2006**, *128*, 4238–4239. (b) Eugene, D. M.; Grayson, S. M. *Macromolecules* **2008**, *41*, 5082–5084. (c) Adachi, K.; Honda, S.; Hayashi, S.; Tezuka, Y. *Macromolecules* **2008**, *41*, 7898–7903. (d) Lepoittevin, B.; Dourges, M. A.; Masure, M.; Hemery, P.; Baran, K.; Cramail, H. *Macromolecules* **2000**, *33*, 8218–8224.
- (11) (a) Amass, A. J.; Bas, S.; Gregory, D.; Mathew, M. C. *Makromol. Chem.* **1985**, *186*, 325–330. (b) Castle, T. C.; Hutchings, L. R.; Khosravi, E. *Macromolecules* **2004**, *37*, 2035–2040. (c) Tritto, I.; Sacchi, M. C.; Grubbs, R. H. *J. Mol. Catal.*

- 1993**, 82, 103–111. (d) Coca, S.; Paik, H. J.; Matyjaszewski, K. *Macromolecules* **1997**, 30, 6513–6516. (e) Li, M. H.; Keller, P.; Albouy, P. A.; *Macromolecules* **2003**, 36, 2284–2292. (f) Matson, J. B.; Grubbs, R. H. *Macromolecules* **2008**, 41, 5626–5631.
- (12) Burtscher, D.; Saf, R.; Slugovc, C. *J. Poly. Sci., Part A: Polym. Chem.* **2006**, 44, 6136–6145.
- (13) Hilf, S.; Kilbinger, A. F. M. *Macromol. Rapid Commun.* **2007**, 28, 1225–1230.
- (14) (a) Cramail, H.; Fontanille, M.; Soum, A. *J. Mol. Catal.* **1991**, 65, 193. (b) Chung, T. C.; Chasmawala, M. *Macromolecules* **1991**, 24, 3118–3120. (c) France, M. B.; Grubbs, R. H.; McGrath, D. V.; Paciello, R. A. *Macromolecules* **1993**, 26, 4742–4747. (d) Hillmyer, M. A.; Grubbs, R. H. *Macromolecules* **1993**, 26, 872–874. (e) Maughon, B. R.; Morita, T.; Bielawski, C. W.; Grubbs, R. H. *Macromolecules* **2000**, 33, 1929–1935.
- (15) (a) Katayama, H.; Urushima, H.; Ozawa, F. *J. Organomet. Chem.* **2000**, 1, 16–25. (b) Bielawski, C. W.; Louie, J.; Grubbs, R. H. *J. Am. Chem. Soc.* **2000**, 122, 12872–12873.
- (16) (a) Katayama, H.; Fukuse, Y.; Nobuto, Y.; Akamatsu, K.; Ozawa, F. *Macromolecules* **2003**, 36, 7020–7026. (b) Owen, R. M.; Gestwicki, J. E.; Young, T.; Kiessling, L. L. *Org. Lett.* **2002**, 4, 2293–2296. (c) Kolonko, E. M.; Kiessling, L. L. *J. Am. Chem. Soc.* **2008**, 130, 5626–5627.
- (17) Lexer, C.; Saf, R.; Slugovc, C. *J. Poly. Sci., Part A: Polym. Chem.* **2009**, 27, 299–305.
- (18) Hilf, S.; Grubbs, R. H.; Kilbinger, A. F. M. *J. Am. Chem. Soc.* **2008**, 130, 11040–11048.
- (19) Murphy, J. J.; Kawasaki, T.; Fujiki, M.; Nomura, K. *Macromolecules* **2005**, 38, 1075–1083.
- (20) (a) Hilf, S.; Berger-Nicoletti, E.; Grubbs, R. H.; Kilbinger, A. F. M. *Angew. Chem., Int. Ed.* **2006**, 45, 8045–8048. (b) Hilf, S.; Kilbinger, A. F. M. *Macromol. Rapid Comm.* **2007**, 28, 1225–1230. (c) Hilf, S.; Hanik, N.; Kilbinger, A. F. M. *J. Poly. Sci., Part A: Polym. Chem.* **2008**, 46, 2913–2921. (d) Hilf, S.; Kilbinger, A. F. M. *Macromolecules* **2009**, 42, 1099–1106.
- (21) Matson, J. B.; Virgil, S. C.; Grubbs, R. H. *J. Am. Chem. Soc.* **2009**, 131, 3355–3362.

- (22) (a) Choi, T. L.; Grubbs, R. H. *Angew. Chem., Int. Ed.* **2003**, *42*, 1743–1746. (b) Camm, K. D.; Castro, N. M.; Liu, Y. W.; Czechura, P.; Snelgrove, J. L.; Fogg, D. E. *J. Am. Chem. Soc.* **2007**, *129*, 4168–4169. (c) Kratz, K.; Breitenkamp, K.; Hule, R.; Pochan, D.; Emrick, T. *Macromolecules* **2009**, *42*, 3227–3229. (d) Colak, S.; Tew, G. N. *Macromolecules* **2008**, *41*, 8436–8440.
- (23) Rawat, M.; Gama, C. I.; Matson, J. B.; Hsieh-Wilson, L. C. *J. Am. Chem. Soc.* **2008**, *130*, 2959–2961.
- (24) Breitenkamp, R. B.; Ou, Z.; Breitenkamp, K.; Muthukumar, M.; Emrick, T. *Macromolecules* **2007**, *40*, 7617–7624.
- (25) Eren, T.; Som, A.; Rennie, J. R.; Nelson, C. F.; Urgina, Y.; Nüsslein, K.; Coughlin, E. B.; Tew, G. N. *Macromol. Chem. Phys.* **2008**, *209*, 516–524.
- (26) Chatterjee, A. K.; Choi, T. L.; Sanders, D. P.; Grubbs, R. H. *J. Am. Chem. Soc.* **2003**, *125*, 11360–11370.
- (27) Raederstoff, D.; Shu, A. Y. L.; Thompson, J. E.; Djerassi, C. *J. Org. Chem.* **1987**, *52*, 2337–2346.
- (28) Dag, A.; Durmaz, H.; Sirkecioglu, O.; Hizal, G.; Tunca, U. *J. Poly. Sci., Part A: Polym. Chem.* **2009**, *47*, 2344–2351.
- (29) Chen, B.; Metera, K.; Sleiman, H. F. *Macromolecules* **2005**, *38*, 1084–1090.
- (30) Blackwell, H. E.; O’Leary, D. J.; Chatterjee, A. K.; Washenfelder, R. A.; Bussman, D. A.; Grubbs, R. H. *J. Am. Chem. Soc.* **2000**, *122*, 58–71.
- (31) Ullman, M.; Grubbs, R. H. *Organometallics* **1998**, *17*, 2484–2489.
- (32) Bielawski, C. W.; Benitez, D.; Morita, T.; Grubbs, R. H. *Macromolecules* **2001**, *34*, 8610–8618.
- (33) Pangborn, A. B.; Giardello, M. A.; Grubbs, R. H.; Rosen, R. K.; Timmers, F. J. *Organometallics* **1996**, *15*, 1518–1520.
- (34) Love, J. A.; Morgan, J. P.; Trnka, T. A.; Grubbs, R. H. *Angew. Chem., Int. Ed.* **2002**, *41*, 4035–4037.
- (35) Moore, J. S.; Stupp, S. I. *Macromolecules* **1990**, *23*, 65–70.

Chapter 6

Pulsed-Addition Ring-Opening Metathesis Polymerization: Catalyst-Economical Syntheses of Homopolymers and Block Copolymers

Portions of the text in this chapter have been reproduced with permission from:

Matson, J. B.; Virgil, S. C.; Grubbs, R. H. *J. Am. Chem. Soc.* **2009**, *131*, 3355-3362.

Copyright 2009 American Chemical Society

Abstract

Poly(*tert*-butyl ester norbornene imide) homopolymers and poly(*tert*-butyl ester norbornene imide-*b*-*N*-methyl oxanorbornene imide) copolymers were prepared by pulsed-addition ring-opening metathesis polymerization (PA-ROMP). PA-ROMP is a unique polymerization method that employs a symmetrical *cis*-olefin chain transfer agent (CTA) to simultaneously cap a living polymer chain and regenerate the ROMP initiator with high fidelity. Unlike traditional ROMP with chain transfer, the CTA reacts only with the living chain end, resulting in narrowly dispersed products. The regenerated initiator can then initiate polymerization of a subsequent batch of monomer, allowing for multiple polymer chains with controlled molecular weight and low polydispersity to be generated from one metal initiator. Using the fast-initiating ruthenium metathesis catalyst $(H_2IMes)(Cl)_2(pyr)_2RuCHPh$ and *cis*-4-octene as a CTA, the capabilities of PA-ROMP were investigated with a Symyx robotic system, which allowed for increased control and precision of injection volumes. The results from a detailed study of the time required to carry out the end-capping/initiator-regeneration step were used to design several experiments in which PA-ROMP was performed from one to ten cycles. After determining the rate of catalyst death, a single, low polydispersity polymer was prepared by adjusting the amount of monomer injected in each cycle, maintaining a constant monomer/catalyst ratio. Additionally, PA-ROMP was used to prepare nearly perfect block copolymers by quickly injecting a second monomer at a specific time interval after the first monomer injection, such that chain transfer had not yet occurred. Polymers were characterized by gel permeation chromatography with multi-angle laser light scattering.

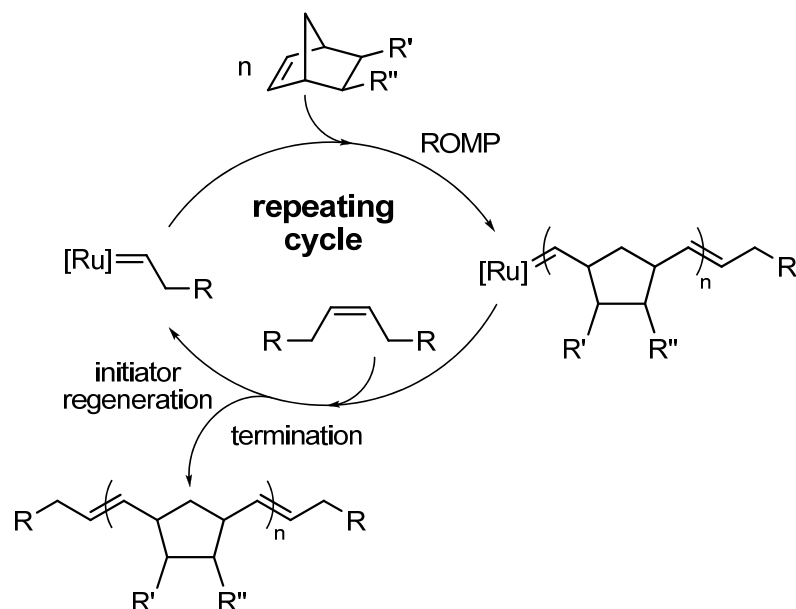
Introduction

Ring-opening metathesis polymerization (ROMP) has emerged as a powerful technique for creating a wide variety of polymer architectures from strained cyclic olefins.¹ Dominated by early transition metal molybdenum catalysts and late transition metal ruthenium catalysts, multi-block,² star,³ graft,⁴ dendronized,⁵ and other types of polymer architectures can be produced by ROMP, often with precise control over molecular weight, molecular weight distribution, and composition. ROMP has been used industrially in various applications,⁶ but the preparation of ROMP polymers with controlled structures often requires high catalyst loadings.

Highly efficient, expensive metal catalysts are used in the synthesis of several types of polymers, most notably polyolefins.⁷ An important quality of polyolefin catalysts is their ability to produce hundreds to thousands of polymer chains from an individual metal center. ROMP catalysts are also extremely efficient, with turnover numbers as high as 4000 in solution⁸ and over 60,000 in bulk in the case of dicyclopentadiene.⁹ However, in the production of living ROMP polymers where the metal complex acts as an initiator, this does not translate into low product cost because each catalyst molecule is capable of producing only one living polymer chain.

Our strategy to regenerate a ROMP initiator is to cleave the metathesis catalyst from the living polymer chain end with a *cis*-olefin chain transfer agent (CTA), simultaneously reform the active initiator species, and subject the regenerated initiator to an additional portion of monomer (Scheme 6.1). If the reactivity of the monomer is much greater than that of the CTA, then polymerization and initiator regeneration can be performed in one pot, making this technique a potentially attractive polymerization

method in industry. In this situation, the ROMP reaction occurs selectively in the presence of CTA until monomer consumption is complete, at which point the end-capping and catalyst regeneration reaction takes place. Attempts to effect this type of repeating cycle have only been described twice.¹⁰ In one report using a molybdenum catalyst, Crowe and coworkers were able to polymerize ten batches of norbornene using styrene as a CTA.^{10a} The product showed a significant high molecular weight shoulder, likely due to a small amount of incomplete chain transfer. Additionally, due to the air, moisture, and functional group sensitivity of this catalyst, the practical applications of this system are limited. In another example by Gibson, the ruthenium olefin metathesis catalyst $(\text{PCy}_3)_2(\text{Cl})_2\text{RuCHPh}$ was recycled eight times in the polymerization of a *tert*-butyl ester functionalized norbornene using *cis*-1,4-diacetoxy-2-butene as the CTA.^{10b} The polymer product in this case showed a low molecular weight tail due to a considerable amount of chain transfer during the polymerization. The occurrence of chain transfer in the presence of a reactive norbornene is likely a result of poor matching of the reactivities of the monomer and the CTA with the catalyst. Although the topic has been only very briefly explored, this polymerization technique, called pulsed-addition ROMP (PA-ROMP), has the potential to improve the efficiency of ROMP and increase the number of applications of ROMP polymers.



Scheme 6.1. Mechanism of PA-ROMP.

In addition to its economic benefits, PA-ROMP would also reduce the ruthenium contamination in the product. The amount of metal needed in metal-catalyzed living polymerization has been reduced to 10 ppm or lower in many examples in the case of copper-mediated atom transfer radical polymerization (ATRP) by the development of ARGET (activators regenerated by electron transfer) ATRP.¹¹ However, reduction of the metal contamination in ROMP polymers remains an unsolved problem. Cleavage of the catalyst from the polymer chain end with ethyl vinyl ether followed by precipitation of the product is typically used to remove the catalyst. However, this method often does not completely remove the catalyst, leaving the resulting polymers contaminated with ruthenium. While low metal contamination is acceptable in polymers in many cases, removal of potentially toxic metals is absolutely crucial in pharmaceutical products. Considering recent studies using ROMP polymers in biological applications, metal

contamination in the products is expected to be a problem as these developments move towards *in vivo* applications.¹² The need for developing new methods to remove metal contaminants in ROMP polymers could be circumvented by simply using less metal to carry out ROMP.

To make PA-ROMP feasible, a highly-active and functional group tolerant metathesis catalyst needs to be used. Recently, pyridine-containing, fast-initiating ruthenium catalysts have shown remarkable reactivity as initiators for living ROMP.^{1b,2c,13} We investigated PA-ROMP with one such catalyst, (H₂IMes)(Cl)₂(pyr)₂RuCHPh (**1**). Additionally, we extended its application to block copolymers, further illustrating the power of this approach.

Results and Discussion

We recently reported on the synthesis of low polydispersity ROMP-ATRP diblock copolymers using catalyst **1**.¹⁴ The ROMP polymers were end-capped by adding the symmetrical *cis*-olefin (*Z*)-but-2-ene-1,4-diyl bis(2-bromopropanoate) to the reaction mixture after ROMP was complete. Because no secondary metathesis reactions (backbiting) occur with substituted norbornenes, the α -bromoester ATRP initiating group was added only to the active chain end. We expected that during this process the ruthenium catalyst was also functionalized with an α -bromoester, and we elected to investigate the possibility of using this regenerated initiator for subsequent polymerization by ROMP. However, the end-capping of the polymer chain with this CTA took 3 h to reach completion. A faster end-capping reaction would be required to make PA-ROMP practically useful.

The end-capping of a ROMP polymer chain with an internal olefin CTA is simply a single cross metathesis event between the ruthenium alkylidene species at the end of a living polymer chain and the internal olefin CTA. Previous studies from our group have demonstrated that sterically unhindered and electron-rich olefins have the highest reaction rates for cross metathesis.¹⁵ In this study, *cis*-4-octene was chosen as the CTA due to its favorable cross metathesis activity, commercial availability, and relatively high boiling point. ROMP of norbornenes is extremely fast due to the release of large amounts of ring strain, with rate constants several orders of magnitude faster than even the best cross metathesis reactions. Similarly, cross metathesis is several orders of magnitude faster than secondary metathesis of substituted polynorbornenes. Based on the great differences in reactivity between ROMP, cross metathesis, and secondary metathesis, we expected that PA-ROMP would be possible in one pot, even with a very reactive CTA.

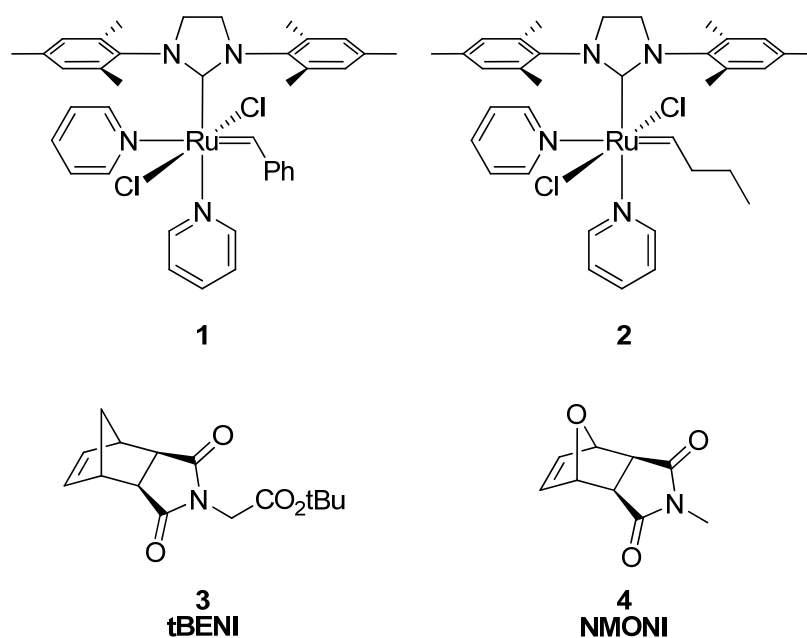


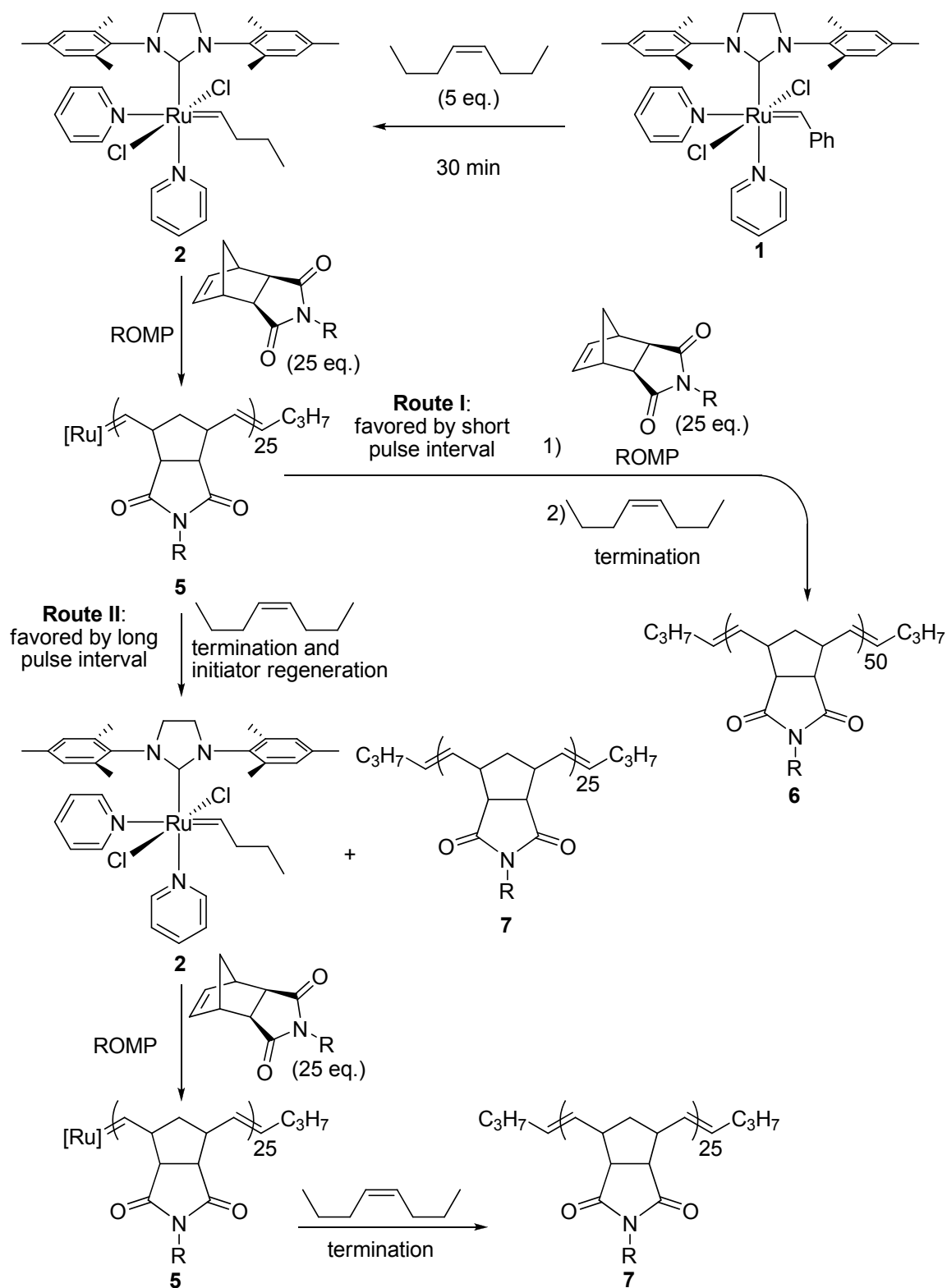
Figure 6.1. Ruthenium olefin metathesis catalysts (**1** and **2**) and monomers (**3** and **4**) used in PA-ROMP reactions.

A Symyx robot system was used for all experiments to provide an extremely high degree of precision and consistency in addition volumes. Our group¹⁶ and others¹⁷ have used robotic systems to assay catalytic activity and optimize reaction conditions, but to our knowledge this is the first report of a systematic study of polymer synthesis done using a robotic system. All stock solutions were prepared in a nitrogen-filled glovebox and capped with screw-cap, septum-topped vials with vent needles. Reactions were run in open vials in a nitrogen-filled glovebox to eliminate potential coupling from oxygen.¹⁸ *tert*-Butyl ester norbornene imide (tBENI) (**3**) was chosen for all homopolymer experiments due to the ease of synthesizing the material in high purity.

Pulse Interval Optimization

An initial experiment designed both to examine whether PA-ROMP was possible over two cycles with catalyst **1** and to optimize the pulse interval (elapsed time between additions) was setup as shown in Scheme 6.2. Equal amounts of a solution containing catalyst **1** and *cis*-4-octene were added to 10 vials. All reaction vials and stock solutions were kept at 25 °C. This solution was allowed to stand for 30 min as catalyst **2** formed. A stock solution containing monomer **3** was also prepared. Vial A was used as a control and received only one addition of the monomer solution. Vials B through J each received two additions of monomer, and the pulse interval was varied between 0.5 min (vial B) and 40 min (vial J). Forty min after the second addition was complete for all vials, the polymer products were recovered by precipitation and filtration. For product mixtures **B** through **J**, a combination of polymer products **6** (DP=50) and **7** (DP=25) was expected, depending on the amount of end-capping that occurred during the time between the two

pulses. Shorter pulse intervals were expected to favor route I because the second addition of monomer occurs before ruthenium-bound polymer **5** has reacted with *cis*-4-octene. This route produces one equivalent of polymer **6**. Longer pulse intervals were expected to favor route II; a longer interval allows for the reaction of *cis*-4-octene with ruthenium-bound polymer **5** to regenerate initiator **2** and form polymer product **7**. A second addition of monomer then produces another equivalent of polymer **7**.



Scheme 6.2. Experiment designed to determine the optimal pulse interval required for PA-ROMP. R = CH₂CO₂tBu.

Gel permeation chromatography (GPC) with multi-angle laser light scattering was used to determine the absolute molecular weight and molecular weight distribution of the polymer products. Figure 6.2 shows the GPC traces of product mixtures **A**, **B**, **F**, and **J**, and Table 6.1 compares the molecular weight and polydispersity index (PDI) of each of the polymer samples. Product mixture **A** (control sample) contains only polymer **7** and shows a molecular weight of 8100 Da, which is in reasonable agreement with the theoretical molecular weight of 7100 Da. Product mixture **B** shows a monomodal GPC peak with a molecular weight of 16200 Da, indicating that only product **6** was formed. This shows that with a pulse time of 30 s, only route I is followed, meaning that no end-capping occurs within 0.5 min of the first monomer addition. The remaining molecular weight data demonstrate that as the pulse interval increases, route II becomes favored, and the molecular weight decreases, approaching that of pure polymer **7**. Another feature of the polymerization is revealed by examining the molecular weight distribution. The PDI increases up to product mixture **F**, which is a mixture of approximately 53% **6** and, 47% **7**.¹⁹ At this point the PDI begins to drop again as an increasing amount of product **7** is formed from the second monomer addition. Product mixture **J** nearly reaches the original molecular weight of polymer **7**, but catalyst death occurring during the time between the pulses prevents a complete return to the original molecular weight of 8100 Da. Based on these results, we chose a pulse interval of 30 min for the subsequent experiments.

It should be noted that this method provides a synthetic route for the production of living, telechelic polynorbornenes with narrow polydispersities. CTAs are typically used to synthesize telechelic ROMP polymers,²⁰ but these polymers all have PDIs near 2.0.

While high PDIs are acceptable for some purposes, low PDIs are required for many applications, such as when specific morphologies of block copolymers are desired. Broad polydispersities are observed when ROMP with extensive chain transfer reaches thermodynamic equilibrium. In our route, the bulky backbone of the P(tBENI) prevents chain transfer except at the chain end. Low polydispersity, telechelic polynorbornenes can thus be obtained by the method described above, even without the use of a robot.

Table 6.1. Characterization of the products formed in the pulse interval optimization experiment.

Product Mixture	Pulse interval (min)	M_n (Da)	PDI	% polymer 7 ^a
A	N/A	8100	1.04	100%
B	0.5	16200	1.04	0%
C	1.3	15600	1.05	7%
D	2.1	14900	1.06	16%
E	2.9	14200	1.06	24%
F	4.9	12400	1.08	47%
G	8.3	10800	1.08	66%
H	14.0	9920	1.06	77%
I	23.7	9380	1.04	84%
J	40	9120	1.04	100% ^b

^a All values except for product **J** are assigned assuming no catalyst death occurred between pulses, meaning that only products **6** and **7** are present in the mixture. ^b This value is assumed to be 100% based on no observations of uncapped polymer in subsequent experiments. The discrepancy in M_n between product **A** and product **J** is assumed to be a result of catalyst death.

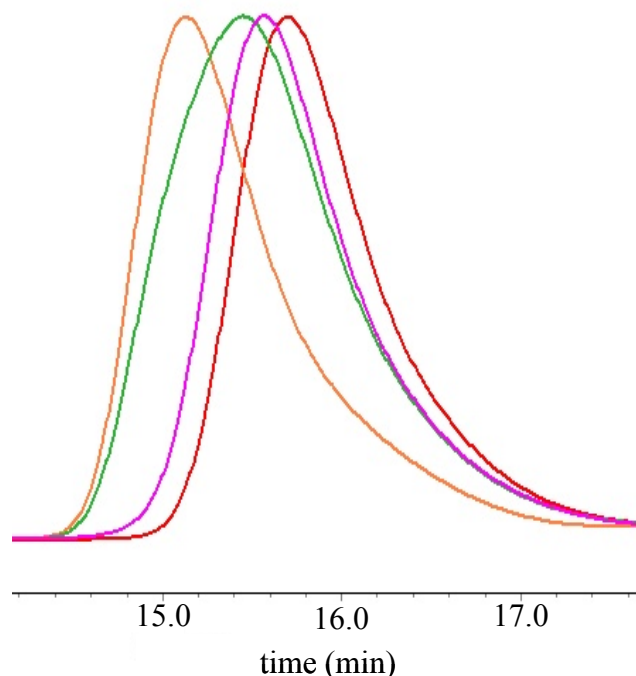
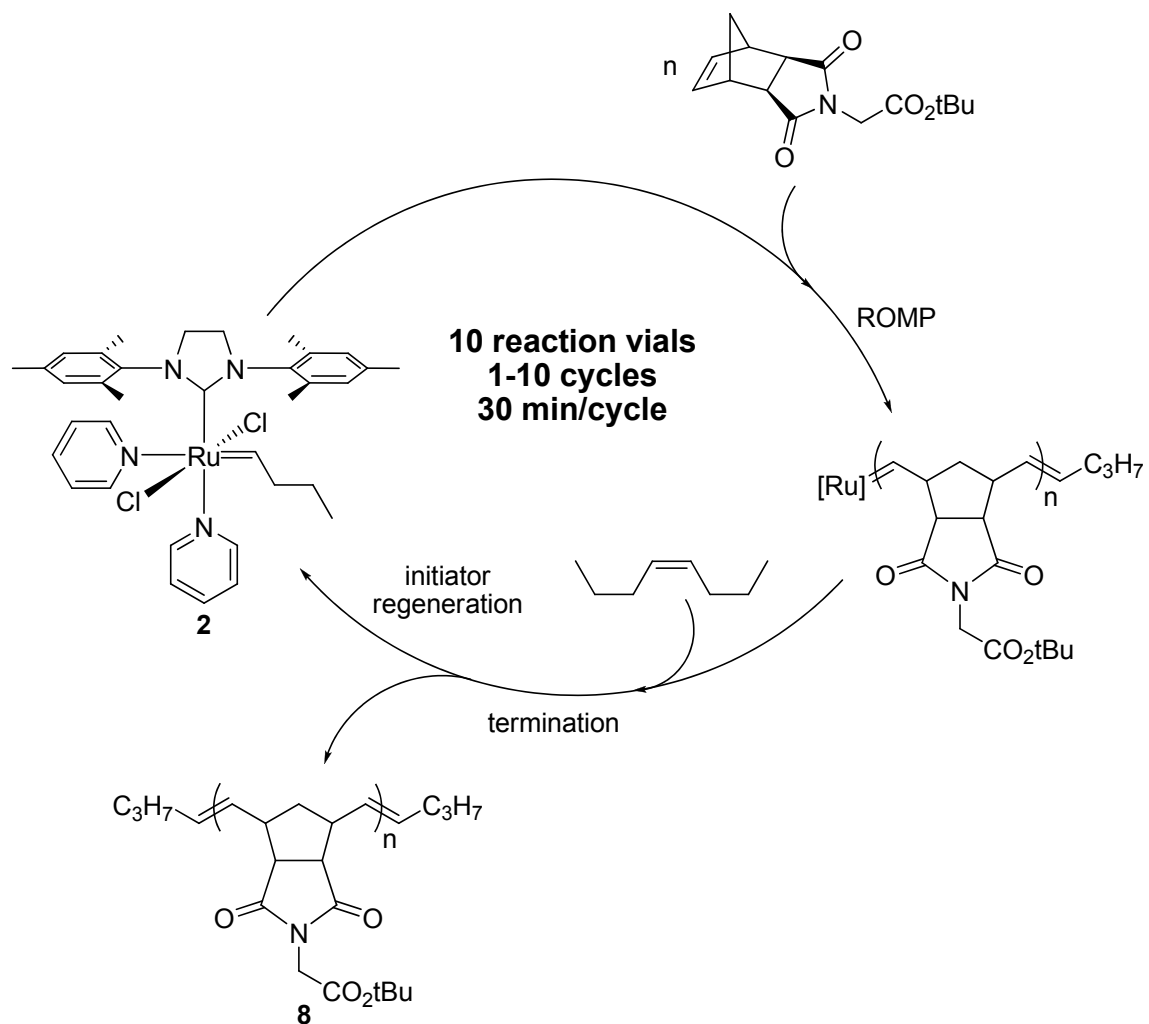


Figure 6.2. GPC traces of products **A** (red; 100% polymer **7**), **B** (orange; 100% polymer **6**), **F** (green; 47% polymer **7**, 53% polymer **6**), and **J** (purple; 100% polymer **7**) from pulse interval optimization experiment.

Homopolymers by PA-ROMP

Based on the data from the pulse interval optimization trials, a set of experiments investigating the feasibility of PA-ROMP over 10 cycles was devised. In these experiments, equal amounts of a stock solution containing catalyst **1** and 5 equiv of *cis*-4-octene were added by the robot to each of 10 vials (designated K through T), each maintained at 25 °C. After allowing 30 min for catalyst **2** to form, 120 μ L from a stock solution containing 25 equiv of monomer **3** and 1.1 equiv of *cis*-4-octene (both relative to catalyst) were added to each vial, ultimately forming polymer **8** (Scheme 6.3). The additional *cis*-4-octene was added to keep the concentration of CTA constant over the entire reaction. After another 30 min, 120 μ L from this stock solution was added only to

vials L through T. This process was continued, eliminating one vial during each 30 min pulse interval, such that vial K received one addition of monomer solution, vial L received two additions, up to vial T, which received ten additions. This allowed us to examine the product mixtures formed in each cycle, shown in Table 6.2.



Scheme 6.3. Synthesis of polynorbornenes by PA-ROMP.

A trend of slowly decreasing peak retention time and slowly increasing peak width is observed in the GPC traces (Figure 6.3). It is important to note that no high molecular weight shoulders or secondary peaks are present. The lack of high molecular weight species indicates that the chain termination and catalyst regeneration portions of

the cycle were complete each time before additional monomer was added. The molecular weight data are shown in Table 6.2. The theoretical molecular weight of the polymer based on the initial monomer/catalyst (M/C) ratio of 25 was 7100 Da, and the molecular weight of the product mixture **K** was 7430 Da, indicating that a small amount of catalyst death occurred during the formation of catalyst **2**. The subsequent products all show slowly increasing molecular weights. We attribute this slow increase to catalyst death during both the polymerization and the end-capping reactions. Because 100% initiator efficiency is observed for pyridine-containing metathesis catalysts such as **1**, the degree of polymerization of a given polymer is determined by the M/C ratio. Even after ten cycles, product mixture **T** has a molecular weight of 11000 Da and a relatively low PDI of 1.12. Figure 6.4 shows the molecular weight and polydispersity data graphed with a well-fitting exponential curve²¹ fitted to the molecular weight data, indicating a nearly constant level of catalyst death. Analysis of the data (see Appendix 2) shows that approximately 8.5% of the catalyst available at the beginning of a cycle dies during the polymerization and end-capping reactions.

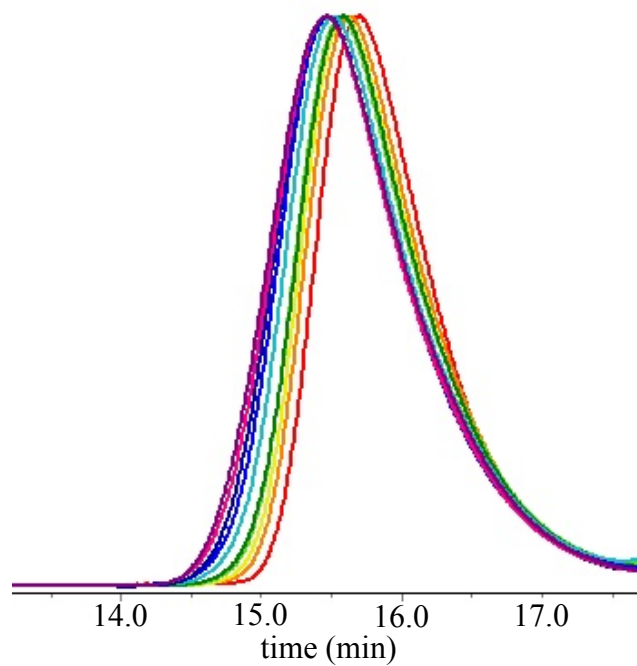


Figure 6.3. GPC traces of product mixtures **K** (red), **L** (orange), **M** (yellow), **N** (light green), **O** (green), **P** (light blue), **Q** (royal blue), **R** (dark blue), **S** (light purple), and **T** (dark purple) from one (product mixture **K**) to ten (product mixture **T**) cycles of PA-ROMP.

Table 6.2. Characterization of P(tBENI) homopolymer products by GPC from 10 cycles of PA-ROMP at 25 °C with M/C = 25 and a pulse interval of 30 min.

Product Mixture	Additions Received	M_n (Da)	PDI
K	1	7430	1.05
L	2	7660	1.09
M	3	7990	1.06
N	4	8180	1.09
O	5	8360	1.09
P	6	9250	1.11
Q	7	9960	1.11
R	8	10800	1.09
S	9	10800	1.16
T	10	11000	1.12

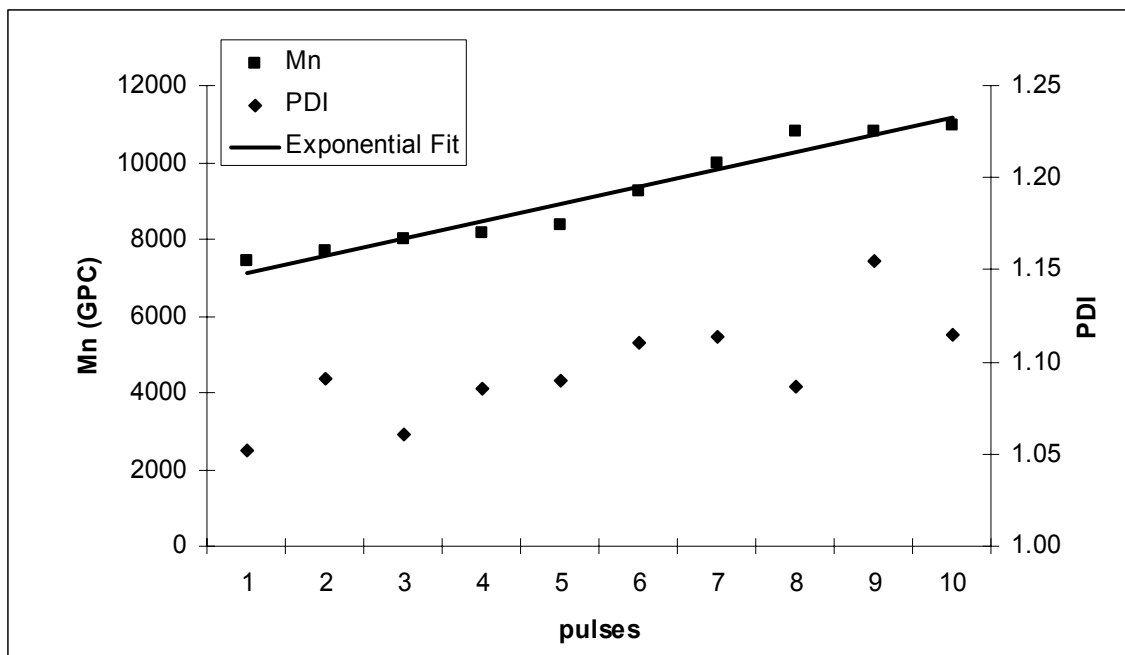
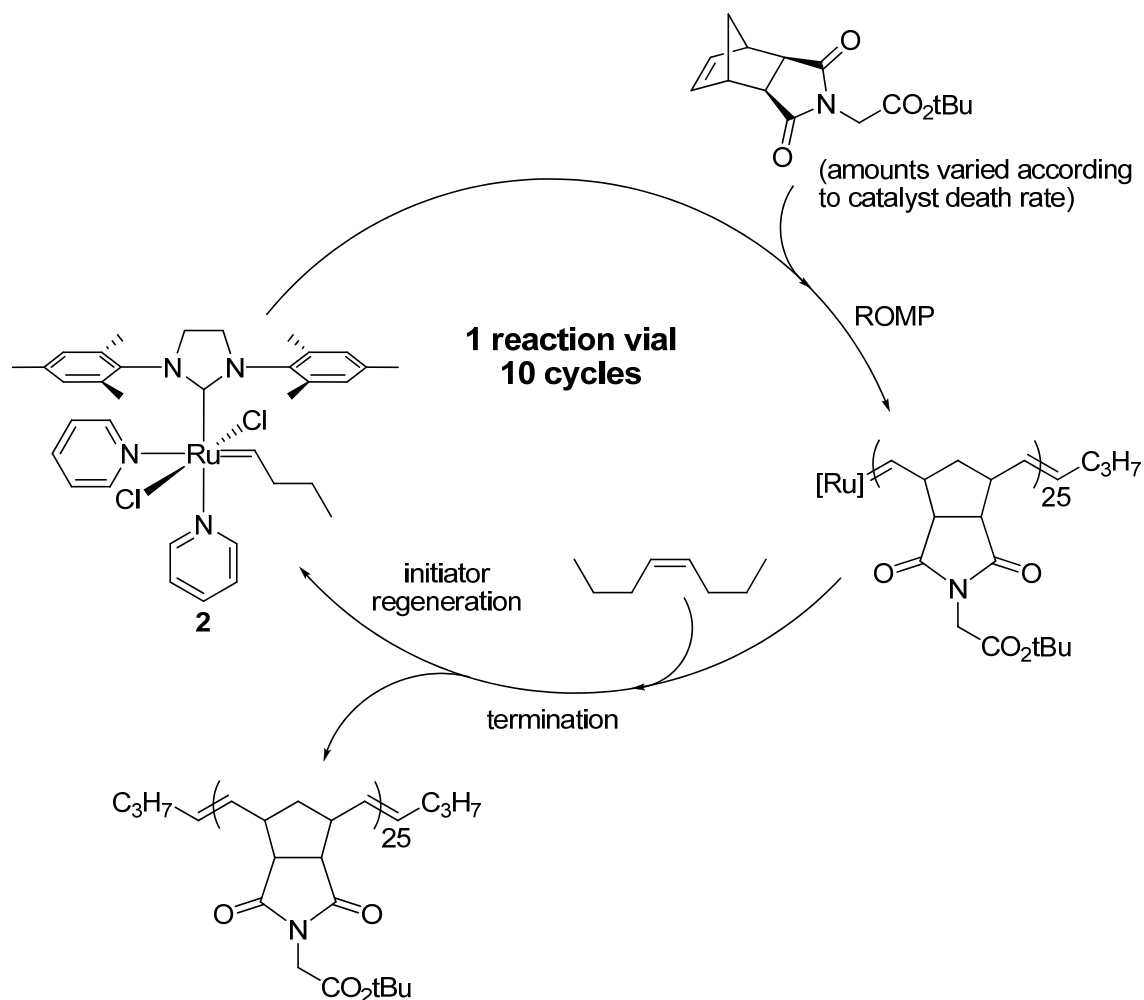


Figure 6.4. Dependence of M_n and PDI on number of cycles of PA-ROMP for P(tBENI) homopolymers with $M/C = 25$.

To demonstrate the usefulness of PA-ROMP for synthesizing a single polymer product with low polydispersity using a low catalyst loading, we constructed a one-vial experiment in which the amount of monomer solution added in each cycle was varied in accordance with the observed rate of catalyst death (Scheme 6.4).



Scheme 6.4. Synthesis of a single batch of low polydispersity homopolymer by PA-ROMP.

By decreasing the amount of monomer added in each pulse to keep a constant M/C ratio, we hoped to observe a single final polymer product with low polydispersity and a controllable molecular weight. Conditions of 25 °C with a pulse interval of 30 min, an initial M/C ratio of 25, and an assumed 8.5% catalyst death rate were used. The robot was programmed to add monomer solution in volumes outlined in Table 6.3, all into a single reaction vial. Ten pulses of 30 min each were performed at 25 °C. The product showed an $M_n = 9640$ Da and $\text{PDI} = 1.08$, which is in reasonable agreement with the theoretical molecular weight of 7100 Da. The GPC trace is shown in Figure 6.5. This

experiment demonstrates that PA-ROMP is capable of producing a single, low polydispersity product with a controllable molecular weight. Notably, 132 mg of polymer was produced from 2 mg of catalyst in this synthesis. A traditional ROMP synthesis of 132 mg of a polymer with this molecular weight would require 14 mg of catalyst, corresponding to a sevenfold increase in catalyst consumption.

Table 6.3. Addition volumes of monomer solution assuming 8.5% catalyst death rate for each of ten cycles of PA-ROMP.

Pulse	% catalyst still alive	volume (μL)
1	100	120.0
2	91.5	109.8
3	83.7	100.4
4	76.6	91.9
5	70.1	84.1
6	64.1	76.9
7	58.7	70.4
8	53.7	64.4
9	49.1	58.9
10	44.9	53.9

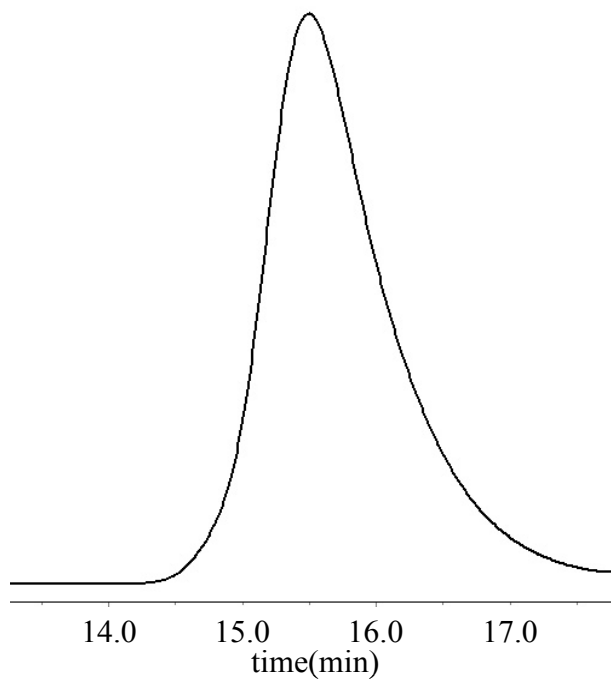


Figure 6.5. GPC trace of PA-ROMP product in single-vial experiment.

In order to probe the limits of PA-ROMP, a second set of ten reactions were performed under identical conditions to the first ten-vial experiment, except an initial M/C ratio of 100 was used (polymer theoretical molecular weight of 27200 Da). The resulting polymer GPCs are shown in Figure 6.6. Characterization data of product mixtures **U** through **DD** are shown in Table 6.4. These data are graphed in Figure 6.7.

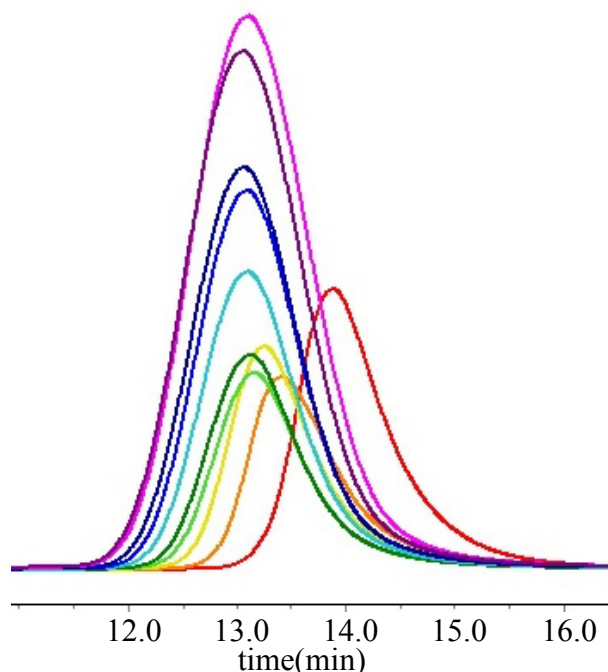


Figure 6.6. GPC traces of P(tBENI) product mixtures **U** (red), **V** (orange), **W** (yellow), **X** (light green), **Y** (green), **Z** (light blue), **AA** (royal blue), **BB** (dark blue), **CC** (light purple), and **DD** (dark purple) from one (product mixture **U**) to ten (product mixture **DD**) cycles of PA-ROMP. Note that the peak heights were not normalized as in the other composite GPC trace figures.

Product **U** matches the theoretical molecular weight, but the subsequent products have much higher molecular weights and broader polydispersities compared with the same experiment using a M/C ratio of 25. Analysis of the molecular weights (see Appendix 2) showed that approximately 16.5% of the available catalyst died during each cycle. This is nearly twice the rate at which catalyst died when polymers with an initial M/C ratio of 25 were synthesized. Evidently this increase in the catalyst death rate can be attributed to decomposition during the ROMP reaction. Because the decomposition pathways of olefin metathesis catalysts active during ROMP have not been studied, it is difficult to predict what modifications could be made to improve PA-ROMP of larger polymers with catalyst **2**. These results clearly demonstrate the need for more stable olefin metathesis catalysts.

Table 6.4. Characterization of P(tBENI) homopolymer products by GPC from 10 cycles of PA-ROMP at 25 °C with M/C = 100 and a pulse interval of 30 min.

Product Mixture	Additions Received	M_n (Da)	PDI
U	1	28600	1.07
V	2	47100	1.08
W	3	58000	1.14
X	4	64500	1.20
Y	5	68700	1.20
Z	6	75700	1.22
AA	7	80700	1.22
BB	8	84600	1.24
CC	9	89400	1.23
DD	10	93600	1.24

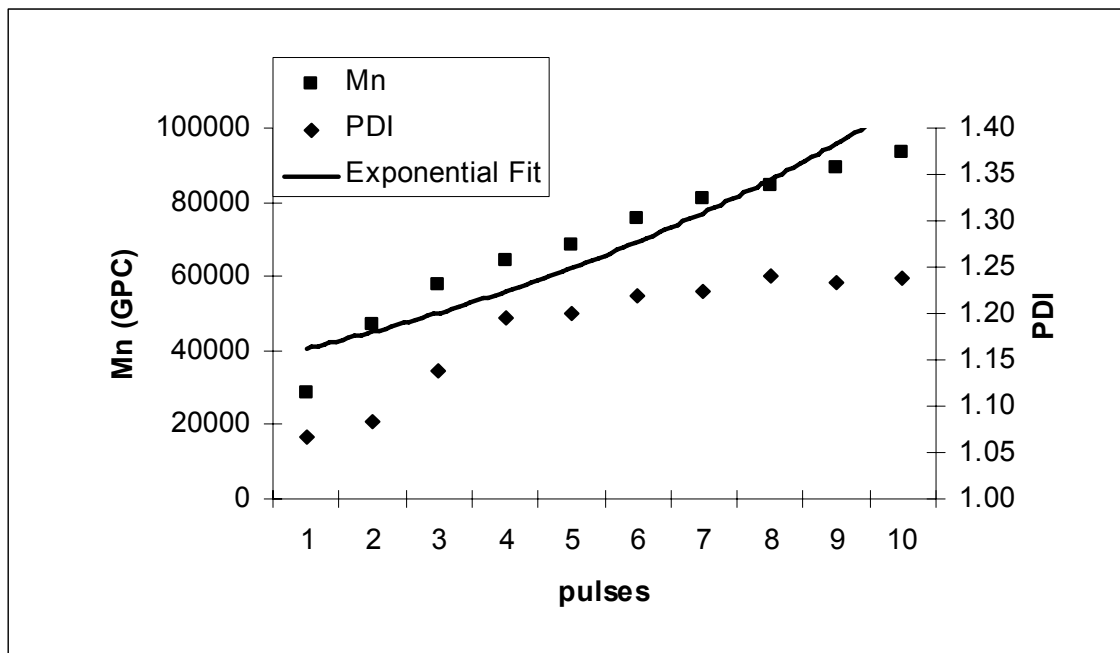


Figure 6.7. Dependence of M_n and PDI on number of cycles of PA-ROMP for P(tBENI) homopolymers with $M/C = 100$.

If catalyst death were occurring predominantly during the end-capping part of the cycle, the catalyst death rate would be expected to remain the same regardless of polymer molecular weight. In contrast, the results from this experiment indicate that catalyst death occurs predominantly during the ROMP reaction. Although little work has been done on the determination of decomposition pathways in ROMP, it can be assumed that these processes are much slower than ROMP itself. Based on this assumption, we attempted to reduce the rate of decomposition while maintaining a high rate of activity for the ROMP and end-capping reactions by performing PA-ROMP at 20 °C.

With this decrease in temperature, we determined that the time between each pulse needed to be increased to 1 h to allow for complete end-capping and initiator regeneration. An experiment was performed with these changes incorporated, and the polymer product mixtures (EE through NN) were isolated and characterized. GPC traces

are shown in Figure 6.8, and the molecular weight and polydispersity data are shown in Table 6.5. The data are graphed in Figure 6.9.

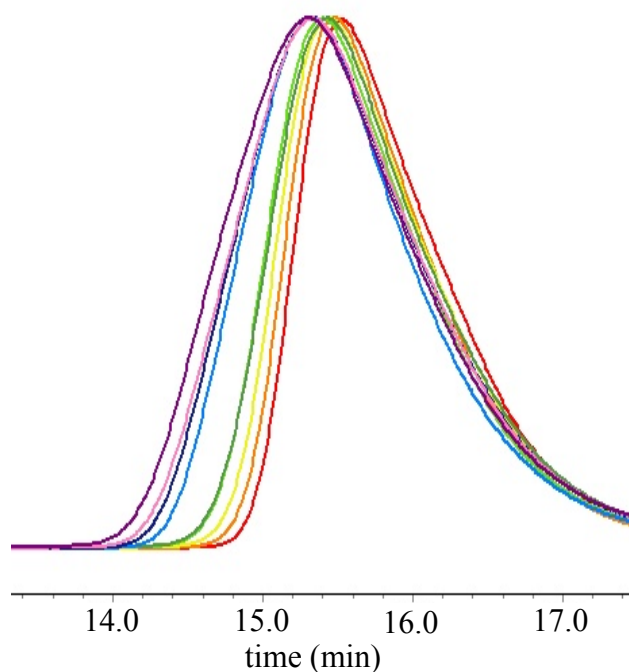


Figure 6.8. GPC traces of P(tBENI) product mixtures **EE** (red), **FF** (orange), **GG** (yellow), **HH** (light green), **II** (green), **KK** (light blue), **LL** (dark blue), **MM** (light purple), and **NN** (dark purple) from one (product mixture **EE**) to ten (product mixture **NN**) cycles of PA-ROMP. Product mixture **JJ** was omitted for clarity.

The results proved that our hypothesis was incorrect, as the catalyst died more quickly under these conditions than the original conditions of 25 °C with 30 min cycles. A death rate of 11.2% was determined from the data analysis (see Appendix 2). This increase in catalyst death rate can be attributed to the longer time between pulses. Although the previous experiment showed that catalyst death occurs predominantly during ROMP, this experiment indicates that a significant amount of catalyst death also occurs during the end-capping and initiator regeneration reactions.

Table 6.5. Characterization of P(tBENI) homopolymer products by GPC from ten cycles of PA-ROMP at 20 °C with M/C = 25 and a pulse time of 60 min.

Product Mixture	Additions Received	M_n (Da)	PDI
EE	1	7730	1.07
FF	2	8470	1.08
GG	3	9270	1.08
HH	4	10030	1.09
II	5	10110	1.10
JJ	6	12000	1.13
KK	7	12970	1.13
LL	8	13020	1.17
MM	9	13100	1.19
NN	10	14210	1.22

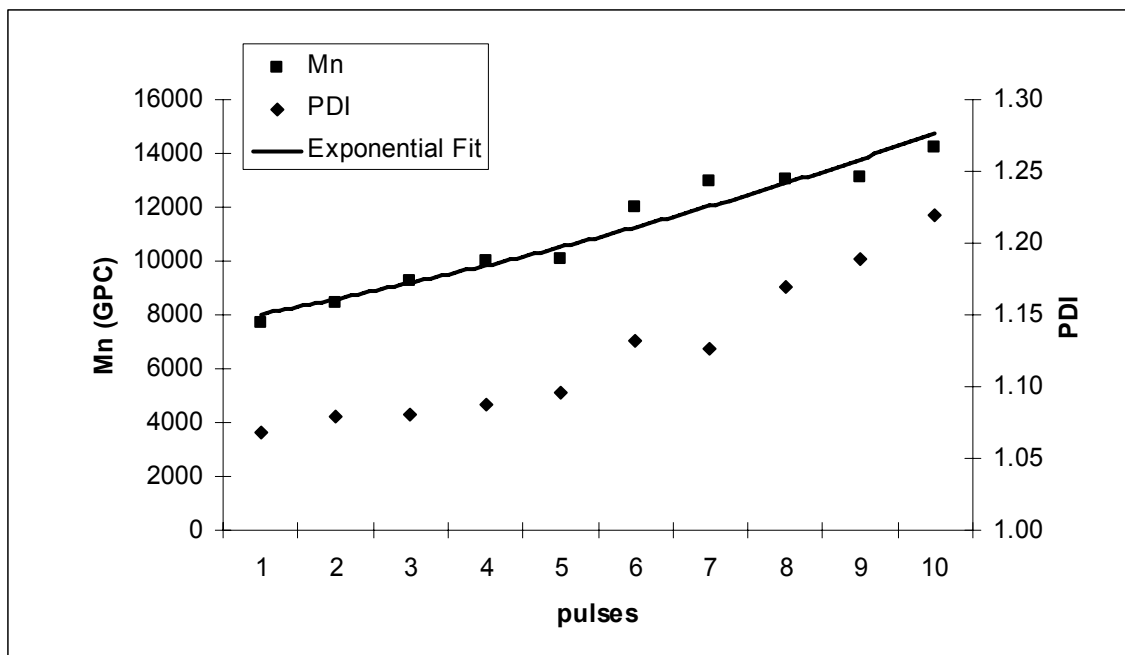


Figure 6.9. Dependence of M_n and PDI on number of cycles of PA-ROMP for P(tBENI) homopolymers with $M/C = 25$ at $20\text{ }^\circ\text{C}$ with 60 min pulse interval.

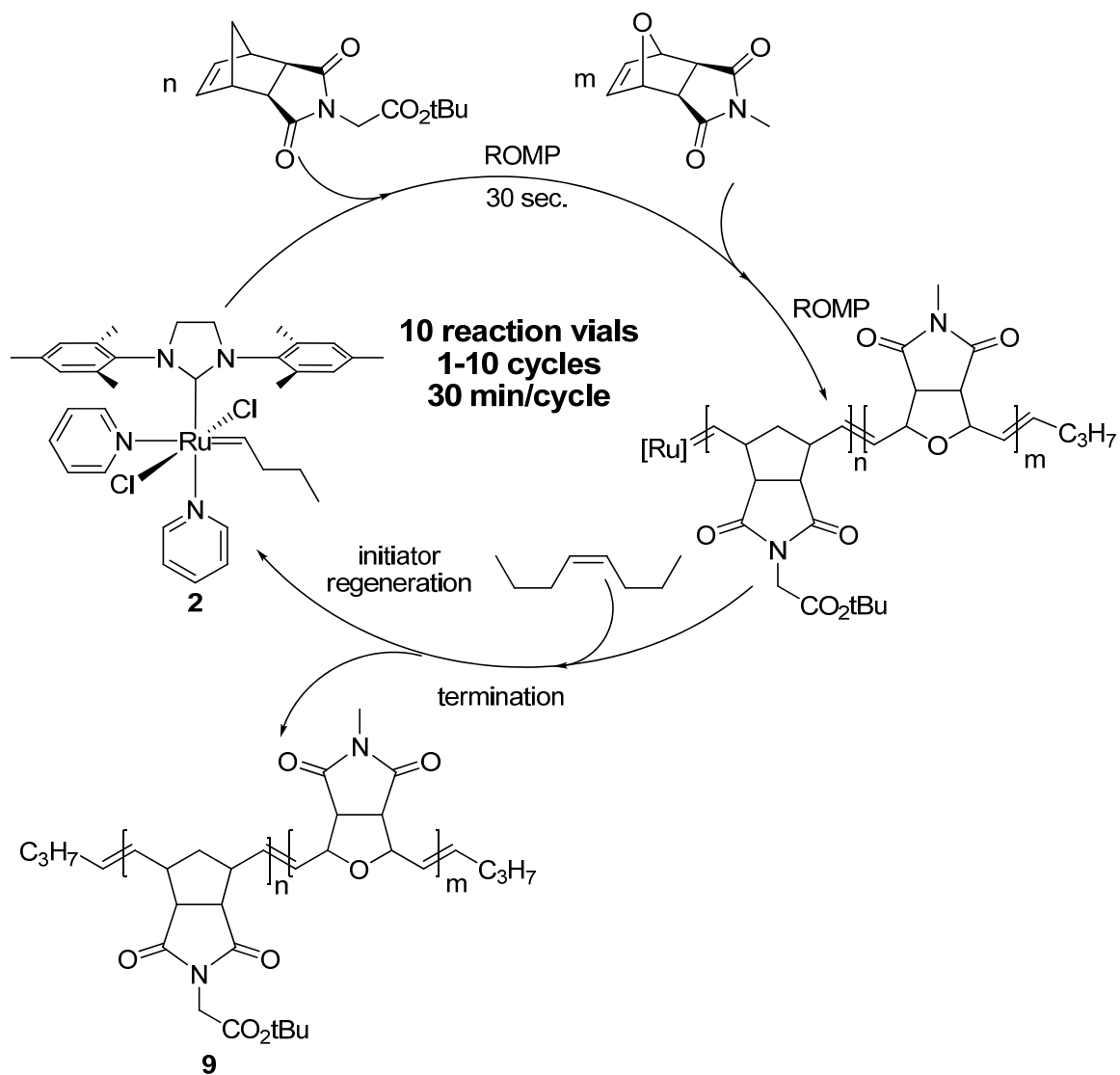
Block Copolymers by PA-ROMP

The ability to synthesize block copolymers with control over block lengths, ratios, and composition has led to a dramatic increase in the number and variety of polymeric materials available to the synthetic chemist. Block copolymers are unique structures that are especially suited to meet specific needs because the desirable properties of two different polymers can be combined into one product.²² The synthesis of block copolymers on a large scale, however, is seldom feasible because nearly all techniques yield only one polymer chain per initiator molecule. Unless this barrier can be overcome, expensive metal catalysts, such as those used for ethylene and propylene polymerization and for ROMP, render block copolymerization uneconomical.

Recently, Arriola et al. developed a method termed chain shuttling polymerization that facilitates the economical synthesis of polyolefin block copolymers by producing many polymer chains from each metal initiator.²³ Inspired by this report, we examined whether catalyst **1** could be used to synthesize block copolymers by the PA-ROMP technique. Because this strategy allows for multiple polymer chains to be produced from one metal center, PA-ROMP may also enable the large scale synthesis of block copolymers by reducing catalyst loading.

In order to synthesize block copolymers, a solution of a second monomer needs to be added to the reaction mixture after ROMP of the first block is complete but before any end-capping has occurred. ROMP is known to be extremely fast,²⁰ but it is vital to the synthesis of block copolymers that no end-capping occurs before the second monomer is added. Results obtained from the pulse interval optimization experiments (Table 6.1) indicate that no observable amount of end-capping occurs in the first 0.5 min after addition of monomer, but end-capping does begin within 1.2 min after monomer addition. With these values in mind, we designed a set of 10 experiments similar to those performed in the homopolymer syntheses. In these experiments, the robot made additions in pairs, adding monomer **3** first, followed 0.5 min later by N-methyl oxanorbornene imide (NMONI) (**4**) to ultimately form polymer **9** (Scheme 6.5). Ten reaction vials, designated EE through NN, were set up at 25 °C with 30 min pulse intervals and a total monomer to catalyst ratio of 25 (12.5 for each monomer), adding monomer solutions to one less vial in each pulse, as was done with the homopolymer experiments. A five-fold excess of *cis*-4-octene was included in the catalyst solution, and additional *cis*-4-octene was added with the second monomer to maintain a constant

concentration of CTA in the reaction mixture. GPC traces of the isolated polymer product mixtures **EE** through **NN** are shown in Figure 6.10.



Scheme 6.5. Synthesis of P(tBENI-*b*-NMONI) block copolymers by PA-ROMP.

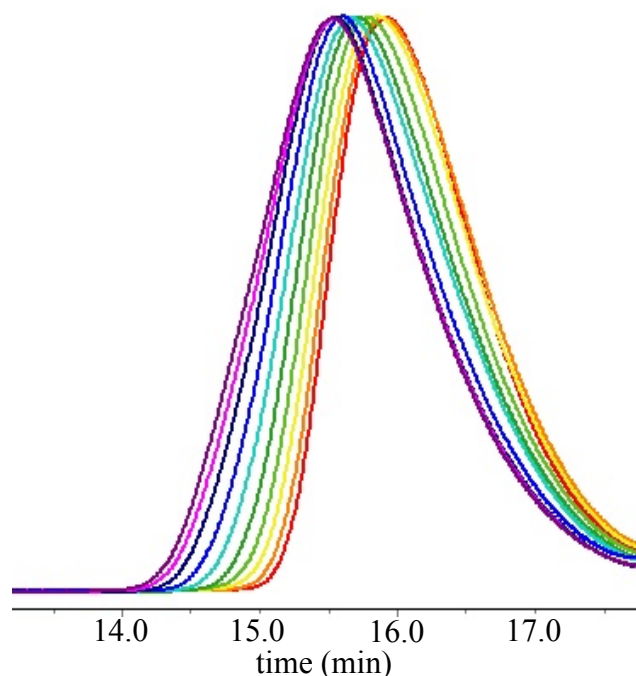


Figure 6.10. GPC traces of block copolymer product mixtures **OO** (red), **PP** (orange), **QQ** (yellow), **RR** (light green), **SS** (green), **TT** (light blue), **UU** (royal blue), **VV** (dark blue), **WW** (light purple), and **XX** (dark purple) from one (product mixture **OO**) to ten (product mixture **XX**) cycles of PA-ROMP.

The polymer characterization data from the block copolymer experiments are shown in Table 6.6. As was observed in the homopolymer experiments, the vial that received only one pair of additions (product mixture **OO**) had a molecular weight of 6320 Da, which is in good agreement with the theoretical molecular weight of 5820 Da, assuming a small amount of catalyst death. The molecular weight of the products slowly increased as catalyst death occurred at a rate of 14.5% per cycle (see Appendix 2). Figure 6.11 shows the data plotted with a well-fitting exponential trendline.

Table 6.6. Characterization of P(tBENI-*b*-NMONI) block copolymer products by GPC from ten cycles of PA-ROMP at 25 °C with M/C = 25 and a pulse interval of 30 min.

Product Mixture	Additions Received	M_n (Da)	PDI
OO	1	6320	1.10
PP	2	6430	1.14
QQ	3	6920	1.14
RR	4	7670	1.14
SS	5	8480	1.16
TT	6	9510	1.18
UU	7	10200	1.23
VV	8	12100	1.22
WW	9	12700	1.26
XX	10	13300	1.30

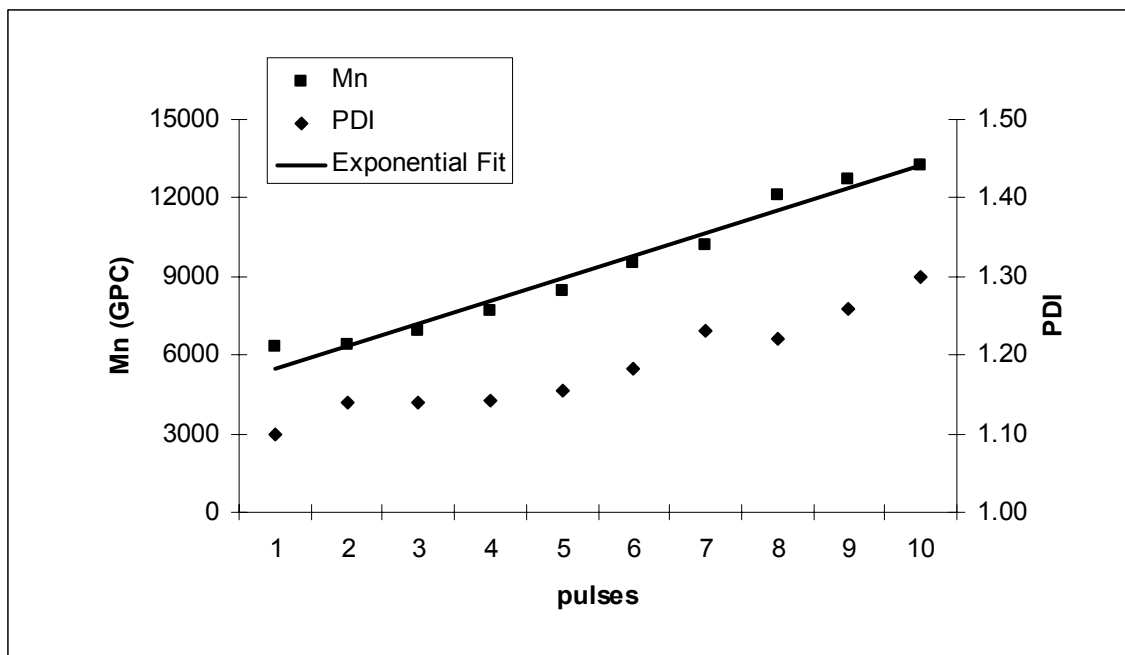


Figure 6.11. Dependence of M_n and PDI on number of cycles of PA-ROMP for P(tBENI-*b*-NMONI) block copolymers.

A single vial experiment was run to determine whether complete consumption of monomer **3** was complete before monomer **4** was added 0.5 min later. This experiment was set up in the same way as the block copolymer experiments, except that the reaction was quenched after 0.5 min with ethyl vinyl ether (100 equiv) instead of adding monomer **4**. Evaluation of the products by ^1H NMR spectroscopy showed that typically 75% of monomer **3** was consumed at this point. This indicates that a small amount of monomer **3** may be present in the second block, but thermal analysis (described below) shows that phase separation of the blocks still occurs. We chose not to increase the interval between the addition of monomer **3** and monomer **4** in order to avoid premature end-capping, which would result in a small amount of dead P(tBENI) homopolymer. A less reactive CTA would likely allow for a longer interval between the two monomer additions, yielding perfect block copolymers.

Differential scanning calorimetry (DSC) was used to evaluate whether the products were indeed block copolymers capable of phase separation. Very broad T_g 's were observed for the unsaturated polymers, which we attribute to the mixture of *cis* and *trans* olefinic stereochemistry in the polymer backbones. Sharper T_g 's were observed when the polymers were hydrogenated using tosyl hydrazide or Wilkinson's catalyst under 600 psi H_2 . A T_g of 111 °C was observed for the hydrogenated P(tBENI) homopolymer, and a T_g of 159 °C was observed for the hydrogenated P(NMONI) homopolymer. For the hydrogenated P(tBENI-*b*-NMONI) block copolymer, T_g 's of 117 °C and 159 °C were observed. These values are in good agreement with the T_g 's of the constituent homopolymers. A P(tBENI-*ran*-NMONI) random copolymer was also prepared and hydrogenated. This polymer showed a single T_g of 136 °C, which lies in between those of the constituent blocks, as is expected for random copolymers. To our knowledge, this is the first example of low polydispersity block copolymers prepared by a regenerated-initiator method. We expect that synthesis of tri- and higher multi-block ROMP polymers could also be prepared by PA-ROMP by simple extension of the current procedure.

Acknowledgement

The author thanks Materia for catalyst as well as Dr. Scott Virgil for programming and operation of the Symyx robotic system and for helpful discussions.

Conclusions

PA-ROMP is a useful strategy for synthesizing homopolymers and block copolymers with much lower catalyst loadings than traditional ROMP. A Symyx robotic system was used to investigate the ability of ruthenium metathesis catalyst **1** to mediate PA-ROMP in several ten-reaction experiments. Using *cis*-4-octene as a CTA to end-cap growing polymer chains and regenerate the ruthenium initiator, up to ten pulses of monomer were successfully polymerized. Under our best conditions, catalyst death was observed to occur at a rate of approximately 8.5% per cycle. This was overcome in a one reaction experiment by varying the amount of monomer injected during each cycle in accordance with the catalyst death rate. This experiment produced a low polydispersity P(tBENI) homopolymer using seven times less catalyst than traditional ROMP. Furthermore, block copolymers were prepared by PA-ROMP. By waiting 0.5 min between injections of tBENI and NMONI into the reaction vials, nearly perfect P(tBENI-*b*-NMONI) block copolymers were prepared in up to ten cycles of PA-ROMP. This represents the first synthesis of low polydispersity block copolymers that is not limited by the one-chain-per-initiator convention. The technique of PA-ROMP is expected to facilitate the emergence of ROMP polymers on the market by reducing cost due to decreased catalyst loading. Additionally, considering the decreased metal contamination in PA-ROMP polymers compared with traditional ROMP polymers, we anticipate that this technique will be valuable for biological applications of ROMP polymers.

Experimental Section

General Information

NMR spectra were measured in CDCl_3 on Varian Mercury 300 MHz spectrometers unless otherwise noted. ^1H and ^{13}C NMR chemical shifts are reported in ppm relative to internal solvent resonances. High-resolution mass spectra (EI and FAB) were provided by the California Institute of Technology Mass Spectrometry Facility. Differential scanning calorimetry was measured on a Perkin-Elmer DSC-7. The results given are for the second heating cycle using a scan rate of $10\text{ }^\circ\text{C}/\text{min}$. Infrared spectra were recorded using a Perkin Elmer Spectrum BXII spectrometer. Gel permeation chromatography (GPC) was carried out in THF on two PLgel $10\text{ }\mu\text{m}$ mixed-B LS columns (Polymer Labs) connected in series with a DAWN EOS multiangle laser light scattering (MALLS) detector and an Optilab DSP differential refractometer (both from Wyatt Technology). No calibration standards were used, and dn/dc values for P(tBENI) and P(tBENI-*b*-NMONI) were obtained by taking the average of the dn/dc measured for at least ten samples by assuming 100% mass elution from the columns. The dn/dc used for P(tBENI) homopolymers was 0.109, and the dn/dc used for P(tBENI-*b*-NMONI) was 0.108. The dn/dc values for all other polymers were obtained in individual runs by assuming 100% mass elution from the columns.

All reactions were performed in an N_2 -filled glovebox unless otherwise indicated. Reactants and reaction vials were kept on plates regulated at $25\text{ }^\circ\text{C}$ unless otherwise noted. Reactions were performed using a Symyx robotic system programmed using Epoch software and were run using $(\text{CH}_2\text{Cl})_2$ as the backing solvent. All stock solutions and reaction vials were maintained at $25\text{ }^\circ\text{C}$. The syringe withdrawal speed was set to 30

$\mu\text{L}/\text{sec}$ with a two second delay after withdrawal. An overshoot volume of 180 μL per 1 mL syringe and a 70 μL dispense back into the stock solution immediately after withdrawal were employed to ensure consistent dispense volumes. A syringe dispense speed of 150 $\mu\text{L}/\text{sec}$ was used, and reaction vials were stirred at a rate of 300 Hz. Reactions were performed in screw-cap, septum-topped vials with holes 5 mm in diameter in the septa. Monomer solutions were kept tightly capped in screw-cap, septum-topped vials, and a 22g vent needle was inserted into each cap. Once the reactions were complete, the vials were removed from the glovebox, and their contents were precipitated into a large volume of hexanes/diethyl ether (1:1). The polymer products were recovered by filtration and drying under vacuum.

Materials

$(\text{CH}_2\text{Cl})_2$ was used as received from an Aldrich Sure-Seal bottle or distilled from CaH_2 . CH_2Cl_2 was purified by passage through a solvent purification system.²⁴ $(\text{H}_2\text{IMes})(\text{pyr})_2(\text{Cl})_2\text{RuCHPh}$ (**1**) was prepared from $(\text{H}_2\text{IMes})(\text{PCy}_3)(\text{Cl})_2\text{RuCHPh}$ (obtained from Materia) according to a literature procedure.²⁵ Monomers *tert*-butyl ester norbornene imide (tBENI) (**3**) and N-methyl oxanorbornene imide (NMONI) (**4**) were prepared as previously described.¹⁴ *cis*-4-Octene was purchased from Alfa Aesar and used as received. All other materials were obtained from Aldrich Chemical Company and used as received unless otherwise noted.

$(\text{H}_2\text{IMes})(\text{Cl})_2(\text{pyr})_2\text{RuCHCH}_2\text{CH}_2\text{CH}_3$ (**2**). A solution of *cis*-4-octene (46 mg) in CH_2Cl_2 (1.5 mL) was added to a 20 mL vial containing catalyst **1** (100 mg). The

solution turned brown, and after 30 min the vial was put in the freezer. After another 10 min, Et₂O was carefully layered on top of the CH₂Cl₂ layer. The vial was put back in the freezer until crystallization occurred. Brown crystals (48 mg) were recovered (50% yield). ¹H NMR (CD₂Cl₂) : δ 0.68 (t, 3H), 1.15 (m, 2H), 1.90 (m, 2H), 2.20-2.60 (m, 18H), 3.80-4.10 (m, 4H), 6.88 (s, 3H), 6.96 (s, 2H), 7.10 (s, 3H), 7.57 (s, 2H), 7.82 (s, 2H), 8.51 (s, 2H) 18.91 (t, 1H). ¹³C NMR (CD₂Cl₂): δ 334.11, 220.75, 157.15, 152.79, 140.44, 139.47, 138.74, 138.27, 137.71, 136.97, 134.45, 131.48, 130.56, 130.14, 129.74, 129.35, 128.25, 124.08, 123.13, 121.66, 61.90, 52.02, 51.15, 21.29, 20.93, 20.55, 20.31, 19.50, 18.72, 14.24. HRMS: [M – C₄H₈] calculated 636.1361; found 636.1346. The complex was occasionally isolated with an impurity that showed a peak at δ 19.07 in the ¹H NMR spectrum.

Varied pulse interval experiment. A stock solution of catalyst **1** (24.80 mg, 1 equiv) and *cis*-4-octene (19.78 mg, 5.2 equiv) in a 5 mL volumetric flask was prepared. A stock solution of monomer **3** (795.40 mg total, 19.09 mg per addition, 25.2 equiv per addition) in a 5 mL volumetric flask was also prepared. The robot added 400 μL of the catalyst/*cis*-4-octene stock solution to each of 10 vials, labeled A through J. Thirty min after catalyst **1** and *cis*-4-octene were mixed to make the stock solution, 120 μL of the monomer **3** solution was added to vials A through J. At varying intervals (outlined in Table 6.1), a second addition of 120 μL of the monomer **3** solution was added to each of vials B through J. Vial A was used as a control and did not receive a second addition of monomer. Thirty min after the final addition was made, all of the vials were removed

from the glovebox. Products **A** through **J** were recovered in 83-95% yield. GPC data are shown in Table 6.1.

P(tBENI) homopolymer syntheses (10 vials, M/C=25, 25 °C). A stock solution of catalyst **1** (25.01 mg, 1 equiv) and *cis*-4-octene (20.65 mg, 5.3 equiv) in a 5 mL volumetric flask was prepared. A stock solution of monomer **3** (1.5879 g total, 19.05 mg per addition, 25.0 equiv per addition) and *cis*-4-octene (28.15 mg total, 0.34 mg per addition, 1.1 equiv per addition) in a 5 mL volumetric flask was also prepared. The robot added 400 μ L of the catalyst/*cis*-4-octene stock solution to each of 10 vials, labeled **K** through **T**. Thirty min after catalyst **1** and *cis*-4-octene were mixed to make the stock solution, 120 μ L of the monomer **3** solution was added to vials **K** through **T**. Thirty min after the first addition, a second addition of 120 μ L of the monomer **3** solution was added to each of vials **L** through **T**. Thirty min after the second addition, a third addition of 120 μ L was added to each of vials **M**-**T**. This process was continued, removing one vial during each cycle, until vial **T** received 10 additions of monomer. Thirty min after the final addition was made, all of the vials were removed from the glovebox. Products **K** through **T** were recovered in 72-96% yield. GPC data are shown in Table 6.2.

P(tBENI) homopolymer syntheses (10 vials, M/C=100). A stock solution of catalyst **1** (6.39 mg, 1 equiv) and *cis*-4-octene (5.00 mg, 5.1 equiv) in a 5 mL volumetric flask was prepared. A stock solution of monomer **3** (1.5860 g total, 19.03 mg per addition, 97.6 equiv per addition) and *cis*-4-octene (7.20 mg total, 0.34 mg per addition, 1.1 equiv per addition) in a 5 mL volumetric flask was also prepared. The reaction

procedure was the same as the P(tBENI) homopolymer syntheses with M/C=25. Products **U** through **DD** were recovered in 71-100% yield. GPC data are shown in Table 6.3.

P(tBENI) homopolymer syntheses (10 vials, M/C=25, 20 °C). The same reaction setup as for the P(tBENI) homopolymer syntheses was used, keeping the reaction mixtures at 20 °C and using a pulse interval of 60 min. GPC data are shown in Table 6.5.

P(tBENI) homopolymer synthesis (1 vial). A stock solution of catalyst **1** (25.20 mg, 1 equiv) and *cis*-4-octene (19.90 mg, 5.1 equiv) in a 5 mL volumetric flask was prepared. A stock solution of monomer **3** (318.55 mg total, 19.11 mg for first addition, 24.9 equiv for first addition) and *cis*-4-octene (5.74 mg total, 0.34 mg for first addition, 1.1 equiv for first addition) in a 2 mL volumetric flask was also prepared. The robot added 400 μ L of the catalyst/*cis*-4-octene stock solution to the reaction vial. Thirty min after catalyst **1** and *cis*-4-octene were mixed to make the stock solution, 120 μ L of the monomer **3** solution was added to the reaction vial. Each 30 min, a volume of the monomer **3** solution was added to the reaction vial, as outlined in Table 6.3. Thirty min after the tenth addition was made, the vial was removed from the glovebox. The P(tBENI) product was recovered in 86% yield. GPC: $M_n = 9640$, $M_w/M_n = 1.08$.

P(tBENI-*b*-NMONI) block copolymer synthesis. A stock solution of catalyst **1** (25.10 mg, 1 equiv) and *cis*-4-octene (19.22 mg, 5.0 equiv) in a 5 mL volumetric flask

was prepared. Stock solutions of monomer **3** (794.85 mg total, 9.54 mg per addition, 12.5 equiv per addition) in a 5 mL volumetric flask, as well as monomer **4** (515.84 mg total, 6.19 mg per addition, 12.5 equiv per addition) and *cis*-4-octene (29.20 mg total, 0.35 mg per addition, 1.1 equiv per addition) in a 5 mL volumetric flask were also prepared. The robot added 400 μ L of the catalyst/*cis*-4-octene stock solution to each of 10 vials, labeled OO through XX. Thirty min after catalyst **1** and *cis*-4-octene were mixed to make the stock solution, 60 μ L of the monomer **3** solution and 60 μ L of the monomer **4** solution were added to vials OO through XX. The robot was programmed such that each vial received the addition of the monomer **4** solution exactly 30 s after it received the addition of the monomer **3** solution. Thirty min after the first set of additions, a second set of additions of the same amounts was performed, adding to each of vials PP through XX. Thirty min after the second set of additions, a third set of additions was performed, adding to each of vials QQ-XX. This process was continued, removing one vial during each cycle, until vial XX received 10 sets of additions of monomer. Thirty min after the final additions were made, all of the vials were removed from the glovebox. Products **OO** through **XX** were recovered in 75-93% yield. GPC data are shown in Table 6.4.

Representative characterization data. Representative NMR and IR spectra of P(tBENI) polymers were obtained from the product of the one-pot homopolymer synthesis of P(tBENI) by PA-ROMP. ^1H NMR: δ 0.90 (t, 6H), 1.20-1.80 (m, 8H + 9n H), 2.00-2.30 (m, n H), 2.70-3.40 (m, 4n H), 4.00-4.10 (m, 2n H), 5.40-5.80 (d, 2n H). IR: 2979, 2931, 1780, 1743, 1710, 1415, 1394, 1369, 1323, 1235, 1167, 919, 846, 750.

Representative NMR and IR spectra of P(tBENI-*b*-NMONI) block copolymers were obtained from product mixture **XX**. ^1H NMR: δ 0.90 (m, 6H), 1.20-1.80 (m, 10n H), 2.00-2.40 (m, n H), 2.70-3.40 (m, 4n H + 5m H), 4.00-4.10 (s, 2n H), 4.30-4.60 (m, 2m H) 4.70-5.10 (m, 2m H) 5.40-6.20 (m, 2n H + 2m H). IR: 2979, 2931, 1779, 1741, 1707, 1416, 1370, 1324, 1281, 1235, 1159, 1130, 1033, 970, 919, 845, 734.

P(tBENI-*ran*-NMONI) synthesis. To a stirring solution of monomer **3** (154 mg, 100 equiv) and monomer **4** (99 mg, 100 equiv) in CH_2Cl_2 (3 mL) under argon flow was added catalyst **1** (4.0 mg, 1 equiv) as a solution in CH_2Cl_2 (0.1 mL). After 5 min, ethyl vinyl ether was added. After an additional 10 min, the reaction mixture was precipitated into a solution of Et_2O /hexanes (1:1). The product was recovered as an off white solid by filtration in 81% yield. ^1H NMR: δ 1.20-1.80 (m, 10n H), 2.00-2.40 (m, n H), 2.70-3.40 (m, 4n H + 5m H), 4.00-4.10 (s, 2n H), 4.30-4.60 (m, 2m H) 4.70-5.10 (m, 2m H) 5.40-6.20 (m, 2n H + 2m H). GPC: $M_n = 54700$, $M_w/M_n = 1.01$.

P(NMONI) homopolymer synthesis. To a stirring solution of monomer **4** (206 mg, 100 equiv) in CH_2Cl_2 (2 mL) under argon flow was added catalyst **1** (8.0 mg, 1 equiv). After 10 min, ethyl vinyl ether (0.5 mL) was added. After an additional 10 min, the reaction mixture was precipitated into a solution of Et_2O /hexanes (1:1). The product was recovered as an off white solid by filtration in 69% yield. ^1H NMR: δ 2.85-3.00 (s, 3n H), 3.20-3.45 (s, 2n H), 4.30-4.60 (m, n H), 4.70-5.00 (m, n H), 5.70-6.10 (m, 2n H).

Typical hydrogenation procedure:

Method A. A vial was charged with the polymer to be hydrogenated (60 mg, 1 equiv per olefin), tosyl hydrazide (220 mg, approx. 4.5 equiv), BHT (3 mg, 0.05 equiv), and 3 mL xylenes. The solution was freeze-pump-thawed three times, then the vial was placed into an oil bath and heated at 130 °C for 5 h. The hot reaction mixture was precipitated into MeOH. Products were recovered by filtration in 42 to 60% yield. Hydrogenation was typically over 99% complete as determined by ¹H NMR spectroscopy. Alternatively, the product can be recovered by precipitation into MeOH followed by precipitation into Et₂O/hexanes (1:1).

Method B. The polymer to be hydrogenated (88 mg, 1 equiv per olefin) was dissolved in 3 mL THF in a scintillation vial. Wilkinson's catalyst (5.5 mg, approx. 0.02 equiv) was added, and the vial was placed in a bomb. Three cycles of pressurizing with 400 psi H₂ and venting were performed. The bomb was then pressurized to 600 psi with H₂ and placed in an oil bath set to 50 °C. After 12 h, more Wilkinson's catalyst (5.5 mg) was added, and the filling procedure was repeated. The bomb was heated at 50 °C for another 24 h. The reaction mixture was filtered and concentrated then precipitated into Et₂O/hexanes (1:1). Products were recovered by filtration in 72 to 85% yield. Hydrogenation was typically over 90% complete as determined by ¹H NMR spectroscopy.

Hydrogenated P(tBENI). Method A was used. ¹H NMR: δ 0.90 (t, 6H), 1.10-1.70 (m, 8H + 11n H), 1.75-1.95 (m, 2n H), 1.95-2.15 (m, 2n H), 2.20-2.30 (m, 2n H),

2.80-2.90 (m, 2n H), 4.00-4.15 (m, 2n H). GPC: $M_n = 13200$, $M_w/M_n = 1.04$. DSC: $T_g = 111$ °C.

Hydrogenated P(tBENI-*ran*-NMONI). Method B was used. ^1H NMR: δ 0.90 (m, 6H), 1.00-1.70 (m, 9n H + 6H), 1.80-2.30 (m, 2n H + 4m H), 2.80-3.20 (m, 4n H + 3m H), 3.75-3.95 (m, 2m H), 4.00-4.10 (m, 2n H). GPC: $M_n = 60700$, $M_w/M_n = 1.01$. DSC: $T_g = 136$ °C.

Hydrogenated P(tBENI-*b*-NMONI). Method B was used. ^1H NMR: δ 0.90 (m, 6H), 1.00-1.80 (m, 9n H + 6H), 1.80-2.30 (m, 2n H + 4m H), 2.80-3.20 (m, 4n H + 3m H), 3.60-3.95 (m, 2m H), 4.00-4.15 (m, 2n H). GPC: $M_n = 11900$, $M_w/M_n = 1.05$. DSC: $T_g = 113$ °C.

Hydrogenated P(NMONI). Method B was used. ^1H NMR (DMSO-*d*6): δ 1.65-1.85 (s, 4n H), 2.70-2.80 (s, 3n H), 3.10-3.25 (m, 2n H), 3.70-3.85 (s, 2n H). DSC: $T_g = 159$ °C. The product was not soluble in THF, so no GPC was obtained.

References

- (1) (a) Grubbs, R. H. *Handbook of Metathesis*; Wiley-VCH: Weinheim, 2003. (b) Bielawski, C. W.; Grubbs, R. H. *Prog. Polym. Sci.* **2007**, *32*, 1–29. (c) Buchmeiser, M. R. *Chem. Rev.* **2000**, *100*, 1565–1604.
- (2) (a) Murdzek, J. S.; Schrock, R. R. *Macromolecules* **1987**, *20*, 2640–2642. (b) Kanaoka, S.; Grubbs, R. H. *Macromolecules*, **1995**, *28*, 4707–4713. (c) Matson, J. B.; Grubbs, R. H. *J. Am. Chem. Soc.* **2008**, *130*, 6731–6733.
- (3) (a) Beerens, H.; Wang, W.; Verdonck, L.; Verpoort, F. *J. Mol. Catal. A-Chem.* **2002**, *190*, 1–7. (b) Bazan, G.; Schrock, R. R. *Macromolecules* **1991**, *24*, 817–823. (c) Conner, E. F.; Lares, M. C.; Hendrick, J. L.; Miller, R. D. *Polymer Preprints* **2002**, *43*, 724.
- (4) (a) Nomura, K.; Takahashi, S.; Imanishi, Y. *Macromolecules* **2001**, *34*, 4712–4723. (b) Hilf, S.; Kilbinger, A. F. M. *Macromol. Rapid Comm.* **2007**, *28*, 1225–1230.
- (5) Rajaram, S.; Choi, T. L.; Rolandi, M.; Frechet, J. M. J. *J. Am. Chem. Soc.* **2007**, *129*, 9619–9621.
- (6) Mol, J. C. *J. Mol. Catal. A-Chem.* **2004**, *213*, 39–45.
- (7) Gibson, V. C.; Spitzmesser, S. K. *Chem. Rev.* **2003**, *103*, 283–315.
- (8) Jha, S.; Dutta, S.; Bowden, N. B. *Macromolecules* **2004**, *37*, 4365–4374.
- (9) Bell, A.; Grubbs, R. H.; Morgan, J. P.; Moore, J. L. High activity metal carbene metathesis catalysts generated using a thermally activated N-heterocyclic carbene precursor. U. S. Patent 6838489, Jan 4, 2005.
- (10) (a) Crowe, W. E.; Mitchell, J. P.; Gibson, V. C.; Schrock, R. R. *Macromolecules* **1990**, *23*, 3536–3538. (b) Gibson, V. C.; Okada, T. *Macromolecules* **2000**, *33*, 655–656.
- (11) Pintauer, T.; Matyjaszewski, K. *Chem. Soc. Rev.* **2008**, *37*, 1087–1097.
- (12) (a) Gordon, E. J.; Gestwicki, J. E.; Strong, L. E.; Kiessling, L. L. *Chem. Biol.* **2000**, *7*, 9–16. (b) Maynard, H. D.; Okada, S. Y.; Grubbs, R. H. *J. Am. Chem. Soc.* **2001**, *123*, 1275–1279. (c) Rawat, M.; Gama, C. I.; Matson, J. B.; Hsieh-Wilson, L. C. *J. Am. Chem. Soc.* **2008**, *130*, 2959–2961.
- (13) (a) Choi, T. L.; Grubbs, R. H. *Angew. Chem., Int. Ed.* **2003**, *42*, 1743–1746. (b) Camm, K. D.; Castro, N. M.; Liu, Y. W.; Czechura, P.; Snelgrove, J. L.; Fogg, D. E. *J. Am. Chem. Soc.* **2007**, *129*, 4168–4169.

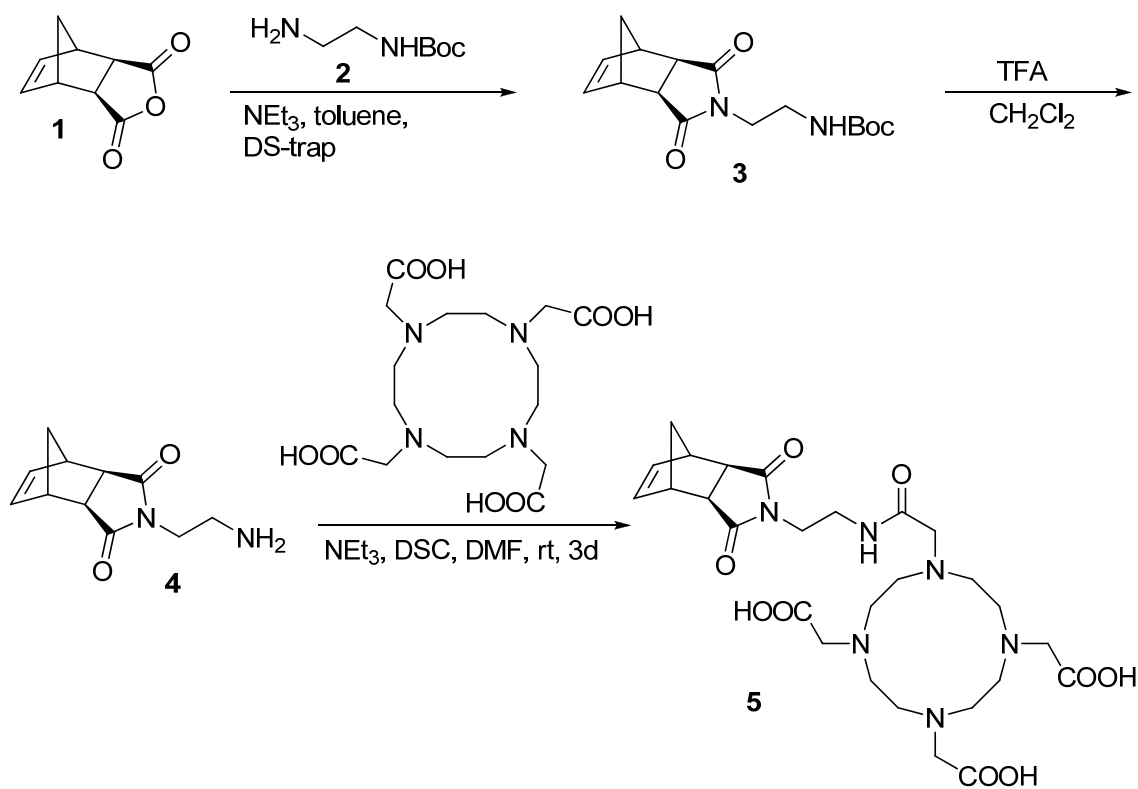
- (14) Matson, J. B.; Grubbs, R. H. *Macromolecules* **2008**, *41*, 5626–5631.
- (15) Chatterjee, A. K.; Choi, T. L.; Sanders, D. P.; Grubbs, R. H. *J. Am. Chem. Soc.* **2003**, *125*, 11360–11370.
- (16) Champagne, T. M.; Hong, S. H.; Lee, C. W.; Ung, T. A.; Stoianova, D. S.; Pederson, R. L.; Kuhn, K. M.; Virgil, S. C.; Grubbs, R. H. *Abstracts of Papers*, 236th ACS National Meeting, Philadelphia, PA; American Chemical Society; Washington, DC, 2008; ORGN-077.
- (17) Bieniek, M.; Michrowska, A.; Usanov, D. L.; Grela, K. *Chem. Eur. J.* **2008**, *14*, 806–818.
- (18) (a) Feast, W. J.; Gibson, V. C.; Khosravi, E.; Marshall, E. L.; Mitchell, J. P. *Polymer* **1992**, *33*, 872–873. (b) Perrott, M. G.; Novak, B. M. *Macromolecules*, **1995**, *28*, 3492–3494.
- (19) These percentages are calculated by assuming that the M_n of 12400 Da is a combination of pure products **6** and **7**.
- (20) Bielawski, C. W.; Benitez, D.; Morita, T.; Grubbs, R. H. *Macromolecules*, **2001**, *34*, 8610–8618.
- (21) While a linear fit to the data presented here is also reasonable, molecular weight is expected to depend on the number of cycles in PA-ROMP in an exponential fashion. When a constant catalyst death rate is assumed, plotting pulses vs. molecular weight out to 40 cycles clearly shows that an exponential fit is the better choice for the data.
- (22) I. W. Hamley, *The Physics of Block Copolymers* (Oxford Univ. Press, Oxford, 1998).
- (23) Arriola, D. J.; Carnahan, E. M.; Hustad P. D.; Kuhlman, R. L.; Wenzel, T. T. *Science* **2006**, *312*, 714–719.
- (24) Pangborn, A. B.; Giardello, M. A.; Grubbs, R. H.; Rosen, R. K.; Timmers, F. J. *Organometallics* **1996**, *15*, 1518–1520.
- (25) Love, J. A.; Morgan, J. P.; Trnka, T. M.; Grubbs, R. H. *Angew. Chem., Int. Ed.* **2002**, *41*, 4035–4037.

Appendix 1

Additional Monomers and Polymers Synthesized

Introduction

Several norbornene monomers were synthesized and polymerized that were not discussed in the text. A brief discussion of their synthesis and polymerization is presented here.



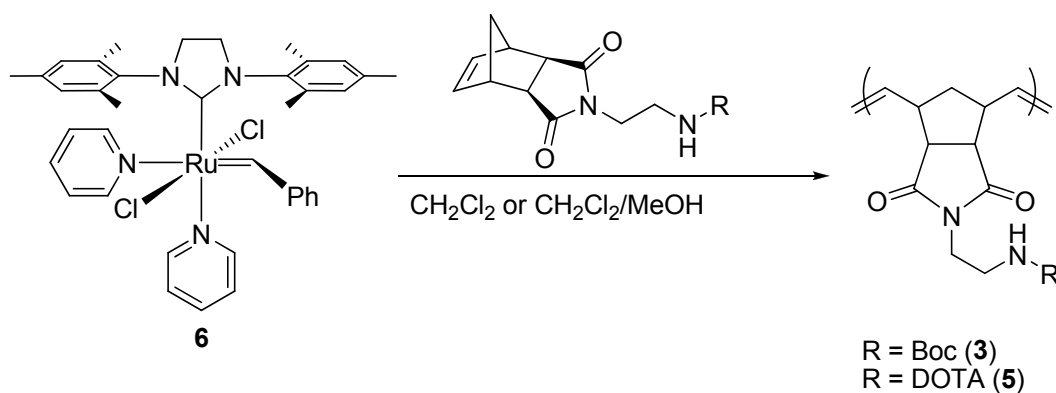
Scheme A1.1 Synthesis of DOTA-containing norbornene monomer.

Results and Discussion

Polymers containing the 1,4,7,10-tetraazacyclododecane- $\text{N},\text{N}',\text{N}'',\text{N}'''$ -tetraacetic acid (DOTA) group have received much interest lately due to their ability to chelate metal ions, most notably the positron-emitting nuclide copper-64, for use as *in vivo* molecular imaging probes.¹ Monomer **5** was synthesized (Scheme A1.1) for

potential use as a comonomer in ROMP polymers to be used in molecular imaging applications. Synthesis of monomer **5** was carried out as follows: Exo-anhydride **1** was reacted with *tert*-butyl-2-aminoethylcarbamate (**2**) in toluene with triethylamine (NEt₃) and a Dean-Stark trap to yield Boc-protected amine **3**. Deprotection of **3** to remove the Boc group was carried out using trifluoroacetic acid in CH₂Cl₂ to afford free amine **4**. DOTA was then coupled to amine **4** using *N,N'*-disuccinimidyl carbonate (DSC) as the coupling agent. Purification by preparatory scale HPLC afforded the desired DOTA-containing monomer **5**.

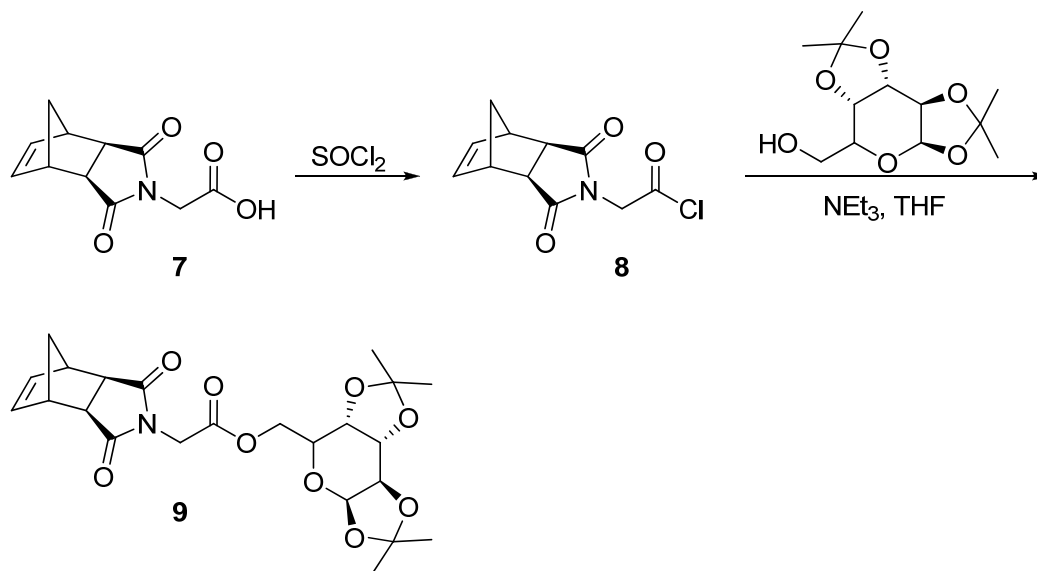
Monomer **3** was found to undergo living ring-opening metathesis polymerization (ROMP) in CH₂Cl₂ using catalyst **6** (Scheme A1.2). The polymer products had controllable molecular weights and narrow polydispersities. Monomer **5** was also found to undergo ROMP in CH₂Cl₂/MeOH (10:1) with catalyst **6** as determined by ¹H NMR spectroscopy. No molecular weight data could be obtained for this product.



Scheme A1.2. ROMP of monomers **3** and **5**.

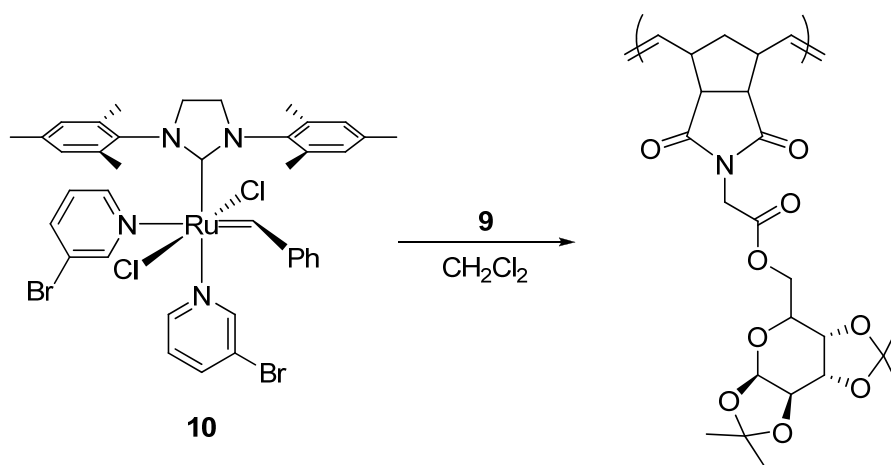
Polymers containing saccharides have also received attention lately, largely due to their abilities to bind receptors on cell surfaces.² For potential use in designing polymers

and nanoparticles with cell-surface receptor binding properties, a galactose-containing norbornene monomer was synthesized. Starting from monomer **7**, whose synthesis has been previously described,³ thionyl chloride was added to form acid chloride **8** (Scheme A1.3). Addition of 1,2:3,4-di-O-isopropylidene-D-galactose furnished the protected galactose-containing monomer **9** in good yield.



Scheme A1.3. Synthesis of galactose-containing norbornene monomer.

ROMP of monomer **9** was carried out using catalyst **10** (described in Chapter 1) in CH_2Cl_2 at room temperature (Scheme A1.4). The polymer product was narrowly dispersed with an observed molecular weight matching the theoretical value.



Scheme A1.4. ROMP of monomer **9**.

Acknowledgement

The author thanks Materia for catalyst, as well as Dave Montgomery, John Phillips, and Young In Oh for HPLC assistance.

Experimental Section

General Information

NMR spectra of small molecules were measured in CDCl_3 on Varian Mercury 300 MHz spectrometers unless otherwise noted. ^1H and ^{13}C NMR chemical shifts are reported in ppm relative to proteosolvent resonances. Flash column chromatography of organic compounds was performed using silica gel 60 (230-400 mesh). High-resolution mass spectra (EI and FAB) were provided by the California Institute of Technology Mass Spectrometry Facility. Gel permeation chromatography (GPC) was carried out in THF on two PLgel 10 μm mixed-B LS columns (Polymer Labs) connected in series with a

DAWN EOS multiangle laser light scattering (MALLS) detector and an Optilab DSP differential refractometer (both from Wyatt Technology). No calibration standards were used, and dn/dc values were obtained for each injection by assuming 100% mass elution from the columns. Analytical HPLC was performed on a Beckman Gold system equipped with a diode array detector using a Phenomenex Gemini column (5 μm particle size, C18 110A, 250×4.6 mm, 5 μm). Preparative HPLC was performed on a Beckman Gold system equipped with a single-wavelength detector monitoring at 310 nm using a Phenomenex Gemini column (5 μm particle size, C18 110A, 250×21.2 mm, 5 μm). Mixtures of acetonitrile and 0.1% aqueous TFA were used as the mobile phase for both analytical and preparative HPLC.

Materials

DOTA was purchased from Strem Chemicals. DSC was purchased from TCI America. Anhydride **1** was prepared as described previously.⁴ CH_2Cl_2 was purified by passage through solvent purification columns.⁵ Anhydrous DMF was obtained from Acros Chemical Company and used as received. $(\text{H}_2\text{IMes})(\text{pyr})_2(\text{Cl})_2\text{RuCHPh}$ (**6**) and $(\text{H}_2\text{IMes})(3\text{Br-pyr})_2(\text{Cl})_2\text{RuCHPh}$ (**10**) were prepared from $(\text{H}_2\text{IMes})(\text{PCy}_3)(\text{Cl})_2\text{RuCHPh}$ (provided by Materia) according to a literature procedure.⁶ All other materials were obtained from Aldrich Chemical Company and used as received unless otherwise noted.

***tert*-Butyl-2-aminoethylcarbamate (2)**. A round-bottom flask was charged with ethylene diamine (20 mL, 9.5 equiv) and CH_2Cl_2 (100 mL). The flask was cooled to 0 °C, then Boc anhydride (6.83 g, 1 equiv) was added dropwise as a solution in CH_2Cl_2

from an addition funnel over 1 h. A white, gummy solid crashed out as the reaction mixture was stirred and allowed to warm to room temperature over 5 h. The solvent was then removed *in vacuo*, and the pale yellow, viscous oil was taken up in H₂O (100 mL) and EtOAc (50 mL). The aqueous layer was separated off, and the EtOAc layer was washed with H₂O (4 x 30 mL). The combined aqueous layers were basified to pH = 13 with NaOH pellets. This aqueous solution was then extracted with EtOAc (4 x 50 mL). The combined organic layers were washed with brine and dried over Na₂SO₄. The solvent was removed *in vacuo* to afford a pale yellow oil, which was further purified by Kugelrohr distillation (135 °C at 250 mTorr) to yield **2** as a clear, viscous oil in 47% yield (2.36 g). ¹H NMR: δ 1.21 (s, 2H), 1.42 (s, 9H), 2.77 (t, *J* = 5.9, 2H), 3.15 (dd, *J* = 11.6, 5.8, 2H), 4.91 (s, 1H).

N-(*tert*-Butyl-2-aminoethylcarbamate)-*cis*-5-norbornene-*exo*-2,3-

dicarboximide (3). A round-bottom flask was charged with amine **2** (2.34 g, 1.1 equiv) and benzene (40 mL). Anhydride **1** (2.13 g, 1 equiv) was added, followed by NEt₃ (200 μL, 0.1 equiv). A Dean-Stark trap was attached, and the flask was immersed in an oil bath and heated at reflux for 2 h. The solvent was then removed *in vacuo*, and the residue was taken up in EtOAc (500 mL). This solution was washed with 0.1 N HCl, water, and brine (200 mL each) and dried over MgSO₄. The solvent was removed *in vacuo* and the product was purified by silica gel chromatography (40% EtOAc in hex) to afford **3** as a white powder in 68% yield (2.71 g). ¹H NMR: δ 1.14 – 1.66 (m, 11H), 2.69 (d, *J* = 1.2, 2H), 3.27 (t, *J* = 1.6 Hz, 2H), 3.30 (q, *J* = 5.3 Hz, 2H), 3.62 (t, *J* = 6.0 Hz, 2H), 4.79 (s,

1H), 6.28 (t, $J = 1.7$ Hz, 2H). ^{13}C NMR: δ 138.00, 156.04, 138.00, 79.63, 48.08, 45.34, 43.04, 39.31, 38.63, 28.51.

N-(2-Aminoethyl)-*cis*-5-norbornene-*exo*-2,3-dicarboximide (4). Boc-protected amine **3** (813 mg, 1 equiv) was dissolved in CH_2Cl_2 (30 mL) in a round-bottom flask. Trifluoroacetic acid (2 mL, 10 equiv) was added, and the flask was capped with a septum pierced with a needle. After 16 h the reaction was slowly quenched by adding 5% NH_4OH (30 mL) portionwise. The reaction mixture was transferred to a separatory funnel, and the organic layer was separated off. The aqueous layer was extracted with CH_2Cl_2 (2 x 15 mL), and the combined organic layers were washed with H_2O and brine (20 mL each) and dried over Na_2SO_4 . The solvent was removed *in vacuo* to afford **4** as a waxy solid in 89% yield (488 mg). ^1H NMR: δ 1.10 (s, 2H), 1.28 – 1.38 (m, 1H), 1.44 – 1.54 (m, 1H), 2.68 (d, $J = 1.4$, 2H), 2.87 (t, $J = 6.4$, 2H), 3.17 – 3.34 (m, 2H), 3.53 (t, $J = 6.4$, 2H), 6.27 (t, $J = 1.8$, 2H). ^{13}C NMR: δ 178.51, 137.95, 48.00, 45.34, 42.98, 41.60, 40.10.

N-((2-Ethyl)-DOTA-amide)-*cis*-5-norbornene-*exo*-2,3-dicarboximide (5). DOTA (325 mg, 3 equiv) was lyophilized from H_2O (5 mL) in a round-bottom flask. To the flask was added DMF (15 mL), NEt_3 (0.9 mL, 24 equiv) and DSC (105 mg, 1.5 equiv). The reaction mixture was stirred at room temperature for 4 h as it became homogeneous and pale yellow, after which amine **4** (55 mg, 1 equiv) was added. After 70 h the solvent was removed *in vacuo*. The residue was taken up in H_2O and purified by preparatory scale HPLC (10-30% ACN in 0.1% aqueous TFA over 40 min.) to yield **5** as

a white powder in 25% yield (39 mg). Purity was confirmed by analytical HPLC. ^1H NMR (CD_3OD): δ 1.24 (d, $J = 9.6$ Hz, 1H), 1.50 (d, $J = 9.6$ Hz, 1H), 2.75 (s, 2H), 3.18 (s, 2H), 3.20-3.45 (m, 4H), 3.68 (m, 4H), 3.80-4.10 (m, 4H), 6.33 (t, $J = 1.8$ Hz, 2H). ^{13}C NMR : δ 180.59, 139.03, 54.87, 51.22, 46.45, 43.84, 39.05, 38.65 (missing protons and carbons are not visible likely due to micelle formation).

ROMP of 3. To a vigorously stirring solution of **3** (21.1 mg, 1000 equiv) in CH_2Cl_2 (0.5 mL) under argon was added catalyst **6** (0.05 mg, 1 equiv) in CH_2Cl_2 (0.1 mL) from a stock solution. After allowing the reaction mixture to stir for 30 min at room temperature under argon, the reaction was quenched by addition of ethyl vinyl ether (0.2 mL). After another 10 min the reaction mixture was precipitated into $\text{Et}_2\text{O}/\text{hex}$ (1:1) (20 mL). The polymer product was recovered by filtration in 95% yield (20 mg). GPC: $M_n = 387,000$, $M_w/M_n = 1.03$.

ROMP of 5. To a stirring solution of **5** (4.5 mg, 22 equiv) in $\text{CD}_2\text{Cl}_2/\text{CD}_3\text{OD}$ (8:1) (0.7 mL) was added catalyst **6** in CD_2Cl_2 (0.1 mL). The disappearance of the proton resonance at 6.3 ppm, which corresponds to the norbornene olefin, was followed by ^1H NMR. After 10 min the reaction mixture was cloudy and the monomer was over 80% consumed.

N-(2-Chloro-2-oxoethyl)-cis-5-norbornene-exo-2,3-dicarboximide (8). A round-bottom flask was charged with carboxylic acid **7** (2.84g, 1 equiv). A condenser was attached to the flask, and a line inlet was attached to the condenser. The flask was

evacuated and backfilled with argon three times, then the gas inlet was quickly traded for a gas inlet attached to tubing connecting to a bump trap, followed by a bubbler filled with a 1M NaOH solution. SOCl_2 (10 mL, 11 equiv) was quickly added to the reaction flask, and the flask was put in an oil bath and heated at reflux until gas evolution had ceased. The SOCl_2 was removed *in vacuo*, leaving a light yellow solid. This crude product was crystallized from EtOAc and pet. ether to afford **8** as pale yellow crystals in 81% yield (2.50 g). ^1H NMR: δ 1.56 (d, $J = 1.2$ Hz, 2H), 2.79 (s, 2H), 3.34 (quintet, $J = 1.6$ Hz, 2H), 4.62 (s, 2H), 6.32 (t, $J = 1.8$ Hz, 2H). ^{13}C NMR: δ 176.53, 168.81, 138.21, 48.44, 48.26, 45.68, 43.17.

N-(1,2:3,4-Di-O-isopropylidene-D-galactose-2-oxoethyl)-cis-5-norbornene-exo-2,3-dicarboximide (9). A 2-necked, round-bottom flask was equipped with a septum and a gas inlet. 1,2:3,4-di-O-isopropylidene-D-galactose (1.06g, 1.07 equiv) was dissolved in THF (10 mL) and added to the flask via syringe. The flask was cooled to 0 °C, and triethylamine was added (680 μL , 1.20 equiv). Acid chloride **8** (1.04 g, 1 equiv) was added dropwise as a solution in THF (10 mL). The reaction mixture was allowed to warm to room temperature. After 36 h the reaction mixture was filtered to remove the precipitated $\text{Et}_3\text{N}\cdot\text{HCl}$, and the filtrate was concentrated *in vacuo*. The residue was taken up in Et_2O and washed with saturated aqueous NaHCO_3 (2 x 10 mL), dried over MgSO_4 , and concentrated *in vacuo*. The crude product was purified by silica gel chromatography (5% MeOH in CH_2Cl_2) to yield **11** as a white solid in 70% yield (1.32 g). ^1H NMR: δ 1.33-1.53 (m, 13H), 1.72 (d, 9.9 Hz, 1H), 2.75 (d, $J = 1.2$ Hz, 2H), 3.31 (m, 2H), 4.00 (m, 1H), 4.19-4.40 (m, 6H), 4.61 (dd, $J = 8.0, 2.5$ Hz, 1H), 5.52 (d, $J =$

4.8 Hz, 1H), 6.31 (t, $J = 1.8$ Hz, 2H). ^{13}C NMR: δ 177.34, 167.15, 138.25, 138.20, 109.92, 109.09, 96.45, 71.12, 70.87, 70.57, 65.96, 64.90, 48.24, 45.65, 43.15, 39.61, 26.24, 26.15, 25.18, 24.67.

ROMP of monomer 9. To a vigorously stirring solution of **9** (49.3 mg, 50 equiv) in CH_2Cl_2 (1.5 mL) under argon was added catalyst **10** (1.9 mg, 1 equiv) in CH_2Cl_2 (1.0 mL) from a stock solution. After allowing the reaction mixture to stir for 90 min at room temperature under argon, the reaction was quenched by addition of ethyl vinyl ether (1.0 mL). After another 10 min the reaction mixture was precipitated into hexanes (40 mL) at 0 °C. The cloudy mixture was centrifuged to sediment the product, and the supernatant was decanted off. The washing and centrifuging procedure was repeated twice more. The remaining solids were dissolved in CH_2Cl_2 , and the solvent was removed to recover the product as a light brown solid in 99% yield (50.7 mg). GPC: $M_n = 24,500$, $M_w/M_n = 1.04$.

References

- (1) (a) Sun, G.; Hagooly, A.; Xu, J.; Nyström, A. M.; Li, Z.; Rossin, R.; Moore, D. A.; Wooley, K. L.; Welch, M. J. *Biomacromolecules* **2008**, *9*, 1997–2006. (b) Gratton, S. A. E.; Williams, S. S.; Napier, M. E.; Pohlhaus, P. D.; Zhou, Z.; Wiles, K. B.; Maynor, B. W.; Shen, C.; Olafsen, T.; Samulski, E. T.; DeSimone, J. M. *Acc. Chem. Res.*, **2008**, *41*, 1685–1695.
- (2) (a) Fraser, C.; Grubbs, R. H. *Macromolecules* **1995**, *28*, 7248–7255. (b) Gestwicki, J. E.; Strong, L. E.; Kiessling, L. L. *Chem. Biol.* **2000**, *7*, 583–591. (c) Camm, K. D.; Castro, N. M.; Liu, Y.; Czechura, P.; Snelgrove, J. L.; Fogg, D. E. *J. Am. Chem. Soc.* **2007**, *129*, 4168–4169.
- (3) See Chapter 3.
- (4) See Chapter 2.
- (5) Pangborn, A. B.; Giardello, M. A.; Grubbs, R. H.; Rosen, R. K.; Timmers, F. J. *Organometallics* **1996**, *15*, 1518–1520.
- (6) Love, J. A.; Morgan, J. P.; Trnka, T. A.; Grubbs, R. H. *Angew. Chem., Int. Ed.* **2002**, *41*, 4035–4037.

Appendix 2

Theoretical PA-ROMP Molecular Weight Data and Determination of Catalyst Death Rates

Portions of the text in this chapter have been reproduced with permission from:

Matson, J. B.; Virgil, S. C.; Grubbs, R. H. *J. Am. Chem. Soc.* **2009**, *131*, 3355-3362.

Copyright 2009 American Chemical Society

Introduction

Additional mathematical data regarding pulsed addition ring-opening metathesis polymerization (PA-ROMP) are presented here. The data were obtained using a Symyx robotic system, which our group and others have used previously in studies of catalyst optimization.¹ The data are presented in Chapter 6 along with a full discussion.

Results and Discussion

Theoretical PA-ROMP Molecular Weight Data

A theoretical data set of 40 cycles of PA-ROMP is constructed below in which 8.5% of all living catalyst dies during each cycle, starting from an initial molecular weight of 7100 (Table 1). The M_n for each cycle and the resulting total M_n in the reaction vial are calculated (columns 3 and 4, respectively), as determined by averaging all previous M_n 's. An exponential trend is clearly observed. The data are graphed in Figure A2.1.

Table A2.1. Theoretical molecular weight trend over 40 cycles of PA-ROMP.

cycle	% catalyst alive	M_n (cycle)	M_n (total)
1	100.00%	7100	7100
2	91.50%	7760	7430
3	83.72%	8480	7780
4	76.61%	9268	8152
5	70.09%	10129	8547
6	64.14%	11070	8968
7	58.68%	12099	9415
8	53.70%	13222	9891
9	49.13%	14451	10398
10	44.96%	15793	10937
11	41.13%	17260	11512
12	37.64%	18864	12125
13	34.44%	20616	12778
14	31.51%	22531	13475
15	28.83%	24624	14218
16	26.38%	26912	15011
17	24.14%	29412	15858
18	22.09%	32144	16763
19	20.21%	35130	17730
20	18.49%	38393	18763
21	16.92%	41960	19868
22	15.48%	45858	21049
23	14.17%	50118	22313
24	12.96%	54774	23665
25	11.86%	59862	25113
26	10.85%	65423	26664
27	9.93%	71501	28324
28	9.09%	78143	30103
29	8.31%	85402	32010
30	7.61%	93335	34054
31	6.96%	102006	36246
32	6.37%	111482	38598
33	5.83%	121838	41120
34	5.33%	133156	43827
35	4.88%	145526	46733
36	4.46%	159045	49852
37	4.08%	173820	53203
38	3.74%	189967	56802
39	3.42%	207614	60669
40	3.13%	226901	64825

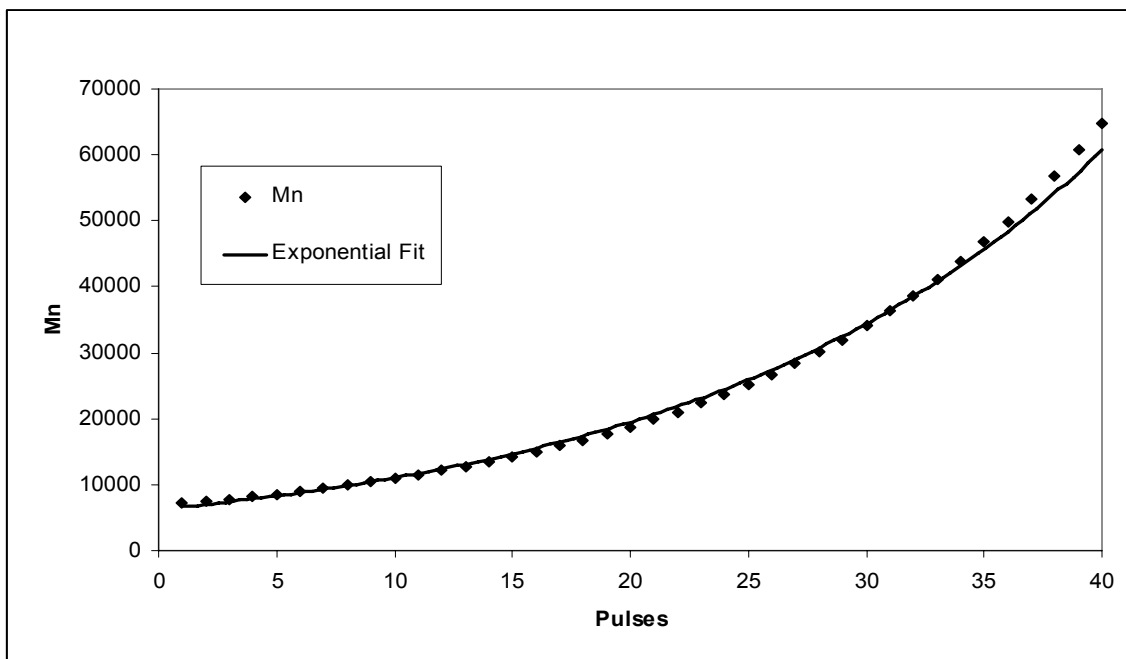


Figure A2.1. Dependence of M_n (total) on molecular weight on the number of cycles of PA-ROMP from a theoretical data set assuming 8.5% catalyst death per cycle and an initial M_n of 7100.

Determination of Catalyst Death Rates

Using the trendlines from exponential fits to the polymer molecular weight data, the observed total M_n for each pulse from the fit (column B), the calculated M_n for each individual pulse (column C), the % catalyst death from initial (column D), and the % catalyst death from the previous cycle (column E) were calculated for each experiment. The calculated M_n for a given pulse (column C, designated here as $M_{n\text{pulse}_n}$) is determined by the formula:

$$M_{n\text{total}_n} = (M_{n\text{total}_{n-1}} + M_{n\text{pulse}_n}) / n$$

Where n = vial number and $M_{n\text{total}_n}$ = value of row n in column B. The calculation for the catalyst death percentage from initial assumes that the polymer M_n for a given cycle is inversely proportional to the amount of living catalyst.

P(tBENI) homopolymers, M/C = 25. The equation determined from the exponential fit to the graph in Figure 6.4 was $y = 6904.1e^{0.0491x}$ ($R^2 = 0.9591$). Values for each pulse are shown in Table A2.2. Averaging the values in column E gives a total average catalyst death percentage of 8.51% per pulse.

Table A2.2. Determination of catalyst death rate for P(tBENI) homopolymers with M/C = 25 and a pulse time of 30 min in PA-ROMP.

A	B	C	D	E
Vial	Observed M_n (total) from fit	Calculated M_n (pulse) for individual pulse	% cat. death from initial	% cat. death from previous cycle
1	7251	7251	0.00%	n/a
2	7616	7981	9.14%	9.14%
3	7999	8766	17.28%	8.95%
4	8402	9610	24.54%	8.78%
5	8825	10516	31.05%	8.62%
6	9269	11489	36.89%	8.47%
7	9735	12534	42.15%	8.33%
8	10225	13655	46.90%	8.21%
9	10740	14857	51.19%	8.09%
10	11280	16145	55.09%	7.98%

P(tBENI) homopolymers, M/C = 100. By graphing the data (Figure 6.7), an exponential fit of pulse vs. M_n with the equation $y = 36286e^{0.108x}$ ($R^2 = 0.8238$) can be calculated. Values for each pulse were calculated and are shown in Table A2.3.

Averaging the values in column E gives a total average catalyst death percentage of 16.51% per pulse.

Table A2.3. Determination of catalyst death rate for P(tBENI) homopolymers with M/C = 100 and a pulse time of 30 min in PA-ROMP.

A	B	C	D	E
Vial	Observed M_n (total) from fit	Calculated M_n (pulse) for individual pulse	% cat. death from initial	% cat. death from previous cycle
1	40424	40424	0.00%	n/a
2	45035	49645	18.57%	18.57%
3	50171	60443	33.12%	17.86%
4	55893	73058	44.67%	17.27%
5	62267	87765	53.94%	16.76%
6	69368	104876	61.45%	16.32%
7	77280	124748	67.60%	15.93%
8	86093	147788	72.65%	15.59%
9	95912	174462	76.83%	15.29%
10	106851	205298	80.31%	15.02%

P(tBENI) homopolymers, M/C = 25, 20 °C, pulse interval of 60 min. The equation determined from the exponential fit to the graph in Figure 6.9 was $y = 7498.7e^{0.0677x}$ ($R^2 = 0.9561$). Values for each pulse are shown in Table A2.4.

Averaging the values in column E gives a total average catalyst death percentage of 11.23% per pulse.

Table A2.4. Determination of catalyst death rate for P(tBENI) homopolymers with M/C = 25, a temperature of 20 °C and a pulse time of 60 min in PA-ROMP.

A	B	C	D	E
Vial	Observed M_n (total) from fit	Calculated M_n (pulse) for individual pulse	% cat. death from initial	% cat. death from previous cycle
1	7251	7251	0.00%	n/a
2	7616	7981	12.29%	12.29%
3	7999	8766	22.77%	11.96%
4	8402	9610	31.78%	11.66%
5	8825	10516	39.55%	11.39%
6	9269	11489	46.29%	11.15%
7	9735	12534	52.17%	10.94%
8	10225	13655	57.31%	10.74%
9	10740	14857	61.81%	10.56%
10	11280	16145	65.78%	10.40%

P(tBENI-*b*-NMONI) block copolymers, M/C = 25. The equation determined from the exponential fit to the graph (Figure 6.11) of the pulse vs. M_n data in Table 5 was $y = 5440.5e^{0.0923x}$ ($R^2 = 0.9844$). Values for each pulse are shown in Table A2.5.

Averaging the values in column E gives a total average catalyst death percentage of 14.53% per pulse.

Table A2.5. Determination of catalyst death rate for P(tBENI-*b*-NMONI) block copolymers with M/C = 25 and a pulse time of 30 min in PA-ROMP.

A	B	C	D	E
Vial	Observed M_n (total) from fit	Calculated M_n (pulse) for individual pulse	% cat. death from initial	% cat. death from previous cycle
1	5982	5982	0.00%	n/a
2	6560	7138	16.19%	16.19%
3	7194	8461	29.29%	15.64%
4	7889	9973	40.01%	15.16%
5	8651	11698	48.86%	14.75%
6	9486	13664	56.22%	14.38%
7	10402	15899	62.37%	14.06%
8	11407	18440	67.56%	13.78%
9	12509	21323	71.94%	13.52%
10	13717	24590	75.67%	13.29%

References

- (1) (a) Kuhn, K. M.; Bourg, J. B.; Chung, C. K.; Virgil, S. C.; Grubbs, R. H. *J. Am. Chem. Soc.* **2009**, *131*, 5313–5320. (b) Bieniek, M.; Michrowska, A.; Usanov, D. L.; Grela, K. *Chem. Eur. J.* **2008**, *14*, 806–818.



L. Bencze